

**Effect of a methylxanthine compound and anticancer agent on
integrin mediated adhesion and induced apoptosis in
Breast cancer cells**

By

Peeyush Goel

[LIFE09200804008]

**Tata Memorial Centre
Mumbai**

A thesis submitted to the Board of Studies in Life Sciences

In partial fulfilment of requirements

For the Degree of

DOCTOR OF PHILOSOPHY

of

HOMI BHABHA NATIONAL INSTITUTE

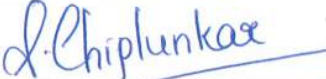
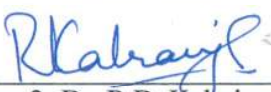


August-2014

HOMI BHABHA NATIONAL INSTITUTE

Recommendations of the Viva Voce Board

As members of the Viva Voce Board, we certify that we have read the dissertation prepared by Peeyush Goel entitled "Effect of a methylxanthine compound and anticancer agent on integrin mediated adhesion and induced apoptosis in breast cancer cells" and recommend that it may be accepted as fulfilling the thesis requirements for the award of Degree of Doctor of Philosophy.

	26.08.2014
Chairperson - Dr. K.B. Sainis	Date:
	26.08.2014
Convener - Dr. S.V. Chiplunkar	Date:
	26.08.2014
Member 1- Dr. R.P. Gude	Date:
	26.8.14
Member 2- Dr. R.D. Kalraiya	Date:
	26.8.14
External Examiner - Dr. Neeta Singh	Date:

Final approval and acceptance of this thesis is contingent upon the candidate's submission of the final copies of the thesis to HBNI.

I hereby certify that I have read this thesis prepared under my direction and recommend that it may be accepted as fulfilling the thesis requirement.

Date: 26.08.2014

Place: Mumbai


(Dr. S.V. Chiplunkar)
Guide

STATEMENT BY AUTHOR

This dissertation has been submitted in partial fulfillment of requirements for an advanced degree at Homi Bhabha National Institute (HBNI) and is deposited in the Library to be made available to borrowers under rules of the HBNI.

Brief quotations from this dissertation are allowable without special permission, provided that accurate acknowledgement of source is made. Requests for permission for extended quotation from or reproduction of this manuscript in whole or in part may be granted by the Competent Authority of HBNI when in his or her judgment the proposed use of the material is in the interests of scholarship. In all other instances, however, permission must be obtained from the author.

Peeyush Goel

DECLARATION

I, hereby declare that the investigation presented in the thesis has been carried out by me.
The work is original and has not been submitted earlier as a whole or in part for a degree
/ diploma at this or any other Institution / University.

Peeyush Goel

List of Publications arising from the thesis

Journal

1. **P.N. Goel** and R.P Gude. Unravelling the antimetastatic potential of pentoxifylline, a methylxanthine derivative in human MDA-MB-231 breast cancer cells. *Molecular and cellular biochemistry*. 358:141-151 (2011).
2. **P.N. Goel** and R.P. Gude. Curbing the focal adhesion kinase and its associated signaling events by pentoxifylline in MDA-MB-231 human breast cancer cells. *Eur J Pharmacol*. 714:432-441 (2013).
3. **P.N. Goel** and R.P. Gude. Pentoxifylline Regulates the Cellular Adhesion and its Allied Receptors to Extracellular Matrix Components in Breast Cancer Cells. *Biomed Pharmacother* (2014) 68:93-99.
4. **P.N. Goel** and R.P. Gude. Delineating the Anti-Metastatic Potential of Pentoxifylline in Combination with Liposomal Doxorubicin against Breast Cancer Cells. *Biomed Pharmacother* (2014) 68:191-200.
5. **P.N. Goel**, S.P Singh, R.P Gude and M.K Chilakapati. Investigating the Effects of Pentoxifylline on Human Breast Cancer Cells Using Raman Spectroscopy *J Innov Opt Health Sci* (2014) 8(2): 1550004.

Conference Proceedings

1. **P. Goel** and R. Gude. Anti-metastatic effects of a methylxanthine derivative in human breast cancer cells. *Eur J Cancer* (Poster abstract) (2014) 50:S210

Peeyush Goel

Presentation at conferences

1. 4th International Conference on Stem Cells and Cancer (ICSCC): Proliferation, Differentiation and Apoptosis at Haffkine Institute, Mumbai in 2013
2. 5th Frontiers in Cancer Science Conference held at Biopolis, Singapore in 2013
3. IX DAE-BRNS Life Sciences Symposium -2013 on Current Advances in Immunobiology and Cancer at BARC, Mumbai in 2013
4. International Symposium on Conceptual Advances in Cellular Homeostasis regulated by Proteasomes and Chaperones at ACTREC, Navi Mumbai in 2013
5. 9th National Research Scholars Meet at ACTREC, Navi Mumbai in 2013
6. 1st International Conference on Chemical Biology (ICCB) at CSIR-IICT, Hyderabad in 2014
7. 33rd Annual Conference of Indian Association for Cancer Research (IACR) at Kollam, Kerala in 2014

Peeyush Goel

Awards

1. CSIR-NET-JRF conducted by Council of Scientific and Industrial Research 2008
2. ICMR-JRF conducted by Indian Council of Medical Research 2008
3. DBT-JRF conducted by Department of Biotechnology 2009
4. The Sajjan Gupta-Konark Memorial Award for excellence in Bio-research at Research Meet in Biotechnology, Environmental Microbiology and Phytochemicals held at GN Khalsa College, Mumbai in 2012
5. Accredited with Travel Award for poster presentation at 4th International Conference on Stem Cells and Cancer held at Haffkine Institute, Mumbai in 2013
6. HBNI-DAE International Travel Fellowship by Department of Atomic Energy in 2013
7. Endorsed with DBT-International Travel Fellowship in 2013 (not availed)
8. Received 1st prize for poster presentation (Best poster) in IX DAE-BRNS Life Sciences Symposium held at BARC, Mumbai in 2013

Peeyush Goel

*Dedicated to my
Beloved family*

Acknowledgement

ACKNOWLEDGEMENT

Labor omnia vincit, a Latin phrase that means “hard work conquers all” and indeed, it does but not solely. This thesis is a culmination of my efforts but includes contributions of several people who stood by my side through the ebbs and rises of my tenure as a Ph.D. student. Although I believe words will not be sufficient to express my gratitude towards the almighty and all those people but in the next few lines I would like to make an honest effort to accomplish this indispensable task.

With immense pleasure, I express my profound gratitude towards my Ph.D. supervisor Dr. R.P Gude (superannuated Jan 2013) for his constant help and support during my doctoral tenure. I gratefully acknowledge his constant encouragement and pragmatic suggestions. I would like to specially thank Dr. S.V Chiplunkar (Director, ACTREC and Current guide) for her indefatigable help and support during the final supervision of my thesis.

I would also like to thank Dr. Rajiv Sarin (Ex-Director, ACTREC) and Dr. S.M Zingde (Ex-Deputy Director, ACTREC) for their help. With a deep sense of appreciation, I owe my thanks to all the doctoral committee members Dr. K.B Sainis (Ex-Director, Biomedical Group, BARC), Dr. Robin Mukhopadhyaya (superannuated) and Dr. R.D Kalraiya for their critical evaluation and suggestions regarding the progress of my work.

A very special vote of thanks to my labmates Yuvraj ji, Manu ji and Sawant ji. Zahid had been my lab mate as well as batch mate and had been with me for support all through the tenure of my doctoral work. I am thankful to Dr. Shimul Salot for the technical expertise during my work and trainees Emmanuel, Sushmita, Himanshu, Nirosha, Shinjini and Pranchi who had helped me in the progress of my work. I would also like to thank my

batch mates Surya, Monica, Lalith, Padma, Lumbini, Manohar, Nikhil, Vikrant and Nitu. The entire microscopy facility (Vaishali, Jairaj, Tanuja and Mansi), flow cytometry facility (Rekha and Shamal), IT department, common instrumentation facility (Dandekar and Kulkarni), Programme office (Maya) and the Animal house facility (Dr. A. Ingle, Mahesh, Shashi and Chavan sir) that had been very co-operative during the course of my work. I would also like to thank all my collaborators (Manjappa, Ankit, Darshana, Shruti, Sanket and Geeta). All my seniors and juniors had been very helpful and supportive. A word of special thanks to all the personnel in the administrative staff, academic and training programme and photography section.

No choice of words will suffice to adequately register the love, care and encouragement provided by my dear friends Payal, Ashish, Kaustubh, Sanket, Sheetal, Aamiya and Rajat. Words are inadequate to express my feelings for my mother, father and brother, who always provided me the best by masking their own needs and desires. Lastly, I am really thankful to ACTREC and CSIR for financial support. I am really thankful to HBNI for providing me travel assistance for the International conference held at Singapore.

I am really indebted to each one of them for their love, help and support.

Peeyush Goel

CONTENTS

Synopsis	1
List of figures	30
List of tables	33
1. Chapter 1: Review of Literature	34
1.1 Cancer: a brief history and its outcome	34
1.2 Metastasis	35
1.3 Processes involved in metastasis	37
1.3.1 Adhesion	37
1.3.2 Invasion	40
1.3.3 Migration	41
1.3.3.1 Lamellipodium extension	43
1.3.3.2 Formation and stabilization of new adhesions	44
1.3.3.3 Cell body contraction	45
1.3.3.4 Rear release	45
1.3.4 Transport, arrest and extravasation	46
1.3.5 Angiogenesis	47
1.4 Breast cancer	48
1.4.1 Incidence and risk factors	48
1.4.2 Development of breast cancer	48
1.4.3 Treatment scenario	49
1.4.3.1 Surgery	49
1.4.3.2 Hormonal therapy	49

1.4.3.3 Radiation therapy and chemotherapy	50
1.4.4 Triple negative breast cancers (TNBC)	51
1.5 Therapeutic implications	52
1.6 Pentoxifylline	54
1.7 Integrins	58
1.7.1 Inside-out signalling	61
1.7.2 Outside-in signalling	62
1.7.3 Integrins and breast cancer	63
1.8 Focal adhesion kinase (FAK)	64
1.8.1 FAK structure	64
1.8.2 FAK signalling and cancer	65
1.9 Protein kinase B/Akt signalling	66
1.10 Apoptosis	67
1.10.1 Integrins and cell death	69
1.11 Combination therapy	70
1.12 Liposomal doxorubicin	71
2. Chapter 2: Aims and Objectives	73
2.1 Rationale of the study	73
2.2 Aims	74
3. Chapter 3: Materials and Methods	75
3.1 Materials	75
3.1.1 Fine chemicals	75
3.1.2 Tissue culture reagents and plasticware	75

3.1.3 General Chemicals	75
3.1.4 Antibodies	76
3.1.5 Kits	76
3.1.6 Solvents and Acids	76
3.1.7 Instruments and machines	77
3.1.8 Cell lines and animals	77
3.2 Methods	77
3.2.1 Maintenance of cell lines	77
3.2.2 MTT cytotoxicity assay	79
3.2.3 Colony formation assay	81
3.2.4 Cell cycle analysis	82
3.2.5 Ethidium bromide/acridine orange (EB/AO) staining	82
3.2.6 AnnexinV/FITC Staining	83
3.2.7 Adhesion assay	83
3.2.8 Preparation of condition media	84
3.2.9 Gelatin zymography	85
3.2.10 Wound scratch assay	86
3.2.11 Flow cytometry for surface expression of integrins	86
3.2.12 Reverse transcriptase (RT) PCR	87
3.2.13 SDS-PAGE	92
3.2.14 Immunofluorescence	99
3.2.15 G-LISA assay for RhoGTPases	100
3.2.16 Actin staining using phalloidin-FITC	100

3.2.17 Caspase-3 and caspase-9 activation assays for apoptosis	101
3.2.18 <i>In vivo</i> xenograft model	102
3.2.19 <i>In vivo</i> intradermal model for angiogenesis	102
3.2.20 <i>In vivo</i> experimental metastasis	103
3.2.21 Chick chorioallontic membrane (CAM) assay	104
3.2.22 <i>In vivo</i> xenograft model for combination study	104
3.2.23 Statistics	105
4. Chapter 4: Results	106
4.1 PTX affects cellular proliferation in dose dependent manner	106
4.2 PTX brings an alteration in cell cycle profile and induces apoptosis	108
4.3 PTX affects cellular adhesion to ECM	112
4.4 PTX impedes cellular motility and affects invasive potential	115
4.5 MDA-MB-231 displays higher adhesion potential than MCF-7 using ECM substrates	118
4.6 MDA-MB-231 exhibit differences in surface expression of integrins compared to MCF-7	120
4.7 PTX demonstrates a differential effect on integrins expression in MDA-MB-231 cells	124
4.8 PTX affects the expression of active FAK and its downstream effectors	131
4.9 PTX enhances the activities of both cleaved caspases 9 and 3	137
4.10 Inhibition of RhoGTPases activity by PTX	139
4.11 PTX affects the actin cytoskeleton arrangement in MDA-MB-231 cells	141
4.12 Tumour growth delay in SCID mice after PTX treatment	142

4.13 Decrease in blood vessel formation upon PTX treatment	144
4.14 PTX affects colony formation using <i>in vivo</i> experimental metastasis model and angiogenesis in Chick chorioallontic membrane assay	147
4.15 Lipodox exhibited lesser cytotoxicity than plain doxorubicin in MDA-MB-231 cells	149
4.16 Synergism in the cytotoxicity profile for the combination regimen of PTX and lipodox	151
4.17 Changes in cell cycle progression and increased apoptosis upon treatment with the combination regimen	156
4.18 Alterations in cellular adhesion, invasion and migration for the combination treatment	161
4.19 Combination delays tumour growth using <i>in vivo</i> xenograft model	166
5. Chapter 5: Discussion	170
6. Summary and Conclusions	185
7. Bibliography	190
8. List of Publications	209

Synopsis



Homi Bhabha National Institute
Ph. D. PROGRAMME

1. **Name of the Student:** Peeyush Goel
2. **Name of the Constituent Institution:** Advanced Centre for Treatment, Research and Education in Cancer, Tata Memorial Centre.
3. **Enrolment No. :** LIFE09200804008
4. **Title of the Thesis:** Effect of a methylxanthine compound and anticancer agent on integrin mediated adhesion and induced apoptosis in breast cancer cells.
5. **Board of Studies:** Life Sciences

SYNOPSIS

Introduction

Cancer is one of the most leading causes of worldwide deaths. The majority of these deaths are due to dissemination of tumour cells from site of origin to distant organs such as lungs, liver, brain and bone, a process referred to as metastasis. Metastasis is thus a crucial area in cancer research as it is the prime cause of mortality by the disease. During the process of metastasis, tumour cells need to invade barriers such as the underlying extracellular matrix (ECM) and surrounding tissues. The ability to alter cellular migration and adhesion to the ECM components helps the tumour cells to by-pass these obstructions, paving a passage into circulation for distant localization.

Breast cancer is the second most common diagnosed cancer worldwide and the leading cause of cancer related deaths in women [1]. Statistically, around 1.3 million cases and almost 0.3 million deaths had been reported by WHO, based on global cancer analysis [2]. It starts as a primary tumour but can later metastasize to the bones, lung, liver and brain [3]. The systemic distribution and resistance to the current therapies indeed makes the process of metastasis hard to manage. Cellular adhesion is an important biological phenomenon required for the functioning of living organisms. The cells transmit signals from their environment via different surface receptors that act as the relaying switches.

Adhesion molecules have traditionally been thought of simply as receptors that permit anchorage to other cells or to the underlying ECM. However, it has become apparent within the past decade that the adhesion molecules such as integrins mediate critical cytosolic signaling events that have a dramatic impact upon cellular proliferation, survival and motility. Each integrin is a heterodimer consisting of an α subunit non-covalently bound to a β subunit [4]. These act as receptors for extracellular matrix

components such as fibronectin, vitronectin, collagen, laminin etc. Intracellularly, integrins are linked to the cytoskeleton and are involved in signal transduction processes. Increased expression of certain integrins such as α_v , α_3 , α_5 , β_1 , β_3 and β_5 as well as adhesion to ECM components correlates with invasive or metastatic potential in breast cancer [5-8]. In the light of these characteristic features, integrins have become attractive targets for drug development and thus targeting cell–matrix adhesions shall provide a critical advantage for cancer therapy. Since integrins lack the intrinsic enzymatic activity they require adaptor molecules to orchestrate cellular signaling. Focal adhesion kinase (FAK) is an intracellular tyrosine kinase that functions as a major mediator of signal transduction by cell surface receptors including integrins [9]. It has been found to be involved in diverse cellular processes such as cell adhesion, migration, cell survival and proliferation [10,11]. It regulates the actin cytoskeleton as well as the functioning of Rho GTPases that aids the process of cellular migration. It also regulates the processes of cellular proliferation via the Mitogen Activated Protein Kinase (MAPK) as well as Akt pathways. FAK inhibition is associated with a decrease in level of activated Akt that forms a part of central pathway regulating the process of apoptosis. Based on these observations it can be regarded as a potential target for anti-cancer therapy.

Triple negative breast cancer (TNBC) is a heterogeneous entity that presents it a daunting task for diagnosis and treatment. TNBC subgroup lacks expression of estrogen receptor, progesterone receptor and HER-2. Further, such tumours are difficult to manage using the conventional hormonal and HER-2 targeted therapies [12]. Thus, no other systemic therapy exist other than chemotherapy.

At present a large number of anti-cancer drugs are available in the market. The initial evaluation requires huge expenditure and longer periods to reach the clinical settings. Hence, it is advisable to evaluate the action of other known drugs that are currently in the market for treatment of other diseases.

The main reasons for this drug repositioning are (a) the pharmacokinetics as well as the safety profiles for the existing drugs are well understood and any newer discovered role can be harnessed for clinical trials. (b) to help drug developers to avoid the assessment costs [13]. In view of this, we have evaluated the anti-metastatic potential of pentoxifylline (PTX) in human breast cancer cells. Previous studies from our laboratory had shown that PTX exerts anti-metastatic activity in B16F10 murine melanoma cells [14-16]. However, no reports are currently available that are suggestive of the fact that PTX exerts anti-metastatic effects in human breast cancer cells. Thus, in the present work we have extended our approach to investigate the efficacy of PTX in MDA-MB-231 human breast cancer cells and elucidate its mechanism of action.

Methylxanthine are methylated derivatives of xanthine, a purine base. These include caffeine, theobromine, theophylline, PTX etc. These act as potent inhibitors of phosphodiesterase activity that elevates intracellular c-AMP levels [17]. PTX is used as a hemorreological agent in the treatment of peripheral vascular diseases. It activates c-AMP dependent Protein kinase A and had been shown to impede migration in B16F10 melanoma by modulating Rho GTPase activity and actin organisation [15]. Further, PTX has been shown to increase the effectiveness of radiotherapy and chemotherapy. PTX inhibits the experimental metastasis of B16F10 murine melanoma cells and modulates cell surface integrin expression and adhesion of B16F10 cells to ECM components [18].

Chemotherapy constitutes a major treatment option in advanced breast cancer. Anthracyclines and taxanes are the most commonly used drugs apart from anti-metabolites (capecitabine, gemcitabine), platinum analogues such as cisplatin, carboplatin. Among these, anthracyclines are one of the most active agents used [21]. Their anti-cancer properties are mainly due to their ability to intercalate between DNA base pairs or form toxic DNA–drug cross-links that trigger the death of rapidly dividing cancer cells. It also leads to generation of free radicals that are toxic to cells, leading to loss of membrane integrity and culminating into cellular death [22]. These anticancer agents suffer from various drawbacks such as induction of cardiotoxicity, alopecia, nausea and vomiting. Thus combination treatments are much required so as to lower the doses of individual drug as well as to increase the therapeutic effectiveness. Based on these properties, we have evaluated the effect of PTX on MDA-MB-231 cells and then used it along with liposomal doxorubicin (LD) or lipodox so as to increase its therapeutic efficacy.

Aims and Objectives

1. To study the anti-metastatic potential of PTX in MDA-MB-231 human breast cancer cells *in vitro* and *in vivo*.
2. To study the effect of PTX on integrin expression profile in MDA-MB-231 cells.
3. To study the effect of PTX on Focal Adhesion Kinase (FAK) and its downstream signaling mediators.
4. To study the chemo-adjuvant potential of PTX in combination with another anti-cancer agent to increase its therapeutic efficacy using *in vitro* and *in vivo* models.

Materials and Methods

Cell Lines

MDA-MB-231, MCF-7 and HT-1080 cell lines were purchased from NCCS, Pune, India. The cell lines were maintained in Dulbecco's Modified Eagle Medium (DMEM, GIBCO) supplemented with 10% heat inactivated foetal bovine serum, FBS (GIBCO) and antibiotics (100 U/ml penicillin and 100 µg/ml streptomycin). Cultures were maintained at 37°C in 5% CO₂ humidified atmosphere.

Cellular cytotoxicity using MTT assay

Cells were seeded in a 96-well plate during the exponential phase of cell cycle. PTX was then added at varying doses and the plates were incubated at 37°C for different time points viz. 24 hr, 48 hr and 72 hr. The drug was removed and (3-(4,5-dimethylthiazol-2-yl)-2,5-diphenyltetrazolium bromide) (MTT) (1mg/ml) was added to the wells and incubated for 4 hr. Plates were then centrifuged and DMSO was added. Subsequently, the plates were read at dual wavelengths of 540/690 nm using a spectrophotometer. IC₅₀, the concentration required to kill 50% of cells was calculated. The cell viability for combination study was also determined by MTT assay. Here, pentoxifylline:lipodox (PTX: LD) were taken in the ratio of 500:1 and synergistic doses were evaluated using compusyn software. The doses evaluated for combination regimens are designated as PTX or P1 (PTX dose 1) 3 mM, PTX or P2 (PTX dose 2) 4 mM, LD or LD1 (lipodox dose 1) 6 µM, LD or LD2 (lipodox dose 2) 8 µM, Combination C1 (P1 and LD1) and Combination C2 (P2 and LD2) respectively.

Colony formation assay for cellular proliferation

Briefly, 600 cells were seeded in a 35 mm plate and incubated for 24 hr. PTX/combination regimens were added later for a period of 24 hr. Cells were washed using PBS and then complete media was added. The cells were allowed to grow into colonies over a period of 8-10 days. Cells were then fixed using chilled methanol and stained with 0.5% crystal violet. Colonies with cells greater than 50 were counted.

Cell cycle analysis using flow cytometry

Sub-confluent plates were treated with varying sub-toxic doses of PTX (1mM, 2.5 mM and 5 mM) or combination regimens for a period of 24 hr. Cells were harvested, washed twice with PBS and later fixed using 70% chilled ethanol. The cells were then treated with RNase (0.5 mg/ml) and stained with propidium iodide (PI) (50 µg/ml). Acquisition was done on FACS Calibur and the results were analysed using Modfit software.

Ethidium bromide/acridine orange (EB/AO) staining for apoptosis

Sixteen thousand cells per well were seeded in triplicates using a 96-well format. Cells were then treated with PTX/combination regimens for 24 hr and then plates were centrifuged. The cells were stained using EB/AO mix and observed under a Zeiss Axio inverted microscope.

AnnexinV/FITC Staining

Apoptosis detection was done using apoptosis detection kit from Invitrogen. Briefly, 1×10^6 cells were suspended in 100 µl Annexin binding buffer and treated with 5 µl Annexin FITC solution along with 1 µl PI(100 µg/ml). The samples were incubated for 15 min and then 400 µl of Annexin binding buffer was added. Acquisition was done using FACS Calibur and analysis was performed using Cell Quest software.

Cellular morphology in presence of PTX

Sub-confluent MDA-MB-231 cells were treated with sub-toxic doses of PTX for 24 hr. Cells were then fixed and subjected to Hematoxylin-Eosin (HE) staining. Coverslips were mounted on glass slides with the aid of DPX mountant and were observed under Zeiss upright microscope.

Adhesion assay

Plates were coated with Matrigel, Collagen type-IV, fibronectin, laminin or vitronectin and then kept at 4°C overnight for polymerization. The plates were washed with PBS, subsequently treated with 1% bovine serum albumin (BSA) for 2 hr and kept in an incubator. Cells treated with sub-toxic doses of PTX or the combination regimens were harvested using saline-EDTA. Subsequently, cells were suspended in 0.1% BSA containing plain DMEM and inoculated at a density of 3×10^4 cells/well. Adhesion was evaluated at different time points viz. 15, 30, 45, 60 and 90 min. The percent cells to respective substrates were then determined by MTT assay.

Preparation of condition media and gelatin zymography

Sub-confluent plates treated with PTX/combination regimens for 24 hr were washed with PBS and then plain DMEM was added to the plates. The condition media was collected after 24 hr and concentrated using 30 kDa cut off filters from Millipore. 50 µl sample were loaded onto 8% SDS-PAGE gel containing 0.1% gelatin. After electrophoresis, the gel was kept in developing buffer and later stained with 0.25% Commassie Brilliant Blue R-250. The gelatinase activity was visible as clear white zones in a dark background. Condition media prepared from HT-1080 was used as a positive control.

Wound scratch assay

Cells grown in 6-well plates were treated with 1 µg/ml mitomycin C for 1 hr and a scratch was made in the middle of plate. PTX/combination regimens were added for 24 hr and plates were fixed with 70% methanol. The wound width was measured using the AxioVision Rel 4.8 imaging software and results were plotted as % wound closure with respect to control.

Flow cytometry for surface expression of integrins

Cells were harvested using saline-EDTA and fixed using 4% paraformaldehyde. Approximately, 1×10^6 cells were treated with 1 µg of the respective anti-integrin antibody. Cells were mixed thoroughly and kept at 4°C for an hour. Subsequently, cells were washed using fluorescence activated cell sorting (FACS) buffer twice and incubated with FITC labeled secondary antibody for 1 hr at 4°C. Cells were washed twice using FACS buffer and then finally suspended in it. Acquisition was done on FACS Calibur and the results were analyzed using Cell Quest software.

Reverse transcriptase (RT) PCR

RNA was extracted from PTX treated cells using the Trizol method. RNA was quantified using Nano Drop. c-DNA preparation and PCR was then performed using kit from Fermentas as per the manufacturer's instructions. Two microgram of c-DNA was used for PCR amplification. GAPDH was used as an internal standard.

Western Blotting

Cells were lysed in modified radioimmunoprecipitation assay (RIPA) buffer. Fifty microgram protein was loaded on 8% SDS-PAGE gel and then electroblotted to PVDF membranes. The membranes were processed by blocking in 5% BSA and subsequently

incubated with respective primary and secondary antibodies. Intermittent washings were done using Tris-Buffered Saline-Tween 20 (TBST). Beta-tubulin was used as a loading control and the signal detection was done on X-ray films using the Pierce Femto chemiluminescence reagent.

Immuno-fluorescence study using confocal microscopy

Cells were grown in 35 mm plates and fixed in 4% paraformaldehyde. Cells were then permeabilized with 0.5% triton X-100 and then blocked in 1% BSA. Incubation with the primary and secondary antibodies was carried out for 1 hr at room temperature. Cover slips were mounted on glass slides in 4% 1,4-diazabicyclo[2.2.2]octane (DABCO). Images were acquired at 63X using the LSM 510 Meta laser scanning microscope from Carl Zeiss, Germany.

G-LISA assay for RhoGTPases

The activity for active RhoGTPases was determined using G-LISA kit from cytoskeleton. Briefly, 50 µg of cell lysates were added to the active Rac or Rho coated plates. Primary and secondary antibodies were added sequentially for 1 h each. Horseradish peroxidase (HRP) was added for color development and the plates were read at 490 nm using a spectrophotometer.

Actin staining using phalloidin-FITC

Briefly, semi-confluent cells were fixed using 4% paraformaldehyde, permeabilised using 0.1% Triton X100 and overlaid with 20 µl of phalloidin mixture and washed with PBS thrice. Coverslips were mounted on a clean glass slide using 4% DABCO and sealed with the help of nail paint. Cytochalasin B was used as a positive control. Images were

acquired at 63X using the LSM 510 Meta laser scanning microscope from Carl Zeiss, Germany.

Caspase-3 and caspase-9 activation assays for apoptosis

Cell lysates were prepared using caspase lysis buffer, supplied as a part of kit from Invitrogen. Two hundred microgram of protein solution was added with subsequent addition of substrates LEHD (Leucine-Glutamate-Histidine-Aspartate), DEVD (Aspartate-Glutamate-Valine-Aspartate) for caspase-9 and caspase-3 respectively. Plate was incubated for at least 2 h at 37⁰C and later read at 405 nm in a spectrophotometer.

***In vivo* xenograft model**

Briefly, 2×10⁶ MDA-MB-231 cells were inoculated into the right flank of 6-8 week old female NOD-SCID mice. When the tumours had grown to an average size of 50 mm³ mice were randomized and divided into 3 groups (n=5). (a) PBS only (b) PTX 40 mg/kg and (c) PTX 60 mg/kg. PTX was administered intraperitoneally (i.p) for a period of 9 days consecutively. Tumour volume was measured using Vernier calipers and calculated using the formula $1/2ab^2$ where a is the longer diameter and b is the shorter one.

***In vivo* intradermal model for angiogenesis**

Briefly, 1×10⁶ MDA-MB-231 cells were injected intradermally into the ventral side of 6-8 week old female NOD-SCID mice. When palpable tumours were observed mice were randomized into 3 groups (n=5) as described previously. (a) PBS only (b) PTX 40 mg/kg and (c) PTX 60 mg/kg. Administration of PTX was done i.p for 9 days. Mice were sacrificed on day 15th after the treatment schedule was completed. The intradermal skin bearing tumours was excised for counting blood vessel density around the localized tumour.

***In vivo* experimental metastasis**

Briefly, 1×10^6 cells were injected intravenously (i.v) in 6-8 weeks old female NOD-SCID mouse. Three groups (n=5) were formed (a) PBS only (b) PTX 40 mg/kg (c) PTX 60 mg/kg. PTX was injected i.p from day 1 to day 9 continuously. Animals were sacrificed when found to be moribund. The lungs were excised and fixed in buffered formalin solution. The tissues were sectioned and stained using haemotoxylin-eosin as done earlier. Images were then captured using an upright microscope from Zeiss (Germany).

Chick Chorioallontic Membrane (CAM) assay

Fertilized eggs from White Leghorn hen were placed in an incubator at 37°C under approximately 70% relative humidity. The eggs were then kept at 37°C for 5 days prior to PTX treatment. PTX (400 µg) was added through a small window made using a sterile scalpel. The eggs were then resealed using parafilm and incubated further at 37°C. The experiment was terminated on the subsequent day and photographs were taken after cut opening of the eggs.

***In vivo* Xenograft model for combination study**

Briefly, 2×10^6 MDA-MB-231 cells were inoculated into the right flank of 6-8 week old female Balb/c nude mice. When the tumours had grown to an average size of 50 mm³ mice were randomized and divided into 6 groups (n=5): (a) PBS only (b) PTX 60 mg/kg and (c) ADR (4 mg/kg) (d) LD (4 mg/kg) (e) PTX+LD (40 mg/kg and 1 mg/kg) (f) PTX+LD (40 mg/kg and 2 mg/kg). PTX was administered intraperitoneally (i.p) for a period of 9 days consecutively while ADR/LD was injected intravenously once a week. Tumour volume was measured using Vernier calipers and calculated using the formula $1/2ab^2$ where a is the longer diameter and b is the shorter one.

Results

PTX affected cellular proliferation in dose-dependent manner

MTT assay was carried out for 24 hr, 48 hr and 72 hr at log doses of PTX to evaluate the anti-proliferative effect of PTX on MDA-MB-231 cells. PTX affected the cellular proliferation in a dose and time dependent fashion. The IC₅₀ values determined were 9 mM, 3 mM and 2 mM for 24 hr, 48 hr and 72 hr respectively (Figure 1). Based on this observation, the subsequent experiments were carried out at sub-toxic doses such as 1, 2.5 and 5 mM of PTX for a 24 hr exposure. Treatment with PTX (1-20 mM) also resulted a decrease in colony formation to 81.7%, 57.14%, 16.11%, 0.75% at 1, 2.5, 10 and 20 mM respectively compared to untreated cells ($P < 0.05$).

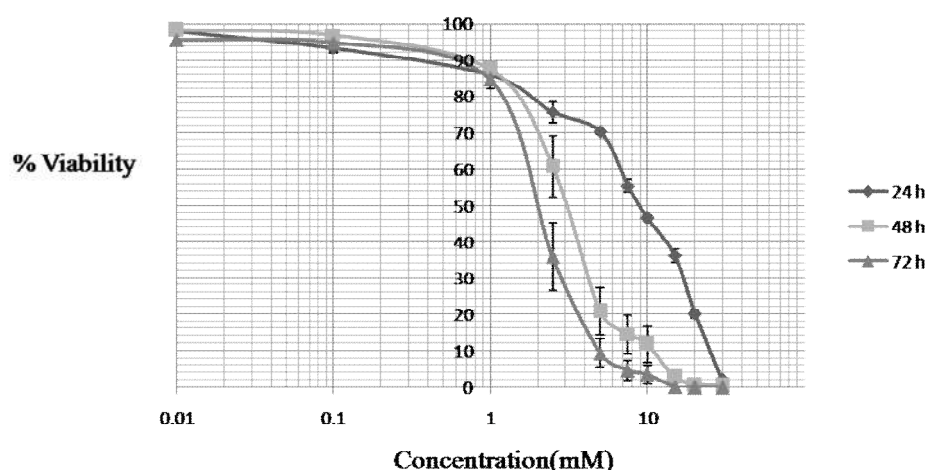


Figure 1: MTT assay for PTX treated cells at 24 hr, 48 hr and 72 hr.

PTX brings an alteration in cell cycle profile and induces apoptosis

Cell cycle analysis using flow cytometry at sub-toxic doses of PTX showed a G1 cell-cycle arrest in MDA-MB-231 cells. A significant increase in number of cells in G1 phase i.e from 36.81% in control to 57.85%, 62.74% at 2.5 mM and 5 mM respectively was observed. Both cyclin D1 as well as cdk4/6 are required to crisscross the G1 cell cycle

phase. PTX treatment at sub-toxic doses lowered the levels of both cyclinD1/cdk6 in a dose dependent manner. However, the levels of cdk4 remained unchanged upon PTX treatment. There was an increase in number of apoptotic cells upon PTX treatment as revealed by staining with ethidium bromide and acridine orange. This was further confirmed by AnnexinV/FITC staining that showed an increase in apoptotic population upon PTX treatment. PTX also affected the process of apoptosis by altering the expression and activities of both Caspases 9, 3 respectively as seen by using western blotting and *in-vitro* caspase activation assay. Further, it decreased the levels of anti-apoptotic proteins such as Bcl-2 and Bcl-xL in a dose dependent manner.

PTX affects cellular morphology and adhesion

Haemotoxylin eosin (HE) staining revealed that PTX treated cells were highly elongated. Further, PTX significantly decreased adhesion to ECM substrates viz matrigel, collagen type IV, fibronectin and laminin in a time and dose dependent manner. Adherence was found out to be 57.63%, 51.65% at 5 mM compared to 80.08% and 69.82% for untreated control at 60 min for matrigel and collagen respectively. There was a reduced adherence to fibronectin and laminin ie 64.84%, 24.82% respectively at 5 mM compared to 90.91%, 45.63% for untreated control at 60 min ($P<0.05$). However, no significant change in adhesion to vitronectin was observed upon PTX treatment.

PTX impedes cellular motility and affects invasive potential

PTX at sub-toxic doses showed a significant reduction in motility of MDA-MB-231 cells. At 1, 2.5, 5 mM wound coverage was 69.54%, 54.87% and 30.84% compared to control ($P<0.05$). Further, PTX affected the activity of gelatinase MMP-9 in a dose dependent

manner. MMP-9 activity showed a 21.59%, 32.37% reduction at 2.5 mM and 5 mM, ($P<0.05$). HT-1080 was used as a positive control.

PTX causes a tumour growth delay and inhibits angiogenesis *in vivo*

PTX significantly resulted in a delay in tumour growth. Tumour volumes on 17th and 21st days were 554.20, 1397 mm³ for untreated control while in PTX treated groups were 280.92, 912.91 mm³ for PTX (40 mg/kg) and 239, 895 mm³ for PTX (60 mg/kg) groups ($P<0.05$).

In the intradermal model of angiogenesis, palpable tumours were visible from day 3rd onwards. PTX inhibited angiogenesis, a process of blood vessel formation from pre-existing ones around the growing tumours. Average tumour volume was 145.6 mm³ for untreated group while it was 75.44, 73.64 mm³ for PTX treated groups viz. 40 mg/kg and 60 mg/kg groups respectively ($P<0.05$). The average number of blood vessels visible were 6.8, 3.8, 2.8 for untreated and PTX treated (40 mg/kg and 60 mg/kg) groups respectively ($P<0.05$). This was also confirmed by Chick chorioallantoic membrane (CAM) assay. PTX also affected the adhesion of MDA-MB-231 cells to lungs in the experimental metastasis model using NOD-SCID mice. PTX treated groups showed lesser and smaller number of colonies compared to the untreated control.

PTX affects integrin expression profile in MDA-MB-231 cells

MDA-MB-231 demonstrated higher adhesive potential compared to MCF-7 to ECM viz. matrigel, collagen type IV, fibronectin, laminin and vitronectin. The adherence for the five matrix components was found to be 25.97%, 11.20%, 29.12%, 23.15, 55.21% for MCF-7 when compared to 80.08%, 69.82%, 90.91, 45.63% and 71.4% respectively for MDA-MB-231 cells at 60 minutes respectively ($P<0.05$). PTX decreased the surface

expression of integrins such as $\alpha 5$, $\beta 1$ and $\alpha 5\beta 1$ in MDA-MB-231 cells as assessed by flow cytometry. Treatment with PTX at sub-toxic doses on integrins αV , $\alpha 3$, $\alpha 5$, $\alpha 2$, $\beta 1$, $\beta 3$ and $\beta 5$ did not affect the levels of transcripts as obtained by RT-PCR. However, the total protein levels of αV , $\alpha 3$, $\alpha 5$, $\beta 1$ and $\beta 3$ integrins was lowered following treatment with PTX at sub-toxic doses (Figure 2). PTX also induces a decrease in surface localization of integrin $\alpha 5\beta 1$ as evident from confocal microscopy of the treated cells.

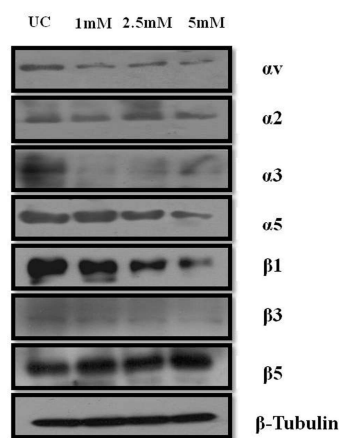


Figure 2: Western blot for integrin subunits upon PTX treatment.

PTX affects the expression of active FAK and its downstream effectors

PTX at sub-toxic doses affected the levels of FAK and ERK1/2 or MAPK in a dose dependent manner (Figure 3). Treatment with PTX resulted in decrease in levels of RhoGTPases ie Rac and Rho in a dose dependent manner. The decrease was found to be significant at 2.5 mM and 5 mM PTX. The corresponding activities being 77.145%, 54.9% and 71.58%, 64.43% for active Rac and Rho respectively ($P < 0.05$). The effect of sub-toxic doses of PTX on actin organization was evaluated in MDA-MB-231 cells using Phalloidin-FITC that specifically stains filamentous actin structures of the cells. Confocal images showed disappearance of filopodia and lamellopodia in a dose dependent manner. Cells treated with cytochalasinB were kept as a positive control. PTX also affected the

levels of Akt (Figure 3) and its downstream effectors such as Bcl-2 and caspases as mentioned earlier.

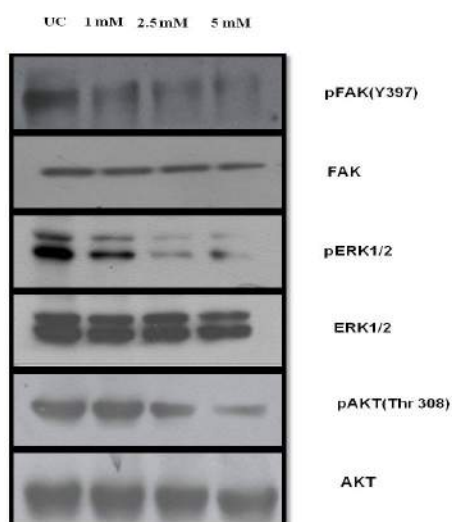


Figure 3: Western blot for FAK and its downstream effectors upon PTX treatment.

Synergism in the cytotoxicity profile for the combination regimen of pentoxifylline and lipodox

LD was used in our present study since it is comparatively lesser toxic compared to DOX alone. The % viability of both PTX and LD in the ratio of 500:1 was determined using MTT assay at different doses both in combination as well as single agents respectively. It was found that PTX at doses of 3 mM, 4 mM and corresponding LD at 6 μ M and 8 μ M showed synergistic action where combination index (CI) tends to be less than unity. Based on these combination doses, anti-metastatic activity of the combination regimen was evaluated. The doses were designated as P1 (3 mM), P2 (4 mM) for PTX, LD1 (6 μ M), LD2 (8 μ M) for LD and C1 (P1 and LD1), C2 (P2 and LD2) for combination. Further, viability at these combination doses (C1 and C2) is much lower than that of individual effects. The anti-proliferative activity of the combination regimen was further

confirmed using colony formation assay. The % colony formation was 54.12% (P1), 44.22 (P2), 16.75 (LD1), 4.88 (LD2), 6.22 (C1) and 1.59 (C2) ($P<0.05$).

Changes in cell cycle progression and increased apoptosis upon treatment with the combination regimen

Flow Cytometry was done to assess the cell cycle status of MDA-MB-231 cells upon PTX and LD treatment as well as their combination. It was found that treatment of MDA-MB-231 cells with PTX lead to a significant increase in G1 phase cells (64.58% for P1, 60.90% for P2 while for UC it was 38.4%) ($P<0.05$). However, treatment with LD caused a significant arrest in G2-M cell cycle phase (49.93% for LD1, 68.35% for LD2 and 14.9% for UC) ($P<0.05$). However, for the combination scenario a G1 phase cell cycle arrest was pronounced. Cells treated with combination doses showed a relatively higher increase in % apoptosis compared to use of PTX and LD alone by flow cytometric analysis using AnnexinV/FITC staining. This was supported by fluorescence microscopic observation after ET/AO staining as well.

Alterations in cellular adhesion, invasion and migration for the combination treatment

It was found that LD *per se* did not alter adhesion of any of the ECM components used. PTX at doses of 3 mM and 4 mM did affect adhesion. Further, the combination regimen showed a similar reduction comparable to that due to use of PTX alone. The combination doses (C1 and C2) showed 52.7%, 40.19% adhesion to matrigel; 49.09%, 49.97% to collagen; 69.55%, 62.28% to fibronectin and 30.3%, 26.2% for laminin considering the adhesion of untreated control to be 100%. No change in adhesion was observed to vitronectin when compared to that in presence of PTX. Further, LD at dose of 8 μ M

showed a slight decrease in migration (approximately 16%). PTX at both the doses impeded migration. In the combination regimen, a similar decrease in migration was observed. The % migration was 41.35%, 31.12%, 101.58%, 84.22%, 39.51, 23.78% for P1, P2, LD1, LD2, C1 and C2 respectively considering the control to be 100% ($P < 0.05$). The effect of PTX, LD and their combinations on activity of gelatinases were studied by performing gelatin zymography. The % MMP-9 activity was 77.60%, 75.12%, 103.51%, 95.1%, 77.08%, 68.94% for P1, P2, LD1, LD2, C1 and C2 respectively considering the control to be 100%.

Combination delays tumour growth using *in vivo* xenograft model

Combination regimen of lipodox and PTX brought about a significant reduction in tumour volume as compared to untreated control using *in vivo* Xenograft model. Tumour volumes were found to be 2429.24 mm³, 1035.53 mm³, 167.9 mm³, 1211.263 mm³, 403.8 mm³ and 327.1 mm³ for untreated, ADR (4 mg/kg), LD (4 mg/kg), PTX (60 mg/kg), PTX+LD (40 mg/kg and 1 mg/kg) and PTX+LD (40 mg/kg and 2 mg/kg) groups respectively.

Discussion

Cancer is manifested as a result of accumulated mutations within the cell and is a leading cause of deaths worldwide. Metastatic breast cancer poses a big challenge to intervene due to limited therapeutic alternatives. Further, failure of a large number of drugs in clinical trials limits the options further. In this regard, therapeutic switching or finding alternatives of known drugs from that are currently in use for other treatments may not only reduce the drug evaluation costs but also provide a better efficacy since pharmacokinetics as well as safety profiles of such drugs are well understood. PTX a well

known methylxanthine derivative, is currently being used in the treatment of peripheral vascular diseases. It is a phosphodiesterase inhibitor that elevates the levels of c-AMP in the cells. It also increases the amount of oxygen reaching the tissues by increasing the flexibility of red blood cells. Thus, it is reported to increase the efficacy of chemotherapy and radiotherapy. Our laboratory has been working extensively to evaluate its metastatic potential against B16F10 melanoma and decipher the mechanism of its mode of action. It had been demonstrated that PTX exerts anti-metastatic effect against melanoma by regulating key processes such as proliferation, migration, invasion and adhesion [14-16, 18]. PTX had been shown to exert anti-metastatic effects on cervical and leukemic cells in combination with other chemotherapeutic drugs [19,20]. However, there are no reports for its efficacy against MDA-MB-231 breast cancer cells. In view of this, we have evaluated its activity against TNBC using MDA-MB-231 as our model system. The anti-proliferative effect of PTX was demonstrated using MTT and clonogenic assays as well as using *in vivo* models. A famous axiom in toxicology by Paracelsus states, 'The dose makes the poison'. In our study, we have therefore evaluated the effects of PTX at sub-toxic doses *i.e.* doses exhibiting a maximal of 30% toxicity. Based on these observations, doses within sub-toxic range were selected *i.e.* 1 mM, 2.5 mM and 5 mM. Further, PTX affected the cellular shape, adhesion to ECM components, invasion, migration and caused apoptosis. The *in vivo* results too complied with the *in vitro* findings. PTX at doses of 40 mg/kg and 60 mg/kg caused a delay in tumour growth, inhibited angiogenesis and affected adhesion of MDA-MB-231 cells to lungs using an experimental metastasis model.

The next step in this regard was to decipher the mechanisms behind these observations. PTX affected adhesion to ECM components viz. matrigel, collagen type IV and laminin. Adhesion to ECM components is chiefly governed by integrins. Thus, effect of PTX was appraised on the integrin expression. A differential effect was observed. PTX affected the surface expression of integrins $\alpha 5$ and $\beta 1$ significantly. Immunofluorescence studies using confocal microscopy also demonstrated reduced fluorescence of integrin $\alpha 5\beta 1$ upon PTX treatment. Integrin $\alpha 5\beta 1$ is a well characterized receptor for fibronectin and had been shown to be highly elevated in breast tumours [23,24]. A decrease in surface expression of both $\alpha 5$ and $\beta 1$ subunits can be plausible explanation for PTX mediated anti-adhesion effects on fibronectin. This was confirmed by western blotting that further showed a dose dependent reduction in total levels of both the integrins. However, for integrins αv , $\alpha 2$, $\alpha 3$, $\beta 3$ and $\beta 5$ no change in surface expression was observed. Although there was a decrease in total protein levels of integrins αv , $\alpha 3$ and $\beta 3$, no change in protein levels was seen for integrins $\alpha 2$ and $\beta 5$. In addition, no change in m-RNA levels was observed upon treatment that confirms that PTX affected the protein machinery. This differential outcome of PTX upon integrin expression might be due to its effect on degradation-synthesis axis for surface receptor modulation or rather integrin transport.

Integrins lack enzymatic activity and thus rely on kinases such as FAK to mediate its downstream effector functions. Thus, effects of PTX on FAK signaling were evaluated as a result of decrease in integrin expression. PTX affected the expression of active FAK and its downstream mediator viz. MAPK and Akt that regulate the processes of cellular proliferation and apoptosis. PTX also disrupted the actin organization by reducing the levels of active Rac and RhoGTPases. It also leads to loss of filopodia and lamellopodia

affecting cellular migration. PTX treatment directed cellular death by altering the levels of Bcl-2, Bcl-xL, caspase-9, caspase-3 and Poly ADP ribose polymerase (PARP). These results thus support the conclusion that PTX induces cell death upon loss of adhesion to ECM components and its allied receptors integrins.

Lastly, we had evaluated the combinatorial effects of PTX and LD both *in vitro* and *in vivo*. The combination regimen showed synergistic activity affecting the processes of cellular proliferation and apoptosis. However, LD did not affect the processes of adhesion, invasion and migration. In the combination scenario, effects on these processes were typically due to presence of PTX *per se*, although, *in vivo* xenograft model showed delayed tumour growth upon treatment with both PTX and LD.

These results highlight the potential of PTX for use as a therapeutic agent in the management of metastatic breast cancer as well as a suitable candidate for developing newer combination regimens at lower concentrations with other known chemotherapeutic drugs.

Conclusion

The present work envisages that PTX inhibits the key metastatic events of MDA-MB-231 human breast cancer cells. It affects cellular processes such as proliferation, adhesion, invasion, migration and apoptosis both as a single agent as well as in combination regimen. Thus, it surely qualifies as a potential anti-metastatic agent for management of metastatic breast cancer.

References

1. R. Siegel, D. Naishadham, and A. Jemal. Cancer statistics, 2013. *CA: a cancer journal for clinicians*. 63:11-30 (2013).
2. J. Ferlay, H.R. Shin, F. Bray, D. Forman, C. Mathers, and D.M. Parkin. Estimates of worldwide burden of cancer in 2008: GLOBOCAN 2008. *International journal of cancer*. 127:2893-2917 (2010).
3. D.X. Nguyen, P.D. Bos, and J. Massague. Metastasis: from dissemination to organ-specific colonization. *Nature Reviews Cancer*. 9:274-284 (2009).
4. D. Bouvard, J. Pouwels, N. De Franceschi, and J. Ivaska. Integrin inactivators: balancing cellular functions in vitro and in vivo. *Nature Reviews Molecular Cell Biology*. 14:432-444 (2013).
5. R. Rathinamand S.K. Alahari. Important role of integrins in the cancer biology. *Cancer and Metastasis Reviews*. 29:223-237 (2010).
6. S. Subbaramand C.M. DiPersio. Integrin $\alpha3\beta1$ as a breast cancer target. *Expert opinion on therapeutic targets*. 15:1197-1210 (2011).
7. J.S. Desgrosellierand D.A. Cheresh. Integrins in cancer: biological implications and therapeutic opportunities. *Nature Reviews Cancer*. 10:9-22 (2010).
8. P.B. dos Santos, J.S. Zanetti, A. Ribeiro-Silva, and E. Beltrao. Beta 1 integrin predicts survival in breast cancer: a clinicopathological and immunohistochemical study. *Diagn Pathol*. 7:104 (2012).
9. V.M. Golubovskaya. Focal adhesion kinase as a cancer therapy target. *Anti-Cancer Agents in Medicinal Chemistry*. 10:735-741 (2010).

10. M. Luo and J.-L. Guan. Focal adhesion kinase: a prominent determinant in breast cancer initiation, progression and metastasis. *Cancer letters*. 289:127-139 (2010).
11. J.T. Parsons, K.H. Martin, J.K. Slack, J.M. Taylor, and S.A. Weed. Focal adhesion kinase: a regulator of focal adhesion dynamics and cell movement. *Oncogene*. 19:5606-5613 (2000).
12. S. Bayraktar and S. Gluck. Molecularly targeted therapies for metastatic triple-negative breast cancer. *Breast cancer research and treatment*:1-15 (2013).
13. J.A. DiMasi, R.W. Hansen, and H.G. Grabowski. The price of innovation: new estimates of drug development costs. *Journal of health economics*. 22:151-185 (2003).
14. P. Dua and R.P. Gude. Antiproliferative and antiproteolytic activity of pentoxifylline in cultures of B16F10 melanoma cells. *Cancer Chemother Pharmacol*. 58:195-202 (2006).
15. P. Dua and R.P. Gude. Pentoxifylline impedes migration in B16F10 melanoma by modulating Rho GTPase activity and actin organisation. *Eur J Cancer*. 44:1587-1595 (2008).
16. P. Dua, A. Ingle, and R.P. Gude. Suramin augments the antitumour and antimetastatic activity of pentoxifylline in B16F10 melanoma. *Int J Cancer*. 121:1600-1608 (2007).
17. L. Hirsh, A. Dantes, B.S. Suh, Y. Yoshida, K. Hosokawa, K. Tajima, F. Kotsuji, O. Merimsky, and A. Amsterdam. Phosphodiesterase inhibitors as anti-cancer drugs. *Biochem Pharmacol*. 68:981-988 (2004).

18. A. Ratheesh, A. Ingle, and R.P. Gude. Pentoxifylline modulates cell surface integrin expression and integrin mediated adhesion of B16F10 cells to extracellular matrix components. *Cancer Biol Ther.* 6:1743-1752 (2007).
19. A. Bravo-Cuellar, P.C. Ortiz-Lazareno, J.M. Lerma-Diaz, J.R. Dominguez-Rodriguez, L.F. Jave-Suarez, A. Aguilar-Lemarroy, S. del Toro-Arreola, R. de Celis-Carrillo, J.E. Sahagun-Flores, J.E. de Alba-Garcia, and G. Hernandez-Flores. Sensitization of cervix cancer cells to Adriamycin by Pentoxifylline induces an increase in apoptosis and decrease senescence. *Mol Cancer.* 9:114 (2010).
20. A. Bravo-Cuellar, G. Hernandez-Flores, J.M. Lerma-Diaz, J.R. Dominguez-Rodriguez, L.F. Jave-Suarez, R. De Celis-Carrillo, A. Aguilar-Lemarroy, P. Gomez-Lomeli, and P.C. Ortiz-Lazareno. Pentoxifylline and the proteasome inhibitor MG132 induce apoptosis in human leukemia U937 cells through a decrease in the expression of Bcl-2 and Bcl-XL and phosphorylation of p65. *J Biomed Sci.* 20:13 (2013).
21. A. Gennari and M. D'Amico. Anthracyclines in the management of metastatic breast cancer: state of the art. *European Journal of Cancer Supplements.* 9:11-15 (2011).
22. G. Minotti, P. Menna, E. Salvatorelli, G. Cairo, and L. Gianni. Anthracyclines: molecular advances and pharmacologic developments in antitumour activity and cardiotoxicity. *Pharmacological reviews.* 56:185-229 (2004).
23. G.E. Morozevich, N.I. Kozlova, I.B. Cheglakov, N.A. Ushakova, M.E. Preobrazhenskaya, and A.E. Berman. Implication of alpha5beta1 integrin in

invasion of drug-resistant MCF-7/ADR breast carcinoma cells: a role for MMP-2 collagenase. *Biochemistry (Mosc)*. 73:791-796 (2008).

24. R. Korah, M. Boots, and R. Wieder. Integrin alpha5beta1 promotes survival of growth-arrested breast cancer cells: an in vitro paradigm for breast cancer dormancy in bone marrow. *Cancer Res*. 64:4514-4522 (2004).

Publications

Published

1. P.N. Goel and R.P. Gude. Unravelling the antimetastatic potential of pentoxifylline, a methylxanthine derivative in human MDA-MB-231 breast cancer cells. *Molecular and cellular biochemistry*. 358:141-151 (2011).
2. P.N. Goel and R.P. Gude. Curbing the focal adhesion kinase and its associated signaling events by pentoxifylline in MDA-MB-231 human breast cancer cells. *Eur J Pharmacol*. 714:432-441 (2013).

Accepted

1. P.N. Goel and R.P. Gude. Pentoxifylline regulates the cellular adhesion and its allied receptors to extracellular matrix components in breast cancer cells. *Biomed Pharmacother*. (2013) doi (10.1016/j.biopha.2013.09.002).
2. P.N. Goel and R.P. Gude. Delineating the anti-metastatic potential of pentoxifylline in combination with liposomal doxorubicin against breast cancer cells. *Biomed Pharmacother*. (2013) doi (10.1016/j.biopha.2013.11.003).

Signature of Student:

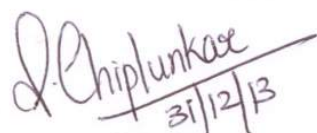


Date: 16.12.2013

Doctoral Committee:

S. No.	Name	Designation	Signature	Date
1	Dr. K.B Sainis	Chairperson		16/12/2013
2	Dr. R.P Gude	Convener		16/12/13
3	Dr. R Mukhopadhyaya	Member		16/12/13
4	Dr. R.D Kalraiya	Member		16/12/13.

Forwarded through,



Dr. S.V. Chiplunkar
 Director, ACTREC
 Chairperson,
 Academic & training Programme, ACTREC

Dr. S. V. Chiplunkar
 Director
 Advanced Centre for Treatment, Research &
 Education in Cancer (ACTREC)
 Tata Memorial Centre
 Kharghar, Navi Mumbai 410210.



Prof. K. Sharma
 Director, Academics
 Tata Memorial Centre



Abbreviations

ABBREVIATIONS

ATP	Adenosine tri phosphate
BSA	Bovine serum albumin
c-AMP	Cyclic adenosine monophosphate
DABCO	1,4-diazabicyclo[2.2.2]octane
DEPC	Diethylpyrocarbonate
DNA	Deoxyribonucleic acid
DMEM	Dulbecco's Modified Eagle's Medium
DMSO	Dimethyl sulphoxide
D/W	Distilled water
ECM	Extracellular matrix
FAK	Focal adhesion kinase
FBS	Fetal bovine serum
gm	Gram
hr	Hour
kDa	Kilo Dalton
LD	Lipodox
mg	Milligram
min	Minute
ml	Millilitre
mM	Milli molar
PBS	Phosphate buffered saline
PTX	Pentoxifylline

RNA	Ribonucleic acid
rpm	Revolutions per minute
SDS	Sodium dodecyl sulphate
V	Volts
μg	Microgram
μM	Micro molar
μl	Microlitre

LIST OF FIGURES

Chapter 1

1.1 Hallmarks of cancer	34
1.2 Different steps involved in metastasis	37
1.3 An overview of cell adhesion molecules	39
1.4 Steps involved in cell migration	43
1.5 Structure of Pentoxifylline	54
1.6 Integrin heterodimers	59
1.7 Integrin Structure	59
1.8 Integrin signaling cascade	61
1.9 Structure of FAK	64

Chapter 4

4.1 PTX affects the proliferation potential of MDA-MB-231 cells	106
4.2 PTX decreases the clonogenic potential	107
4.3 PTX brings an alteration in the cell cycle	109
4.4 EB/AO Staining shows the apoptotic inducing activity of PTX	110
4.5 AnnexinV/FITC staining showing the apoptotic inducing activity of PTX	111
4.6 PTX decreases the adhesion to ECM substrates	113
4.7 Cellular motility impeded by PTX	115
4.8 Gelatin zymography of PTX treated condition media	117
4.9 MDA-MB-231 cells exhibit higher adhesive potential to ECM components than MCF-7 cells	118
4.10 MDA-MB-231 displayed higher surface expression	

of integrins compared to MCF-7 cells	121
4.11 PTX affects surface expression of integrins $\alpha 5$, $\beta 1$ and $\alpha 5\beta 1$ using flow cytometry in MDA-MB-231 cells	125
4.12 Immunofluorescence analysis of PTX treated cells on surface expression of integrin $\alpha 5\beta 1$	129
4.13 Effect of PTX on RNA levels of integrins using RT-PCR	130
4.14 Changes in total protein levels of integrins upon PTX treatment in MDA-MB-231 cells	131
4.15 Dose dependent effects of PTX on FAK pathway and other associated molecules	133
4.16 Increase in activity of cleaved caspase-9 and caspase-3 upon PTX treatment	138
4.17 Decrease in activity of active RhoGTPases upon PTX treatment	140
4.18 Effect of PTX on actin staining in MDA-MB-231 cells	141
4.19 PTX shows a tumour growth delay in xenograft model	143
4.20 PTX affects blood vessel formation in intradermal model of angiogenesis	145
4.21 PTX treatment displayed lessened metastatic potential using <i>in vivo</i> experimental metastasis model	148
4.22 PTX affects blood vessel formation using <i>in ovo</i> CAM assay	149
4.23 Comparison of cytotoxicity for Doxorubicin (DOX) and liposomal doxorubicin (Lipodox or LD)	150
4.24 Effect of combination doses of PTX and LD	152
4.25 Clonogenic assay for the combination	155

4.26 Cell cycle distribution upon combination treatment	157
4.27 EB/AO staining for differentiating live and dead cells upon combination treatment	159
4.28 AnnexinV/FITC staining for apoptotic determination upon combination treatment	160
4.29 Adhesion assay to ECM components upon combination treatment	163
4.30 Gelatin zymography using condition media upon combination treatment	163
4.31 Changes in cellular motility upon combination treatment	165
4.32 <i>In vivo</i> xenograft model upon combination treatment	167

LIST OF TABLES

4.1 Tabulation of different cell cycle phases upon PTX treatment	110
4.2. Combination index (CI) values for actual experimental points	154
4.3. Data for $F_a=0.5$ i.e. Effect at 50% inhibition	154
4.4. Tabulation for cell cycle analysis using flow cytometry upon combination treatment	158

Chapter 1
Review of Literature

1.1 Cancer: a brief history and its outcome

The inception of the word cancer meaning “crab” like is attributed to the Greek physician Hippocrates (460-370 B.C) also referred to as the “Father of medicine”. However, the oldest description of cancer dates back to its discovery by the Egyptians in 1600 B.C. Cancer in the current scenario tends to be one of the most leading causes of worldwide deaths [1]. It is rather a syndrome characterized by uncontrolled proliferation and the spread of abnormal cells. As per the latest global statistics an estimated 12.7 million cancer cases around the world (6.6 million cases in men and 6.0 million in women) were reported by International agency for research on cancer (IARC), WHO. This number is anticipated to rise towards 21 million by the year 2030 [2]. Breast cancer is the second most common cancer with nearly 1.38 million cases [3].

The 10 major hallmarks of cancer are sustained proliferation, self sustenance by evading growth suppressors, resistance to apoptosis, replicating immortality, activating invasion and metastasis, angiogenesis, deregulated cellular energetics, immune evasion, genomic instability and tumor promoting inflammation [4,5] being represented in Figure 1.1.

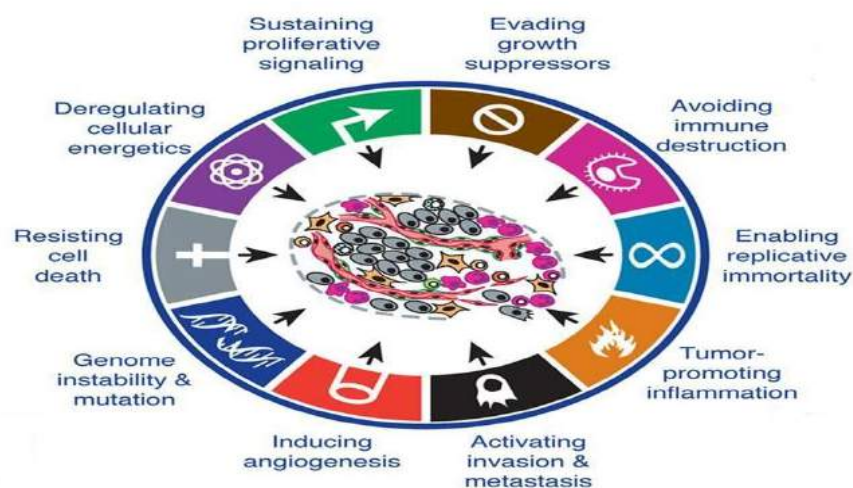


Figure 1.1: Hallmarks of cancer. Adapted from [5].

Several mutations are necessitated by a cell to transform and eventually proliferate forming a primary tumour. This primary tumour when localized or confined at a particular site can easily be treated by surgically removing the same. However, most cancer related deaths are not caused by this primary mass but due to disseminated tumour cells from these primary tumours at distant sites via the bloodstream. This process is referred to as metastasis and is the prime cause of cancer deaths [5-7].

1.2 Metastasis

Metastasis is both a process and outcome of the process. However, only small subpopulations of a mostly heterogenic tumour harbor metastatic capability [8]. Accumulating mutations leads to cellular transformation. This eventually leads to carcinoma in situ. Cancer cells then need to loosen the contacts with the neighboring cells as well as with the underlying matrix evolving towards the invasive carcinoma stage. These are characterized by deregulated adhesion, enabling them to detach from the primary mass and then re-adhere at target organ(s) distant from the primary tumour. During the process of invasion cancer cells secrete enzymes such as the matrix metalloproteinases (MMPs) that degrades the extracellular matrix (ECM). Cells then migrate and intravasate into the blood vessels and are carried to distant target sites [7-10]. Cancer cells can disseminate from the primary tumour via lymphatic or haematogenous routes. They can form solid metastases in the lymph nodes and subsequently can disseminate from the established lymph node metastases to distant sites, where they form distant metastases. This ability might be gained during the progression in the lymph node environment. Haematogenous dissemination can occur from the primary tumour, lymph node metastases or distant metastases. Metastatic cells evade immune cell killing and

processes resistance to anoikis, the programmed cell death induced by loss of cell matrix interaction. Finally, metastatic cells are able to modulate the secondary site (e.g. reorganization of the ECM) and proliferate with the aid of cues from the microenvironment.

There are at least five major prerequisite for a tumour cell to successfully complete the sequence of events outlined above. These include interaction with the local microenvironment, migration, invasion, resistance to apoptosis and the ability to induce angiogenesis. All these functions are regulated by the processes of adhesion and proteolysis, which together provide the most fundamental molecular effectors mechanisms upon which a metastatic cell relies [9]. Adhesion and proteolysis determine tumour cell interaction with other cells and with the ECM, help create a path for migration, promote angiogenesis, and both directly or indirectly trigger survival signals. In light of these facts, the metastatic process is indeed a very complex phenomenon. The various steps involved in the process of metastasis are outlined in Figure 1.2.

However, it may be noted that these cancer cells may end up in a dormancy phase, where in the cells neither die nor proliferate. Thus, not all the primary tumours are able to metastasize and this makes the process of metastasis rather inefficient [10].

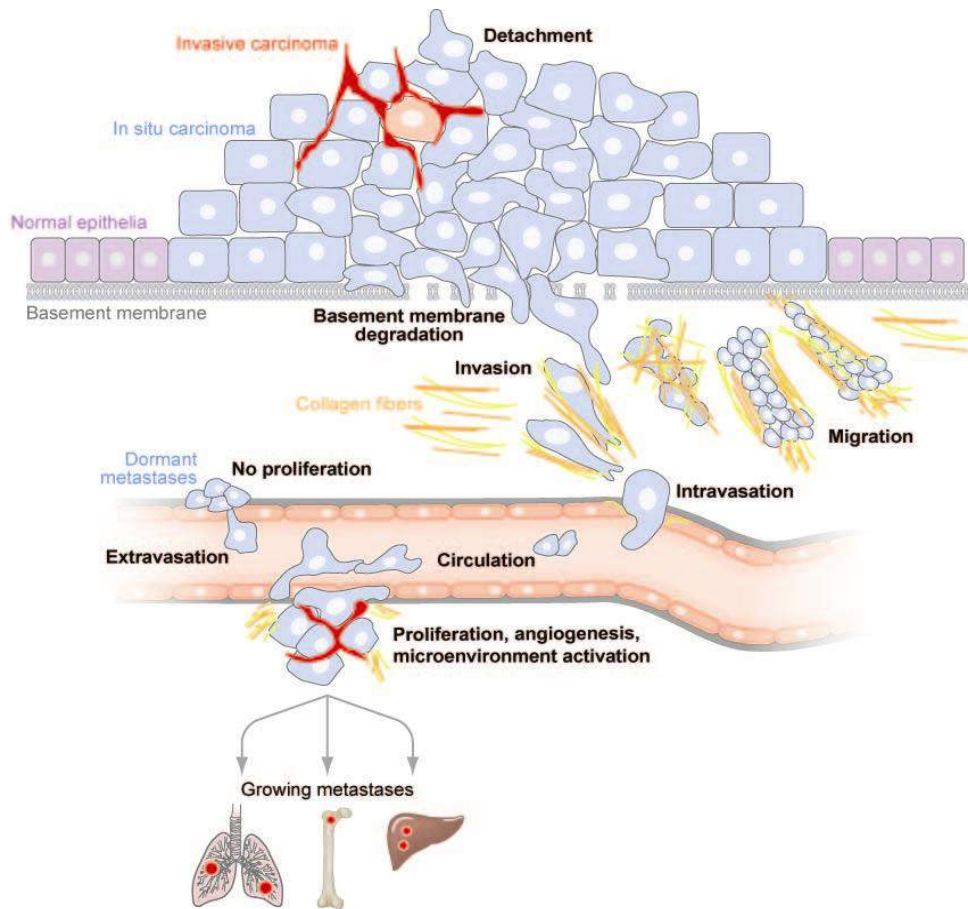


Figure 1.2: Different steps involved in metastasis. Adapted from [9].

1.3 Processes involved in metastasis

1.3.1 Adhesion

Cells that need to metastasize must detach from their primary site by modifying the expression and localization of cell surface molecules responsible for their attachment to the primary tumour. This process is associated with the down-regulation of intercellular adhesion [11,12]. Though, adhesion mechanisms must be disrupted for tumour cells to become motile, the reattachment of the malignant cells to metastatic sites requires an increase in cellular adhesive capacity [13]. This concept of “disordered adhesion” was first put forward in 1944 when Coman recognized that

adhesion between malignant cells must be down-regulated as a prerequisite for invasive behavior [14]. Since then our knowledge of the molecular basis for these alterations in adhesive capacity has increased considerably and now it is well recognized that cell-cell and cell-substratum adhesion mediated by specific cell surface molecules, play a critical role in tumour cell metastasis. The different cell adhesion molecules are highlighted in Figure 1.3.

Adhesion molecules fall into one of four key groups: integrins, cadherins, selectins, and members of the immunoglobulin superfamily. While integrins mediate cell-ECM interactions, cadherins mediate intercellular interactions. Selectins play a part in endothelial cell adhesion, whereas members of the immunoglobulin superfamily share a diversity of expression on cells of the immune system, neuronal tissue, as well as cells of the epithelial origin such as colonocytes. There is now ample experimental evidence for adhesion mechanisms, in particular these molecules, in the development of metastasis [15-17].

The loss of intercellular cohesion in the primary tumour results in detachment and release of certain cells. This loss of cohesion is aided by a decreased expression of homotypic cell adhesion molecules (CAMs), specifically the cadherins, in these metastatic cells. Cadherins are glycoproteins and are of numerous types, among which E-cadherins are most extensively studied in reference to cancer biology. Analysis of a variety of epithelial carcinoma cell lines revealed that E-cadherin expression is correlated inversely with invasive potential [18,19] and is a common feature of several epithelial malignancies.

	SOME FAMILY MEMBERS	Ca ²⁺ OR Mg ²⁺ DEPENDENCE	HOMOPHILIC OR HETEROPHILIC	CYTOSKELETON ASSOCIATIONS	CELL JUNCTION ASSOCIATIONS
<i>Cell-Cell Adhesion</i>					
Classical cadherins	E, N, P, VE	yes	homophilic	actin filaments (via catenins)	adherens junctions
Desmosomal cadherins	desmoglein	yes	homophilic	intermediate filaments (via desmoplakin, plakoglobin, and other proteins)	desmosomes
Ig family members	N-CAM	no	both	unknown	no
Selectins (blood cells and endothelial cells only)	L-, E-, and P-selectins	yes	heterophilic	actin filaments	no
Integrins on blood cells	$\alpha_1\beta_2$ (LFA-1)	yes	heterophilic	actin filaments	no
<i>Cell-Matrix Adhesion</i>					
Integrins	many types	yes	heterophilic	actin filaments (via talin, filamin, α -actinin, and vinculin)	focal adhesions
	$\alpha_6\beta_4$	yes	heterophilic	intermediate filaments (via plectin)	hemidesmosomes
Transmembrane proteoglycans	syndecans	no	heterophilic	actin filaments	no

Figure 1.3: An overview of cell adhesion molecules. Adapted from [17].

Along with the cell-cell communication, interactions between tumour cells and the ECM occur during the initial invasive action of metastatic cells and following their extravasation.

These interactions are mediated chiefly by the integrins that are transmembrane receptors which bind to a variety of ECM molecules including laminin, fibronectin, vitronectin, and collagens. The integrin repertoire on normal epithelium and

malignancies has been determined on carcinomas of the colon, pancreas, kidney, breast, lung, prostate and skin [20-26].

A number of cell adhesion molecules have been shown to have one or more Ig-like domains and are thus classified as members of the immunoglobulin superfamily. These receptors mediate both homophilic and heterophilic adhesion involving a variety of ligands. A number of pro-inflammatory cytokines which induce the expression of several of these receptors include ICAM-1, ICAM-2, PECAM, and V-CAM on the endothelial cell wall. Several of these receptors have been shown to bind to integrins [27] and thus may serve as a mechanism to induce adhesion of tumour cells to the endothelium. Members of selectin superfamily are also over expressed under conditions of inflammation and these may serve a role in tumour metastasis. Increased expression of Sialyl Le^x has been found to correlate with the metastatic potential [28]. Several other CAMs including CD-44 have been found to be implicated in metastatic progression [29].

Thus, in all the engagement of adhesion receptors triggers assembly of functional matrix contacts, in which bound matrix components, adhesion receptors and associated intracellular cytoskeletal and signaling molecules form large, localized multiprotein complexes [30]. The malignant progression of cancer cells involves down-regulation of ECM, alterations in the profile and expression levels of integrins and proteoglycans, decreased focal adhesions in culture and a switch to a more migratory phenotype associated with invasive and metastatic behavior [31].

1.3.2 Invasion

The engagement of integrins and other attachment molecules is accompanied by the recruitment of proteases to degrade the ECM, providing a pathway for invasion. The

term invasiveness describes the ability of cells to cross anatomic barriers, e.g., basement membranes, interstitial stroma, and intercellular junctions that separate tissue compartments. A common feature of invasion processes is the degradation of ECM, using specific enzymes, which is required for invasive cells to migrate into adjacent tissues. Extensive work on the mechanisms of tumour invasion and metastasis has identified MMPs as key players in the events that underlie tumour dissemination [32-34]. The MMPs are a family of zinc dependent endopeptidases. Their primary function is degradation of proteins in the ECM. Currently, at least 19 members of this family are known to exist [32]. Recent data from model systems suggest that MMPs are involved in breast cancer initiation, invasion and metastasis. Consistent with their role in breast cancer progression, high levels of a few MMPs have been found to correlate with poor prognosis in patients with breast cancer [33]. Because MMPs are apparently involved in breast cancer initiation and dissemination, inhibition of these proteinases may be of value both in preventing breast cancer and in blocking metastasis of established tumours [35].

1.3.3 Migration

The next important step in the process of metastasis is cellular migration. It is a multistep process involving changes in the cytoskeleton, cell-substrate adhesions, and the ECM, which is initiated upon the reception of cues from the extracellular milieu. Migration requires that cells must acquire a spatial asymmetry enabling them to turn forces generated intracellularly into cell body translocation [36-39].

A family of GTPases named RhoGTPases had been found to be critical for cell migration. Of the nearly 20 Rho family members found in humans, Rho A/B, Rac 1/2 and

cdc-42 have been shown to have important roles in cell migration. Rho proteins generally cycle between an active, GTP-bound, conformation and an inactive GDP bound conformation. In the active form, they interact with downstream target proteins to induce cellular responses. Rho proteins can exchange nucleotide and hydrolyze GTP at slow rates in vitro, and these reactions are catalyzed by guanine nucleotide-exchange factors (GEFs) and GTPase-activating proteins (GAPs), respectively. Rho proteins can also bind to proteins known as GDIs (guanine-nucleotide dissociation inhibitors), which prevent their interaction with the plasma membrane but not necessarily with downstream targets [40-42].

The process of cell migration is divided into four mechanistically separate steps: lamellipodium extension, formation and stabilization of new adhesions, cell body contraction, and rear release. The process is highlighted in Figure 1.4.

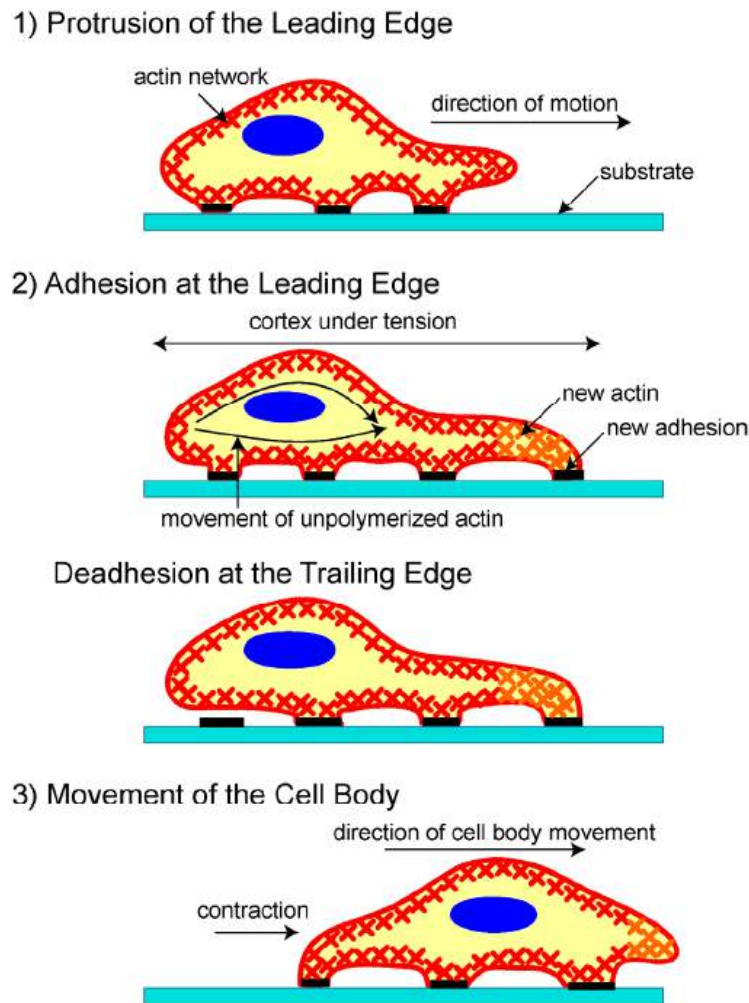


Figure 1.4: Steps involved in cell migration. Adapted from [43].

1.3.3.1 Lamellipodium extension

Lamellipodia are flat foot like projections whereas filopodia are thin needle like projections. These projections do not usually contain any cytoplasmic organelles and is rich in branching filament networks made of actin. On response to migratory stimuli, cells put out lamellipodia and this is coupled with local actin polymerization understood to be through the actin nucleating complex Arp2/3 [44]. An increase in the sites of actin polymerization marks the first step of lamellipodial formations followed by fast polymerization. During actin polymerization, the G-actin monomers are added to

preexisting F-actin filaments. New sites for actin polymerization may occur because of a number of mechanisms including uncapping or severing of already existing actin filaments as well as de novo formation of actin nucleation sites. When a cell moves, during the initial formation of lamellipodia, protrusive forces are required which are normally provided by actin polymerization and organization. It has been suggested that at the leading edge of migrating cells, integrins bind the ECM, recruit the actin cytoskeleton, and initiate local reorganization of the actin network, promoting different types of membrane protrusion. Rac activity has been shown to be important for lamellipodial formation induced by most extracellular cues including growth factor [45] and cytokine activation [46]. Rac activation by both tyrosine kinases and G-protein-coupled receptors is often dependent on phosphoinositide 3-kinase (PI3K) activity [47] and inhibitors of PI3K block Rac activation [48].

1.3.3.2 Formation and stabilization of new adhesions

When lamellipodia are formed at the leading edges of the cell, nascent adhesion contacts also seem to form. These adhesion sites form as small aggregates that become larger during cell migration. Cell adhesion to the ECM itself activates Rac and Cdc42 where Rac is required for focal adhesion complex assembly [45,46]. Since these complexes require a fine cytoskeletal structure, molecules that initiate nucleation might be present in these complexes. While this possibility has not found solid evidence so far, data suggests the existence of a preformed cytoskeletal complex into which the adhesion molecules are incorporated. As the cell migrates, membrane proteins such as integrins move rapidly to the cell periphery and focal adhesion turnover is essential during this

process. Too strong an attachment to the substratum will inhibit cell migration. Regulated receptor trafficking must be essential to replenish these proteins at the leading edge.

1.3.3.3 Cell body contraction

After the formation of stable adhesions, the cell needs to move forward and this is accomplished by the use of contractile forces that push the cell forward. The cell exerts traction on the substratum, which is directly related to the intracellular generated force. The substratum in turn exerts a force on the cell and the ratio of contractile force to cell-substratum adhesion strength has been speculated to determine the rate of locomotion [49]. Cell body contraction is dependent on actomyosin contractility [50] and can be regulated by Rho. Macrophages upon inhibition of Rho continue to extend processes without significant movement of the cell body. Rho acts via ROCKs (also known as Rho-kinases) to affect Myosin light chain (MLC) phosphorylation both by inhibiting MLC phosphatase and by phosphorylating MLC [51,52]. The effect of inhibiting Rho on cell migration rate depends on the cell type and in cells that have stress fibres, the high level of substrate adhesion through stress fibre-associated focal adhesions inhibits cell migration. Thus, Rho can act here in two ways- it promotes migration by lowering adhesion, but decreases cell migration by inhibiting cell body contraction. In less adherent cells that lack focal adhesions, such as macrophages, neutrophils and various cancer cell lines, Rho does not affect adhesion but induces cell body contraction [45,53].

1.3.3.4 Rear release

Rates of lamellipodial protrusion and rear release both normally contribute towards the rates of migration, but in some cells, the rate of rear release determines the rate of

migration [54]. This step is normally considered as the rate-limiting step in cell migration [55]. Integrins play a very important role in rear release. In some cells such as fibroblasts, when the cell migrates a fraction of the integrins are left behind on the substratum in a process called membrane ripping [54]. Integrins remaining on the cell surface can undergo two fates: they redistribute on the cell surface and undergo endocytosis into vesicles that accumulate on the cell body [56]. At the rear of the cell, these aggregates normally tend to release. There they disperse and are either used for new adhesions in the cell front or move along the cell edges and form a new aggregate. This suggests a mechanism by which integrins are replenished during cell migration. RhoGTPases are involved in cell rear release. Rho inactivation causes cytoskeletal breakdown, cell rounding, and inhibits migration [57]. In slowly moving cells, tail detachment appears to depend on the action of the protease calpain, which degrades focal adhesion components at the rear of cells [55,58]. The mechanisms that move integrins from the trailing edge toward the advancing lamellipodium are likely to be the key for the speed and directionality of cell migration. However, the precise way in which integrin vesicular transport acts to drive the heterodimers toward the advancing lamellipodium is not yet clear.

1.3.4 Transport, arrest and extravasation

The ability of a cancer cell to undergo migration and invasion allows it to change position within the tissues. These processes allow neoplastic cells to enter lymphatic and blood vessels for dissemination into the circulation, and then undergo metastatic growth in distant organs [59]. The cancer cell, having entered the blood or lymph system, then has to survive in the circulation and is transported to distant sites in the

body. During this time, the vast majority of cancer cells will be torn to shreds in the circulation or will die entrapped in a vessel, but a few will have productive interactions with blood cells and platelets [59-61]. The actin cytoskeleton likely plays a role in protecting cancer cells from destruction and promoting junction formation with various types of blood cells. These heterotypic cell interactions likely have important signaling and survival roles, as well as offering physical strength and protection from immune surveillance [62]. The next step for a few cancer cells is extravasation, which is escape from the vasculature. This process requires adherence to the endothelium and passage through the basement membrane into the new tissue to establish growth as a metastasis. The cancer cell uses its actin cytoskeleton to orchestrate protrusive migration and to burrow through the ECM to establish a new tumour site [63].

1.3.5 Angiogenesis

The establishment of a new tumour site requires the commencement of another important process in metastasis, angiogenesis. It is the formation of new blood vessels from existing vasculature. It is a multi-step process that includes endothelial cell (EC) proliferation, migration, basement membrane degradation, and new lumen organization. Within a given microenvironment, the angiogenic response is determined by a net balance between pro and anti-angiogenic regulators released from activated ECs, monocytes, smooth muscle cells and platelets [64]. In addition to the genetic and epigenetic changes that occur during transformation, angiogenesis is required to allow tumour propagation, progression and metastasis. Like normal tissues, tumours require an adequate supply of oxygen, metabolites and an effective way to remove waste

products [65]. Gaining access to the host vascular system and the generation of a tumour blood supply are rate-limiting steps in tumour progression. Angiogenesis is a crucial feature of solid tumour biology and anti-angiogenic therapies have become a major strategy for cancer treatment [66].

1.4 Breast cancer

1.4.1 Incidence and risk factors

Breast cancer is the second most common cancer among women. Despite earlier detection of the disease and improved anti-cancer therapies, it is still the second leading cause of cancer related deaths among women [2,3]. Like many diseases, there are multiple risk factors for the development of breast cancer. Among lifestyle related factors are alcohol, obesity and oral contraceptives. In contrast to other cancers, such as lung cancer, in which there is a very strong correlation between the occurrence of the disease and smoking, with breast cancer the non-lifestyle risk factors are far more important. These include aging and genetic predisposition, but the most important risk factor, increasing the chance 100 times, is being a woman. This is not because women have more breast tissue, but because female breast cells are continuously exposed to high concentrations of the female hormones estrogen and progesterone, providing growth-promoting effects [67-70].

1.4.2 Development of breast cancer

Hallmark of cancer is the uncontrolled proliferation of cells. Cancer cells, unlike normal cells, ignore signals to specialize, stop dividing and die [4,5]. The disturbed life cycle of cancer cells is caused by one or multiple mutations, either somatic or germline (inherited), in the DNA of the cells. Somatic mutations, occur during the life-span of a

cell and can be caused by exogenous stimuli e.g. chemicals and UV radiation. These mutations may be rapidly repaired by the cell its gene-repair mechanisms, or may be reason for the cell to commit suicide (undergo apoptosis) or to be killed by cells of the immune system. Thereby, growth of cells with mutated DNA is prevented. However, when mutated cells escape these repair/killing routes, uncontrolled division can take place and a tumour is formed. About 5 to 10% of all breast tumours are hereditary as a result of mutations in the DNA. Inherited mutations of genes that increase the risk of breast cancer include BRCA1, BRCA2, p53, ATM and PTEN [71-73]. Only cells that obtain multiple mutations (somatic, germline or a combination of both) are thought to be able to eventually form tumours.

1.4.3 Treatment scenario

1.4.3.1 Surgery

The most effective way to treat breast cancer is surgical removal of the tumour. The stage of the disease determines whether the surrounding tissue, the whole breast or the lymph nodes should be removed in addition to the primary tumour. Importantly, all individual tumour cells have to be removed to prevent outgrowth of residual cells into new tumours. Therefore, surgery is almost never the sole therapy in (breast) cancer [74,75].

1.4.3.2 Hormonal therapy

As mentioned previously, the continuous exposure of the female breast cells to the hormone estrogen is a high risk factor for the development of breast cancer. Majority of all breast cancers are positive for the estrogen receptor. In these cells, binding of estrogen to the estrogen receptor provides proliferation signals and therefore the uncontrolled division of these cells is (at least partly) dependent on estrogen [76]. Hormonal therapy of

estrogen-positive breast cancer consists of blocking these receptors, without activating them, thereby inhibiting the division of the cancer cells. The most well known anti-estrogen drug used in breast cancer therapy is tamoxifen [76-78].

1.4.3.3 Radiation therapy and chemotherapy

A third method that is often used to treat breast cancer is the induction of cell cycle arrest and/or apoptosis in cancer cells by either irradiation or chemotherapy. During radiation therapy, ionizing radiation is applied locally at the site of the tumour [79-81], while chemotherapy is administered systemically. Chemotherapeutic drugs (or cytostatics) act primarily on dividing cells and therefore, in addition to the dividing cancer cells, cells of the digestive tracts, hair follicles and cells of the immune system are also affected [82,83]. This results in classic side-effects like nausea, hair loss and increased vulnerability towards pathogens. Chemotherapeutic drugs can be divided into several groups on how they act on the cancer cells that includes alkylating agents, anthracyclines, topoisomerase inhibitors and mitotic inhibitors [84,85]. Alkylating agents bind directly to DNA and thereby prevent the cancer cell from reproducing [84,86]. Anthracyclines interfere with enzymes involved in DNA replication and also work in all phases of the cell cycle. A major concern is the effect they can have on heart muscle cells. Examples include daunorubicin and doxorubicin (Adriamycin) [87]. Topoisomerase inhibitors interfere with enzymes called topoisomerases, which are important in DNA replication [88]. Finally, mitotic inhibitors are plant alkaloids and other compounds derived from natural products. They can stop mitosis or inhibit enzymes from making proteins needed for reproduction of the cell. These drugs act during the M phase of the cell cycle. Examples include the taxanes (paclitaxel, docetaxel) and the vinca alkaloids (vinblastine,

vincristine, and vinorelbine) [84,89]. Due to the upregulation or constitutive activation of certain protein pathways that are protective against apoptosis are activated. This can result in the reduced efficacy of the chemotherapeutic agents.

In addition Herceptin, inhibitors of the EGFR (Iressa) and c-KIT (Imatinib) are already used as anti-cancer drugs, whereas several other tyrosine kinase inhibitors are currently under investigation for their use as anti-cancer drug. These new drugs have been (or are) developed because of the improved insights into the development and progression of breast cancer [90-92].

Thus, unravelling the mechanisms of metastasis will surely provide additional useful targets to combat the lethal metastases leading to the development of newer or improvements in the current breast cancer treatment.

1.4.4 Triple negative breast cancers (TNBC)

The term TNBC is used to describe a subtype of breast cancer that lacks expression of the estrogen receptor (ER), progesterone receptor (PR) and does not over-express human epidermal growth factor 2 receptor (HER2) protein. These are biologically aggressive in nature and respond to chemotherapy much better than other types of breast cancer. TNBC are classified under the basal type subclass of tumours [93-95]. It is an important area of research for both researchers and clinicians alike because it (1) is a poor prognostic factor for disease-free and overall survival, (2) no effective specific targeted therapy is readily available for TNBC. Thus, conventional chemotherapy is the only effective systemic treatment [96]. Moreover, there had been fewer advances in the treatment of TNBC compared with other subtypes. For these reasons, new research initiatives for TNBC are critical.

1.5 Therapeutic implications

Advances in the successful treatment of cancer by existing approaches such as surgery, radiotherapy and chemotherapy remains limited because of the presence of metastatic disease. Thus, treatments targeting cancer metastasis are extremely attractive. In theory, inhibition of any of the steps in the metastatic process, from the initial release of cells in the circulation at the primary tumour, to the final stages of growth in the new organ, could offer therapeutic targets.

In the past two decades many potential therapeutic molecules have been identified. Major being MMPs, uPA, integrins, growth factors like VEGF, EGF and kinases. Many synthetic and natural compounds, monoclonal antibodies, peptides have been generated against these potential targets, some of which are in clinical trials and still more are undergoing preclinical research. In the drug discovery research, a very viable and promising approach is to investigate anti-cancerous and anti-metastatic activity of the drugs that had already been demonstrated to treat other diseases. This process is referred to as drug repositioning and has gained a wide acceptance providing success to various pharma companies [97-99]. Aspirin, a non-steroidal anti-inflammatory drug has been shown to inhibit metastasis [100]. Artemisin an antimalarial compound has been recently shown to have anticancerous properties [101]. Silybin and silymarin compounds used so far as hepatoprotectants are also pro-apoptotic and anti-angiogenic in nature [102]. Thalidomide, the antiemetic drug for pregnancy, has come through a long way, as an anti-angiogenic agent and is in clinical trials for the same [103].

Data from numerous studies have shown that massive changes, some which are transient and some which are retained over long periods, occur in the tumour cells, host

cells and tumour cell- host cell interactions during metastatic cascade. Hence, it is obvious that targeting any one or more of the events in the metastatic cascade would provide viable therapeutic strategies, which can be translated into clinical benefits. Therefore, over the last couple of decades, a lot of importance has been placed on developing drugs or therapeutic strategies, which can target one or more steps in the metastatic cascade. Studies in our lab have concentrated on the potential of several methylxanthine derivatives to act as anti-metastatic agents [104-108].

A xanthine is a purine base that can be found in a majority of body tissue and fluid. It can also be found in some plants which are used for medicinal purposes. Methylxanthine is a methylated derivative of xanthine. Three important classes of methylxanthines are caffeine, theobromine and theophylline. These inhibit phosphodiesterase and antagonize adenosine thus elevating c-AMP levels in the cells. The first report suggesting role of c-AMP in cell growth came way back in the year 1968 in which HeLa cells used in this study were all inhibited by 3', 5'-AMP (c-AMP) whereas, the non-malignant strain was almost unaffected by the presence of c-AMP [109]. The greater sensitivity of the malignant cells to c-AMP may result from a variety of causes e.g. lower levels of phosphodiesterase, the enzyme that hydrolyzes c-AMP, or higher levels of adenyl cyclase enzyme that converts ATP to c-AMP. Since then c-AMP elevating agents like c-AMP analogues, methylxanthines [110-113], prostaglandins [114,115], histamines, catecholamines [116] have been studied as therapeutic agents for various cancers.

Caffeine, Theophylline, iso-butylmethylxanthine (IBMX) and Pentoxifylline (PTX) have shown anti-cancerous and anti-metastatic effects in melanoma and some other

cancers using *in vitro* and *in vivo* assays [117-123]. They have also been in clinical trials in combination with some anti-cancerous compounds where they had been used as sensitizers for radiotherapy and chemotherapy [105,119,122, 124-129].

1.6 Pentoxifylline

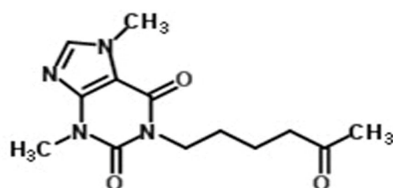


Figure 1.5: Structure of Pentoxifylline.

Pentoxifylline ([1-(5-oxohexyl)-3,7-dimethyl-xanthine], oxpentifylline, PTX) represented in Figure 1.5 is a theobromine derivative used in treatment of peripheral vascular diseases. PTX was developed by Hoechst Aktiengesellschaft in the seventies. It is a phosphodiesterase inhibitor and used for the treatment of intermittent claudication on the basis of chronic occlusive arterial disease of the limbs [130,131]. Studies have shown that pentoxifylline improves peripheral blood flow [132]. The mechanisms for this are several. Blood flow in the capillaries and blood viscosity are influenced by red cell deformability and aggregation, haematocrit, and plasma viscosity. PTX significantly reduced whole blood viscosity in patients with peripheral arterial disorders, significantly increased red cell deformability in healthy subjects and patients with peripheral vascular disease [133,134]. It decreased platelet adhesion and aggregation to vessel walls in patients with peripheral vascular disorder and decreased fibrinogen levels. In blood from healthy volunteers PTX increased the filterability of monocytes and polymorphonuclear leucocytes [134]. After incubation with PTX both mononuclear and polynuclear cells

increase intracellular c-AMP levels through inhibition of phosphodiesterase [135]. Increased c-AMP contents of platelets interfere with platelet aggregation and leads to inhibition of cyclooxygenase [136]. Further, elevated intracellular c-AMP levels inhibit cytokine production through inhibition of activation of monocytes and lymphocytes. The exact mechanism of how PTX alters red blood cell physiology is not entirely understood but might be a reduction of intracellular calcium due to inhibition of calcium influx. It is known that older erythrocytes accumulate more Ca^{2+} and are less deformable. Transglutaminase is a Ca^{2+} dependent enzyme that irreversibly cross links membrane proteins, and thereby rigidifies the erythrocytes. PTX can reduce intracellular Ca^{2+} and inhibited activation of Ca^{2+} dependent transglutaminases [137,138]. This enables the erythrocytes to remain deformable and makes it easier for them to pass through the capillaries. However, exactly how PTX alters red blood cells is not completely understood. Another study showed that PTX improved whole blood filterability in healthy volunteers, but the investigators did not find any increased red cell deformability [139].

Seven phase 1 metabolites (denoted M1-M7) were identified in human urine during the study of PTX biotransformation [140]. The structures of the metabolites were determined: the biotransformation yielded three hydroxy metabolites (M1, M2, M3a, and M3b), two carboxy metabolites (M4, M5) and two de-methylated metabolites (M6, M7). The major metabolite excreted in urine is M5 followed by M4. The excretion of unchanged PTX and M1 each accounts for less than 1% of the dose [140]. When PTX is administered to healthy humans the areas under the plasma concentration curves (AUC) for M5 and M1, but not M4 are larger than PTX [141-143]. It is eliminated from the

circulation with a short mean elimination half-life of about 0.9 hr after oral and about 1 hr to 2 hr after intravenous (IV) administration [141,144]. A sustained release 400 mg tablet is currently available commercially, which allows a patient to reduce dosing frequency while maintaining the therapeutic plasma concentrations.

Besides being a hemorreological agent, PTX have been shown to have therapeutic effects in various other diseases and cellular processes. These include liver degeneration [145,146], sperm motility [147], oxidative stress, chronic inflammatory diseases, muscular dystrophy [148], renal failure, HIV infection [149] and cancer [121-124]. The therapeutic effects of PTX have been mainly attributed to its property to elevate c-AMP levels and affect associated genes. However, some of these effects have been found to be independent of c-AMP signaling and show involvement of other pathways.

PTX inhibits IEC-18 intestinal epithelial cell proliferation via a differential modulation of TGF- α and TGF- β 2 expression [150]. It inhibits PDGF induced PI3K pathway which further inhibits AKT activation in smooth muscle cells [151]. In mesengial cells this effect has been shown due to elevation of PKA activity [152]. Tissue factor (TF), the membrane glycoprotein that initiates blood coagulation, is constitutively expressed by many tumour cells and is implicated in peri-tumour fibrin deposition and hyper-coagulability in cancer [153]. Upregulation of tumour TF correlated with enhanced metastatic potential [154]. Furthermore, TF has been co-localized with VEGF in breast cancer, especially at sites of early angiogenesis [155]. PTX inhibited TF expression and VEGF release under hypoxic as well as normal conditions in A375 melanoma, MCF-7 breast carcinoma and A549 lung carcinoma

[156]. It has also been shown to affect PDGF induced ERK and MAPK activities [157].

As an anti-cancer agent, PTX has been used to enhance tumour sensitivity to both radiation and chemotherapeutic agents [124-126, 158,159]. PTX induces tumour perfusion therefore better oxygenation. This enhances radiosensitivity as well as facilitates delivery of anti-cancerous drugs. The drug also interferes with cytokine-mediated inflammatory reactions, which occur in the acute phase after irradiation, thus reducing the side effects post-radiation exposure. Further, it abrogates G2M phase block created by treatment with cytotoxic agents and radiations leading to increased apoptosis. PTX had been reported to increase radiosensitivity in chronically hypoxic WiDr tumours [160,161], head and neck cancer [158,162] and hepatoma cell lines [163,164]. It augments the effect of alkylating agents on FSaIIc fibrosarcoma and mammary adenocarcinoma both *in vitro* as well as *in vivo* [165]. It showed synergistic combination with adozelesin in Chinese hamster ovary cells [166]. PTX decreased spontaneous metastases in a Wilms' tumour model in Furth-Wistar rats and in neuroblastoma C1300 in A/J mice. It inhibited metastasis of DEN induced hepatocellular carcinomas to lung [167]. However, it was ineffective in the NIH renal adenocarcinoma in BALB/c mice [168] and promoted the development of murine colon adenocarcinoma derived metastatic tumours in liver [169]. This differential effect of PTX on metastasis is said to be dependent on tissue type and drug exposure.

Further, there are recent reports of its usage in variety of other cancers such as cervix, leukemia in combination with anti-cancer drugs [124-126]. However, no reports regarding its anti-metastatic activity against breast cancer cells have been reported.

Our lab had been working with the effects of methylxanthine derivatives on tumour metastasis. PTX was shown to inhibit hematopoietic stem cell homing [170] and inhibited the lung homing of B16F10 melanoma cells in an experimental metastasis model system [171]. Further studies on PTX showed that this drug could also inhibit proliferation of endothelial cells and tumour induced angiogenesis [172]. Studies on the mechanism of action of PTX suggested that the effects of this methylxanthine derivative are probably mediated at least in part through its effects on cell adhesion and adhesion receptors. It was found to inhibit the adhesion of tumour cells to reconstituted basement membrane and type IV collagen [173]. The inhibition of adhesion of B16F10 melanoma cells to ECM components suggested that PTX might have an effect on cell surface receptors that mediate cell adhesion to ECM i.e. integrins. PTX was also shown to inhibit the integrin-mediated adherence of IL-2 activated human peripheral blood lymphocytes to human endothelial cells, matrix components and cultured tumour cells [174]. It also inhibited the integrin mediated adhesion and activation of human T lymphocytes [175]. Further, studies from our lab had demonstrated that PTX affects the integrin expression in B16F10 cells [106].

Thus, it shall be important to elucidate its role in regulating the integrin levels in breast cancer cells along with its mechanism of action.

1.7 Integrins

Integrins are heterodimeric cell surface receptors composed of a variable α subunit of 150-170 kDa and a conserved 95 kDa β -subunit. There are 18 known α and 8 β subunits that can combine to form at least 24 $\alpha\beta$ heterodimers as shown in Figure 1.6 [176].

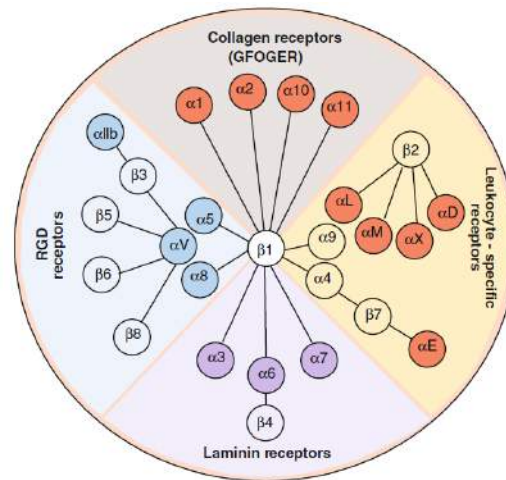


Figure 1.6: Integrin heterodimers. Adapted from [176].

These contain a large extracellular domain responsible for ligand binding, a single transmembrane domain, and a cytoplasmic domain as depicted in Figure 1.7.

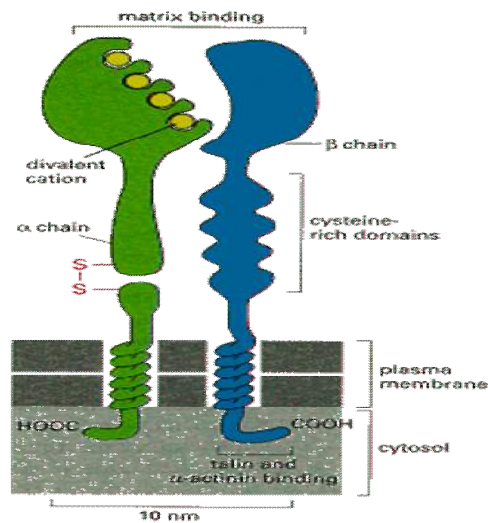


Figure 1.7: Integrin Structure. Adapted from [17].

The exact combination of various α and β subunits dictates the binding specificity of integrins to different ECM components. Although, both subunits are required for adhesion, the binding specificity primarily depends on the extracellular region of the subunit. The structural similarities between α subunits of various integrins are remarkable.

Their extracellular domains contain seven homologous repeats of 30-40 amino acids spaced by stretches of 20-30 amino acids. The three or four repeats, which are in extreme extracellular region, are involved in ligand binding. The α subunits of all integrins share the five amino acid motif, GFFKR, located directly under the transmembrane region. The exact function of this motif has not been elucidated. The β subunits contain tandem repeats of four cysteine rich regions that are essential for maintaining the tertiary structure of integrins. The recognition site for most integrins that bind the ECM consists of an RGD (arginine-glycine-aspartic acid) sequence [176,177]. Integrins bind to their ligands with low affinity and this binding occurs only when a certain minimum number of integrins are present at specific points known as focal contacts. In resting cells integrins are diffused over the cell surface and lack sufficient adhesive force. In response to specific stimuli they cluster in focal contacts and their combined affinities create a region on the cell surface, which presents sufficient adhesive capacity to adhere to the ECM [176-178]. This allows cells to bind a large number of matrix molecules simultaneously while maintaining their ability to explore their environment without losing all attachments. Any stronger binding to their ligands will cause an irreversible binding to the matrix, depriving them of their motility.

Although integrins do not possess any enzymatic activity or a kinase domain, they initiate signaling through association with non-receptor kinases, such as focal adhesion kinase (FAK) and src family of kinases. These kinases in turn activate several downstream pathways such as PI3K, Akt and Mitogen activated protein kinase (MAPK/ERK). Integrins also interact with a number of regulatory adaptor molecules and structural proteins that couple integrin to the actin cytoskeleton [15,31,177-181]. As already stated

binding of ECM molecules/ligands to the integrins leads to clustering and subsequently promotes the localized aggregation of signaling moieties leading to downstream intracellular signaling. Conversely, cytoplasmic signals modulate the integrin functioning and thus regulate cellular dynamics. Hence, integrins orchestrate both outside-inside and inside-outside signaling events [182]. Extracellular ligation of integrins triggers a large variety of signal transduction events such as proliferation, invasion, migration, survival or apoptosis, angiogenesis, immunity and homeostasis [179-183] as shown in Figure 1.8.

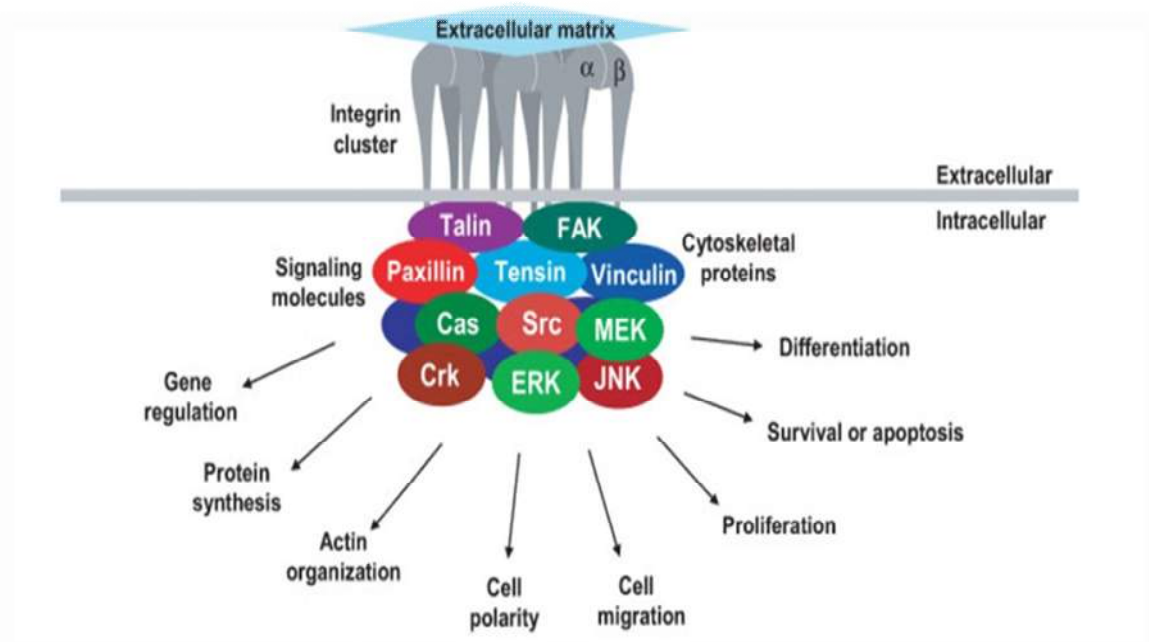


Figure 1.8: Integrin signaling cascade. Adapted from [178]

1.7.1 Inside-out signaling

Inside-out signaling or integrin activation is important in physiological situations such as in the blood, where cells are in close proximity to their ligands, yet cell–ligand interactions occur only following integrin activation in response to specific external cues

such as injury to the vasculature or the induction of inflammation [182,184]. This characteristic of integrin regulation is also important in the developmental processes when cells are required to migrate for specific periods of time during morphogenic processes. In normal resting inactive state integrin extracellular domains are unbound to ligands and exist in a bent conformation. Activation signals from within the cell induce straightening of the extracellular domains and stabilize the extended active conformation. This conformational change exposes the external ligand binding site to which ligands bind, allowing the transmission of signals from the outside to the inside. The exact changes that occur in the extracellular head domain once integrins undergo conformational change to the high affinity state are still unclear. The role of integrin cytoplasmic tails in the regulation of integrin affinity has been extensively examined in the rapidly activated $\alpha\text{IIb}\beta\text{3}$ and β2 integrin families [185].

1.7.2 Outside-in signaling

Integrins themselves lack intrinsic catalytic activity. Ligand binding to the extracellular domain of integrins results in signal transduction to the cytoplasm in the classical direction from outside towards inside. These intracellular signals affect cellular growth, differentiation and apoptosis. Further, the intracellular signals generated lead to the assembly of the focal adhesion (FA) complex, a large, dynamic multiprotein complex involving over 150 intracellular proteins [182,186]. FAs serve as the hub for transmission of intracellular signals. Within FAs, proteins are in constant flux, continually associating and dissociating with each other.

1.7.3 Integrins and breast cancer

Numerous studies have documented marked differences in surface expression and distribution of integrins in malignant breast tumours compared with pre-neoplastic tumours of the same type. Integrins such as α_v , α_3 , α_5 , β_1 and $\alpha_v\beta_3$ are being involved in the process of cancer progression [181]. A large number of reports are suggestive of the correlation between integrin expression and breast cancer metastasis. Integrin $\alpha_3\beta_1$ is associated with the process of tumourigenesis and invasion [187] while $\alpha_v\beta_3$, $\alpha_v\beta_5$, $\alpha_5\beta_1$ are associated with breast cancer progression [31]. Expression of $\alpha_5\beta_1$ is highly up-regulated in drug resistant breast carcinoma cells and associated with the ability to regulate invasion via MMP-2 [188]. Moreover, $\alpha_v\beta_3$ is associated with MAPK signaling affecting proliferation [189] while β_1 is an indicator for survival in breast cancer [190]. However, $\alpha_2\beta_1$ has been shown to play a key role of metastasis suppressor in the spontaneous model of breast carcinoma [191].

1.8 Focal adhesion kinase (FAK)

FAK is a 125-kDa non-receptor protein tyrosine kinase that was identified almost 20 years ago during the 1990s by identification of an increased phosphorylated protein after v-Src transformation of chicken embryo cells [192]. It is associated with regulating a large number of cellular processes such as cellular proliferation, adhesion, migration and cell survival [193-201]. Further, it is a ubiquitously expressed kinase and shares about 90% homology with human, chicken, mouse and frog [193]. It mediates signaling by phosphorylation and/or localization of its downstream effectors.

1.8.1 FAK structure

FAK consists of three major domains that includes N-terminal FERM domain, a central kinase domain and C-terminal focal adhesion targeting domain (FAT) as shown in Figure 1.9.

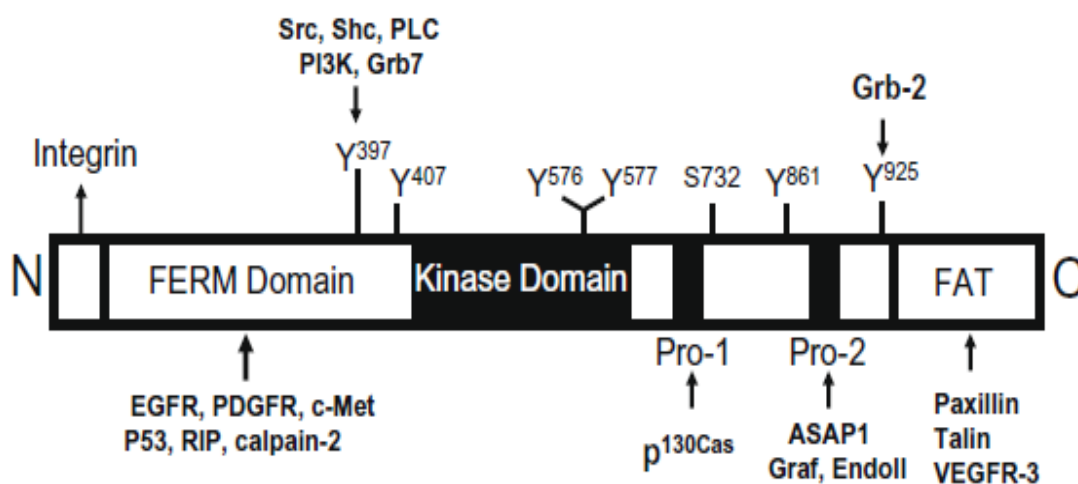


Figure 1.9: Structure of FAK. Adapted from [194].

The kinase domain of FAK shares a high degree of sequence similarity with other protein tyrosine kinases. Clustering of the integrins facilitates the auto-phosphorylation of tyrosine 397, which increases the catalytic activity of FAK [195,196]. The motif surrounding tyrosine 397 facilitates the binding of SH2 (Src-homology 2) domain containing proteins. Most important SH2 containing protein that interacts with FAK-tyrosine 397 is Src. The catalytic loop harbors two tyrosines, Y576 and Y577, whose phosphorylation is induced in response to binding of Src to FAK-tyrosine 397 and is necessary for the full adhesion-induced activation of the kinase domain. In addition to auto-phosphorylation, the kinase domain is implicated in the phosphorylation of several focal adhesion associated proteins such as paxillin, Grb2 and p130CAS. The N-terminus consists of an auto-phosphorylation site, tyrosine 397, and a FERM domain (erythrocyte

band 4.1-ezrin-radixin-moesin), both mediating protein-protein interactions [193-198]. The most well known interaction partner of the FAK-FERM domain is the cytoplasmic tail of β -integrins. In addition to protein binding, there are indications that the FERM domain functions as a regulator of FAK activity. In suspension, interaction of the FERM domain with the kinase domain prevents auto-phosphorylation of tyrosine 397, necessary for the activation of FAK. During attachment of cells the integrins cluster enabling the binding of the FERM domain to the cytoplasmic tail of the β -integrin. This results in the unfolding of FAK, thereby releasing its auto-inhibition and allowing its auto-phosphorylation and activation. The C-terminal domain can be divided into FAT sequence and the region between the FAT sequence and the kinase domain. As suggested by the name, the FAT sequence is required for localization at the focal adhesions. Although the FAT domain is able to directly interact with the cytoplasmic tails of integrins, increasing evidence supports an indirect interaction with the integrins via integrin associated proteins like talin and paxillin [195-198].

1.8.2 FAK signalling and cancer

FAK has long been known to play an important role in mediating integrin signaling [202-206]. When integrins bind to ECM proteins, they cluster on the cell surface resulting in clustering of FAK at these sites of adhesion. FAK clustering induces auto-phosphorylation of Y397, which creates docking sites for proteins with SH2 domains and mediates further downstream signaling events. FAK is thought to regulate cell proliferation via MAPK signaling [199,200]. It is also implicated in integrin-mediated cell motility as well as apoptosis [202,203,206,207]. Detachment from the ECM induces

apoptosis in many cell types. Apoptosis due to loss of cell attachment is termed anoikis and is regulated by integrins and FAK signaling [205-207].

A large number of reports describe the expression and activity of FAK in primary and metastatic human tumour tissue. Most studies show an enhanced expression of FAK mRNA and/or protein in a variety of human cancers, including squamous cell carcinoma of the larynx, invasive colon and breast tumours, metastatic prostate carcinoma and malignant melanoma [194,208-214]. These reports envisage FAK to be an important therapeutic target for breast cancers.

1.9 Protein kinase B/Akt signalling

Akt (protein kinase B), a serine/threonine kinase has emerged as a critical enzyme in several signal transduction pathways involved in cell proliferation, apoptosis and angiogenesis [215-219]. Akt is fully activated following its phosphorylation at two regulatory residues, a threonine residue on the kinase domain and a serine residue on the hydrophobic motif. Phosphorylation at Thr308 and Ser473 is required of Akt1 while phosphorylation at Thr309 and Ser474 activates Akt2. Phosphorylation of a threonine residue on the kinase domain, catalyzed by PDK1, is essential for Akt activation. It causes a charge-induced conformational change, allowing substrate binding and increased rate of catalysis. Without threonine phosphorylation, the hydrophobic motif of Akt is more susceptible to the action of phosphatases, however, the dually phosphorylated and fully active enzyme is stable, allowing its localization to the nucleus and other sites. The activity of Akt is negatively regulated by PTEN (phosphatase and tensin homolog deleted on chromosome 10, a PIP3-specific phosphatase) and SHP (SH2 domain containing inositol 5'-phosphatase). The principal role of Akt is to facilitate cell survival and to

block apoptotic cell death [215-217,220]. This is achieved by phosphorylating and deactivating pro-apoptotic factors such as Bad, caspase-9 and forkhead transcription factors. Akt regulates the activity of caspase-9 by phosphorylating it, preventing its activation and also up regulates the Bcl-2 expression via c-AMP response element binding protein [221,222].

Akt and p53 play opposing roles in signaling pathways that determine cell survival. Under conditions where the apoptotic effect of p53 is dominant, destruction of Akt plays a role in accelerating the apoptotic process. In apoptosis-prone cells, p53 dependent signaling enables down-regulation of Akt, which predisposes cells to rapid apoptosis in response to stress signals. Under certain circumstances Akt activation may overcome the death promoting effects of p53 and rescue cells from apoptosis [223,224].

1.10 Apoptosis

Apoptosis occurs when cells have sufficient time to organize and participate in their own demise. In response to specific signals, cells undergo apoptosis, which is manifested by a number of distinctive biochemical and morphological changes. Cells undergoing apoptosis exhibit shrinkage, membrane blebbing, chromatin condensation, and extensive nuclear fragmentation. Apoptosis or type 1 cell death is a carefully controlled programmed cell death that does not lead to any inflammation in the organisms. On the other hand, necrosis or type 3 cell death is a more frenzied cell death resulting from circumstances outside the cells leading to edema and disruption of the plasma membrane [225-227]. Many cells can be activated to undergo apoptosis following the interaction of selected ligands with cell surface receptors. The most well studied receptors are the Fas/APO-1 (apoptosis inducing protein 1) and tumour necrosis factor receptor 1

(TNFR1). Apoptosis mediated by both signaling cascades end in activation of caspases. Thus far, 14 caspases had been identified and are divided into three groups, which include initiator caspases (caspase 2, 8, 9, and 10), executioner caspases (caspase 3, 6, and 7), and caspases involved in cytokine processing (caspase 1, 4, 5, 11-14). Caspases are synthesized as single chain, ~45 kDa proenzymes that are activated by two cleavages. The first cleavage separates the N-terminal pro-domain and the second cleavage separates the large (~p20) and the small (~p10) subunits that form a heterodimeric active caspase with two symmetrically arranged active sites at opposite ends of the molecule. Caspase activation is generally considered as the “point of no return” in apoptotic pathways [228]. Activated caspases cleave key substrates required for normal cellular functions, such as the cytoskeletal proteins, nuclear proteins, and DNA repair enzymes. One of the major substrates of caspases is PARP (poly- (ADP-Ribose) polymerase) whose cleavage by caspases renders it inactive and leads to cessation of DNA repair mechanisms. Caspases are activated either via the receptor mediated (Fas ligand or TNF α -mediated) pathway or via the mitochondrial pathway. The receptor mediated pathway leads to the activation of pro-caspase-8. In the mitochondrial pathway, pro-apoptotic members of the Bcl-2 family associate with mitochondria and direct the release of cytochrome c (Cyt c) and other proteins, which activate pro-caspase-9 [225-231]. Defects in p53 and bcl-2 genes are associated with proliferative disorders and apoptosis. It is believed that p53, a key tumour-suppressor protein, accumulates when DNA is damaged and arrests the cell cycle at the G1 phase to allow extra time for repair. However, if the repair process fails, p53 triggers apoptosis. When p53 is dysfunctional, apoptosis fails to occur. Also, an over-expression of Bcl-2 retards normal apoptotic process [231-234]. Anticancer drugs

mediate their effect by triggering apoptosis. There is strong evidence suggesting that cancer cells can increase their resistance to anti-cancer drugs by increasing the expression of Bcl-2 that leads to inhibition of apoptosis [235,236]. Inactivation of p53 also contributes to the initiation and progression of cancer. Hence, the p53 status becomes a strong determinant of response to treatment with anticancer agents [233,234]. The mitochondrial (intrinsic) apoptotic pathway, activated by cytotoxic drugs ultimately leads to the activation of caspases that cause cell death in tumour cells. In addition, activation of the receptor-linked (extrinsic) apoptotic pathway leads to enhanced sensitivity of tumour cells toward cytotoxic agents. Hence, apoptosis is an important area of study where the ability to achieve a significant therapeutic index and differentiating normal cells from tumour cells may lower the threshold at which cell injury triggers apoptosis.

1.10.1 Integrins and cell death

Integrin-mediated cell attachment is essential for survival signaling in many types of normal cells and offers protection against a variety of apoptotic stimuli. Epithelial and endothelial cells that are largely dependent on integrin-mediated cell attachment for their survival undergoes apoptosis upon loss of integrin-mediated cell attachment [180,205-207]. Cancer cells deprived of contact with the matrix die rather than circulate and colonize distant sites. Hence, integrins have a significant effect on the progression of malignant tumours. Integrin-mediated cell attachment has been shown to modulate cancer cell responses to chemotherapeutic agents [237,238]. Hence, elucidation of the molecular mechanisms contributing to defective adhesion is important in developing new drugs for treatment of various diseases.

1.11 Combination therapy

Combination therapy aims to overcome individual drug limitations, which may include lack of effectiveness, progressive decline in effectiveness over prolonged use, or adverse events. Most drug combinations select diverse targets of action for each of the individual drugs and aim to enhance effectiveness synergistically. Alternatively, one molecule may improve the action of another by increasing its penetration or preventing its destruction or efflux [239].

In almost all cancer types, single drug targeted therapy is only effective in about half of the patients. This is because cancer cells utilize either alternate pathways or compensatory mechanisms to evade inhibition. Therefore, development of drug combinations that target diverse pathways and modulate tumour microenvironment is currently in focus for treatment of breast cancer. Further, a combination therapy should meet three basic criteria before it is taken to clinics. These include a) each component should have single agent activity with no cross-resistance b) there should be preclinical evidence of synergy between the components c) the components should have no overlapping toxicity issues [239-241].

Studies regarding combination therapy of PTX and doxorubicin have been studied against various cancers such as leukemia and cervical cancer cells [125,126]. However, no reports indicating its usage against breast cancer had been reported. In view of this, it shall be interesting to evaluate the effects of combination of PTX and lipodox (liposomal doxorubicin) in breast cancer cells.

1.12 Liposomal doxorubicin

Chemotherapy represents one of the major therapeutic interventions in the treatment of advanced breast cancer [82,84,85,90-92,242]. Among the various classes of known anti-cancer agents, anthracyclines {such as doxorubicin (DOX) or adriamycin (ADR)} comprise one of the primary options in this scenario [242]. However, there are a large number of toxicity related issues such as cardiotoxicity, suppression of bone marrow, nausea, vomiting and baldness associated with the usage of doxorubicin [243,244]. In order to overcome these limitations, drug delivery systems such as the entrapment of DOX in pegylated liposomes are preferred [244,245].

Lipodox is doxorubicin hydrochloride encapsulated in long circulating pegylated liposomes. Liposomes are microscopic vesicles composed of a phospholipid bilayer that are capable of encapsulating active drugs. The pegylated liposomes of doxorubicin are formulated with surface bound methoxypolyethylene (MPEG), a process often referred to as pegylation, to protect liposomes from detection by the mononuclear phagocyte system (MPS) and to increase blood circulation time [245]. Pegylated liposomes have a half-life of approximately 55 hr in humans. These are stable and direct measurement of liposomal doxorubicin shows that at least 90% of the drug remains liposome encapsulated during circulation. It is hypothesized that because of their small size and persistence in the circulation, the pegylated doxorubicin liposomes are able to penetrate the altered and often compromised vasculature of tumours. Once the pegylated liposomes distribute to the tissue compartment, the encapsulated doxorubicin HCL becomes available. The exact mechanism of release is not well understood.

Doxorubicin is a cytotoxic anthracycline antibiotic isolated from *Streptomyces peucetius* var. *caesius* [244]. It is indicated for the treatment of metastatic carcinoma of the ovary, metastatic breast cancer and AIDS related Kaposi's sarcoma (KS) [246-250].

The exact mechanism of anti-tumour activity of doxorubicin is not known. It is generally believed that inhibition of synthesis of DNA, RNA and protein is responsible for the majority of the cytotoxic effects. Liposomal doxorubicin penetrates the cells rapidly, binds to chromatin and inhibits nucleic acid synthesis by intercalation between adjacent base pairs of the DNA double helix and thus preventing their unwinding for replication [87,244,245].

Chapter 2
Aims and Objectives

2.1 Rationale of the study

Despite improvements in diagnosis, surgical techniques, general patient care, local and systemic adjuvant therapies most deaths from cancer result due to progressive growth of metastases, that are resistant to conventional therapies. Conventional treatment modalities for cancer are surgery, followed by radiation and/or chemotherapy. Currently treatment for possible metastases is initiated along with treatment for primary tumour. Hence, a combination of different therapies is popular where cytotoxic drugs are used in combination with anti-metastatic and anti-angiogenic drugs to successfully combat the disease. In order to plan an effective combination strategy, knowledge of the molecular mechanisms of action of each of the therapeutic agents is very essential. One of the most common causes of failure of a number of potential drugs is their high degree of cytotoxicity. Hence, investigations are often directed to the potential of drugs which are used in the treatment of other diseases and hence been shown to be non-cytotoxic, to act as anti-cancer or anti-metastatic agents. Also since cancer, as well, the subsequent metastases are in essence, normal cellular processes have gone deregulated, most of the drugs, which are useful in other pathological conditions in the body, find use as anti-cancer agents.

Our lab has been working with the effects of methylxanthine derivatives on tumour metastasis. PTX was shown to inhibit hematopoietic stem cell homing and inhibited the lung homing of B16F10 melanoma cells in an experimental metastasis model system. Further, studies on PTX showed that this drug could also inhibit proliferation of endothelial cells and tumour induced angiogenesis. Studies on the mechanism of action of PTX suggested that the effects of this methylxanthine derivative are probably mediated

at least in part through its effects on cell adhesion and adhesion receptors. PTX was found to inhibit the adhesion of tumour cells to reconstituted basement membrane and type IV collagen. Further, PTX was found to modulate the integrin expression in B16F10 cells and affect the RhoGTPases. For the successful establishment of metastases, the cells should be able to modulate their ability to adhere, invade, and migrate through the ECM. Hence, in this study we aim to look at the anti-metastatic action of PTX with emphasis on its effects on integrin mediated adhesion and induced apoptosis in human MDA-MB-231 breast cancer cells (a model system for TNBC). TNBC that has no alternative option for treatment other than chemotherapy. Thus, we had evaluated the anti-metastatic effects of PTX against the same and unraveled the underlying mechanism of action.

Next, we had demonstrated the effect of PTX in combination with anti-cancer drug lipodox (liposomal doxorubicin) so as to increase the therapeutic efficacy of the latter by not only limiting the dose but also minimizing the toxicity.

2.2 Objectives

1. To study the anti-metastatic potential of PTX in MDA-MB-231 human breast cancer cells *in vitro* and *in vivo*.
2. To study the effect of PTX on integrin expression profile in MDA-MB-231 cells.
3. To study the effect of PTX on Focal Adhesion Kinase (FAK) and its downstream signaling mediators.
4. To study the chemo-adjuvant potential of PTX in combination with another anti-cancer agent to increase its therapeutic efficacy using *in vitro* and *in vivo* models.

Chapter 3
Materials and Methods

3.1 Materials

3.1.1 Fine chemicals

Acrylamide; Akt inhibitor IV; Bovine serum albumin fraction V; Bradford reagent; collagen type IV; 1,4 -diazabicyclo[2.2.2]octane (DABCO); Dimethylsulphoxide (DMSO) (tissue culture grade); cytochalasin-B; ethylene diamine tetra acetic acid (EDTA); fibronectin; FAK inhibitor PF-573228; laminin; matrigel; Methyl tetrazolium bromide (MTT); Mitomycin C; N,N'-Methylene-bis-acrylamide; Poncue-S; Polyoxyethylene sorbitan monolaurate (Tween 20); paraformaldehyde; Sodium orthovanadate; Sodium dodecyl sulphate (SDS); sodium citrate; sodium deoxycholate; Triton-X-100; TRITM; Tris; NNN'N'-Tetra-methylethylene-diamine and vitronectin were purchased from Sigma Aldrich, USA.

3.1.2 Tissue culture reagents and plasticware

Fetal Bovine Serum US origin (FBS), DMEM from Gibco, USA; Benzyl penicillin from Alembic Ltd. India; Streptomycin from Nicholas Piramel, India; 35 mm culture dishes, 60 mm culture dishes, 90 mm culture dishes, 96 well flat bottom plates with lid, 24 well plate with lid from BD Falcon, USA; cell scrapers from Nunc Nalgene Int., USA; 0.2 micrometre syringe driven filters and 30 kDa centrifugal cut-off filters from Millipore, USA.

3.1.3 General Chemicals

Agarose from Sigma Aldrich, USA; Ammonium persulphate from Sisco Laboratories, India; Calcium chloride from S.D fine Ltd, India; Coommasie brilliant blue R from Sisco Laboratories, India; Magnesium chloride, Potassium chloride, Phenol red from S.D. fine Ltd, India; Skimmed milk powder from Biorad, USA; Sodium azide from Spectrochem

Pvt. Ltd., India; Sodium bi-carbonate from S.D. Fine Ltd, India; Sodium hydroxide from Sisco Laboratories, India; Disodium hydrogen phosphate from Qualigens, India; Dihydrogen sodium phosphate from S.D.Fine Ltd, India and Trypsin from Himedia Pvt Ltd, India.

3.1.4 Antibodies

Integrins α_v , α_2 , α_3 , α_5 , β_1 , β_3 and β_5 from Santa Cruz, USA; Integrins $\alpha_v\beta_3$, $\alpha_v\beta_5$ and $\alpha_5\beta_1$ from Millipore, USA; FAK, VEGF and p53 from Santa Cruz, USA; pFAK, ERK1/2, pERK1/2, Akt, pAkt, cyclin D1, cdk4, cdk6, Bcl-2, Bcl-xL, Mcl-1, Cleaved caspase 9, Cleaved caspase 3, cleaved PARP from Cell signaling, USA; while β -Tubulin from Sigma Aldrich, USA. All the secondary antibodies such anti-rabbit/mouse labeled with FITC/Alexa fluor 568 were purchased from Invitrogen, USA while anti-rabbit/mouse labeled with HRP were purchased from Sigma Aldrich, USA.

3.1.5 Kits

AnnexinV-FITC labelled kit, Caspase detection kit from Invitrogen, USA; c-DNA synthesis kit, DNA ladder 1 kb from MBI Fermentas; G-LISA kit from Cytoskeleton, USA; PCR amplification kit from MBI Fermentas, USA; Phalloidin-FITC labelled, Primers, Protease inhibitor cocktail from Sigma Aldrich, USA; Protein ladder pre-stained, Ribonuclease A from MBI Fermentas, USA and Supersignal west femto detection kit from Thermo Scientific, USA.

3.1.6 Solvents and Acids

Acetic acid from Qualigens, India; Ethyl Alcohol from S.D. Fine Ltd., India; Methanol from S.D. Fine Ltd., India; Sulphuric acid from Qualigens, India; 37-41% formaldehyde from Merck, India; 2-Mercapto ethanol from Fluka AG, Germany; Hydrochloric acid, glycerol,

chloroform from Qualigens, India; iso-propanol and ethanol from Sigma Aldrich, USA.

3.1.7 Instruments and machines

ELISA plate reader (Spectra Max 190) from Molecular Devices, USA; Centrifuge RC 5C plus from Sorvall, USA; Flow cytometer from BD FACS Calibur, USA; Table top ultracentrifuge (TL100) from Beckman, USA; spectrophotometer (UV 160A) from Shimadzu, Japan; UV illuminator from UVP Bio-imaging Sys., USA; upright light microscope, Inverted microscope, Laser confocal microscope (510 Meta) from Zeiss, Germany, Rota 4-R Centrifuge from Plasto-crafts Ind. Pvt. Ltd.; rocker from Neolab, India; Rotary shaker from Remi Equipments, India; Trans-blot cell from Biorad, USA; Powepack Electragel-100 from Techno Source, India; Horizontal gel apparatus from Monokin Techno Source, India and water-bath from Neolabs, India.

3.1.8 Cell lines and animals

MDA-MB-231, MCF-7 and HT-1080 cell lines were purchased from NCCS, Pune, India. NOD-SCID and Nude mice were supplied from Animal House, ACTREC after the ethical committee clearance (IEAC).

3.2 Methods

3.2.1 Maintenance of cell lines

Reagents

DMEM (Dulbecco's modified Eagles media): 13.5 gm of media powder was dissolved in 1 litre of fresh distilled water (D/W). 3.7 gm of NaHCO₃ was added to the dissolved media. Media was sterilized by filtration through 0.2 micrometre filter and stored in aliquots at 4°C.

FBS (Fetal bovine serum): Aliquot and stored at -20°C.

Penicillin: A 5,00,000 unit vial was dissolved in 25 ml of PBS and filter sterilized. Aliquots were made and kept at -20°C, sterilized and stored at -20°C in aliquots.

Phosphate buffered saline (PBS)

NaCl	8 gm
KCl	0.2 gm
Na ₂ HPO ₄	1.44 gm
KH ₂ PO ₄	0.24 gm

The salts were dissolved in D/W, pH was adjusted to 7.2 and the volume was made up to 1 litre. Sterilization was done by autoclaving.

Trypsin EDTA: 0.25% Trypsin and 0.2% EDTA in PBS, sterilized by filtration and stored at 4°C.

Saline EDTA: 0.02% EDTA in PBS, sterilized by filtration and stored at 4°C.

Trypan Blue: 0.4% trypan blue powder was dissolved in PBS, filtered using Whatman filter paper and kept at 4°C.

Protocol

The breast cancer cell lines MDA-MB-231, MCF-7 and fibrosarcoma HT-1080 cells were cultured in complete medium made up of DMEM supplemented with 10% FBS and antibiotic solution (10 units/ml of penicillin G-sodium and 10 µg/ml of streptomycin sulphate). Cultures were incubated in a humidified atmosphere containing 5% CO₂ and 95% air, at 37°C and passaged when sub-confluent (70-80%). Sub-confluent monolayers were rinsed in PBS and harvested with trypsin EDTA. Subsequently, to this dissociated cell suspension, complete media was added to inactivate trypsin. Cells were centrifuged at 2000 rpm for 5 minutes and the pellet was resuspended in 1 ml of complete medium. Cell

viability was determined using trypan blue dye exclusion test. Cell suspension was diluted in trypan blue and counted in a haemocytometer. The viable cells excluded the dye while the dead cells retained it and appeared blue coloured under the microscope. Cell count was determined using the formula:

No of cells /ml= no of cells x 10^4 x dilution factor

It was ensured that the cells were at least 95% viable for all the *in vitro* and *in vivo* assays. Routine cryopreservation of the cell line was done in which cells were harvested and to it chilled freezing mixture (DMEM with 20% FBS and 10% DMSO) was added drop wise. Approximately, 1×10^6 cells were added in each cryovial and kept at -20°C for an hr. The vial was then transferred to -80°C , kept overnight and then stored in liquid nitrogen. The revival of the frozen cells was carried out by taking the cryovial out of liquid nitrogen and immediately thawing it in a 37°C water bath. To this cell suspension complete media was added to dilute the DMSO. Cells were centrifuged and given a PBS wash. The cells were then seeded in a culture dish and grown to confluence.

3.2.2 MTT cytotoxicity assay [251]

Reagents

Drugs: Trental vial containing 300mg of PTX in 15 ml saline (71.86 mM) sterile solution.

MTT reagent: MTT powder was dissolved in sterile PBS at a concentration of 5 mg/ml and stored frozen in aliquots.

DMSO (dimethyl sulphoxide)

Protocol

MDA-MB-231 cells were harvested in exponential phase and a cell suspension was made in complete medium at a concentration of 5×10^4 cells/ml, 2.5×10^4 cells/ml and 1.5×10^4 cells/ml. 100 μ l of this cell suspension was seeded in each well of 96-well flat bottom tissue culture plates except for blank. The cells were allowed to grow and stabilize for 24 hr. Subsequently the media from the wells was removed and replaced with complete media containing the serial dilutions of the drug being studied. PTX dilutions were made from stock solutions prepared in PBS. All the dilutions were made in complete medium. Each treatment was performed in six wells replicates. Post incubation (24 hr, 48 hr and 72 hr) cells were washed with PBS and 100 μ l of complete medium was added in each well. Cell viability was determined by MTT colorimetric assay. 20 μ l of MTT reagent was added to each well to make a final concentration of 1mg/ml of media and incubated for 4 hr at 37°C. Plates were then centrifuged at 2000 rpm for 10 minutes. Medium from the plate was removed by gently tapping the plate against a pad of blotting paper. Formazon crystals were dissolved in 100 μ l of DMSO. The optical density was measured in ELISA plate reader at 540 nm with a reference wavelength of 690 nm. Absorbance of blank was subtracted from each. Cell viability was plotted as percentage of untreated control and dose effect plot was generated. Results are expressed as Mean \pm S.E.M. Inhibitory Concentration 50 (IC₅₀) of the drugs was determined from the dose effect curve as the drug concentration that decreased the cell viability to 50 %.

The interaction between PTX and Lipodox (liposomal doxorubicin) was analyzed using the compusyn software program to determine whether the combination was antagonistic, additive or synergistic [252]. Data from cell viability assay (MTT) were expressed as the

fraction of cell viability inhibited by the individual drugs or the combination verses untreated cells. This program is based upon the Chou-Talalay method which calculates a combination index (CI) and analysis is performed based on the following equation: $CI = (D)_1 / (D_x)_1 + (D)_2 / (D_x)_2 + (D)_1(D)_2 / (D_x)_1(D_x)_2$. Here (D)₁ and (D)₂ are the doses of drug 1 and drug 2 that have x effect when used in combination and (D_x)₁ and (D_x)₂ are the doses of drug 1 and drug 2 that have the same x effect when used alone. When CI = 1, this equation indicates additive effects. CI below 1.0 indicates synergism and greater than 1 indicates antagonism. Here, (PTX:LD) were taken in the ratio of 500:1 and synergistic doses were evaluated. The doses evaluated for combination regimens were abbreviated as PTX or P1 (PTX dose 1) 3 mM, PTX or P2 (PTX dose 2) 4 mM, LD or LD1 (lipodox dose 1) 6 μM, LD or LD2 (lipodox dose 2) 8 μM, Combination C1 (P1 and LD1) and Combination C2 (P2 and LD2) respectively.

3.2.3 Colony formation assay [104,253]

Reagents

0.5% Crystal violet stain: weigh 0.25 gm of crystal violet and dissolve in 50 ml of methanol.

Protocol

35 mM petri plates were seeded with 600 cells and incubated for 24 hr. The cells were treated with sub-toxic doses of PTX or its combinations for a period of 24 hr. Cells were washed with PBS and replaced with complete medium. The plates were incubated further for 8-10 days till in the untreated control the colonies attain a size of more than 50 cells. The cells were fixed with chilled methanol and stained with 0.5% crystal violet. The plate was divided in various quadrants with the marker. Colonies

with cell number 50 or more were counted in all the plates.

3.2.4 Cell cycle analysis [104]

Reagents

RNAse: 10 µg/µl solution

Propidium Iodide: 1 mg/ml solution in PBS

Protocol

Sub confluent MDA-MB-231 cells were treated with the PTX and its combination regimens. Cells were harvested, washed twice with PBS and fixed in chilled 70% ethanol. The fixed cell pellet was washed with PBS and re-suspended in 200 µl of PBS. Cells were treated with 10 µl RNAse solution (0.5 mg/ml concentration) for 15 min at 37°C. The volume was made upto 1 ml and 50 µl propidium Iodide (50 µg/ml concentration) was added to it. Cells were incubated for 10 min at room temperature. 10,000 events were acquired on FACS Calibur and analyzed using Modfit software.

3.2.5 Ethidium bromide/acridine orange (EB/AO) staining [254]

Reagents

Ethidium bromide (EB): 100 µg/ml

Acridine orange (AO): 100 µg/ml

Protocol

The basis of this assay is the discrimination of membrane integrity between live and dead cells. Approximately, 16000 cells/well were seeded in triplicates in a 96-well format. Cells were treated with PTX/combination for 24 hr and then centrifuged. The cells were stained using EB/AO mix and observed under a Zeiss Axio inverted microscope. Images were captured at 10X magnification for three different fields of each particular well.

3.2.6 AnnexinV/FITC Staining

Reagents

AnnexinV/FITC kit from Invitrogen

Protocol

Detection of apoptosis cells was performed as per the manufacturer's instructions (Invitrogen). Briefly, 1×10^6 cells for each of the PTX and its combination groups were suspended in 100 μ l 1X Annexin binding buffer and then treated with 5 μ l AnnexinV/FITC solution along with 1 μ l of Propidium Iodide (100 μ g/ml). The samples were mixed thoroughly and then incubated at room temperature for 15 minutes. Thereafter, the final volume was made upto 500 μ l using Annexin binding buffer and the samples were kept on ice. Acquisition was done using FACS Calibur and the analysis performed using Cell Quest Pro software.

3.2.7 Adhesion assay [105]

Reagents

Matrigel: 10 μ g/ml working solution made in PBS

Collagen type IV: 10 μ g/ml working solution in PBS

Laminin: 5 μ g/ml working solution made in PBS

Fibronectin: 2.5 μ g/ml working solution made in PBS

Vitronectin: 2.5 μ g/ml working solution made in PBS

BSA: 1% in PBS

Protocol

96-well flat bottom plates were coated with ECM substrates (50 μ l/well): Matrigel (10 μ g/ml), collagen type-IV (10 μ g/ml), fibronectin (2.5 μ g/ml), laminin (5 μ g/ml) and

vitronectin (2.5 µg/ml). Plates were kept overnight at 4°C for polymerization. Un-polymerized substrates were washed with PBS and the plates were blocked with 1% BSA in PBS for 2 hr at 37°C. Sub-confluent MDA-MB-231 cultures were treated with PTX and its combinations. The cells were harvested using saline EDTA, washed and diluted to a final concentration of 3×10^5 cells/ml in DMEM containing 0.1% BSA. 100 µl of the cell suspension was added to each substrate coated well and kept for incubation at 37°C for 15 min, 30 min, 45 min, 60 min or 90 min. Non-adherent cells were removed by giving two washes with PBS. Wells containing unwashed cells were kept as control. The adherent cells were quantified using MTT assay and expressed as relative % of the respective total unwashed cells (adherent as well as non-adherent).

3.2.8 Preparation of condition media [104,255]

Secretion and activity of gelatinases MMP-2 and MMP-9 was studied by gelatin zymography Sub-confluent cultures were seeded in 90 mm plates. The cells were allowed to proliferate and when the confluency had reached to about 70-80% the cells were treated with sub-toxic doses of PTX/combination doses for 24 hr. Cells were washed twice with PBS and incubated with plain DMEM for another 24 hr. Condition media so obtained was collected and clarified by centrifugation at 2000 rpm for 10 minutes and concentrated using 30 kDa cut off filters. The cells remaining in the plates were harvested using saline EDTA and the total cell count was measured. The volume of condition media was normalized with respect to the cell count and used for gelatin zymography. The concentrated conditioned media was normalized with respect to cell count and stored at -80°C until further use. HT-1080 conditioned media was used as a positive control.

HT-1080 cells were cultured in DMEM containing 10% FBS and the condition media was prepared in the same way as was done for MDA-MB-231 cells.

3.2.9 Gelatin zymography [104,255]

Reagents

Non-reducing lamelli buffer- 6X lamelli buffer without β -mercapto-ethanol.

2% Gelatin: Take 50 ml of sterile milli Q water and heat it to 70°C. To this add 1 gm of porcine gelatin. Let it dissolve and make 2 ml aliquots. Store at -20°C. Add 1.5 ml of this to 30 ml of resolving gel mixture.

Developing and washing buffer: 50 mM Tris chloride containing 100 mM CaCl₂, 1 μ M ZnCl₂, 1% Triton X 100, 0.02% NaN₃, pH-7.5. Filter, sterilize and store at 4°C.

Staining solution: 0.5% Coomassie brilliant blue R-250 powder in a destaining solution. Filter and store.

De-staining solution: methanol, water and acetic acid mixture (5:4:1 v/v).

Other reagents includes SDS –PAGE, coomassie stain and destainer.

Protocol

To assess the gelatinase activity, samples were incubated in non -reducing lamelli buffer for 30 minutes at room temperature and run on 10% SDS -PAGE containing 0.1% gelatin (w/v) in maxi gel apparatus. 50 μ l of HT-1080 condition media was loaded as a positive control. Gels were washed twice in washing and developing buffer for 1 hr at room temperature and further incubated in the same buffer at 37°C for 48 hr. The gels were stained in staining solution for 2 hr and destained further in the destainer till the bands appeared. Enzymatic activity was visualized as clear zones on a blue background. Gel image was taken in the gel documentation machine and densitometry analysis was done.

3.2.10 Wound scratch assay [256]

Reagents

Mitomycin C: 1 mg/ml stock diluted to 1 µg/ml

Protocol

Confluent monolayers of MDA-MB-231 cells were washed twice with PBS and then treated with mitomycin C (1 µg/ml) for 1 hr. Cells were then wounded with a sterile plastic tip in the centre of the plate. The pealed off cells were removed with two PBS washes. PTX/combination regimens were added for 24 hr and plates were fixed with 70% methanol. The wound width was measured using the AxioVision Rel 4.8 imaging software and results were plotted as % wound closure with respect to control.

3.2.11 Flow cytometry for surface expression of integrins [106,257]

Reagents

Fixing solution: 4 gm paraformaldehyde was added to PBS and warmed gently until the whole of paraformaldehyde was dissolved.

FACS Buffer: 0.01% sodium azide was dissolved in PBS containing 1% FBS (ice cold)

Protocol

MDA-MB-231 cells were grown to 90% confluency in complete medium. The cells were then treated with sub-toxic doses of PTX for 24 hr. The media was then removed and the cells were washed twice with ice cold PBS. The cells were then harvested using trypsin EDTA and washed twice with FACS buffer. The cells were then fixed by incubation in 4% paraformaldehyde for 30 minutes at room temperature. The cells were again washed in FACS buffer and resuspended in FACS buffer containing the primary antibody (1 µg antibody for 1 million cells) against the integrins of interest (α_v , α_2 , α_3 , α_5 , β_1 , β_3 , β_5 ,

$\alpha v\beta 3$, $\alpha v\beta 5$ and $\alpha 5\beta 1$) and incubated for 1 hr at 4°C. The cells were then washed and resuspended in FACS buffer containing the 2° antibody (1:200) conjugated to FITC. Incubation was done for 1 hr in dark. Cells were then washed and resuspended in 300 μ l of FACS buffer for acquisition using FACS Calibur. 10,000 cells were acquired and the data was analyzed using the software cell quest. Mean fluorescent intensity of the samples were used to ascertain the integrin expression on the cell surface.

3.2.12 Reverse transcriptase (RT) PCR [258]

a) Sample preparation

Reagents

Trizol(TRITM) reagent, chloroform, Isopropanol, 75% ethanol

DEPC treated water: 1 ml of DEPC was added to 1 litre of fresh D/W. It was mixed thoroughly for 30 minutes, incubated overnight at room temperature and autoclaved the next day.

Protocol

Harvested cells were pelleted and TRITM Reagent was added to the cell pellet. The cell pellet was passed through a pipette several times to form a homogenous lysate. The samples were allowed to stand for 5 minutes on ice. 0.2 ml chloroform was added for every 1ml of TRITM Reagent used. The sample was covered tightly, shaken vigorously for 15 seconds and was allowed to stand for 2-5 minutes at room temperature. The resulting mixture was centrifuged at 12,000 rpm for 30 minutes at 4°C. Centrifugation separated the mixture into 3 phases: a red organic phase, containing proteins, an interphase containing DNA and a colourless upper aqueous phase containing RNA. The aqueous phase was transferred to a fresh tube and an equal volume of isopropanol was

added to it and mixed. The mixture was allowed to stand at -20°C for 2 hr followed by centrifugation at 12,000 rpm for 30 minutes at 4°C. The RNA precipitate formed a pellet at the bottom of the tube. The supernatant was removed and the RNA pellet was washed with 1 ml of 75% ethanol. The sample was centrifuged at 12,000 rpm for 20 minutes at 4°C. The RNA pellet obtained after centrifugation was dried for 5-10 minutes by air drying. The pellet was suspended in nuclease free water. The purity and quantification of the RNA sample was performed using a biophotometer.

b) 1st strand cDNA synthesis

Reagents

First strand cDNA synthesis kit

DNaseI and DnaseI buffer

Nuclease free water

Dry Bath

Protocol

Total RNA was converted into c-DNA using M-MuLV Reverse transcriptase. To a nuclease-free tube, the following were added:

RNA	2 µg
10X DNaseI reaction buffer	1 µl
DNaseI	1 µl
Ribonuclease inhibitor	1 µl
Nuclease free water	Up to 11 µl

This was incubated at 37°C for 30 minutes. The reaction was terminated by adding 1 µl of EDTA and heating at 65°C. For synthesizing the c-DNA the following were added to the same tube:

5X reaction buffer	4 µl
10mM dNTP mix	2 µl
Reverse Transcriptase	1 µl
Oligo dT	1 µl

The mixture was incubated at 42°C for 60 minutes. The reaction was terminated by heating at 70°C for 5 minutes.

c) Polymerase chain reaction (PCR)

Reagents

PCR kit

Nuclease free water

TE buffer: 10 mM Tris pH-8, 1 mM EDTA

Thermal cycler

Protocol

All primers were dissolved in TE buffer according to manufacturer's instructions. The PCR reaction mixture for 1 reaction (20 µl) was made as follows:

10X PCR Buffer	2 µl
10 mM dNTP mix	0.4 µl
Primer 1	0.08 µl
Primer 2	0.08 µl
Taq DNA polymerase	0.1 µl

25 mM MgCl ₂	0.4 µl
Template c-DNA	0.8 µl
Nuclease free water	Up to 20 µl

To demonstrate the linearity of PCR conditions GAPDH (house keeping gene) transcripts were also amplified.

d) PCR Primers and conditions

c-DNA	Forward Primer	Reverse Primer	Cycles	Amplicon Size, bp
αv	GTT GGG AGA TTA GAC AGA GGA	CAA AAC AGC CAG TAG CAA CAA	94°C, 45 sec 56°C, 45 sec 72°C, 60 sec 30 cycles	288
α2	TGG GGT GCA AAC AGA CAA GG	GTA GGT CTG CTG GTT CAG	94°C, 45 sec 58°C, 60 sec 72°C, 60 sec 30 cycles	541
α3	TAC GTG CGA GGC AAT GAC CTA	TTT GGG GGT GCA GGA TGA AGC T	94°C, 45 sec 60°C, 60 sec 72°C, 60 sec 30 cycles	306
α5	CAT TTC CGA GTC TGG GCC AA	TGG AGG CTT GAG CTG AGC TT	94°C, 60 sec 58°C, 60 sec 72°C, 60 sec 30 cycles	324

β1	ACG CCG CGC GGA AAA GAT GA	GCA CCA CCC ACA ATT TGG CCC T	94°C, 35 sec 58.8°C, 35 sec 72°C, 35 sec 30 cycles	160
β3	GGG GAC TGC CTG TGT GAC TC	CTT TTC GGT CGT GGA TGG TG	94°C, 60 sec 58°C, 60 sec 72°C, 60 sec 30 cycles	544
β5	CGA GCT TGG GAT AAA GCA AG	TCA ACA GGC ATC TCA ACA GC	94°C, 60 sec 46°C, 60 sec 72°C, 60 sec 30 cycles	327
GAPDH	GAG TCA ACG GAT TTG GT CGT	TGT GGT CAT GAG TCC TTC CA	94°C, 35 sec 58.3°C, 35 sec 72°C, 35 sec 30 cycles	512

e) Agarose Gel Electrophoresis

Reagents

1 % Agarose: 1 gm agarose was melted at 100°C in 100 ml TBE buffer.

Tris Base 121 gm

Boric acid 61.7 gm

EDTA 7.44 gm

Dissolved in autoclaved D/W and volume made upto 1 litre.

Loading dye (MBI Fermentas).

Ethidium bromide: 1 mg/ml stock diluted to 0.5 µg/ml.

Protocol

1% Agarose was prepared TBE (containing EtBr) and the gel was poured into the apparatus and cooled. 10 µl of PCR product was mixed along with 2 µl loading dye and loaded onto the agarose gel along with molecular weight markers. The gel was run at a constant voltage of 80 V. The gel was then visualized and documented on a UVP gel doc system.

3.2.13 SDS-PAGE [258]

a) Sample preparation

Reagents

Lysis buffer: Triton X-100 (1%), NaCl (150 mM), EDTA (5 mM), EGTA (2 mM), Sodium fluoride (50 mM), Sodium orthovanadate (1 mM) and protease inhibitor cocktail (1 µl/100µl).

Protocol

Cells were harvested using Trypsin EDTA and washed with PBS. The cells were pelleted and incubated on ice for 40 minutes in the presence of lysis buffer. Lysate was clarified by centrifugation at 10,000 rpm for 20 minutes and stored at -80°C until further use.

b) Protein Estimation

Reagents

0.5 mg/ml Bovine serum albumin (BSA) in D/W, Bradford's reagent

Protocol

In a 96-well plate 1.25, 2.5, 3.75 and 5 µg of BSA i.e. 2.5 µl, 5 µl, 7.5 µl and 10 µl of 0.5 mg/ml of BSA was taken. Volume was made up to 10 µl with distilled water. 10 µl of sample was taken in the rest of the wells. Water was kept as blank. To it 100 µl of

Bradford's reagent was added. Absorbance was taken at 595 nM using SoftMax Pro software. The estimation was done in triplicates. Sample concentration was automatically given by the software, using the BSA standard.

c) Sample Buffer (6X)

Reagents

Glycerol	6 ml
1M Tris pH 6.8	3 ml
SDS	1.2 gm
β-ME (2-mercaptoethanol)	600 μl
Bromophenol blue 0.05%	0.005 gm

Protocol

50 μg of protein lysate (untreated and PTX treated) was mixed with 6X sample buffer in a ratio of 5:1. The volume of the samples was normalized with D/W and the samples were boiled for 5 minutes in a boiling water bath for denaturation and then resolved on SDS-PAGE.

d) Gel Casting and electrophoresis

Reagents

30% Acrylamide mixture (29.2% acrylamide + 0.8% bis-acrylamide) solution was prepared in D/W, filtered through Whatmann filter # 3 and stored at 4°C in an amber coloured bottle.

1.5 M Tris-HCl pH 8.8 (resolving buffer)

1M Tris-HCl pH 6.8 (stacking buffer)

10% SDS solution: 10 gm of SDS was added to 100 ml of water, heated to 70°C for SDS to dissolve completely.

10% Ammonium persulphate (APS) solution

N,N,N',N'-Tetramethylethylenediamine (TEMED)

Pre-stained molecular protein marker

Tank Buffer: 196 mM Glycine, 50 mM Tris HCl and 0.1% SDS. pH was adjusted to 8.3

Agarose 1%

Mini gel dual assembly

Power Pack

Resolving gel recipe 30 ml volume (for 2 mini gels):

D/W 13.9 ml

Acrylamide mixture 8 ml

1.5 M Tris pH 8.8 7.5 ml

10% SDS 300 µl

10% APS 300 µl

TEMED 18 µl

Stacking gel Recipe 10 ml volume (for 2 mini gels):

D/W 6.8 ml

Acrylamide mixture 1.7 ml

1M Tris pH6.8 1.25 ml

10% SDS 100 µl

10% APS 100 µl

TEMED 10 µl

Protocol

The glass plates were wiped with 70% alcohol and assembled. The bottom and the sides of the glass plates were sealed using 1% molten agarose. When solidified the resolving gel mixture was poured gently leaving some space for the stacking gel. The gel mixture was overlaid with methanol to give a uniform gel front and kept for polymerization for 20-30 minutes. When polymerization was over, the methanol and the un-polymerized gel mixture was removed, washed with D/W. The stacking gel mixture was poured on top of the resolving gel and a comb was inserted. Stacking gel was allowed to polymerize, following which the wells were washed with D/W and marked. The assembly cathodic and anodic chamber was filled with tank buffer and the wells were loaded with the denatured sample. A molecular weight marker was loaded in one well. Electrophoresis was carried out at 25 mA for the stacking and then the further run was carried out at 30 mA. Run was stopped when the dye front reached 1 mm above the gel end.

e) Protein transfer

Protein transfer

Reagents

Wet Transfer buffer: 25 mM Tris, 192 mM glycine, 20% v/v methanol, pH 8.3

Poncue S solution: 0.1% Poncue powder in 5% acetic acid

Polyvinylidene difluoride (PVDF) membrane

Protocol

The PVDF membrane was cut according to the size of the gel and pre-wetted with methanol for 5 minutes before equilibration. The resolved gel and the membrane both were equilibrated with the transfer buffer for 20 minutes. Four whatmann filter #3 sheets

were cut according to the size of membrane. After equilibration the membrane was kept over the gel and this was sandwiched between the folds of filter paper, two on either side. Care was taken to avoid any bubbles being trapped. The sandwich was then kept between the electrode plates of the transfer assembly (gel towards the cathode). The transfer assembly was filled with the transfer buffer. Transfer was carried out for 16 hr at constant 10 V or for 1 hr at 100 V in a cold room. The membrane was stained with Poncue solution till the pink bands appeared. The side containing the bands were marked and then destained by rinsing in D/W.

f) Western blotting [258]

Reagents

TBS: 50 mM Tris pH 7.5, 0.85% NaCl; pH was adjusted to 7.6, solution was autoclaved and stored at 4°C.

TBST: To 1 litre of TBS 1 ml of Tween 20 was added, stirred well and used.

Blocking Solution: 5% non-fat skimmed milk powder in TBST; kept at 37°C for 15 minutes to dissolve completely, 5% BSA in TBST or 5% goat serum made in TBST.

Primary and Secondary antibody dilutions: The antibodies were diluted in 2.5% non-fat skimmed milk/BSA/serum made in TBST.

Super-Signal West Femto kit

Developing cassette

Plastic boxes

X-ray films

Protocol

The membrane was blocked with the blocking reagent for the mentioned duration. The blots were then washed vigorously with TBST for 5 minutes. The blot was taken in a plastic bag, overlaid with primary antibody and kept on a rocker for the mentioned time. After incubation, blots were washed with TBST 3 times, for 10 minutes each. Blots were then incubated for 1 hr with HRP conjugated secondary antibody. The nonspecific binding was removed by 3 TBST washes, 10 minutes each. The table below provides the details of the western blotting carried out.

Protein	Mol Wt. KDa	Blocking	1° Antibody	Incubation	2° Antibody
αv	125	5% Skimmed milk (1 h)	1:250	1 h	1:6000
$\alpha 2$	150	5% goat serum (1 h)	1:2000	1 h	1:6000
$\alpha 3$	150	5% Skimmed milk (1 h)	1:500	1 h	1:6000
$\alpha 5$	150	5% Skimmed milk (1 h)	1:1000	1 h	1:6000
$\beta 1$	125	5% Skimmed milk (1 h)	1:3000	1 h	1:6000
$\beta 3$	125	5% goat serum (1 h)	1:2000	1 h	1:6000
$\beta 5$	100	5% Skimmed milk (1 h)	1:250	1 h	1:6000
FAK	125	5% BSA (1 h)	1:500	Overnight	1:6000
pFAK	125	5% BSA (1 h)	1:3000	Overnight	1:3000
ERK1/2	44,42	5% BSA (1 h)	1:3000	Overnight	1:6000
pERK1/2	44,42	5% BSA (1 h)	1:3000	Overnight	1:6000
AKT	60	5% BSA (1 h)	1:3000	Overnight	1:3000

Materials And Methods...

pAKT	60	5% BSA (1 h)	1:1000	Overnight	1:6000
VEGF	42	5% Skimmed milk (1 h)	1:1000	1 h	1:6000
Cyclin D1	36	5% BSA (1 h)	1:3000	Overnight	1:6000
Cdk4	30	5% BSA (1 h)	1:2000	Overnight	1:6000
Cdk6	36	5% BSA (1 h)	1:2000	Overnight	1:6000
p53	53	5% Skimmed milk (1 h)	1:500	1 h	1:6000
Bcl-2	28	5% BSA (1 h)	1:1000	Overnight	1:6000
Bcl-xL	30	5% BSA (1 h)	1:1000	Overnight	1:6000
Mcl-1	40	5% BSA (1 h)	1:1000	Overnight	1:6000
Cleaved caspase 9	35	5% BSA (1 h)	1:2000	Overnight	1:6000
Cleaved caspase 3	19	5% BSA (1 h)	1:2000	Overnight	1:6000
Cleaved PARP	89	5% BSA (1 h)	1:2000	Overnight	1:6000
β-Tubulin	55	5% BSA (1 h)	1:3000	1 h	1:6000

The blots were then taken to the dark room for visualization of the signal. Super-signal west femto developing reagent was made as per the manufacturer's instructions. The blot was kept on a clean glass plate and on the probed side Super signal west femto mixture was added and incubated for 5 minutes. After incubation excess reagent was drained on the filter paper and the blot was kept in the developing cassette in between two transparent plastic sheets. On to the protein side X-ray sheet was kept and exposed for various times depending upon the signal intensity. The exposed films were developed in the developing machine. Equal loading was checked by studying β -tubulin expression.

3.2.14 Immunofluorescence

Reagents

Fixative: Methanol at -20°C, Paraformaldehyde- 0.4 gm of paraformaldehyde was added to 10 ml of boiling PBS. pH was adjusted to 7.4.

Permeabilizing solution: 0.1% Triton X-100 in PBS.

Blocking solution: 1% BSA made in PBS

Primary antibodies against integrin $\alpha 5\beta 1$: Diluted in PBS

Secondary antibodies conjugated with Alexa 568: Diluted in PBS

Mountant: 4% DABCO in 90% of glycerol PBS. Aliquot and stored at -20°C

Transparent nail polish

Protocol

MDA-MB-231 cells were grown on coverslips and then treated with sub-toxic doses of PTX for 24 hr. The coverslips were then washed twice with PBS and fixed in 4% paraformaldehyde for 10 minutes at 37°C. The coverslips were washed twice with PBS, permeabilized with 0.5% triton X-100 for 10 minutes and then blocked in 1% BSA for half an hour. The coverslips were overlaid with $\alpha 5\beta 1$ primary antibody (1:20) and incubated in a humidifying chamber for overnight at 4°C. After incubation, the coverslips were given 3 washes with PBS and overlaid with secondary antibody conjugated with the dye Alexa568 (1:200) and kept in dark. After 1 hr, 3 washes were again given with PBS and the coverslips were mounted on glass slides in 4% DABCO glycerol. Cells incubated with the fluoro-chrome conjugated secondary antibodies alone (no primary antibody) were used as negative controls. Images were acquired at 63X using the LSM

510 META laser scanning microscope from Carl Zeiss, Germany. Images were analyzed using the software LSM 510.

3.2.15 G-LISA assay for RhoGTPases

Reagents

G-LISA kit from Cytoskeleton, PBS

Protocol

The assay was performed as per the manufacturer's instructions from cytoskeleton™. Both Rac and Rho activation assay kits were used for determination of active levels of GTPases in cellular lysates. Briefly, 50 µg of cell lysates (untreated, PTX treated 1 mM, 2.5 mM and 5 mM) were added to the active Rac or Rho coated plates. Plates were then incubated with intermittent shaking. Primary and secondary antibodies were added sequentially for 1 hr each. (Rac-1°antibody is 1:200 and 2° is 1:100 while for RhoA 1°antibody is 1:250 and 2° is 1:62.5). Color development was seen by addition of HRP detection reagent and then the reaction was stopped by addition of stop reagent. Plates were then read at 490 nm using a spectrophotometer. The results were plotted as % activity considering untreated control as 100%.

3.2.16 Actin staining using phalloidin-FITC [107]

Reagents

4% Paraformaldehyde (PFA): 4 gm PFA was dissolved in PBS and the temperature was brought to 37°C

Phalloidin staining solution: A 50 µg/ml solution of phalloidin-FITC was made in 0.05% BSA and used.

Protocol

Cells grown on coverslips (untreated and PTX treated) were washed with PBS and fixed by incubating them for 10 minutes at 37°C with freshly prepared 4% paraformaldehyde. Coverslips were washed with PBS and permeabilized using 0.1% Triton X100 at room temperature for 10 minutes. Coverslips were then overlaid with 20 µl of Phalloidin mixture and incubated at 37°C for 10 minutes in a humid chamber. Coverslips were overlaid with equal volume (20 µl) of 4% BSA and incubated for 10 minutes at room temperature. Coverslips were washed with PBS and were mounted on a clean glass slide in the mounting media and sealed with the help of nail polish. Cytochalasin-B was used as a positive control. Images were acquired at 63X using the LSM 510 META laser scanning microscope from Carl Zeiss, Germany. Images were analyzed using the software LSM 510.

3.2.17 Caspase-3 and caspase-9 activation assays for apoptosis

Reagents

ApoTarget™ caspase colorimetric protease assay kit from Invitrogen.

Protocol

Cell lysates were prepared for untreated control and PTX treated samples *viz.* 1 mM, 2.5 mM and 5 mM using caspase lysis buffer, supplied as a part of kit component. 200 µg of protein solution was added with subsequent addition of substrates LEHD (Leucine-Glutamate-Histidine-Aspartate), DEVD (Aspartate-Glutamate-Valine-Aspartate) for caspase-9 and caspase-3 respectively in a 96-well plate format. Plate was incubated for at least 2 hr at 37°C and later read at 405 nm in a spectrophotometer. Results were plotted as % fold increase considering untreated control to be unity.

3.2.18 *In vivo* xenograft model [259]

Reagents

70% ethanol, PBS, PTX stock 71.86 mM.

Female NOD-SCID mice

Syringes

Vernier caliper

Protocol

Briefly, 2×10^6 MDA-MB-231 cells suspended in plain DMEM were injected in the flanks of female SCID mice (5 mice were taken per group) after the flanks were cleaned with 70% ethanol. The latency period was found to be around 5 days. Tumours were allowed to grow and when the tumours had grown to an average size of 50 mm^3 [260] mice were randomized and divided into 3 groups (a) PBS only (b) PTX 40 mg/kg and (c) PTX 60 mg/kg. PTX was administered intraperitoneally (i.p) for a period of 9 days consecutively ie from day 9th to 17th respectively. Tumour volume and animal weight were measured on alternate days. Tumour volume was calculated by the formula $1/2(a \times b^2)$, where a is the long diameter and b is the short diameter. Mice were sacrificed on day 21st and photographs were taken. The results were plotted as tumour volume vs. days post tumour transplantation.

3.2.19 *In vivo* intradermal model for angiogenesis [105]

Reagents

70% ethanol, PBS, PTX stock 71.86 mM.

Female NOD-SCID mice

Syringes

Vernier caliper

Dissection box

Protocol

Briefly, 1×10^6 MDA-MB-231 cells were injected intradermally into the ventral side of 6-8 week old female NOD-SCID mice. The tumour latency period was 3 days. Mice were randomized into 3 groups (n=5) as described previously (a) PBS only (b) PTX 40 mg/kg and (c) PTX 60 mg/kg. PTX treatment was started from day 4th till day 12th i.p for 9 days. Tumour volume and animal weights were measured alternatively as performed previously. Mice were sacrificed on day 15th and the animals bearing tumours were photographed. Later, the skin bearing tumours was excised and blood vessels around the growing tumour mass were counted.

3.2.20 *In vivo* experimental metastasis [105]

Reagents

70% ethanol, PBS, PTX stock 71.86 mM, 10% buffered formalin.

Female NOD-SCID mice

Syringes

Dissection box

Protocol

Briefly, 1×10^6 cells were injected intravenously (i.v) in 6-8 weeks old female NOD-SCID mouse. The animals were divided into 3 groups (a) PBS only (b) PTX 40 mg/kg (c) PTX 60 mg/kg. PTX was injected i.p from day 1 to day 9 continuously. The animals were later sacrificed after a period of 30 days when mice were found to be moribund. Animals were dissected and lungs were taken out and fixed in buffered formalin solution. The tissues

were sectioned and then stained using haemotoxylin-eosin. Images were then captured using an upright microscope from Zeiss (Germany) and the colonies were counted.

3.2.21 Chick chorioallontic membrane (CAM) assay

Reagents

70% ethanol, PBS, PTX

White Liver horn Eggs

Protocol

To study the effect of PTX on angiogenesis CAM assay was carried out. Eggs were incubated at 37°C and 70% relative humidity for a period of 5 days. The eggshells were swiped with 70% alcohol and a small aperture was made on the air sac with the help of a sterile scalpel. 10 µl of the drug solution (400 µg) was added in the air space with the help of a micropipette. The aperture was then sealed with parafilm. Eggs were kept at 37°C. The experiment was terminated on the subsequent day and photographs were taken after cut opening of the eggs.

3.2.22 *In vivo* xenograft model for combination study [259]

Reagents

70% ethanol, PBS, PTX stock 71.86 mM, 10% buffered formalin

Doxorubicin and lipodox stock 2 mg/ml.

Female NIH-3 nude mice

Syringes

Vernier caliper

Dissection box

Protocol

Briefly, 2×10^6 MDA-MB-231 cells were injected into the right flank of 6-8 week old female Nude (NIH-3) mice. Mice were then divided into 6 groups (n=5) namely (a) Untreated or UC (PBS only), (b) DOX (4 mg/kg), (c) LD (4 mg/kg), (d) PTX 60 mg/kg (e) PTX+LD (40 mg/kg and 1 mg/kg) (f) PTX+LD (40 mg/kg and 2 mg/kg). Tumour latency period was found to be 4 days. Treatment was started from day 7th. PTX was administered intraperitoneally (i.p) for a period of 9 days consecutively while DOX/LD were injected intravenously (i.v) once a week for 2 weeks respectively. The tumour volumes and animal weights were measured alternately as described previously. Mice were sacrificed on day 17th and photographs were taken.

3.2.23 Statistics

The experiments were performed at least thrice independently and the values represented are indicative of Mean \pm SEM. One way ANOVA (Equal variances assumed) was used for statistical significance where $P < 0.05$ was considered to be statistically significant.

Chapter 4

Results

4.1 PTX affects cellular proliferation in dose dependent manner

MTT assay was performed to determine the IC_{50} of PTX in a time and dose dependent manner (24 hr, 48 hr and 72 hr). As seen in (Figure 4.1), IC_{50} showed a significant decrease as exposure time of PTX was increased. The observed IC_{50} of PTX on MDA-MB-231 cells was found to be 9 mM, 3 mM and 2 mM after 24 hr, 48 hr and 72 hr respectively. These results clearly demonstrated the anti-proliferative effect of PTX as observed by a dose dependent decrease in cell viability at all the time intervals under investigation. Based on this observation, the subsequent experiments were carried out at sub-toxic doses such as 1 mM, 2.5 mM and 5 mM of PTX for a 24 hr exposure. Cancer cells have a self sufficiency to growth signals and can form clones. PTX (1-20 mM) showed a dose dependent decrease in colony formation (Figure 4.2a and 4.2b) leading to $81.7 \pm 2.69\%$, $57.14 \pm 2.12\%$, $16.11 \pm 0.87\%$, $0.75 \pm 0.37\%$ at 1 mM, 2.5 mM, 10 mM and 20 mM respectively compared to untreated cells ($P < 0.05$). Thus, only a fraction of seeded cells are able to self reproduce them with increasing concentration of PTX.

Figure 4.1

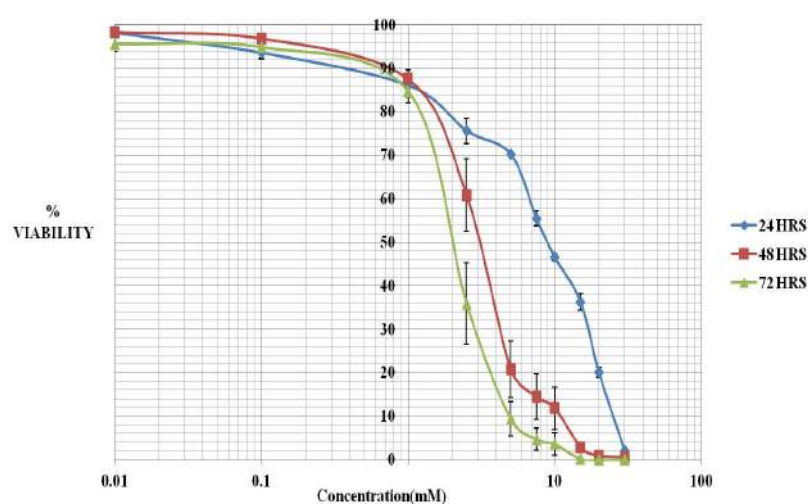
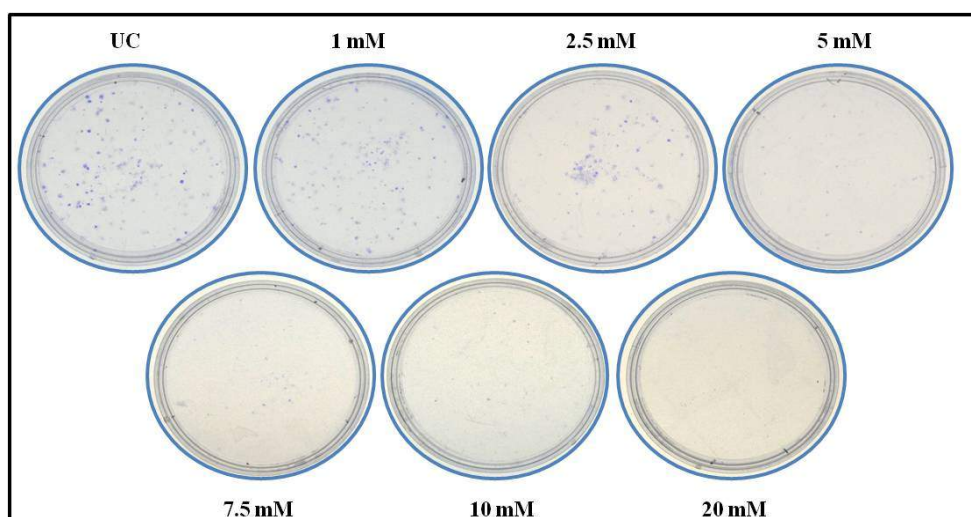


Figure 4.1: PTX affects the proliferation potential of MDA-MB-231 cells.

MTT assay was carried out to study the effect of 24 hr, 48 hr and 72 hr of PTX (0.01-30 mM) treatment on MDA-MB-231 cells. IC_{50} was calculated from the dose effect plots considering untreated control as 100% viable. IC_{50} for 24 hr, 48 hr and 72 hr was 9 mM, 3 mM and 2 mM respectively. Results are representative of three independent experiments (Mean \pm SEM).

Figure 4.2

(a)



(b)

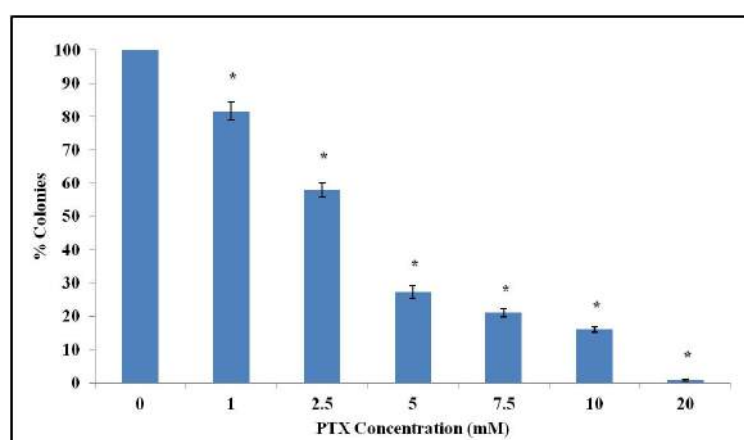


Figure 4.2: PTX decreases the clonogenic potential.

Cells were treated with PTX (1-20 mM) for 24 hr and then allowed to grow further. Number of colonies at the end of 8 days of incubation were stained and counted. (a) Qualitative representation of colonies (b) plot representing percentage colonies against increasing PTX concentration, considering the untreated control as 100% colonies. A significant dose dependent decrease in colony formation is observed. Results are representative of three independent experiments Mean \pm SEM. * $P < 0.05$.

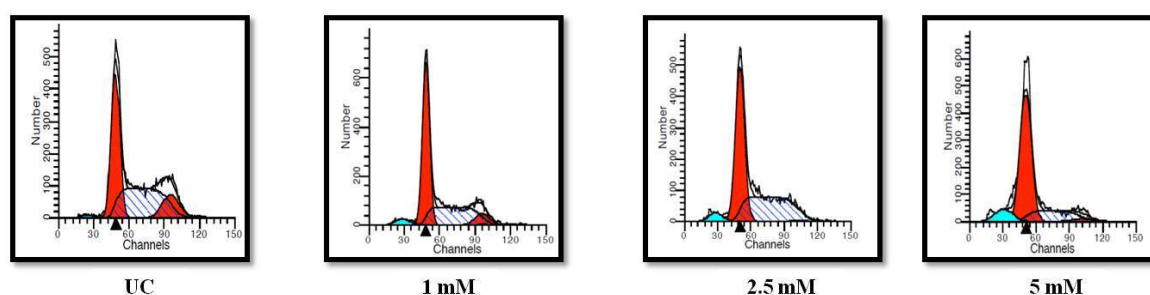
4.2 PTX brings an alteration in cell cycle profile and induces apoptosis

PTX affected cellular proliferation in a dose and time-dependent manner. However, its effect on cell cycle needs to be demonstrated. Flow cytometry was performed to evaluate the ploidy status of MDA-MB-231 cells treated with sub-toxic doses of PTX. As evident from (Figure 4.3a and 4.3b) PTX induces a G0-G1 block. There was a significant increase in percentage of cells in G1 phase i.e from 36.81 \pm 2.87% in untreated control to 57.85 \pm 2.5%, 62.74 \pm 4.68% at 2.5 mM and 5 mM respectively ($P < 0.05$) (Table 4.1). Since, PTX exerted a cell cycle blockade it leads to cellular apoptosis. Thus, EB/AO staining was performed to validate the same. There was an increase in number of apoptotic cells at sub-toxic doses of PTX represented as red coloured cells compared to live green coloured cells (Figure 4.4). To further corroborate our findings, AnnexinV/FITC staining was done to determine the apoptosis inducing ability of PTX at sub-toxic doses. AnnexinV has an affinity for phosphatidylserine (PS) found in the inner leaflet of non-apoptotic cells. However, PS translocates to the outer membrane of apoptotic cells. There is a significant increase in the early apoptotic cells (shown in the lower right quadrant) as well as late apoptotic cells (upper right quadrant) in a dose

dependent manner compared to the untreated control ($P < 0.05$) (Figure 4.5a and 4.5b). In addition, we had assessed the effects of sub-toxic doses of PTX on apoptotic signaling molecules. PTX decreased the levels of anti-apoptotic proteins such as Bcl-2 and Bcl-xL in a dose dependent manner. It also affected the expression and activities of both caspase 9 and caspase 3 in a dose dependent manner (Figure 4.15c and 4.15d).

Figure 4.3

(a)



(b)

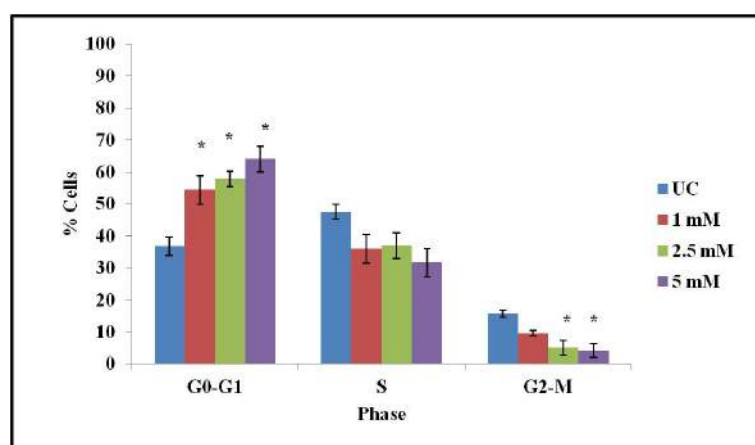


Figure 4.3: PTX brings an alteration in the cell cycle.

MDA-MB-231 cells treated with sub-toxic concentrations of PTX for 24 hr were stained with PI and acquired using FACS Calibur. (a) Ploidy level at sub-toxic doses compared

to control. (b) Graphical representation of PTX treated cells in different phases of cellular cycle. PTX treated cells showed accumulation in G0-G1 phase, decrease in S and G2-M phases. Results are representative of three independent experiments Mean \pm SEM. * P <0.05.

Table 4.1. Tabulation of different cell cycle phases upon PTX treatment.

	G0-G1	S	G2-M
Untreated	36.81	47.5	15.68
1 mM	54.38	36.01	9.6
2.5 mM	57.85	37.04	5.1
5 mM	64.05	31.64	4.3

Figure 4.4

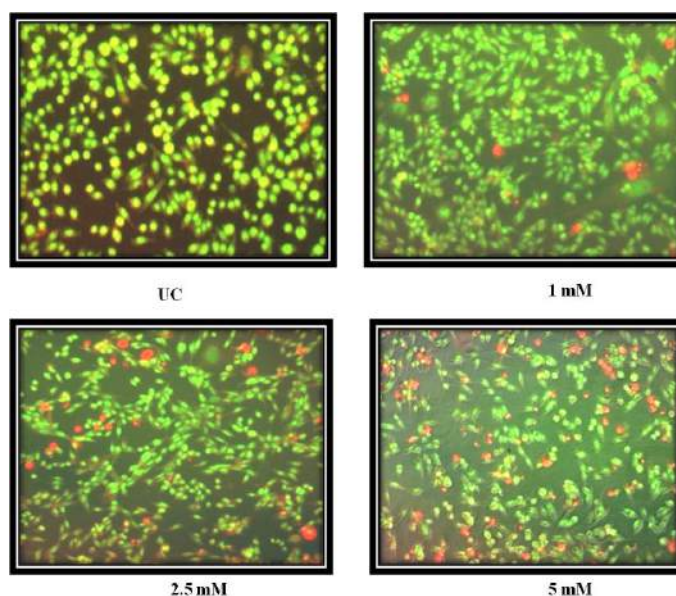


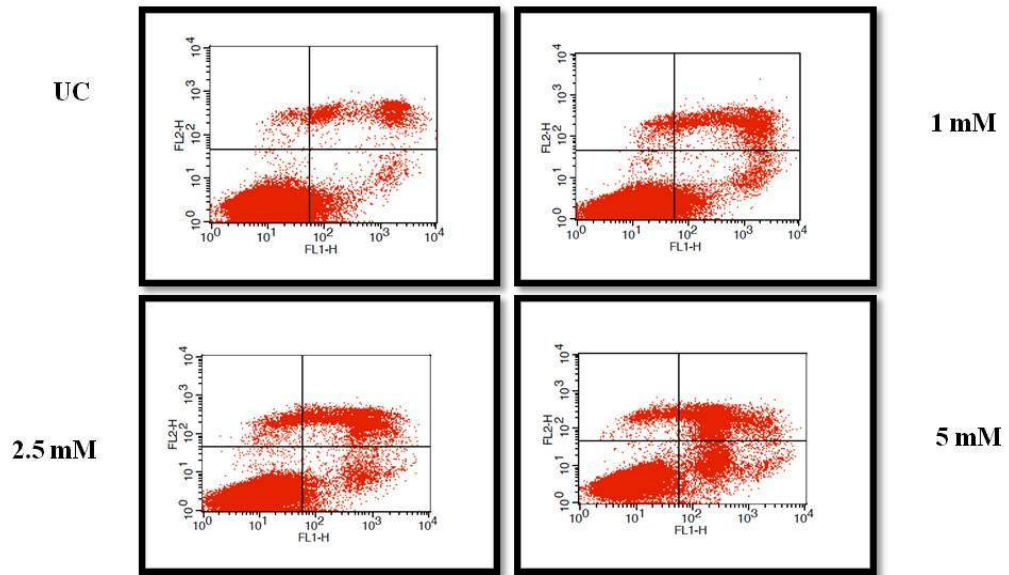
Figure 4.4: EB/AO Staining shows the apoptotic inducing activity of PTX.

Cells treated with PTX in 96-well plates for 24 hr were centrifuged and equal volumes of EB/AO were added. AO fluoresce green in live cells while EB fluoresces orange/red

when intercalated with DNA in dead cells. PTX treated cells showed an increase in apoptosis. Results are representative of three independent experiments.

Figure 4.5

(a)



(b)

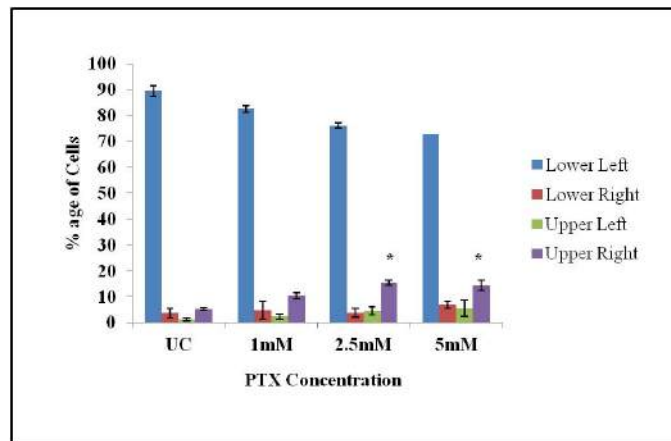


Figure 4.5: AnnexinV/FITC staining showing the apoptotic inducing activity of PTX.

Cells treated with sub-toxic doses of PTX were stained with AnnexinV, a molecule with high affinity towards Phosphotidyl Serine (PS) found on outer surface of apoptotic cells.

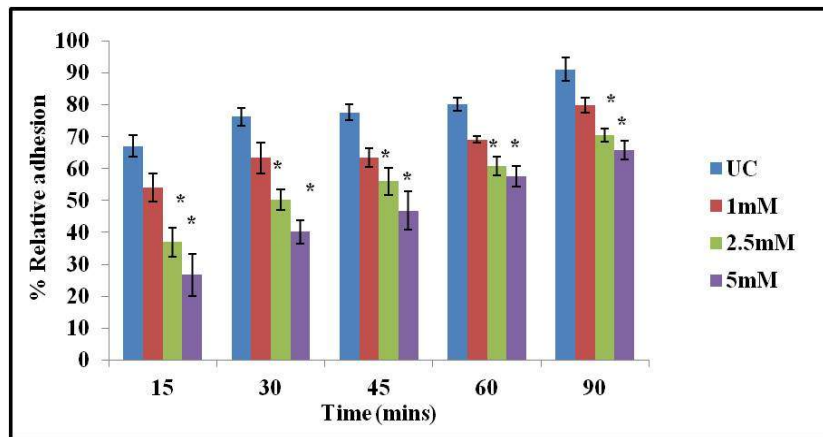
(a) Increase in number of apoptotic cells is visible with increasing doses of PTX (lower and upper right quadrants) respectively. (b) Graphical representation. X-axis represents AnnexinV/FITC while Y-axis denotes Propidium Iodide (PI).

4.3 PTX affects cellular adhesion to ECM

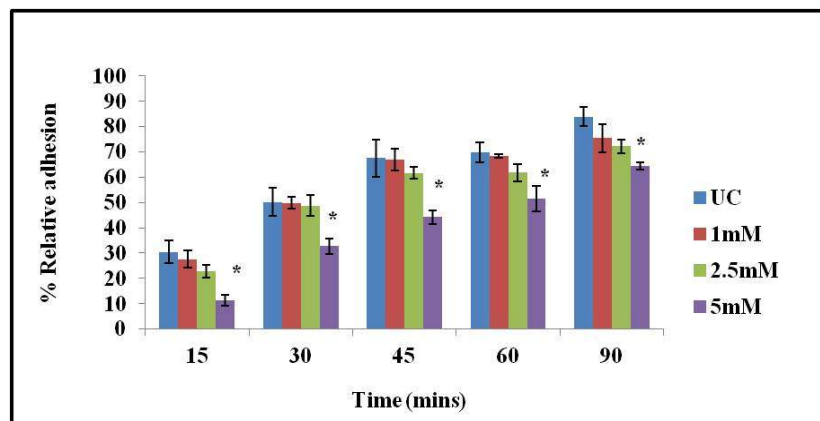
During the process of metastasis, the transformed cells need to alter their adhesive behavior for successful migration and invasion through the surrounding/underlying matrix so as to reach the bloodstream. In light of this, effect of PTX was evaluated on adhesion to ECM substrates viz. matrigel, collagen type IV, fibronectin, laminin, vitronectin using sub-toxic doses at different time points 15 min, 30 min, 45 min, 60 min and 90 min respectively using adhesion assay. Treatment with PTX significantly affected the adhesion to matrigel, collagen type IV, fibronectin and laminin in a dose and time-dependent manner (Figure 4.6a-d). However, no significant change in adhesion was observed for vitronectin (Figure 4.6e). Adherence was found out to be $57.63 \pm 3.22\%$, $51.65 \pm 5.02\%$, $64.84 \pm 2.35\%$, $24.82 \pm 4.37\%$ at 5 mM compared to $80.08 \pm 2.1\%$, $69.82 \pm 3.86\%$, $90.91 \pm 0.58\%$, $45.63 \pm 2.99\%$ for untreated control at 60 min against matrigel, collagen type IV, fibronectin and laminin respectively ($P < 0.05$). Thus, PTX exerts anti-adhesive effects against MDA-MB-231 cells.

Figure 4.6

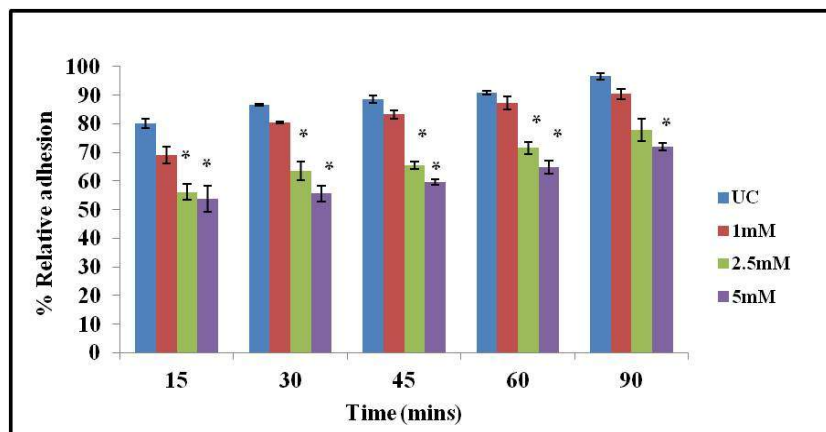
(a) Matrigel

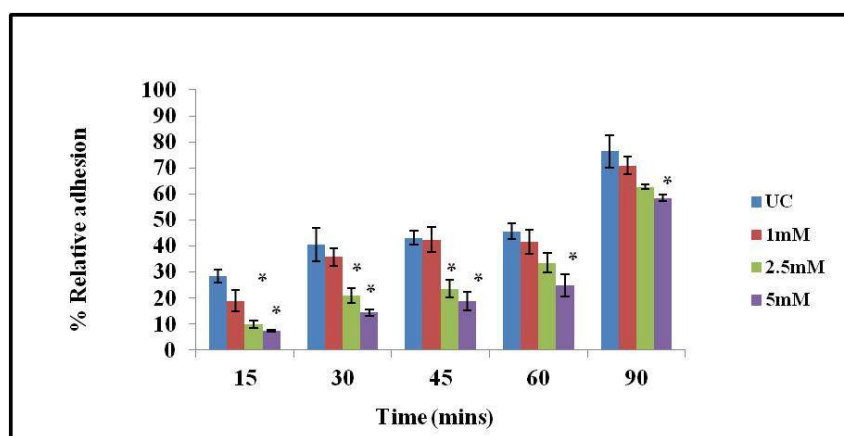
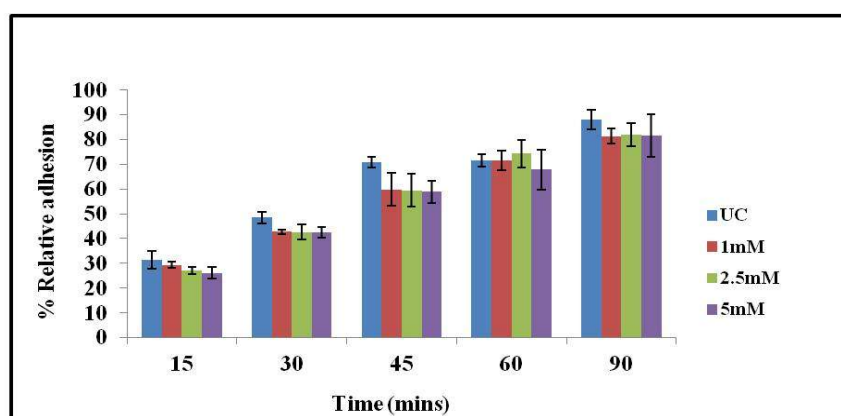


(b) Collagen Type IV



(c) Fibronectin



(d) Laminin**(e) Vitronectin****Figure 4.6: PTX decreases the adhesion to ECM substrates.**

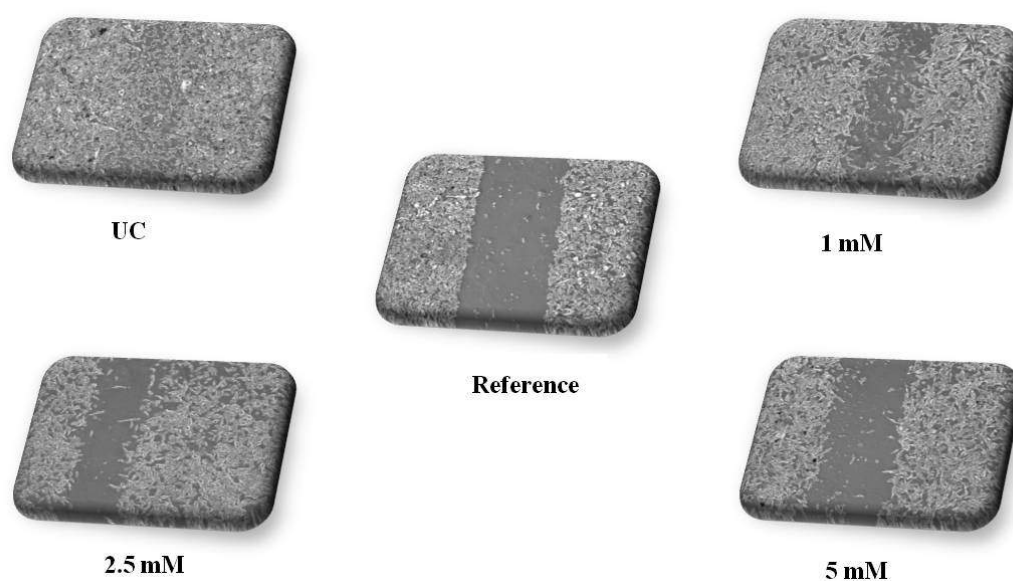
Cells were treated with sub-toxic doses of PTX for 24 hr, harvested and allowed to adhere to plates for 15, 30, 45, 60 and 90 min. Time and dose-dependent kinetics of adhesion to (a) Matrigel (b) collagen type-IV (c) fibronectin (d) laminin and (e) vitronectin. PTX treated cells showed a decrease in adherence at all time points. Values are representative of three independent experiments Mean \pm SEM.* P <0.05.

4.4 PTX impedes cellular motility and affects invasive potential

PTX at sub-toxic doses showed a significant reduction in motility of MDA-MB-231 cells (Figure 4.7a and 4.7b). At 1 mM, 2.5 mM, 5 mM wound coverage was found to be $69.54 \pm 2.93\%$, $54.87 \pm 2.02\%$ and $30.84 \pm 3.53\%$ considering the control as 100% ($P < 0.05$). Further, the activities of both gelatinases MMP-2 and MMP-9 were checked by subjecting the condition media to gelatin zymography. A dose dependent decrease in MMP-9 activity was observed (Figure 4.8a and 4.8b). At 2.5 mM, 5 mM a reduction in MMP-9 activity by $21.59 \pm 1.15\%$ and $32.37 \pm 4.16\%$ was seen as compared to the untreated control ($P < 0.05$).

Figure 4.7

(a)



(b)

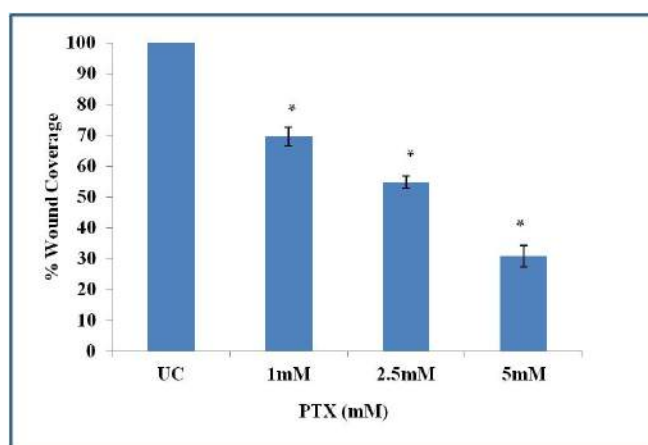
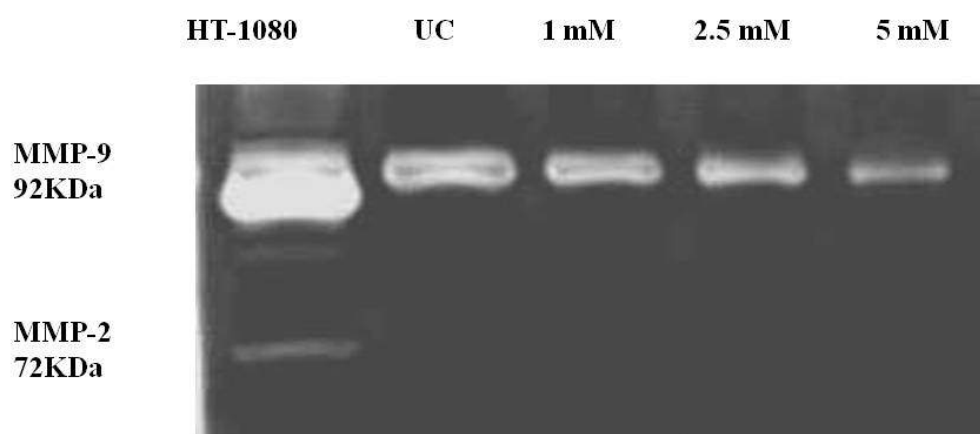


Figure 4.7: Cellular motility impeded by PTX.

Cells grown in 6-well plates were scratched using a sterile tip. Wound coverage was then monitored in the presence of PTX for 24 hr at sub-toxic doses. Initial and final wound widths were measured for control and treated groups. A representative picture of 10X magnification is shown as reference taken at initial zero time point. (a) Wound coverage in untreated control and PTX treated groups. (b) Quantitative representation of wound coverage. A significant reduction in migration at all the sub-toxic doses can be seen. Values are representative of three independent experiments Mean \pm SEM. * P <0.05 compared with untreated control.

Figure 4.8

(a)



(b)

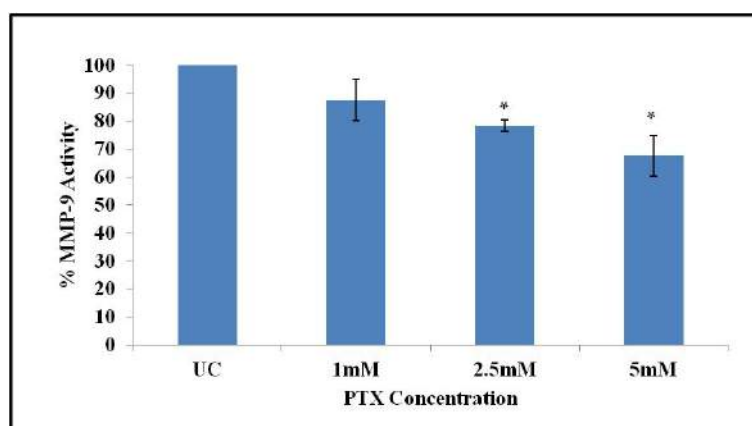


Figure 4.8: Gelatin zymography of PTX treated condition media.

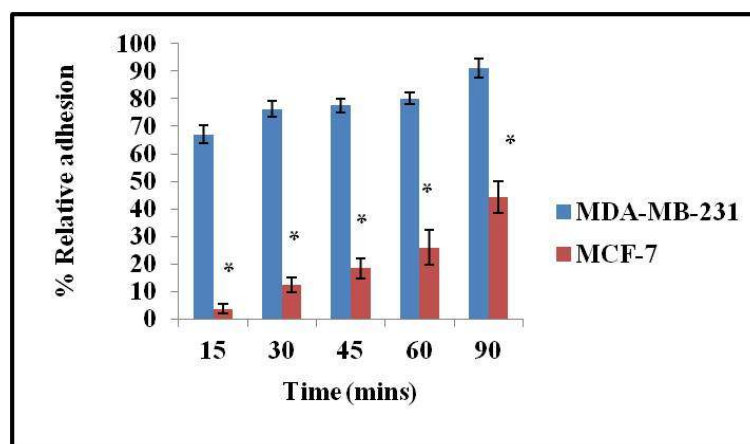
Condition media was collected from untreated and PTX treated cells after 24 hr. Gelatinase activity is visible as clear white zones in dark background. (a) Zymogram (b) quantification was done using densitometry considering untreated as 100%. Values are representative of three independent experiments Mean \pm SEM. * P <0.05.

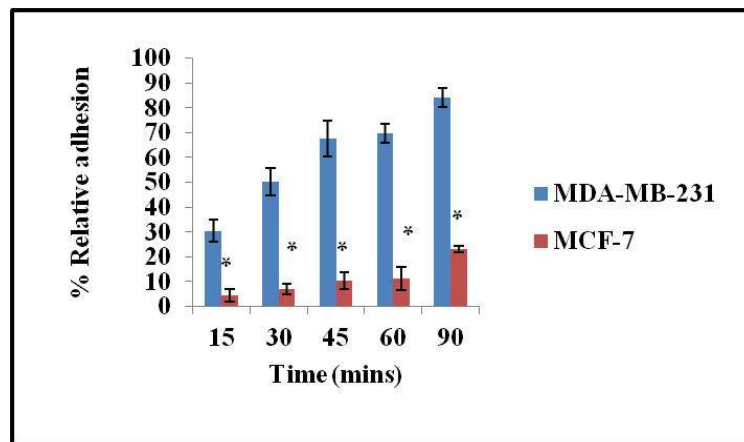
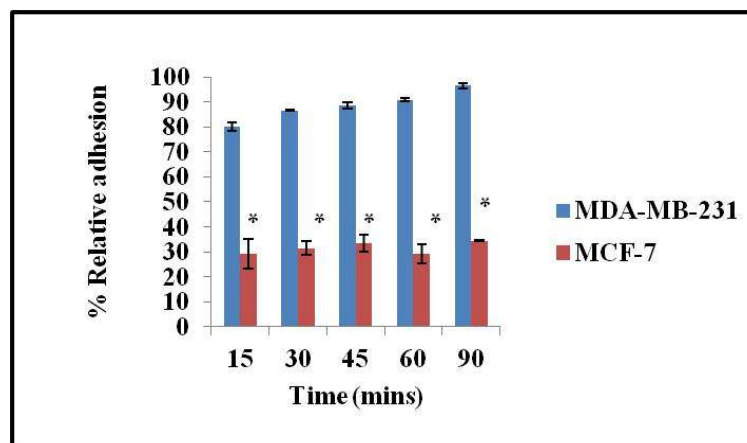
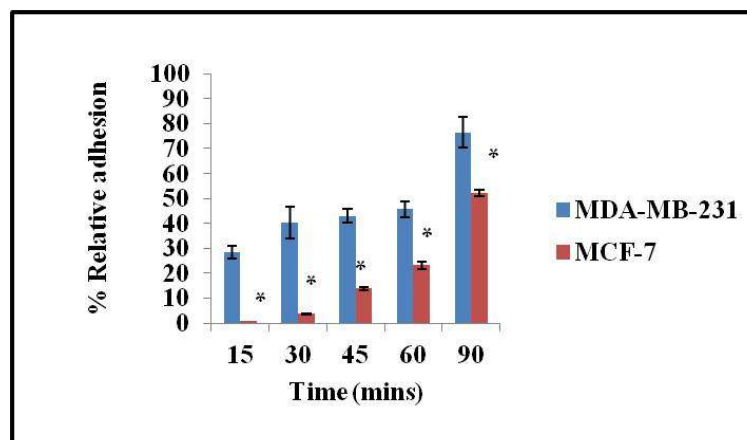
4.5 MDA-MB-231 displays higher adhesion potential than MCF-7 using ECM substrates

MDA-MB-231 cells displayed a significant and high adhesive potential to the ECM components at different time points 15 min, 30 min, 45 min, 60 min and 90 min respectively (Figure 4.9a-e). The % relative adhesion for MCF-7 was found to be 25.97±6.30%, 11.2±4.71%, 29.12±3.84%, 23.15±1.40%, 55.21±5.95% as compared to 80.08±2.1%, 69.82±3.86%, 90.91±0.58%, 45.63±2.99%, 71.4±2.48% for MDA-MB-231 against matrigel, collagen type IV, fibronectin, laminin and vitronectin respectively at 60 min ($P<0.05$).

Figure 4.9

(a) Matrigel



(b) Collagen Type IV**(c) Fibronectin****(d) Laminin**

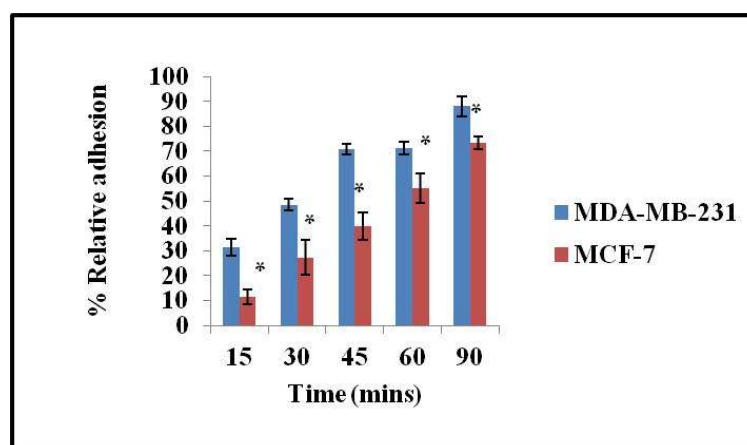
(e) Vitronectin

Figure 4.9: MDA-MB-231 cells exhibit higher adhesive potential to ECM components than MCF-7 cells.

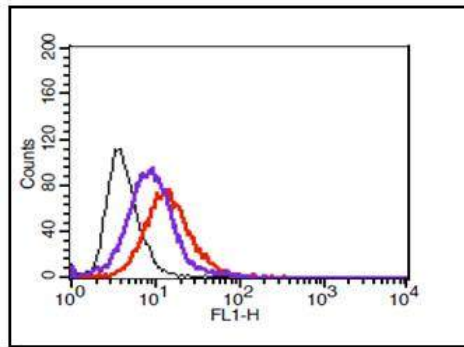
Adhesive potential was compared between MDA-MB-231 and MCF-7 cells towards ECM components at different time points (15, 30, 45, 60 and 90 min). MDA-MB-231 cells showed higher adhesion to (a) Matrigel (b) collagen type IV (c) fibronectin (d) laminin (e) vitronectin compared to lower metastatic MCF-7 cells. Values are representative of three independent experiments Mean \pm SEM. * $P < 0.05$.

4.6 MDA-MB-231 exhibit differences in surface expression of integrins compared to MCF-7

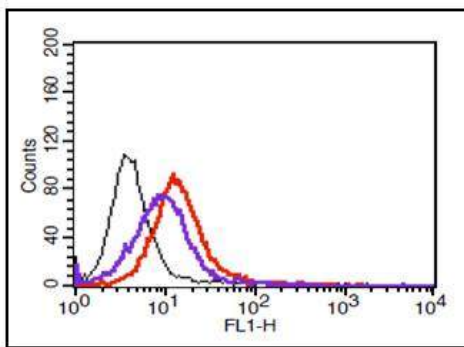
Both breast cell lines i.e MDA-MB-231 and MCF-7 were being tested for differences in surface expression of integrins using flow cytometry. MDA-MB-231 cells exhibited significantly higher levels of integrins such as α_v , α_3 , α_5 , β_1 , β_3 , β_5 , $\alpha_v\beta_3$, $\alpha_v\beta_5$ and $\alpha_5\beta_1$ (Figure 4.10a, 4.10c-i) compared to MCF-7. However, there was no marked difference observed in the surface expression of integrin α_2 between the two cell lines as shown in (Figure 4.10b).

Figure 4.10

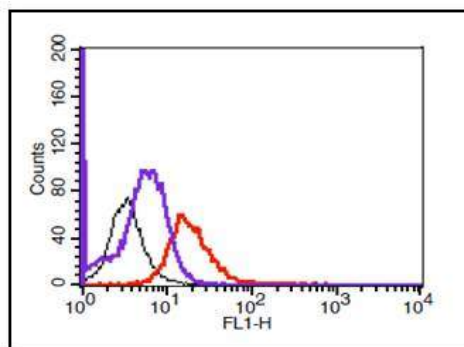
(a)



(b)

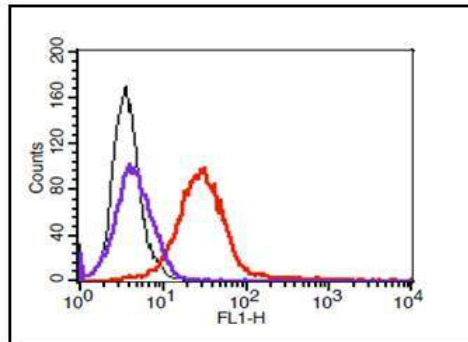


(c)

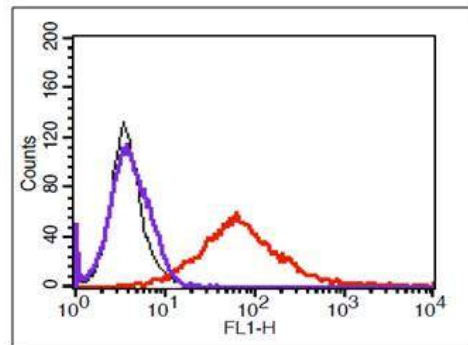


— 2⁰ Control
— MDA-MB-231
— MCF-7

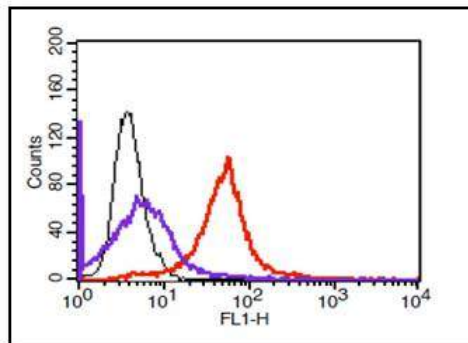
(d)



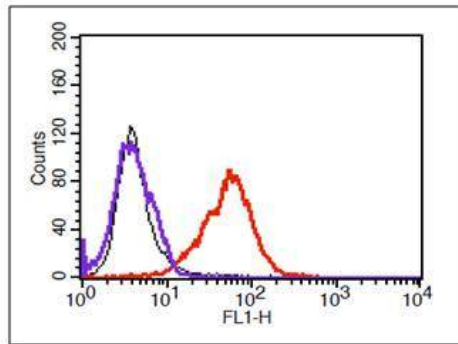
(e)



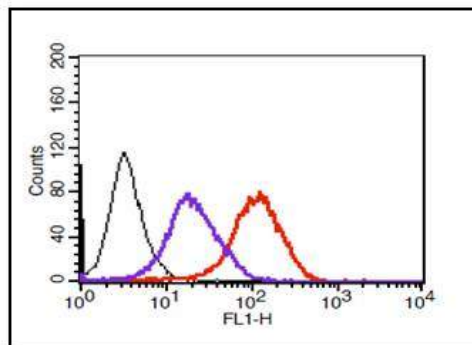
(f)



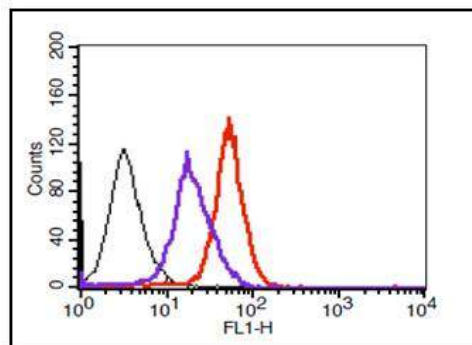
(g)



(h)



(i)



(j)

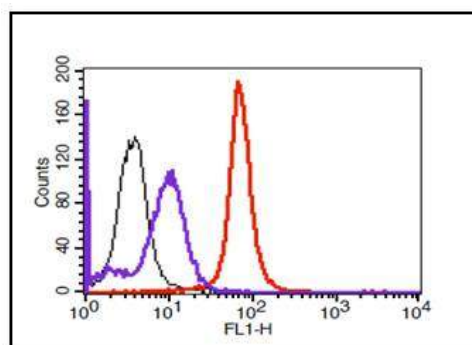


Figure 4.10: MDA-MB-231 displayed higher surface expression of integrins compared to MCF-7 cells.

Flow cytometry was performed to compare the surface expression of integrins (a) αv (b) $\alpha 2$ (c) $\alpha 3$ (d) $\alpha 5$ (e) $\beta 1$ (f) $\beta 3$ (g) $\beta 5$ (h) $\alpha v\beta 3$ (i) $\alpha v\beta 5$ and (j) $\alpha 5\beta 1$ between MDA-MB-231 and MCF-7 cells respectively. MDA-MB-231 cells expressed higher levels of all the integrins under investigation except $\alpha 2$.

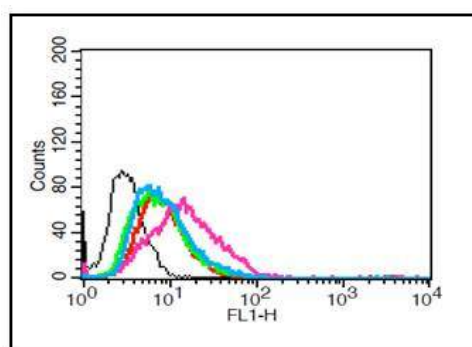
4.7 PTX demonstrates a differential effect on integrins expression in MDA-MB-231 cells

PTX affected the surface expression of integrins $\alpha 5$, $\beta 1$ or $\alpha 5\beta 1$ significantly. The relative mean fluorescence intensity (MFI) was found out to be 90.55 ± 6.81 , 70.49 ± 7.27 , 57.34 ± 1.22 for integrin $\alpha 5$; 81 ± 11.80 , 64.65 ± 4.74 , 61.23 ± 3.84 for integrin $\beta 1$ while 93.28 ± 2.28 , 76.97 ± 0.52 , 49.73 ± 0.29 for integrin $\alpha 5\beta 1$ at PTX doses of 1 mM, 2.5 mM and 5 mM, considering the MFI for untreated control to be 100% ($P < 0.05$) (Figure 4.11a and 4.11b). A decrease in surface expression was also observed for integrin $\beta 3$ at 5 mM but it was rather insignificant (Figure 4.11). However, for integrins αv , $\alpha 2$, $\alpha 3$, $\beta 3$ and $\beta 5$ there was no change in surface expression observed (Figure 4.11). PTX caused a decrease in surface localization of integrin $\alpha 5\beta 1$ using confocal microscopy as seen by the reduced

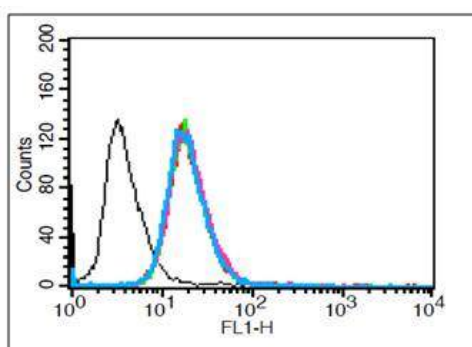
Fluorescence of PTX treated cells when compared to the untreated control (Figure 4.12). However, treatment with PTX did not affect the levels of transcripts at sub-toxic doses of the integrins αV , $\alpha 3$, $\alpha 5$, $\alpha 2$, $\beta 1$, $\beta 3$ and $\beta 5$ using RT-PCR (Figure 4.13). The changes in total protein levels was confirmed by western blotting that further showed a dose-dependent reduction in total levels of $\alpha 5$ and $\beta 1$ integrins (Figure 4.14). Further, a decrease in total protein levels was also observed for integrins αv , $\alpha 3$ and $\beta 3$ except for integrins $\alpha 2$ and $\beta 5$ respectively (Figure 4.14).

Figure 4.11

(a)

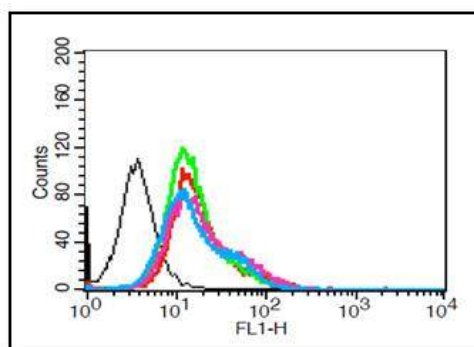


(b)

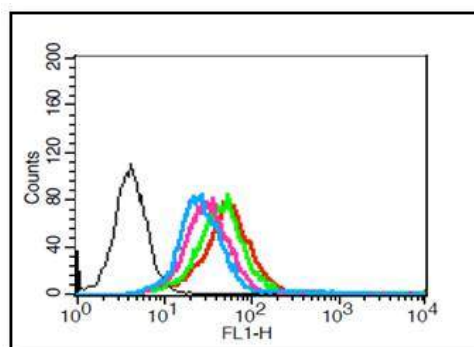


— 2⁰ Control
— UC
— 1 mM
— 2.5 mM
— 5 mM

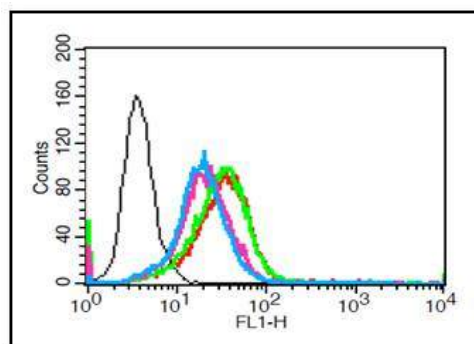
(c)



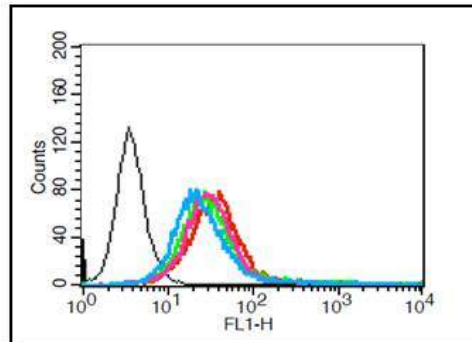
(d)



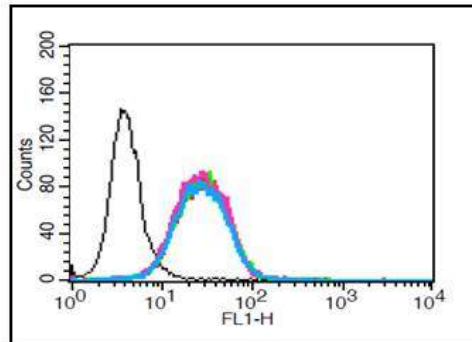
(e)



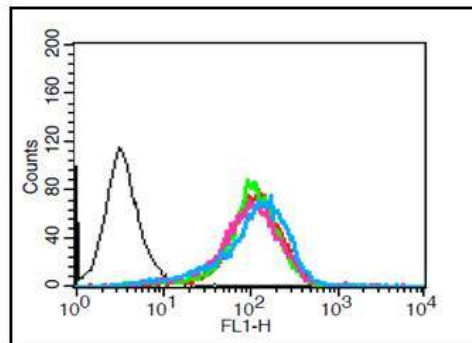
(f)



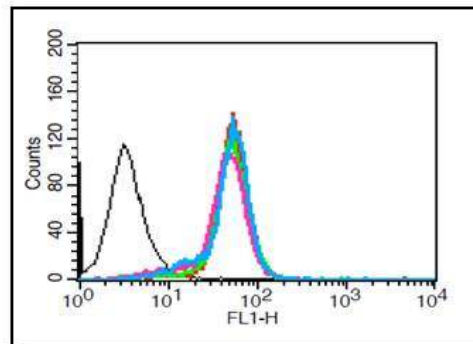
(g)



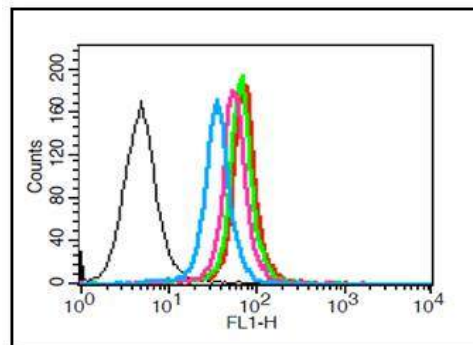
(h)



(i)



(j)



(k)

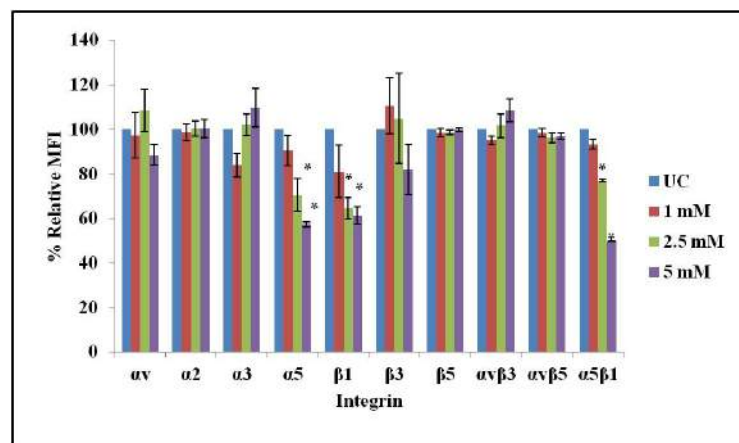


Figure 4.11: PTX affects surface expression of integrins $\alpha 5$, $\beta 1$ and $\alpha 5\beta 1$ using flow cytometry in MDA-MB-231 cells.

MDA-MB-231 cells were treated with sub-toxic doses of PTX (0 mM, 1 mM, 2.5 mM and 5 mM) for 24 hr to evaluate its effect on surface expression of integrins (a) αv (b) $\alpha 2$ (c) $\alpha 3$ (d) $\alpha 5$ (e) $\beta 1$ (f) $\beta 3$ (g) $\beta 5$ (h) $\alpha v\beta 3$ (i) $\alpha v\beta 5$ and (j) $\alpha 5\beta 1$. (i) Quantitative representation. PTX affects surface expression of integrins $\alpha 5$, $\beta 1$ and $\alpha 5\beta 1$ markedly while no effect was observed for integrins αv , $\alpha 2$, $\alpha 3$, $\beta 3$, $\beta 5$, $\alpha v\beta 3$ and $\alpha v\beta 5$ respectively.

Figure 4.12

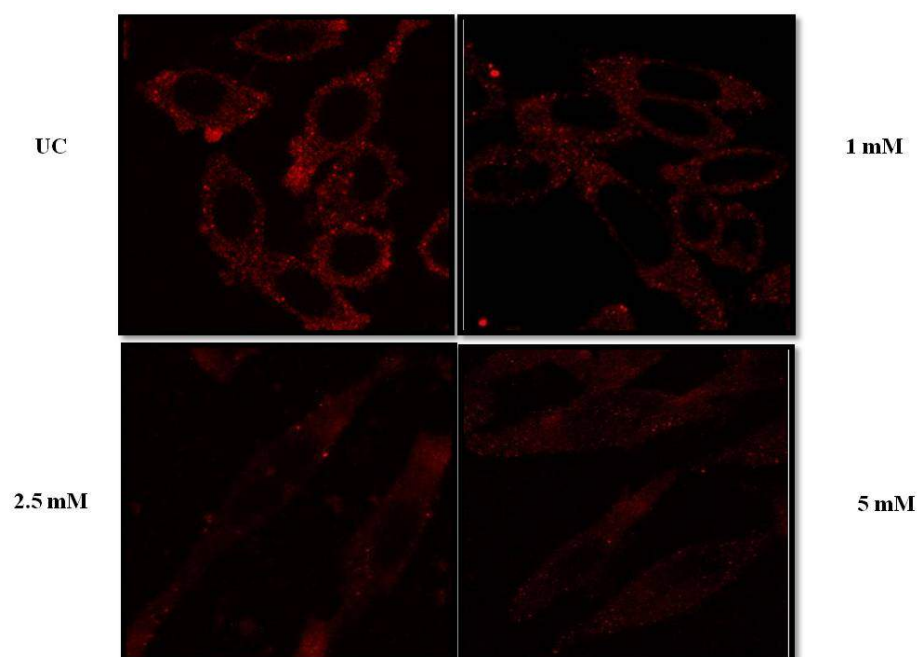
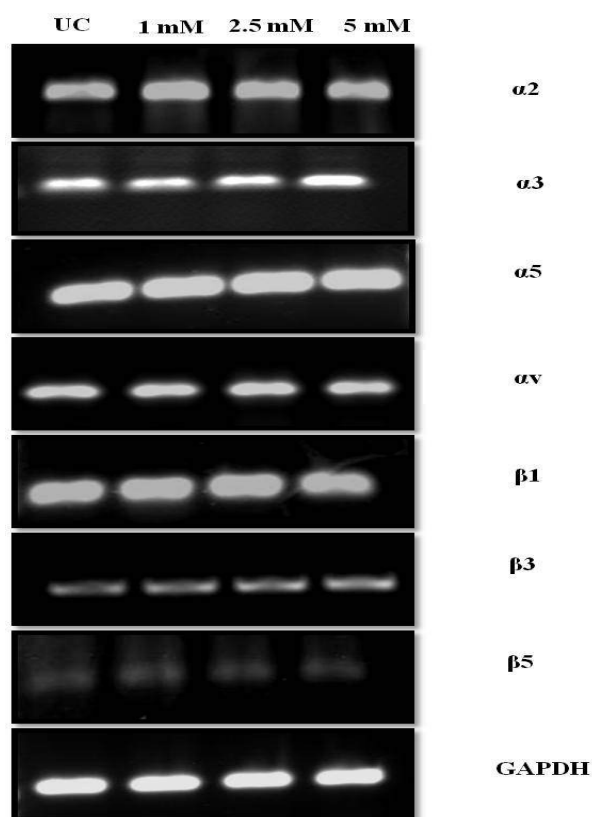


Figure 4.12: Immuno-fluorescence analysis of PTX treated cells on surface expression of integrin $\alpha 5\beta 1$.

PTX treated cells showed a decrease in cell surface fluorescence at sub-toxic doses for integrin $\alpha 5\beta 1$. Further, cells showed an altered morphology with a more extended spindle shape.

Figure 4.13

**Figure 4.13: Effect of PTX on RNA levels of integrins using RT-PCR.**

Treatment with PTX for 24 hr at sub-toxic doses does not affect the transcription of integrins $\alpha 2$, $\alpha 3$, $\alpha 5$, αv , $\beta 1$, $\beta 3$ and $\beta 5$.

Figure 4.14

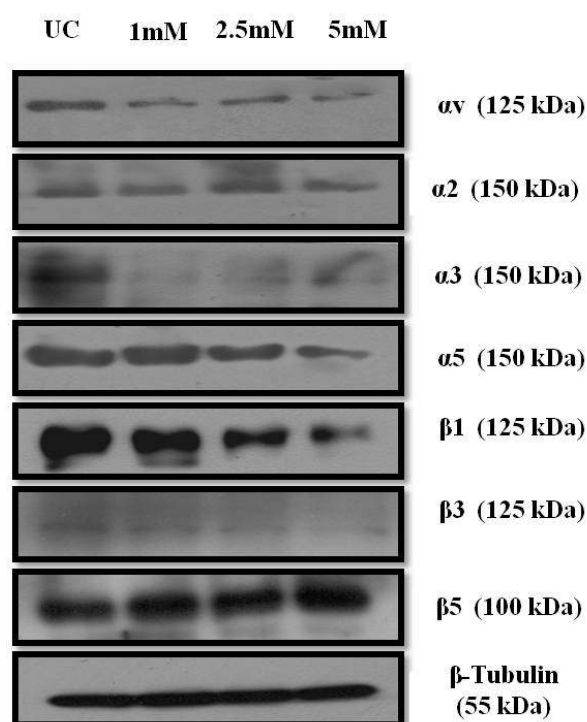


Figure 4.14: Changes in total protein levels of integrins upon PTX treatment in MDA-MB-231 cells.

Western blotting was done to assess PTX associated changes in total protein levels of integrins αv , $\alpha 2$, $\alpha 3$, $\alpha 5$, $\beta 1$, $\beta 3$ and $\beta 5$. PTX at sub-toxic doses 1 mM, 2.5 mM, 5 mM affected the levels of αv , $\alpha 3$, $\alpha 5$, $\beta 1$ and $\beta 3$. However, no change was observed for $\alpha 2$ and $\beta 5$ subunits. β -tubulin was used as a loading control.

4.8 PTX affects the expression of active FAK and its downstream effectors

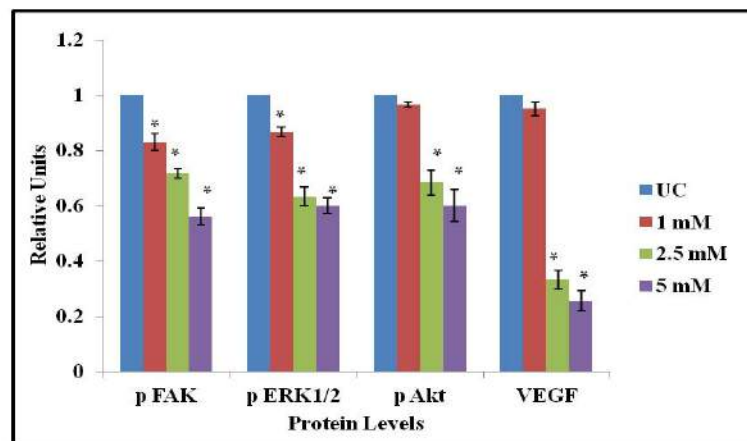
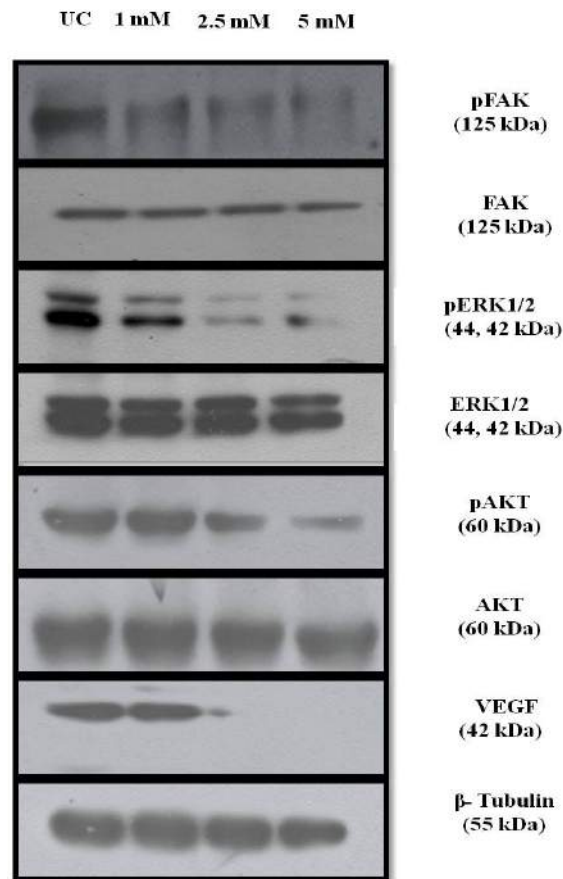
Integrins lack enzymatic activity to regulate the downstream signaling. Thus, it requires accessory molecules such as FAK to mediate the same. Several studies had demonstrated that FAK regulates the processes of cell proliferation, angiogenesis, migration and apoptosis. To evaluate whether PTX inhibits the phosphorylation of FAK/ERK/Akt, protein levels of VEGF and the other apoptotic proteins, MDA-MB-231 cells were

treated with sub-toxic doses of PTX. It was found that PTX inhibited the activation of FAK, ERK1/2 and Akt as shown by a decrease in phosphorylation (Figure 4.15a). Further, it inhibited the levels of VEGF, cyclin D1, cdk6, Bcl-2 and Bcl-xL in a dose dependent manner (Figure 4.15a-c). However, a dose dependent increase in levels of cleaved caspase-9, 3 and PARP was also observed, indicating an increase in apoptosis (Figure 4.15d). There was no change in the levels of p53, cdk4 and McL-1 respectively (Figure 4.15b and 4.15c).

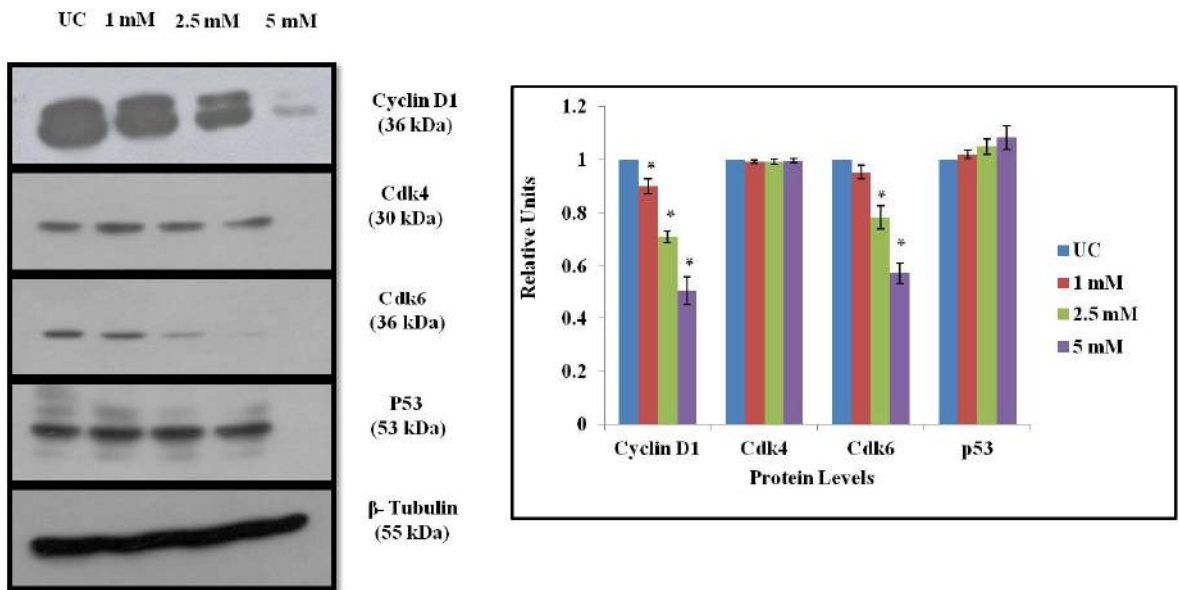
To check whether FAK affects the levels of MAPK and Akt, cells were treated with PF-573228 (FAK inhibitor or FAKi). Inhibition of FAK resulted in lowering of the levels of both ERK1/2 and pAkt (Figure 4.15e). Further, treatment with FAKi also impedes migration of MDA-MB-31 cells suggestive of the fact that FAK indeed has a tumourigenic role in the process of metastasis (Figure 4.15f). Lastly cells treated with Akt inhibitor IV affected the expression of cleaved caspase 9, 3, cleaved PARP and Bcl-2 (Figure 4.15g). These results suggested that inhibition of FAK signaling due to altered adhesion to ECM components through integrins causes cellular apoptosis via Akt pathway.

Figure 4.15

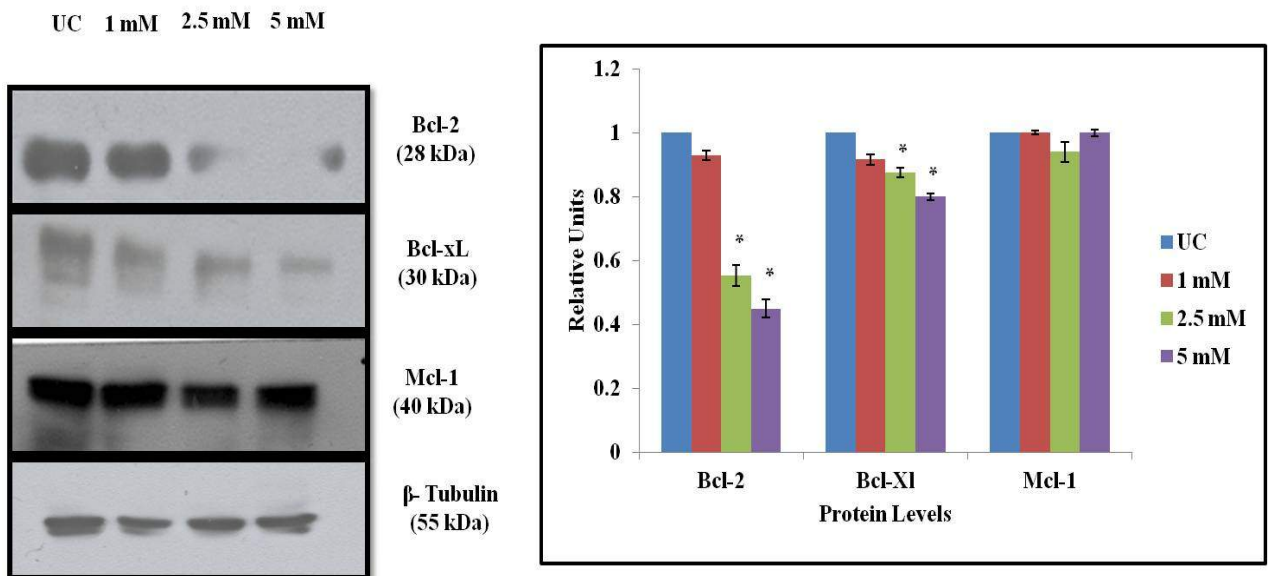
(a)



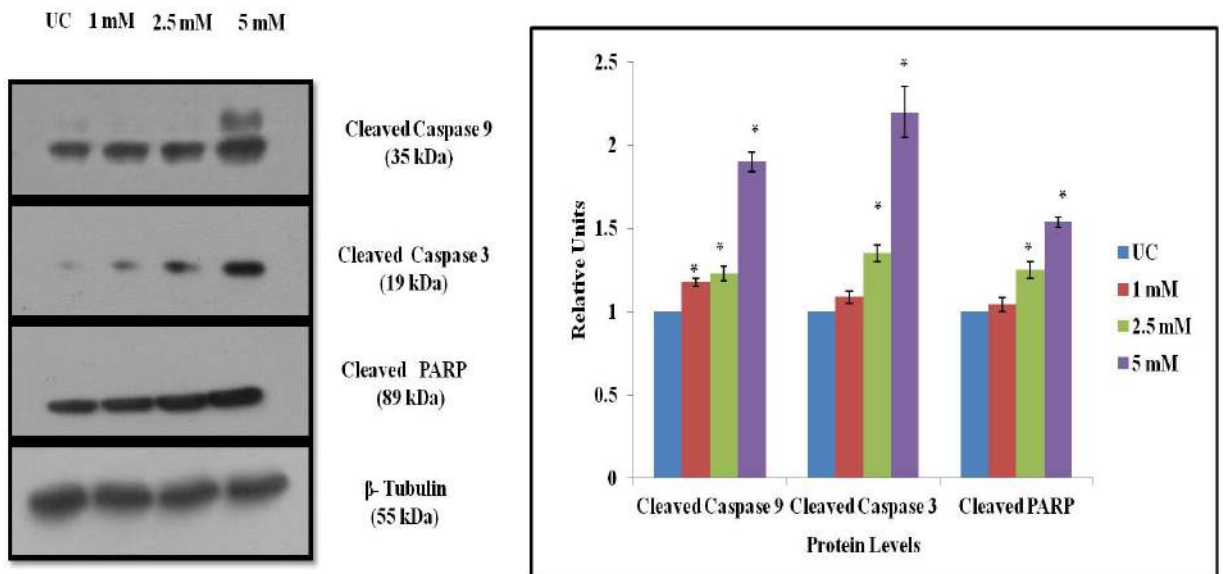
(b)



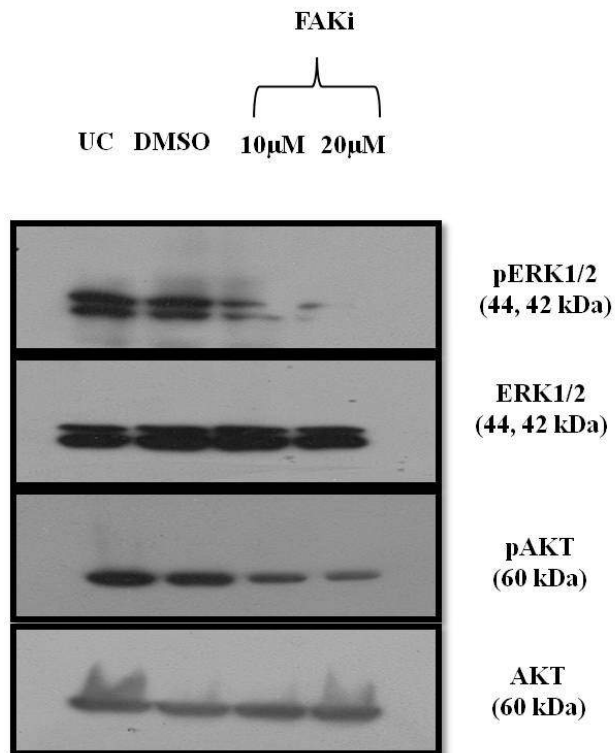
(c)



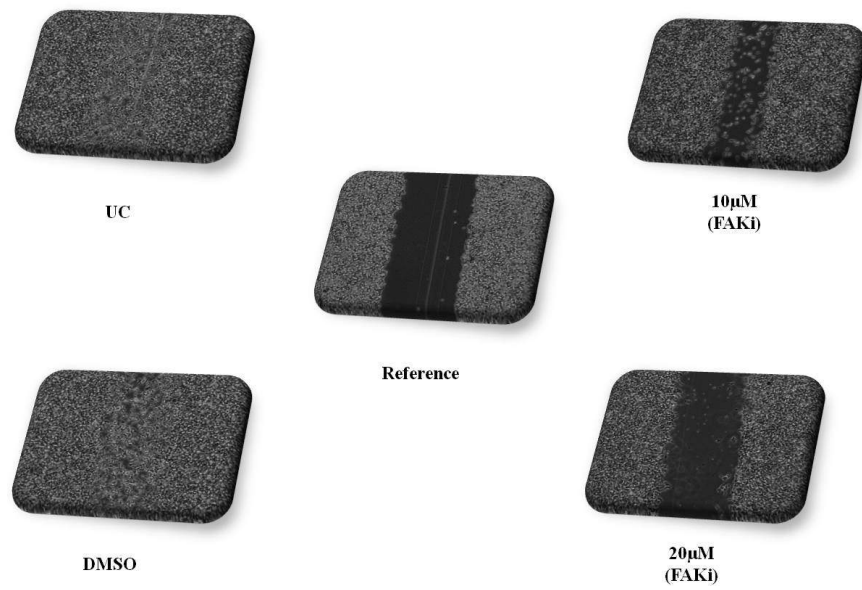
(d)



(e)



(f)



(g)

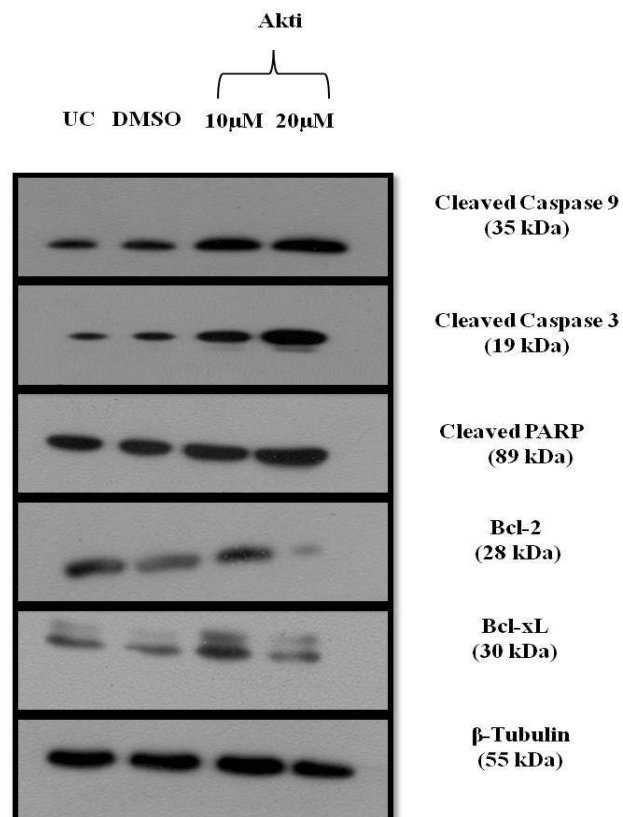


Figure 4.15: Dose dependent effects of PTX on FAK pathway and other associated molecules.

MDA-MB-231 cells were treated with sub-toxic doses of PTX (1 mM, 2.5 mM and 5 mM) along with untreated control for 24 hr. Western blotting was done to study the effects of PTX on protein expression (a) Dose dependent decrease in activated levels of FAK, ERK1/2 and Akt is seen along with decreased levels of VEGF (b) PTX affects G1/S cell cycle mediators cyclinD1/cdk6 while levels of cdk4 and p53 remains unchanged. (c) and (d) shows an increase in levels of active caspases 9 and 3 along with the downstream effector PARP that result in apoptosis, while levels of anti-apoptotic proteins (Bcl-2, Bcl-xL) were decreased. No change in levels of Mcl-1 observed. (e) treatment of cells using PF-573228 (FAK inhibitor or FAKi) at 10 μ M and 20 μ M resulted in lowering of the active levels of both ERK1/2 and pAkt (f) decrease in cellular migration of MDA-MB-31 cells upon treatment with FAKi in wound healing assay, suggestive of the fact that FAK indeed has a role in the process of metastasis. (g) Treatment with Akt inhibitor/Akt IV or Akti at 10 μ M and 20 μ M affected the levels of caspase 9, caspase 3, PARP and Bcl-2 while no change was observed for Bcl-xL. DMSO was used as a vehicle control.

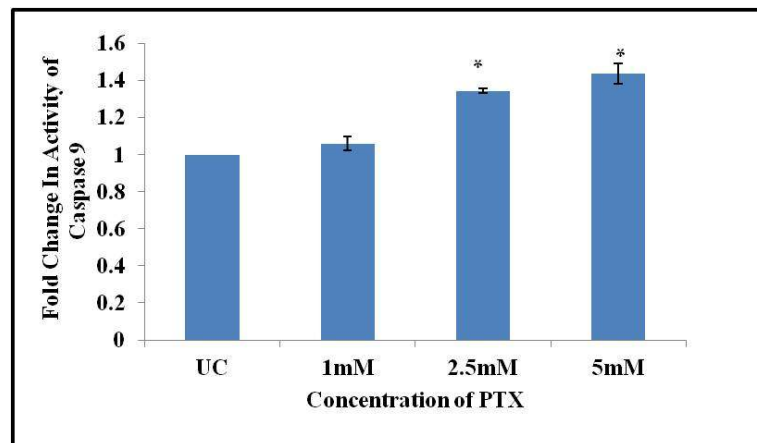
4.9 PTX enhances the activities of both cleaved caspases 9 and 3

Caspases exist in an inactive zymogenic form that needs to be processed to be active. This functional form can then recognize target sequences in its substrates initiating the apoptotic process. PTX showed a significant dose-dependent increase in activities of both cleaved caspase-9, 3 at 2.5 mM and 5 mM respectively compared to untreated control. The synthetic peptides labeled with para-nitroaniline used were LEHD for caspase-9 and

DEVD for caspase-3. The active form of these caspases is directly proportional to their substrate specific cleavage ability. Caspase-9 activity showed a fold change of $1.34 \pm 1.26\%$, $1.43 \pm 5.5\%$ while in case of caspase-3 the increase was $1.34 \pm 5.2\%$, $1.65 \pm 2.2\%$ at 2.5 mM and 5 mM compared with the untreated control set to be unity ($P < 0.05$) (Figure 4.16a and 4.16b).

Figure 4.16

(a)



(b)

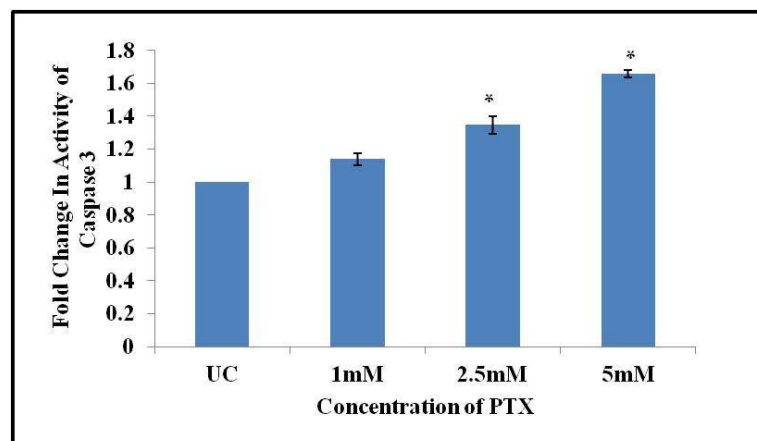


Figure 4.16: Increase in activity of cleaved caspase-9 and caspase-3 upon PTX treatment.

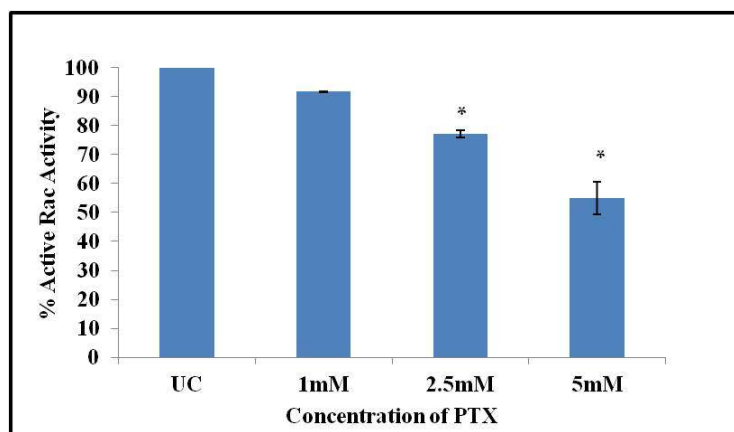
Cells treated with sub-toxic doses of PTX were harvested and cell lysates were prepared. A 96-well format was used to determine the activity of caspases. Caspase activity was determined using substrates: LEHD, DEVD specific for caspase 9 and caspase 3. A significant fold change is observed at 2.5 mM and 5 mM in activities of (a) Caspase -9 and (b) Caspase-3 respectively. Values are representative of three independent experiments Mean±S.E.M. * $P < 0.05$.

4.10 Inhibition of RhoGTPases activity by PTX

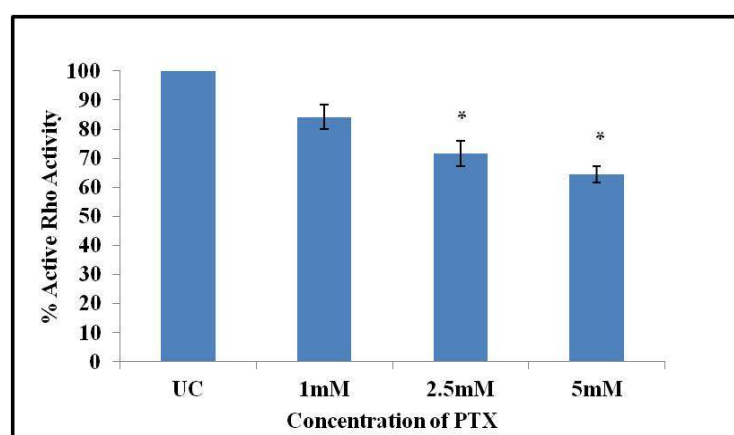
The effect of PTX on the family of RhoGTPases such as Rac, Rho which are largely associated with cytoskeletal alterations and migration was seen in MDA-MB-231 cells using G-LISA assay. The latter has an advantage over other traditional methods such as pull-down assays as it requires lesser starting material, time and the results are quantitative. The Rac or Rho G-LISA® kit contains a Rac/Rho-GTP-binding protein linked to the wells of a 96-well plate. Active, GTP-bound Rac/Rho in cell lysates binds to the well while inactive GDP-bound Rac/Rho is removed during successive washing steps. Cell lysates treated with sub-toxic doses of PTX (1 mM, 2.5 mM and 5 mM) showed a concentration dependent decrease in activities of both the GTPases respectively. The decrease is significant at 2.5 mM, 5 mM and was found to be $77.145 \pm 1.2\%$, $54.9 \pm 5.54\%$ and $71.58 \pm 4.31\%$, $64.43 \pm 2.83\%$ for Rac and Rho respectively, compared to untreated control (Figure 4.17a and 4.17b).

Figure 4.17

(a)



(b)

**Figure 4.17: Decrease in activity of active RhoGTPases upon PTX treatment.**

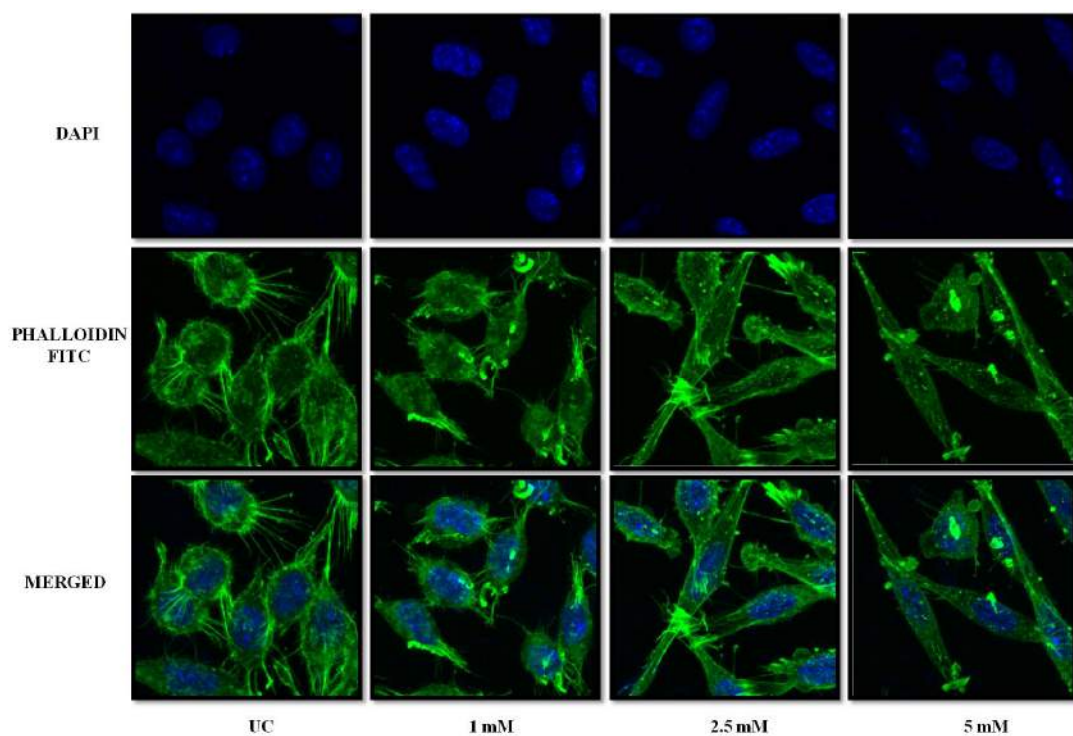
G-LISA assays were performed to score the activities of PTX on active Rac and RhoA. A significant reduction is observed at sub-toxic doses of 2.5 mM and 5 mM in levels of (a) Active Rac and (b) RhoA respectively. Values are representative of three independent experiments Mean±S.E.M * $P < 0.05$.

4.11 PTX affects the actin cytoskeleton arrangement in MDA-MB-231 cells

The effect of sub-toxic doses of PTX on actin organization was seen in MDA-MB-231 cells. Cells treated with various sub-toxic doses of PTX were fixed and stained with Phalloidin-FITC that specifically stains filamentous actin in the cell. Confocal images captured at 600X magnification showed disappearance of extensions protruding at cellular surface i.e filopodia as well as lamellopodia in a concentration dependent manner upon PTX treatment (Figure 4.18a). A positive control using cytochalasin B showed disruption of actin fibers (Figure 4.18b).

Figure 4.18

(a)



(b)

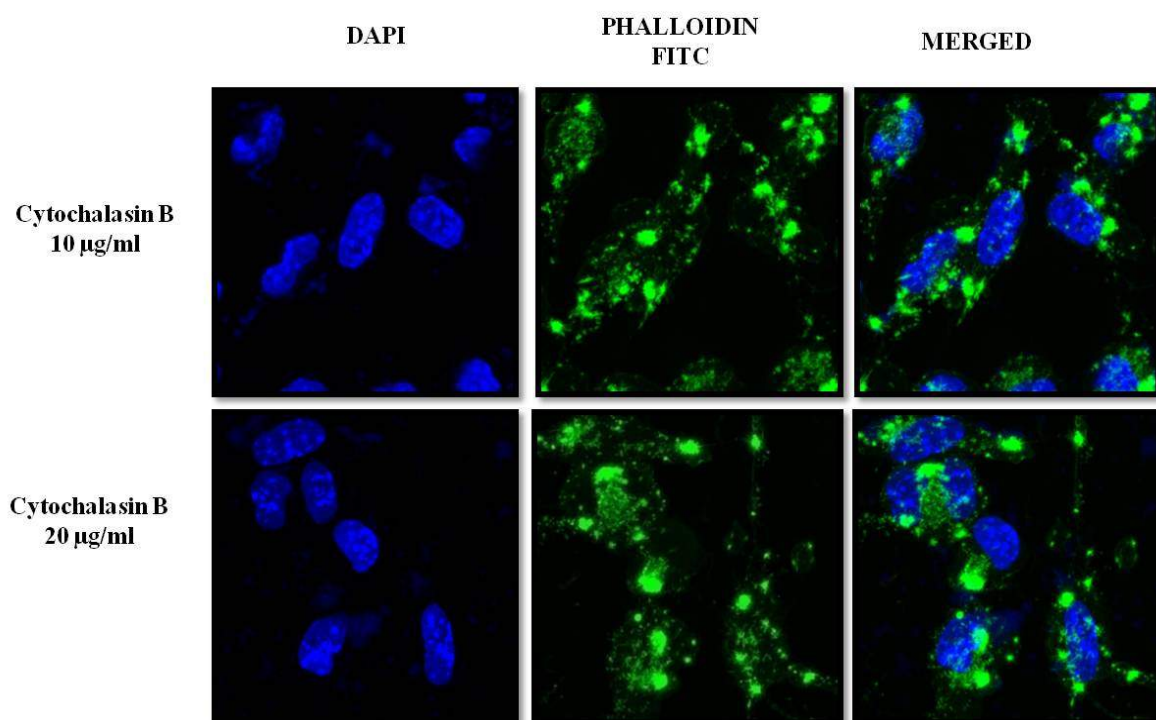


Figure 4.18: Effect of PTX on actin staining in MDA-MB-231 cells.

Sub-confluent cells were treated with PTX and then subjected to Phalloidin/FITC staining (a) A dose dependent decrease in actin structures such as filopodia (seen as protrusions arising from cell surface) and lamellopodia is seen (b) Cells treated with Cytochalasin B at concentrations of 10 µg/ml and 20 µg/ml were used as positive control. Loss of actin structures is distinctly visible.

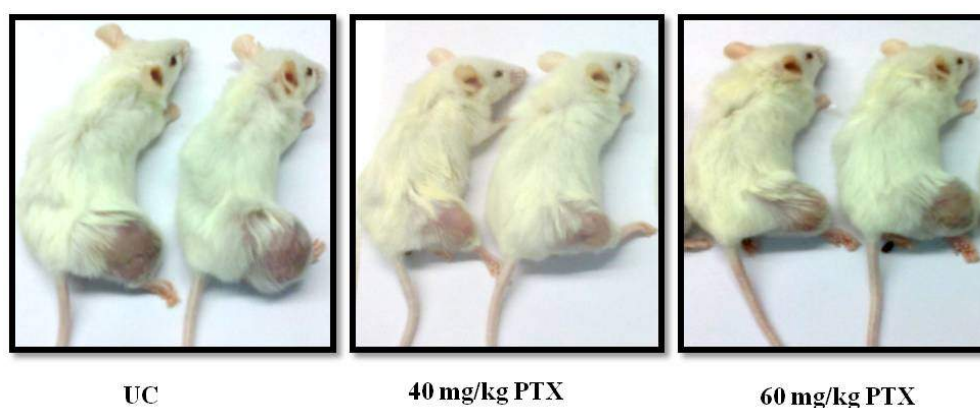
4.12 Tumour growth delay in SCID mice after PTX treatment

MDA-MB-231 cells were implanted subcutaneously into the right flank to allow tumours to grow. Tumour latency period observed was 5 days. PTX was administered intraperitoneally from the day 9, when the average tumour volume was more than 50 mm³ till day 17 i.e for a period of 9 days. PTX showed a significant tumour growth delay from day 13th till 21st when animals were sacrificed (Figure 4.19a). Tumour volume on

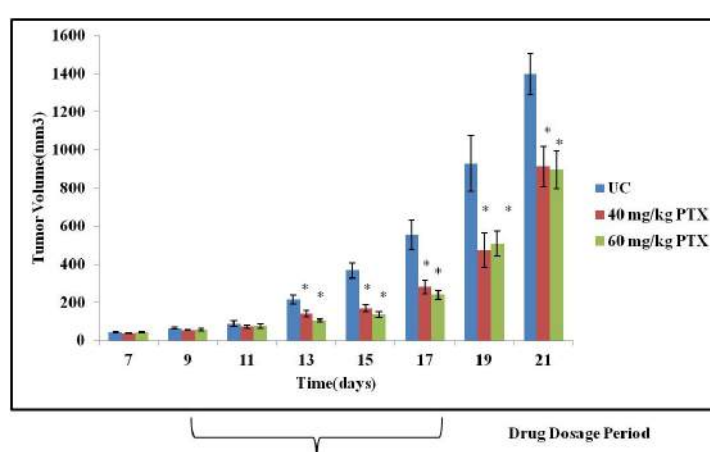
17th and 21st days were $554.20 \pm 78.05 \text{ mm}^3$, $1397 \pm 108.2 \text{ mm}^3$ for untreated control while $280.92 \pm 37.13 \text{ mm}^3$, $912.91 \pm 106.16 \text{ mm}^3$ for PTX (40 mg/kg) and $239 \pm 22 \text{ mm}^3$, $895 \pm 98.50 \text{ mm}^3$ for PTX (60 mg/kg) groups respectively (Figure 4.19b). Animal weights were measured alternately after PTX administration to observe the dose associated toxicity in animals. There was no decrease in body weights on PTX treatment (Figure 4.19c).

Figure 4.19

(a)



(b)



(c)

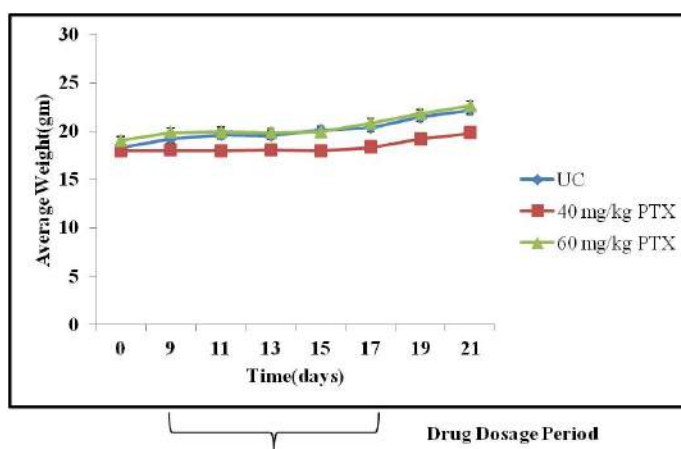


Figure 4.19: PTX shows a tumour growth delay in xenograft model.

MDA-MB-231 cells were implanted into the right flanks of 6-8 week old female NOD-SCID mice. PTX treatment (40 mg/kg and 60 mg/kg) was given intraperitoneally when tumours attained a minimum tumour volume of 50 mm^3 ie from day 9th to day 17th (a) Representative animals of PTX treated groups (b) Tumour growth delay is observed upon PTX treatment (c) No significant weight loss was observed during the course of PTX treatment. Values are representative of Mean \pm S.E.M. * $P < 0.05$.

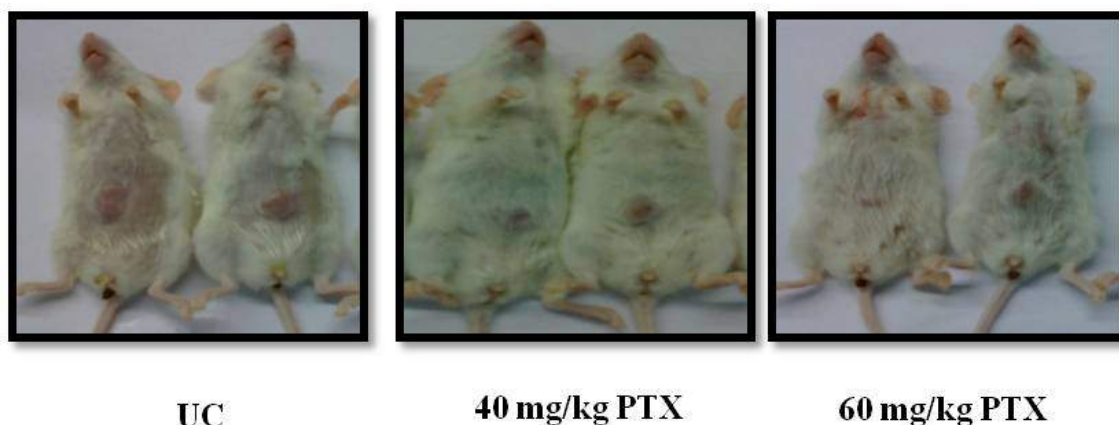
4.13 Decrease in blood vessel formation upon PTX treatment

MDA-MB-231 cells implanted intradermally showed palpable tumours on day 3rd. PTX was administered from 4th day onwards when an average tumour volume was greater than $1\text{-}2 \text{ mm}^3$ since lesser volumes restrain the tumours to derive nutrition. Hence, angiogenesis occurs only after achieving volumes greater than 2 mm^3 . PTX was administered for a period of 9 days as done earlier. Tumour volumes and animal weight were measured every alternate day. There was a delay in tumour growth as seen by reduced tumour burden compared to control group (Figure 4.20a). Tumour volume was $145.6 \pm 24.32 \text{ mm}^3$ for untreated while it was $75.44 \pm 10.95 \text{ mm}^3$, $73.64 \pm 15 \text{ mm}^3$ for PTX

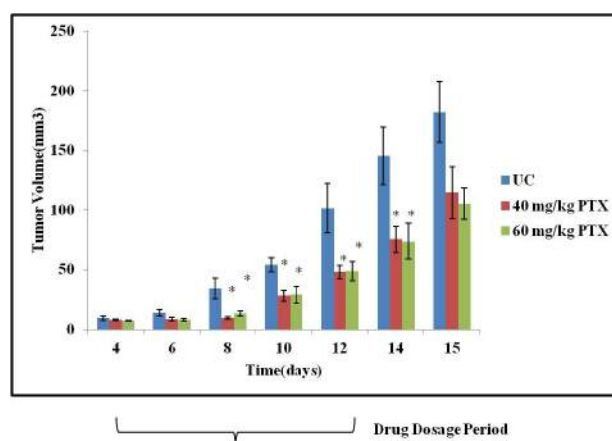
treated viz 40 mg/kg and 60 mg/kg groups respectively (Figure 4.20b). No significant weight loss was observed (Figure 4.20c). Mice were sacrificed on day 15th and the skin was carefully removed using forceps to visualize the growth of blood vessels around the tumour (Figure 4.20d). A significant reduction in blood vessels was being observed. Average number of blood vessels visible was 6.8 ± 0.8 , 3.8 ± 0.8 , 2.8 ± 0.58 for untreated and PTX treated (40 mg/kg and 60 mg/kg) groups respectively (Figure 4.20e).

Figure 4.20

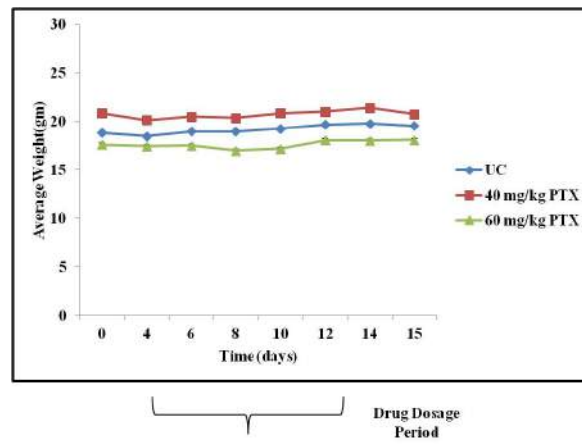
(a)



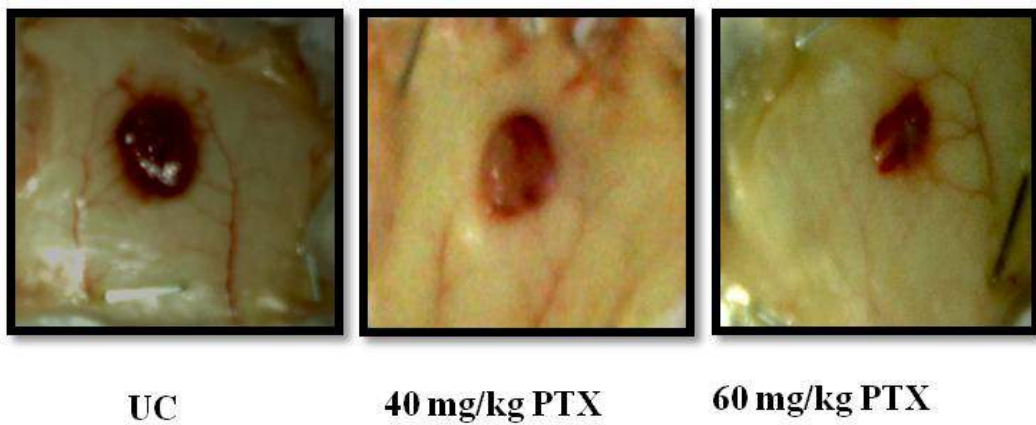
(b)



(c)



(d)



(e)

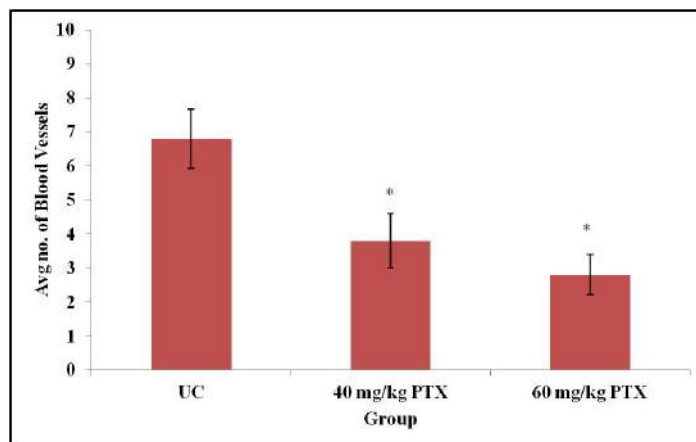


Figure 4.20: PTX affects blood vessel formation in intradermal model of angiogenesis.

MDA-MB-231 cells were implanted intradermally into 6-8 week old female NOD-SCID mice respectively. After palpable tumours were visible, PTX was given intraperitoneally at doses of 40 mg/kg and 60 mg/kg ie from day 4th to day 12th (a) Mice bearing tumours (b) Tumour burden decreased during the course of PTX treatment (c) Changes in body weight were insignificant upon PTX treatment (d) and (e). Skin bearing the tumours was later excised and photographed. Blood vessels around tumours were then counted and plotted. Values are representative of Mean±S.E.M. * $P < 0.05$.

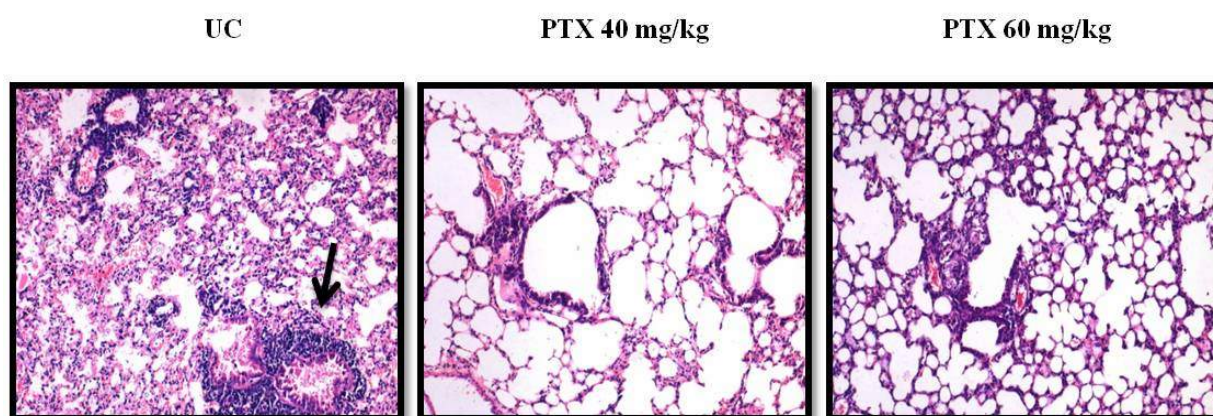
4.14 PTX affects colony formation using *in vivo* experimental metastasis model and angiogenesis in chick chorioallontic membrane assay

MDA-MB-231 cells were injected intravenously and PTX administration was started at the same day for a period of 9 days. Mice were sacrificed after a period of approximately 30 days and the lungs were excised. Numerous tumour islands were being present in the untreated group. These islands were both large and small being present throughout the lung parenchyma. However, in the treatment group PTX 40 mg/kg, tumour cells were present at few places while other areas were found to be devoid of tumour cells and were clear. In addition, animals treated with PTX 60 mg/kg group showed presence of metastatic cells and formation of smaller tumour islands (Figure 4.21a). The quantitative assessment results showed an average of 7 ± 0.69 , 2.3 ± 0.3 , 3 ± 0.34 tumour islands/field for untreated, 40 mg/kg and 60 mg/kg PTX groups respectively ($P < 0.05$) (Figure 4.21b). This observation clearly demonstrated anti-adhesive properties of PTX using *in vivo* model system. Further, we had evaluated the effect of PTX on angiogenesis using *in ovo*

model CAM assay. CAM assay was performed as an additional validation to corroborate our earlier findings and we did observe a decrease in blood vessel formation around the growing embryo (Figure 4.22).

Figure 4.21

(a)



(b)

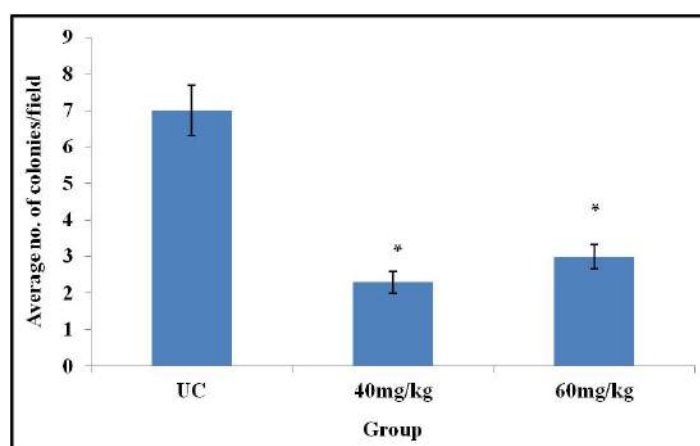


Figure 4.21: PTX treatment displayed lessened metastatic potential using *in vivo* experimental metastasis model.

MDA-MB-231 cells were injected intravenously into the tail vein of 6-8 week old female NOD-SCID mice. Mice were divided into three groups (a) Control treated with PBS, PTX

40 mg/kg and PTX 60 mg/kg and treated for a period of 9 consecutive days via intraperitoneal route. Mice were sacrificed after a month, lungs were excised and later Haematoxylin-Eosin stained. Control groups showed presence of many large and small tumour colonies compared to PTX treated groups (b) Quantitative measurement of colonies formed.

Figure 4.22

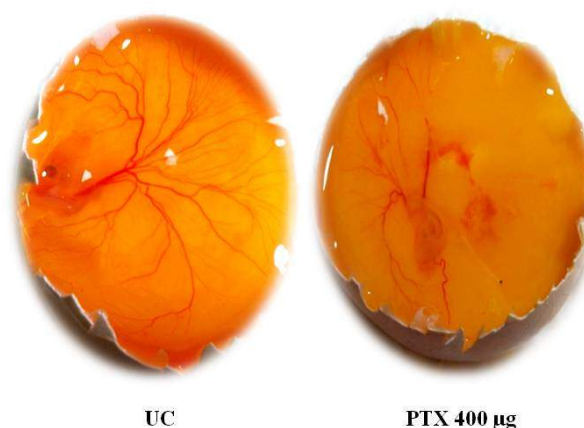


Figure 4.22: PTX affects blood vessel formation using *in ovo* CAM assay.

Fertilized eggs were procured and kept in an incubator maintained at 37°C under humidifying conditions. The eggs were kept for a period of 5 days before PTX treatment and then incubated further. Photographs were taken after the eggs were cut open. PTX treatment caused reduction in blood vessel density around the growing embryo, suggestive of its anti-angiogenic activity.

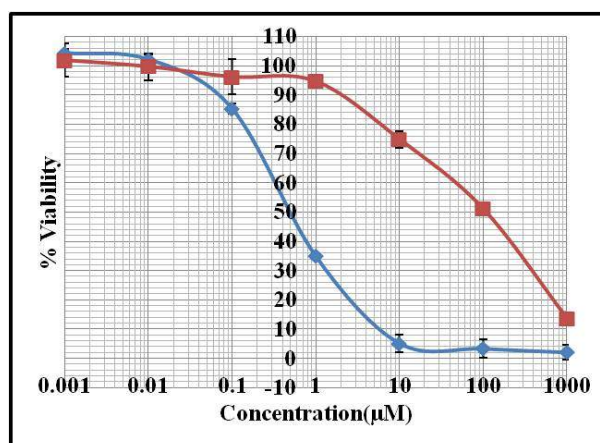
4.15 Lipodox exhibited lesser cytotoxicity than plain doxorubicin in MDA-MB-231 cells

MTT assay was done to evaluate the toxicity of DOX and LD at different time points, *viz.* 24 hr, 48 hr and 72 hr respectively (Figure 4.23a-c). It was found that DOX is highly toxic to MDA-MB-231 cells when compared to LD at these time points. IC₅₀ was found

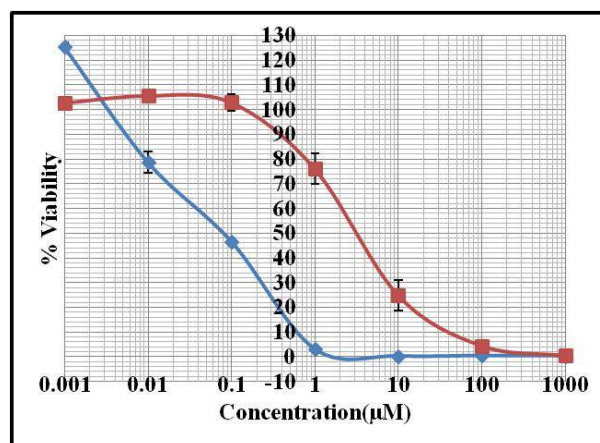
to be 0.5 μM , 0.09 μM , 0.006 μM for DOX compared to 100 μM , 3.5 μM , 0.4 μM in case of LD at 24 hr, 48 hr and 72 hr. Hence, LD was chosen for combination therapy in our model system due to sustained release of the drug and least toxicity.

Figure 4.23

(a)



(b)



(c)

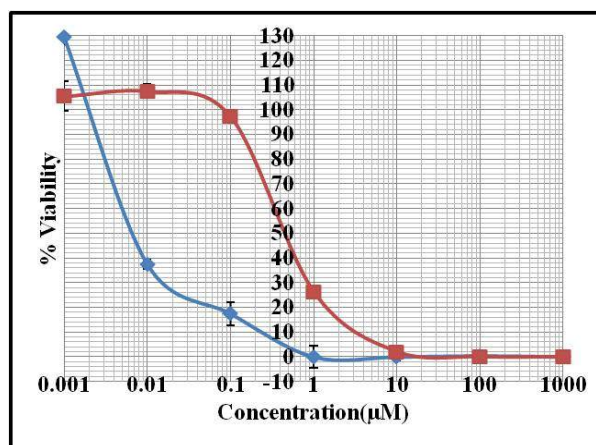


Figure 4.23: Comparison of cytotoxicity for Doxorubicin (DOX) and liposomal doxorubicin (Lipodox or LD).

MTT assay was performed to determine the percent viability in MDA-MB-231 cells at (a) 24 hr (b) 48 hr (c) 72 hr in MDA-MB-231 cells using DOX and LD. Results are representative of three independent experiments Mean \pm SEM. Red (LD) and blue(DOX).

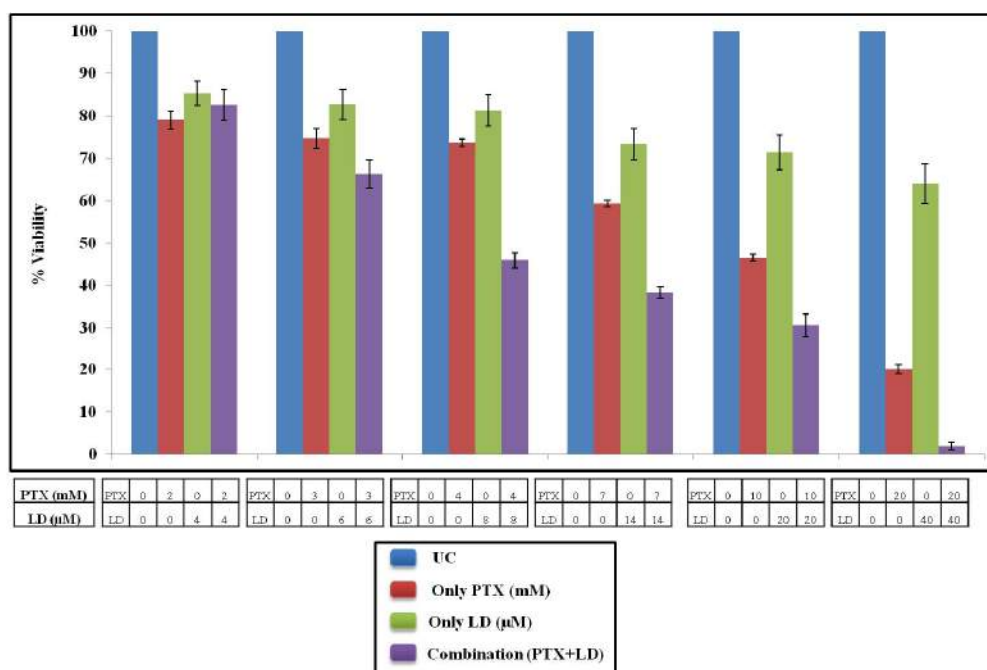
4.16 Synergism in the cytotoxicity profile for the combination regimen of PTX and lipodox

The % viability of both PTX and LD in the ratio of 500:1 was determined using MTT assay at different doses both in combination as well as single agents respectively (Figure 4.24a). Combination Index (CI) was determined by use of compusyn software (Table 4.2). A value of $CI > 1$ means antagonism, $CI = 1$ represents additive and $CI < 1$ indicates synergism. It was found that PTX at doses of 3 mM, 4 mM and corresponding LD at 6 μ M and 8 μ M showed synergistic action where CI tends to be less than unity (Table 4.2). The dose-effect curve and CI plot are represented in (Figure 4.24b and 4.24c) respectively. Further, it can be seen that there is a reduction in IC_{50} values for both the drugs used (Table 4.3). The IC_{50} computed by software comes to be approximately 8.1

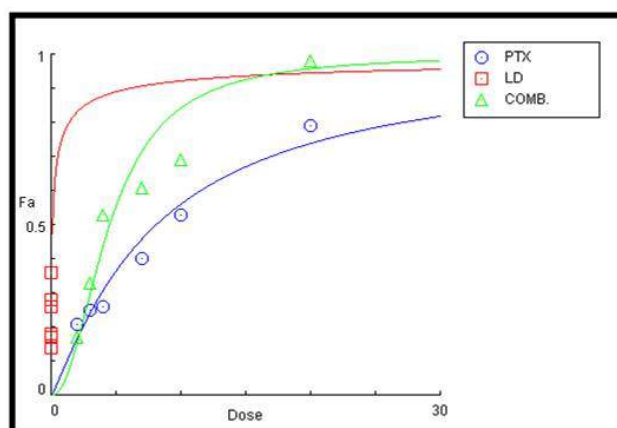
mM, 110 μ M for PTX and LD. However, in the combination scenario it is found to be close to 4.5 mM, 9 μ M for PTX and LD with CI<1. This clearly indicates that the combination doses act synergistically and is more potent than individual drugs. Based on these combination doses, anti-metastatic activity of the combination regimen was evaluated. The doses were designated as P1 (3 mM), P2 (4 mM) for PTX, LD1 (6 μ M), LD2 (8 μ M) for LD and C1 (P1 and LD1), C2 (P2 and LD2) for combination. It can be further seen that the viability at these combination doses (C1 and C2) is much lower than that of individual effects (Figure 24a). The anti-proliferative activity of the combination regimen was further confirmed using colony formation assay. The % colony formation was 54.12 \pm 4.14% (P1), 44.22 \pm 1.90% (P2), 16.75 \pm 0.70% (LD1), 4.88 \pm 1.17% (LD2), 6.22 \pm 1.24% (C1) and 1.59 \pm 0.23% (C2) (P <0.05). The results are shown in (Figure 4.25a and 4.25b).

Figure 4.24

(a)



(b)



(c)

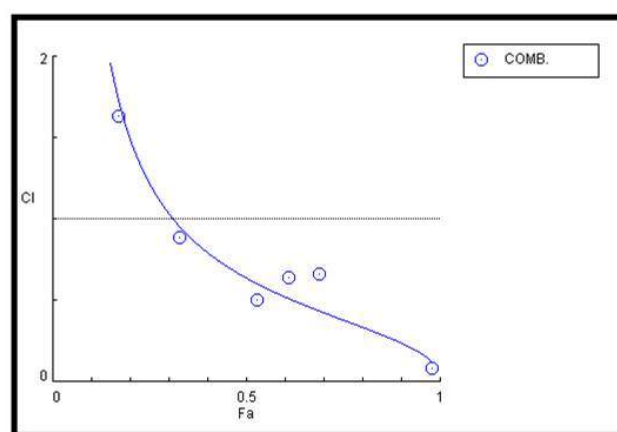


Figure 4.24: Effect of combination doses of PTX and LD.

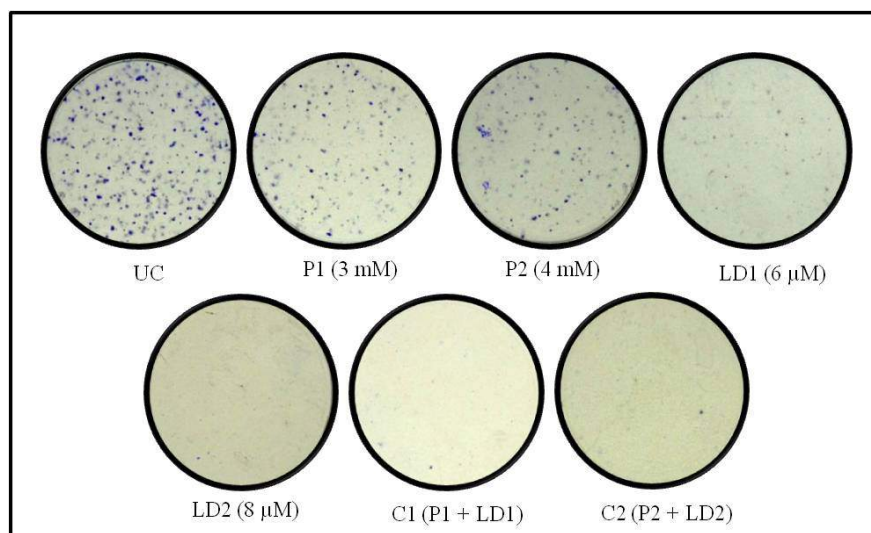
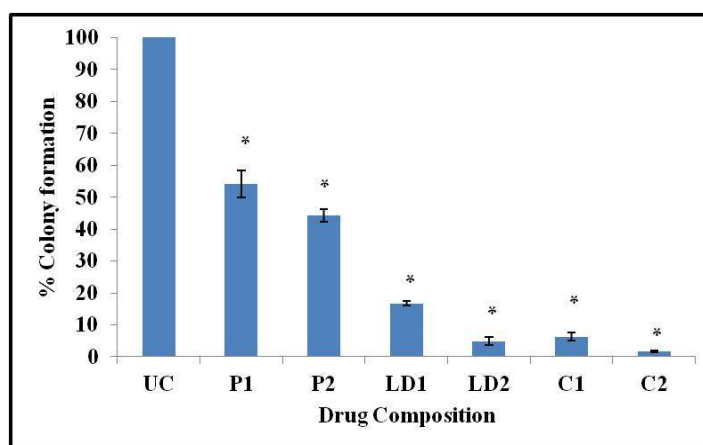
Combination regimen was evaluated for PTX and LD for 24 hr study in the ratio of 500:1. (a) Representation of % viability for individual doses of PTX, LD as well as their combination doses (b) Dose-effect curve of PTX, LD and combination (c) Combination Index (CI) plot for different combinations. CI values less than 1 are representative of synergism.

Table 4.2. Combination index (CI) values for actual experimental points.

Total Dose (PTX and LD)	Effect (Fa)	Combination Index (CI)
2.004	0.17	1.63463
3.006	0.33	0.88569
4.008	0.53	0.50458
7.014	0.61	0.64374
10.02	0.69	0.65971
20.04	0.98	0.08417

Table 4.3. Data for Fa=0.5 i.e. Effect at 50% inhibition.

Drug/Combination	Combination Index (CI)	PTX Dose (mM)	LD Dose (mM)
PTX		8.07922	
LD			0.10972
COMBINATION	0.63782	4.49159	0.00898

Figure 4.25**(a)****(b)****Figure 4.25: Clonogenic assay for the combination.**

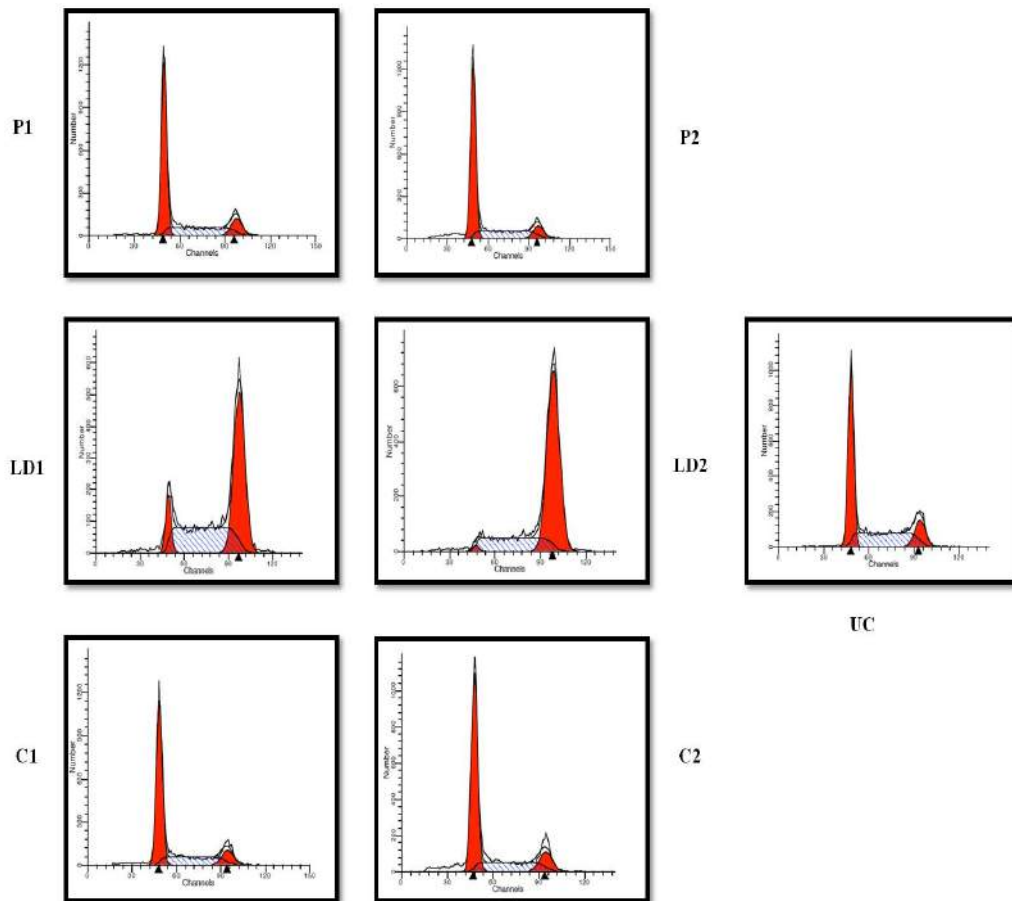
Colony formation assay was done to evaluate the anti-proliferative effect of PTX (P1 and P2), LD (LD1 and LD2) and their combinations. (a) Qualitative representation (b) graphical representation showed a significant decrease in colony formation in case of C1 and C2. Results are representative of three independent experiments Mean \pm SEM. (* $P < 0.05$).

4.17 Changes in cell cycle progression and increased apoptosis upon treatment with the combination regimen

Flow cytometry was done to assess the cell cycle status of MDA-MB-231 cells upon PTX and LD treatment as well as their combinations (C1 and C2) represented in (Figure 4.26a). PI is an intercalating dye that has an affinity towards nucleic acids and thus upon binding to DNA its fluorescence changes. It was found that treatment with PTX leads to a significant increase in G1 phase of the cell cycle ($64.58 \pm 2.58\%$ for P1, $60.90 \pm 2.57\%$ for P2 while for UC it was $38.4 \pm 3.22\%$) ($P < 0.05$). However, treatment with LD causes a G2-M cell cycle arrest significantly ($49.93 \pm 2.14\%$ for LD1, $68.35 \pm 3.44\%$ for LD2 and $14.9 \pm 1.11\%$ for UC) ($P < 0.05$) as shown in (Figure 4.26b). However, in the combination scenario a G1 phase cell cycle arrest was pronounced (Table 4.4). Further, we wanted to check whether these doses cause an increase in apoptosis or not. ET/AO staining was performed as done earlier to confirm the same. An increase in apoptosis indicated by red colored cells was dominant in the combination groups (Figure 4.27). To further corroborate our findings, AnnexinV/FITC staining was performed to demonstrate the same in MDA-MB-231 cells. There was an increase in apoptosis in case of combination doses compared to individual treatments as can be seen by increase in number of apoptotic cells in both the upper right and lower right quadrants of both C1 and C2 plots (Figure 4.28a and 4.28b). These results clearly indicate that the combination of both PTX and LD caused an increase in apoptosis.

Figure 4.26

(a)



(b)

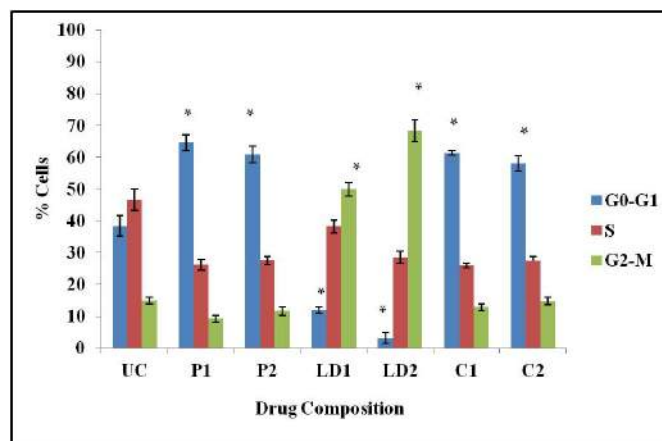


Figure 4.26: Cell cycle distribution upon combination treatment.

Flow cytometry was done to determine the cell cycle status in MDA-MB-231 cells treated with PTX, LD or combinations. (a) Ploidy status of the cells (b) graphical representation of the cells present in different phases of cellular cycle. Results are indicative of three independent experiments Mean \pm SEM. (* $P < 0.05$).

Table 4.4. Tabulation for cell cycle analysis using flow cytometry upon combination treatment.

	G0-G1	S	G2-M
UC	38.4 \pm 3.22	46.5775 \pm 3.40	14.9025 \pm 1.11
P1	64.5875 \pm 2.57	26.2125 \pm 1.64	9.2 \pm 0.98
P2	60.905 \pm 2.57	27.4925 \pm 1.31	11.605 \pm 1.36
LD1	11.8625 \pm 0.92	38.21 \pm 1.93	49.93 \pm 2.14
LD2	3.07 \pm 1.69	28.58 \pm 1.92	68.35 \pm 3.44
C1	61.2775 \pm 0.75	25.95 \pm 0.78	12.7725 \pm 1.13
C2	58.0275 \pm 2.45	27.275 \pm 1.43	14.695 \pm 1.17

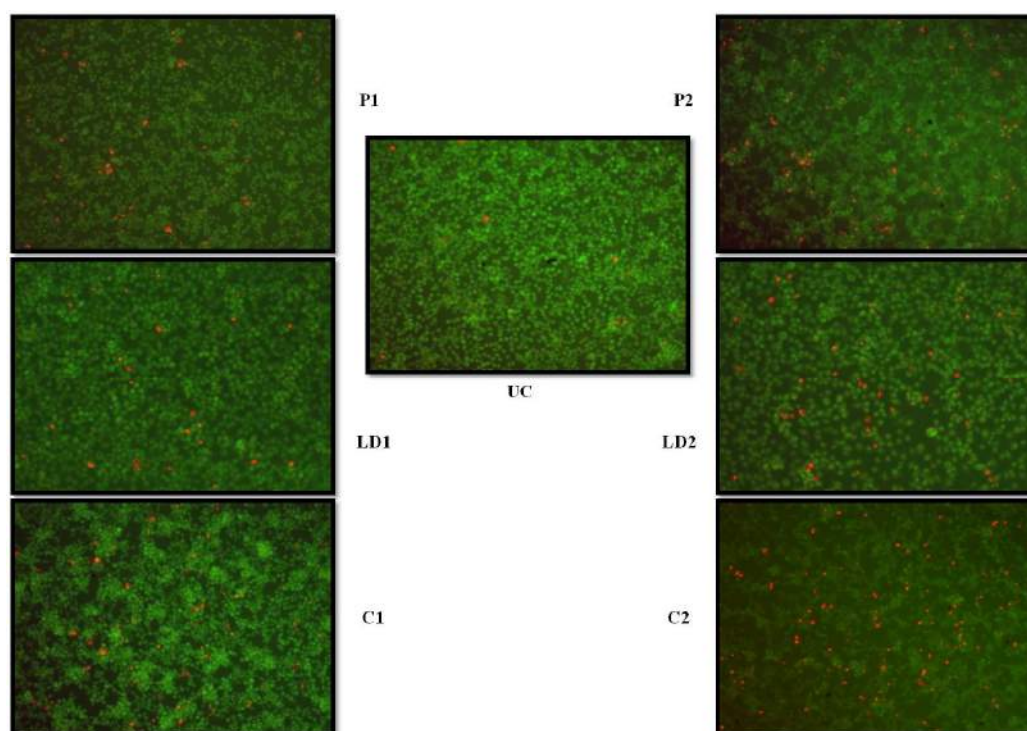
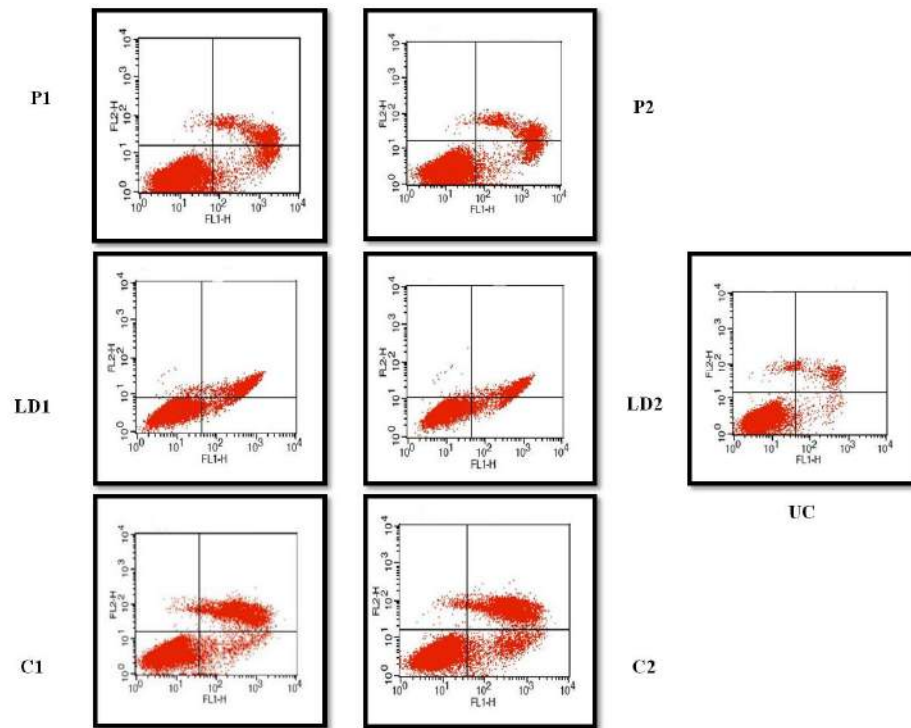
Figure 4.27

Figure 4.27: EB/AO staining for differentiating live and dead cells upon combination treatment.

The differences between live and dead cells for MDA-MB-231 cells treated with different combinations were determined using EB/AO staining. AO stains the live cells that appear green while apoptotic cells appear reddish coloured. Images were captured using Axio Inverted microscope (Germany).

Figure 4.28

(a)



(b)

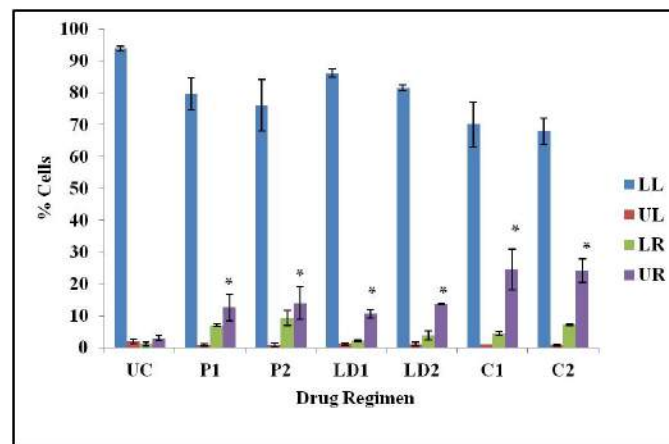


Figure 4.28: AnnexinV/FITC staining for apoptotic determination upon combination treatment.

(a) Sub-confluent cells treated with combination doses showed an enhancement in apoptosis compared to treatment with single drugs alone. AnnexinV binds to the phosphatidylserine present on the outer membrane of apoptotic cells. (b) Graphical representation. X and Y axis represents FITC and PI fluorescence respectively.

4.18 Alterations in cellular adhesion, invasion and migration for the combination treatment

Adhesion assay was done to evaluate the adhesive potential of MDA-MB-231 cells upon PTX, LD as well as their combinations to various ECM components viz. matrigel, collagen type IV, fibronectin, laminin and vitronectin. It was found that LD *per se* does not alter adhesion to any of the mentioned substrates. PTX at doses of 3 mM and 4 mM does affect adhesion. The adhesion for (P1 and P2) was found out to be $55.96 \pm 7.78\%$; $43.87 \pm 10.48\%$ for matrigel, $52.8 \pm 8.52\%$; $54.44 \pm 8.81\%$ for collagen type IV, $64.55 \pm 5\%$; $56.34 \pm 6.53\%$ for fibronectin and $34.53 \pm 4.68\%$; $30.3 \pm 4.6\%$ for laminin ($P < 0.05$). Further, the combination regimen showed a slight reduction in adhesion in comparison to use of PTX alone on matrigel, collagen type IV and laminin respectively. The combination doses (C1 and C2) showed $52.7 \pm 3.94\%$, $40.19 \pm 4.21\%$ adhesion to matrigel, $49.09 \pm 2.91\%$; $49.97 \pm 6.17\%$ to collagen, $69.55 \pm 8.59\%$; $62.28 \pm 9.4\%$ to fibronectin and $30.3 \pm 8.04\%$; $26.2 \pm 6.78\%$ for laminin considering the adhesion of untreated control to be 100%. No change in adhesion was observed against vitronectin (Figure 4.29). These results clearly indicate that LD does not affect cellular adhesion to ECM components. However, in the combination regimen it is PTX that alters the same. The effect of combination was then

evaluated on the activity of gelatinases such as MMP-2 and MMP-9 using gelatin zymography. The % MMP-9 activity was $77.60\pm 3.46\%$, $75.12\pm 5.21\%$, $103.51\pm 1.75\%$, $95.1\pm 2.98\%$, $77.08\pm 0.57\%$, $68.94\pm 2.08\%$ for P1, P2, LD1, LD2, C1 and C2 respectively considering the control to be 100% (Figure 4.30a and 4.30b). The condition media from HT-1080 was used as a positive control that shows the activity of both gelatinases i.e. MMP-9 (92 kDa) and MMP-2 (72 kDa).

Wound healing assay was done to assess the anti-migratory effect of combination regimens in MDA-MB-231 cells. It was observed that LD does not affect the process of motility though at dose of 8 μM there was a decrease in migration (approximately 16%). PTX at both the doses (P1 and P2) impedes migration. In the combination regimen, a similar decrease in migration was observed. The % migration was $41.35\pm 6.63\%$, $31.12\pm 3.45\%$, $101.58\pm 10.49\%$, $84.22\%\pm 16.20$, $39.51\pm 0.24\%$, $23.78\pm 2.90\%$ for P1, P2, LD1, LD2, C1 and C2 respectively considering the control to be 100% ($P<0.05$). The changes in cellular motility are represented in (Figure 4.31a and 4.31b).

In short, we found out that LD *per se* does not affect the processes of adhesion, invasion and migration but it is rather the doses of PTX that brings about an alteration in the above mentioned processes.

Figure 4.29

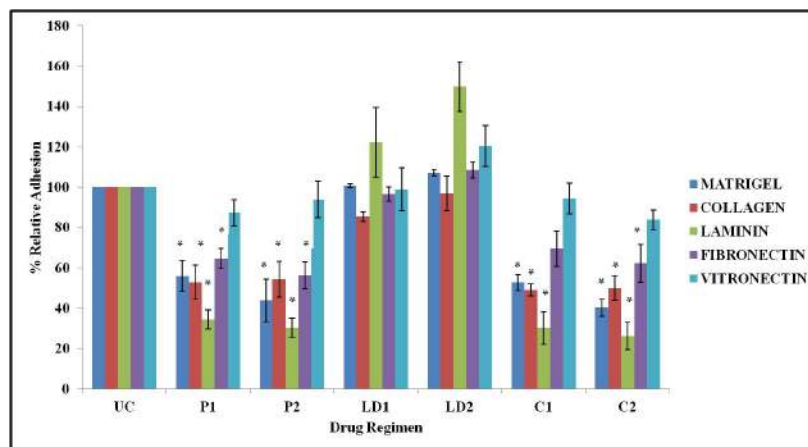
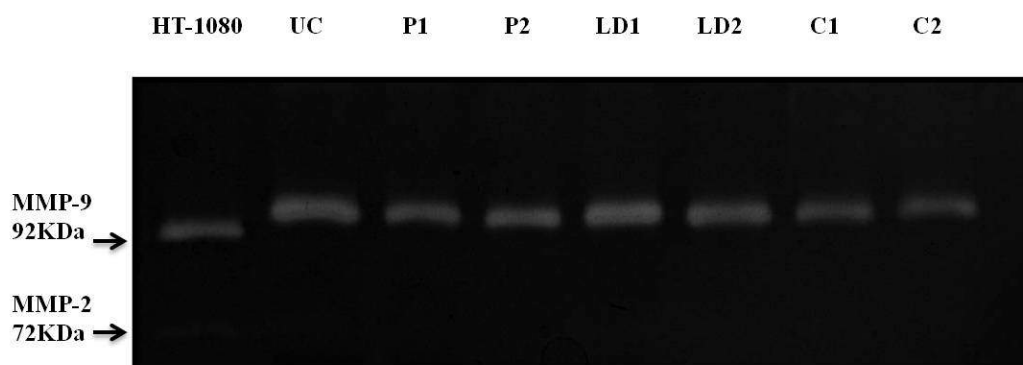


Figure 4.29: Adhesion assay to ECM components upon combination treatment.

Adhesion was evaluated in drug treated cells for 30 min using different ECM substrates *viz.* Matrigel, collagen type IV, fibronectin, laminin and vitronectin. The % relative adherence was then calculated. Results are representative of three independent experiments Mean \pm SEM. (* $P < 0.05$).

Figure 4.30

(a)



(b)

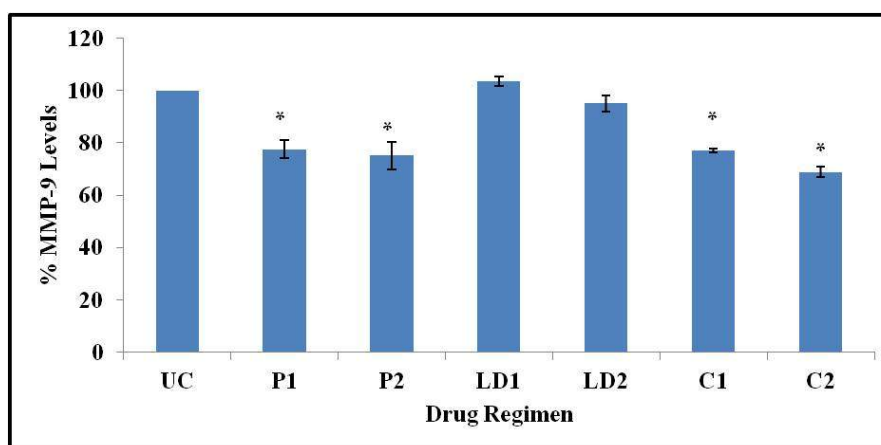
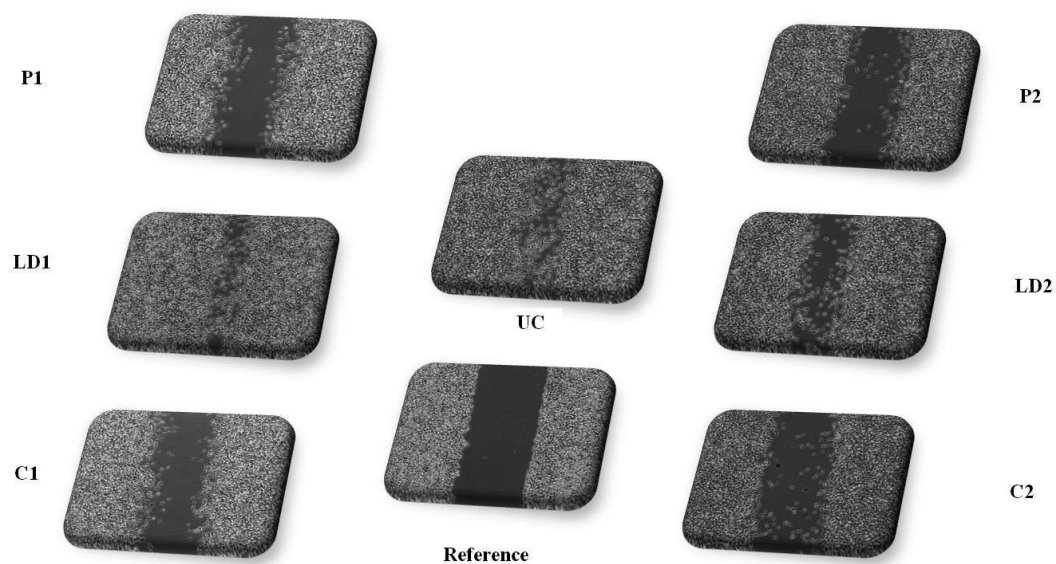


Figure 4.30: Gelatin zymography using condition media upon combination treatment.

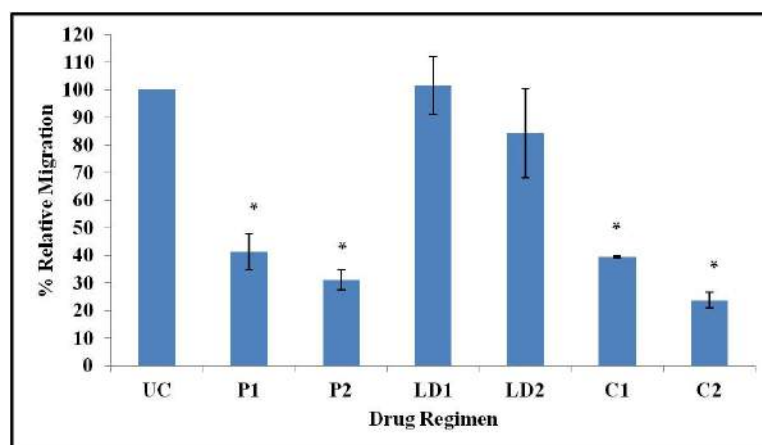
The effect of PTX, LD and combinations was done to evaluate changes in the activity of gelatinases. HT-1080 was used as positive control. (a) Representative zymograms and (b) graphical representation for changes in activity of MMP-9 considering activity in control to be 100%. Results are representative of three independent experiments Mean \pm SEM. (* $P < 0.05$).

Figure 4.31

(a)



(b)

**Figure 4.31: Changes in cellular motility upon combination treatment.**

Wound healing assay was performed to ascertain the anti-motility effects in MDA-MB-231 cells using different combination regimens. (a) Wound images captured after 24 hr of drug exposure. Reference represents wound at zero hr (b) % wound coverage considering

wound closure in control to be 100%. The results are indicative of three independent experiments Mean \pm SEM. (* P <0.05).

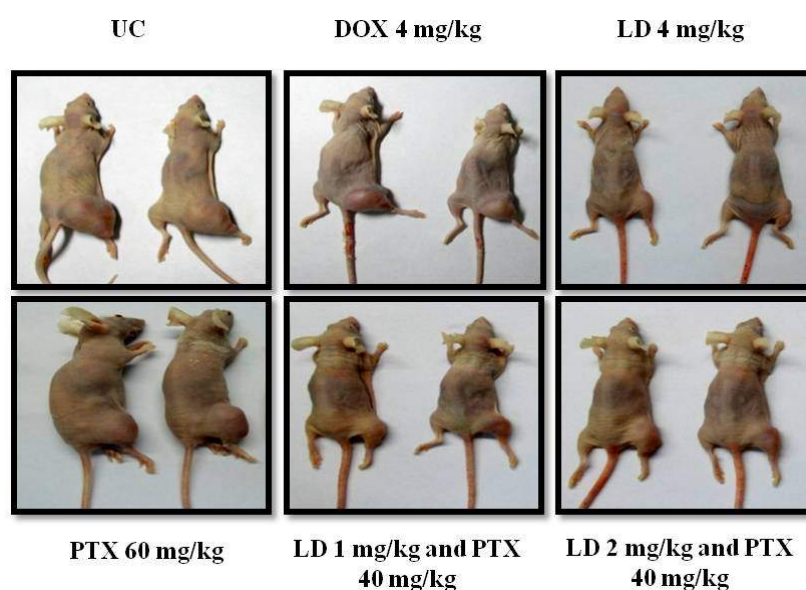
4.19 Combination delays tumour growth using *in vivo* xenograft model

Here, we had used immuno-compromised nude mice (NIH-3) as the xenograft model system to demonstrate the *in vivo* efficacy of PTX, DOX and LD using MDA-MB-231 breast cancer cells. Tumour latency period was found out to be around 4 days. Mice were separated into 6 groups (n=5) as already mentioned. When tumours had reached an approximately 50 mm³ i.e. by day 7th drug dosage was initiated. The treatment regimen given was as followed (a) Group 1 [Untreated or UC (PBS only)], (b) Group 2 [DOX (4 mg/kg)], (c) Group 3 [LD (4 mg/kg)], (d) Group 4 [PTX 60 mg/kg] (e) Group 5 [PTX+LD (40 mg/kg and 1 mg/kg)] and (f) Group 6 [PTX+LD (40 mg/kg and 2 mg/kg)]. PTX was administered intraperitoneally (i.p) in Groups 4, 5 and 6 for a period of 9 days consecutively (day 7th till 15th) while DOX/LD was being injected intravenously (Groups 2, 3, 5 and 6), once a week for 2 weeks respectively (day 7th and 14th). Mice were sacrificed on day 17th. Representative images are shown in (Figure 4.32a). The tumour volumes were found out to be 2429.24 \pm 275.85 mm³, 1035.53 \pm 298.97 mm³, 167.9 \pm 38.06 mm³, 1211.263 \pm 161.96 mm³, 403.8 \pm 69.06 mm³ and 327.1 \pm 53.79 mm³ for untreated, DOX (4 mg/kg), LD (4 mg/kg), PTX (60 mg/kg), PTX+LD (40 mg/kg and 1 mg/kg) and PTX+LD (40 mg/kg and 2 mg/kg) groups respectively (Figure 4.32b) (P <0.05). Further, there were no significant changes in average animal weights in any of the groups under investigation (Figure 4.32c). The tumours were also excised and weighed. There was significant difference in combination groups i.e. Group 5 and 6 compared to the untreated control (Figure 4.32d). The tumours from group 2 and 3 (DOX 4mg/kg as well as LD

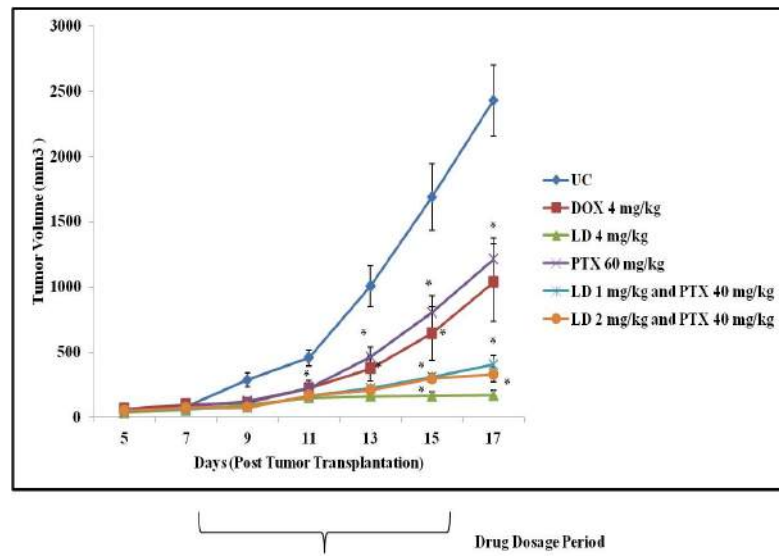
4mg/kg) clearly demonstrates the effect of LD in the *in vivo* system leading to lower tumour volumes along with weights, because of the better half life and thereby increased potency of LD. It should be clearly noted that although the tumour volumes represented for group 3 (LD 4 mg/kg) is much lesser than the combination groups i.e. group 5 PTX+LD (40 mg/kg and 1 mg/kg) and group 6, PTX+LD (40 mg/kg and 2 mg/kg), but the dose for LD given is two and four times the amount given to the latter groups. Thus, the combination surely plays a substantial role in delaying the tumour growth in nude mice at lower doses of both LD and PTX.

Figure 4.32

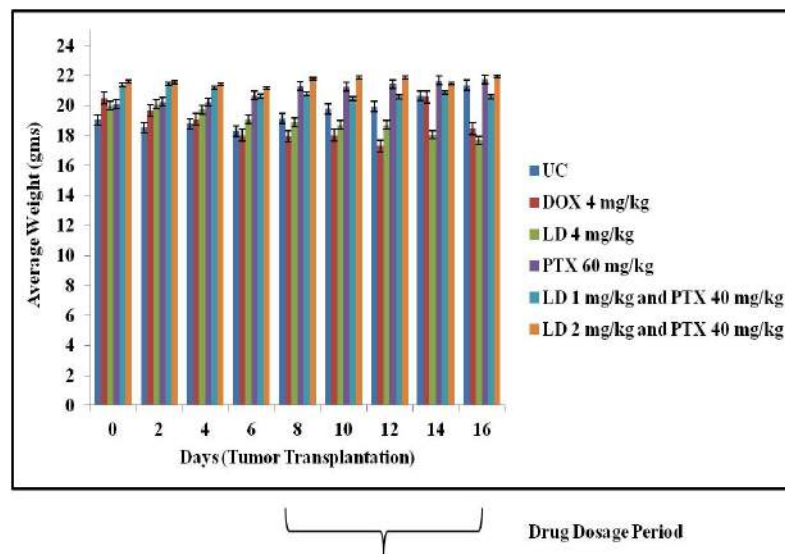
(a)



(b)



(c)



(d)

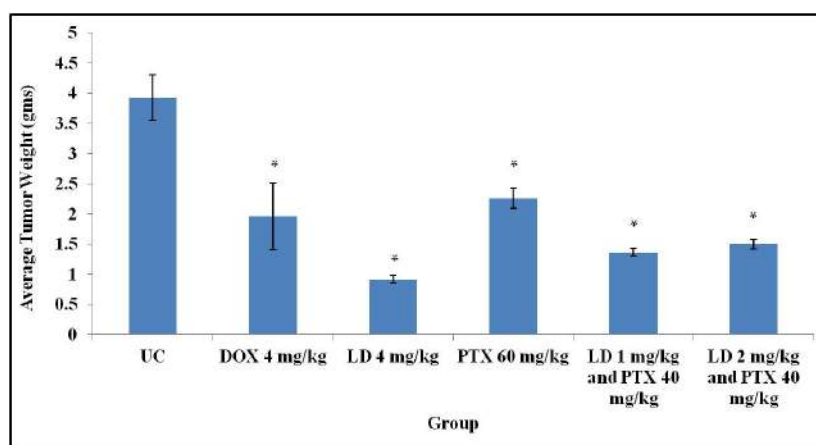


Figure 4.32: *In vivo* xenograft model upon combination treatment.

MDA-MB-231 cells injected sub-cutaneously into nude mice were subjected to treatment using DOX, LD, PTX and their combinations. Mice were sacrificed on day 17th and tumours were excised. (a) Images of animals showing tumour grown on the right flank (b) tumour volumes (c) animal weights at alternate days and (d) average weights of excised tumours.

Chapter 5
Discussion

Breast cancer is the second most diagnosed cancer worldwide [1-3]. The multistep event of metastatic breast cancer involves the invasion of mammary carcinoma cells into the flanking tissues, paving their way to enter systemic circulation, intravasating to target sites mainly the bones, lungs and central nervous system [7,261]. The primary cause for cancer related deaths is the dissemination of tumour cells into the bloodstream making a destination to different target sites. This process starts when a transformed cell accumulates mutations in the genes regulating the key essential pathways, leading to uncontrolled proliferation and its outgrowth [4,5]. The detachment from the primary mass makes it a liable candidate to participate in the next round of confrontation with other physical barriers. Cells having the capability to show increased adhesion, invasion and migration participate in further metastatic sequel [6-8]. Thus, targeting the initial metastatic events such as adhesion, migration and invasion which are the key cardinal signatures surely holds a promise to target the multistep metastatic occurrence. There has been a significant progress in the development of new diagnostic, prognostic and therapeutic strategies but the survival rates for patients with metastatic disease has not changed markedly [262].

Conventional treatment modalities include surgery, followed by radiation and/or chemotherapy. One of the most common causes of failure of a number of potential drugs is their high degree of cytotoxicity and induction of resistance culminating to cause a limitation in therapy. Hence, investigations are often directed to understand the potential and therapeutic efficacy of drug/s which are used in the treatment of other diseases and hence been shown to be non-cytotoxic, to act as anti-cancer or anti-metastatic agents. The pharmacokinetics as well as the safety profiles for the existing drugs is well understood.

Thus, any newer discovered role/s can be harnessed to the fields of clinical trials. This can eventually help drug developers to bypass the assessment costs [97-99]. In view of this, we have evaluated the anti-metastatic potential of PTX in human breast cancer cells. PTX is the drug of choice based on its hydrophilic nature due to its maximal solubility in aqueous among other derivatives such as caffeine [263]. This indeed is a pharmacological advantage in therapeutic scenario.

PTX is a methyl xanthine derivative (3,7, dimethyl-1-(5-oxohexyl xanthine) used as a hemorreological agent in the treatment of peripheral vascular diseases [264]. This primarily occurs through reduction in whole blood viscosity and improved red blood cell flexibility [265]. It can reduce cancer cell stickiness, thereby increasing the circulating time of tumour cells in blood which can become a spotlight for the circulating immune cells [266]. It has shown to exert therapeutic benefits in cardiovascular diseases [267] and as an anti-inflammatory agent by decreasing the levels of TNF- α as well as other inflammatory cytokines [268,269]. It improves tumour oxygenation by increasing tumour blood flow and sensitizes tumours to both irradiation and alkylating agents [263,270]. Further, being a phosphodiesterase inhibitor it increases c-AMP levels [135]. This could lead to suppression of Ras and MAPK activity in variety of cells such as NIH3T3 fibroblasts affecting proliferation [271]. Increased c-AMP is also associated with the attenuation of anti-apoptotic proteins such as Bcl-2, Mdm2 [272] and cytoskeletal reorganization affecting motility in HeLa and B16F10 cells [107,273]. Our lab had earlier demonstrated the anti-metastatic activity of PTX in B16F10 melanoma cells [104-108]. Based on the literature survey suggesting no reports of PTX on human breast cancer cells prompted us to demonstrate its anti-metastatic potential viz. cellular proliferation,

adhesion, migration and invasion in human breast cancer cells using MDA-MB-231(TNBC) cell line as a model for *in vitro* study. Further, we had chosen TNBC as our model system primarily because such type of tumours can be managed by chemotherapy alone as no targeted therapies exist [93-96].

The initial evaluation of PTX in MDA-MB-231 cells was done using a MTT cytotoxic assay for 24 hr, 48 hr and 72 hr. A dose and time dependent decrease in cellular proliferation was observed that confirms the anti-proliferative potential of PTX. There was a decrease in IC_{50} at all the time points. The clonogenic assay further corroborated its anti-proliferative potential. A famous axiom in toxicology by Paracelsus states, 'The dose makes the poison'. Thus, in view of this fact, we had evaluated the effects of PTX at sub-toxic doses *i.e.* doses exhibiting a maximal of 30% toxicity. Hence, doses in sub-toxic range *i.e.* 1 mM, 2.5 mM and 5 mM were selected for further experimentation. PTX induced a cell cycle arrest at G1 phase of cell cycle. This observation is consistent with other anticancer agents that are phosphodiesterase inhibitors [274,275]. Both cyclin D1 as well as cdk4/6 are required to crisscross the G1 phase of the cell cycle [276]. PTX has been associated to lower cyclin D1 levels in mesangial cells that may abolish cdk4 activity [152]. However, PTX inhibited both cyclinD1/cdk6 in our model system without affecting cdk4 levels. Thus, it attenuates the G1 phase of cell cycle by affecting cyclinD1/cdk6 in our model system. EB/AO staining was performed to distinguish live from apoptotic cells. AO fluoresce green in live cells while EB fluoresces orange/red when intercalated with DNA in dead cells. AO being an inclusion dye penetrates cells making the nucleus look green while ET, an exclusion dye penetrates only those cells whose membrane integrity is lost [254]. PTX treated MDA-MB-231 cells showed an

increase in apoptosis at a concentration of 5 mM. This result was further confirmed using AnnexinV/FITC staining that showed a higher number of apoptotic cells compared to the controls. Thus, apart from inducing a cell cycle block it also leads to apoptosis. One of the major family of proteinases associated with the process of tumourigenesis are MMPs [34]. Both MMP-2 and MMP-9 are the major gelatinases playing a key role in degradation of collagen type-IV and gelatin [277]. We observed that PTX inhibited MMP-9 significantly using gelatin zymography. It had been earlier reported that MMP-9 expression is a positive prognostic marker in node-negative breast cancer [278]. TNF- α is a potent transcriptional activator of MMP-9 [279,280]. PTX has been shown to inhibit TNF- α induced MMP-9 secretion in HL60 leukemia cells [281]. Based on these evidences, we propose a similar mechanism of action in this scenario as well. Treatment with PTX also impedes cellular migration in breast cancer cells. A distinct family of small GTPases such as RhoGTPases functions by alternating between an active, GTP bound and an inactive, GDP bound states. These members are involved in diverse processes such as migration, cytoskeletal reorganization and metastasis [40-42]. PTX had been shown to inhibit migration in B16F10 melanoma by the modulation of RhoGTPase activity [107]. We observed a significant decrease in the active levels of both Rac, RhoGTPases at 2.5 mM and 5 mM in the present model system. Further, we postulated that this effect might be due to certain cytoskeletal disruption responsible required for maintenance of cellular integrity. PTX has shown to act as an actin depolymerising agent in B16F10 cells [107,171]. Based on this fact, we had performed actin staining using Phalloidin labeled with fluorochrome FITC. There was a loss of filopodia and lamellopodia, as well as change in cellular morphology upon PTX treatment that further

corroborates our findings. These results clearly document that PTX affected cellular motility and cytoskeletal organization via inhibition of RhoGTPases.

Cells inside the body are firmly glued to supporting matrix i.e the ECM. This ECM not only provides structural support but also provides a means of regulating cellular behavior [282]. It had been well documented that metastatic cancer cells showed a differential adhesive behavior to tumour microenvironment [283]. Based on these observations, we have carried out the experiments to understand the differences in adhesion between the two breast cancer cell lines viz. MDA-MB-231 and MCF-7. The latter is a non-metastatic cell line compared to MDA-MB-231 which is highly invasive and exhibits a high metastatic potential [284]. MDA-MB-231 cells displayed a significant and high adhesive potential to the ECM components at different time points against matrigel, collagen type IV, fibronectin, laminin and vitonectin respectively. This observation supports the fact that metastatic cells do show a differential affinity towards their microenvironment. Based on the ability of higher adhesion of MDA-MB-231 cells prompted us to evaluate the effects of PTX at sub-toxic doses on the ECM substrates as well. A significant reduction in the adhesion potential of MDA-MB-231 cells to ECM substrates such as matrigel, collagen type-IV, fibronectin and laminin was observed upon PTX treatment. No change in adhesion upon PTX treatment was seen against vitronectin. It had been well documented that ECM governs the life cycle and expression of integrins [285,286]. Thus, these results clearly envisage the need to appraise the effect of PTX on integrin receptors that might play a crucial role in regulating the adhesion potential of MDA-MB-231 cells. Both breast cell lines were being tested for differences in surface expression of integrins using flow cytometry. MDA-MB-231 cells exhibited significantly higher levels of

integrins such as α_v , α_3 , α_5 , β_1 , β_3 , β_5 , $\alpha_v\beta_3$, $\alpha_v\beta_5$ and $\alpha_5\beta_1$ compared to MCF-7. However, there was no marked difference observed in the surface expression of integrin α_2 between the two cell lines. These observations are consistent with the earlier report [287]. Hence, these results clearly demonstrate that deviations in surface expression of integrins between the two cell lines might be one of the possible reasons for differential adhesive behavior. Based on our previous observations regarding differences in integrin expression between two breast cancer cell lines, we have evaluated the effects of PTX treatment at sub-toxic doses on integrin expression. A differential effect was being observed upon PTX treatment. PTX affected the surface expression of integrins α_5 , β_1 and $\alpha_5\beta_1$ significantly. Treatment with PTX also caused a reduction in fluorescence of integrin $\alpha_5\beta_1$ using confocal microscopy. A decrease in surface expression was also observed for integrin β_3 at 5 mM but it was rather insignificant. It has been well documented that MDA-MB-231 cells show the highest adhesion potential to fibronectin [288] and this was also confirmed by adhesion assay. Further, PTX decreased the adhesion towards fibronectin in a dose-dependent manner. Integrin $\alpha_5\beta_1$ is well characterized receptor for fibronectin and shown to be highly elevated in breast tumours and is associated with resistance to apoptosis by chemotherapeutic drugs [180,188,237,289]. A decrease in surface expression of both α_5 and β_1 subunits could be a plausible explanation for PTX mediated anti-adhesive effects on fibronectin. This observation is consistent with the earlier report that loss of fibronectin leads to decrease in expression of $\alpha_5\beta_1$ integrin [290]. The changes in total protein levels was also confirmed by western blotting that showed a dose-dependent reduction in total levels of both the integrins. Although, there was no change in surface expression for integrins α_v ,

α_2 , α_3 , β_3 and β_5 but a decrease in total protein levels was observed for integrins α_v , α_3 and β_3 . No change in protein levels was seen for integrins α_2 and β_5 . Integrin $\alpha_2\beta_1$ is known to play a role in metastatic suppression [191] and thus no effect of PTX on surface and total protein levels of $\alpha_2\beta_1$ could thus be well justified. In addition, no change in integrin transcriptional levels was seen upon PTX treatment. Thus, PTX affects the integrins at the protein/post translational level at least in our model system. This differential outcome of PTX upon integrin expression might be due to its effect on degradation-synthesis axis for surface receptor modulation or rather integrin transport. These findings do implicate the anti-metastatic activity of PTX by regulation of cell-ECM adhesion via integrins.

Integrins are devoid of any enzymatic activity and thus require the engagement of kinases such as FAK to mediate its downstream signaling. FAK, a non-receptor tyrosine kinase regulates myriad of cell signaling pathways. This orchestration network embraces key metastatic attributes such as proliferation, migration, invasion, apoptosis as well as angiogenesis [193-198]. The increased levels of FAK form a positive correlation with the invasive behavior from a benign state [194,208-214]. It phosphorylates a large number of substrates which in turn regulate downstream signaling events. Once activated by a key phosphorylation at tyrosine397 residue ensures successive signaling events such as activation of PI3K/Akt signaling, a central pathway regulating apoptosis [198]. Levels of both FAK and PI3K/Akt are unregulated in breast cancers [194,217]. It also regulates the functioning of RhoGTPases and MAPK signaling that aids the process of cellular migration and proliferation respectively [291,292].

Treatment with PTX affects the active levels of FAK in a dose-dependent manner. Further, FAK regulates the processes of cellular proliferation via the MAPK as well as Akt pathways [197,293]. Earlier studies had shown that PTX inhibited ERK or MAPK pathway in human ovarian cancer cells [124]. It had also shown to inhibit Akt activation as well as its translocation in smooth muscle cells and mesangial cells respectively [151,152]. FAK inhibition is associated with decrease in Akt levels where it is a critical downstream intercessor of FAK survival signaling, protecting the cells from apoptosis. A dose dependent decrease was observed in the levels of both activated forms of ERK1/2 and Akt. In the present study we also found out a dose dependent effect of FAKi on activated form of MAPK and Akt levels. It also impedes the cellular migration using wound scratch assay. These results further confirm that FAK is a key regulator of tumorigenesis and thus targeting FAK holds a key promise for therapeutic intervention. ERK2 has been shown to regulate levels of VEGF, a potent activator of angiogenesis [292]. Earlier studies had shown that PTX inhibits VEGF release in human MCF-7 and A549 cancer cells [156]. We observed a similar decrease in cellular levels of VEGF, suggestive of its anti-angiogenic action as well. This result was further affirmed by our *in-vivo* findings where PTX at 40 mg/kg and 60 mg/kg inhibited blood vessel and tumour formation.

Akt regulates the activity of caspase-9 by phosphorylating it, preventing its activation and upregulates the Bcl-2 expression via c-AMP response element binding protein [221,222]. We found a dose dependent increase in levels as well as activities of cleaved caspase-9 and its downstream effector caspase i.e cleaved caspase-3. A dose dependent increase in protein levels of cleaved PARP was also observed. Caspase-3 is an executioner caspase

since it is responsible for the proteolytic cleavage of many key proteins such as the PARP [294]. Further, decrease in both Bcl-2 and Bcl-xL levels were ascertained. However, decrease in Bcl-xL was less pronounced than Bcl-2 levels, while no changes in Mcl-1 levels were observed. These observations clearly indicated that PTX might be able to modulate the FAK/Akt axis to induce apoptosis in MDA-MB-231 cells that further potentiates our earlier findings that PTX treatment induces cellular apoptosis in MDA-MB-231 cells. We had also evaluated the effects of Akti on apoptotic machinery and found that treatment with Akti affects the expression of caspase 9, caspase 3, PARP and Bcl-2. This confirmed that inhibition of Akt pathway leads to cellular apoptosis. Thus, inhibition of integrins at the cell surface modulates the adhesive potential towards ECM components. This in turn affects the FAK signaling that causes cellular death by affecting the Akt pathway.

Preclinical evaluation of any chemotherapeutic agent forms an integral aspect in therapeutic scenario. *In vivo* studies were done to test the efficacy of PTX using NOD-SCID mice. The doses were calculated based on body surface area [295]. There was a significant tumour growth delay upon PTX treatment, indicative of a stronger evidence for clinical potential. However, no significant difference in tumour volume was observed between the two groups of PTX 40 mg/kg and 60 mg/kg per se. Integrins are known to be involved in the process of angiogenesis as well [183]. Intradermal model for evaluating anti-angiogenic activity showed a promising role for PTX as well. Dose dependent decrease in blood vessel as well as tumour development was observed. There was no significant weight loss noticeable during the course of the treatment. Further, we have evaluated the effect of PTX on angiogenesis using *in ovo* model CAM assay. CAM assay

was performed as an additional validation to corroborate our findings and we did observe a decrease in blood vessel formation around the growing embryo. Previous reports from our lab have established that PTX pre-treated melanoma cells showed lesser tumour island formation in C57/BL6 mice [106]. In our model system MDA-MB-231 cells were injected intravenously and PTX administration was started at the same day for a period of 9 days. Mice were being sacrificed after a period of approximately 30 days and the lungs were excised. Numerous tumour islands were being present in the untreated group. These islands were both large and small being present throughout the lung parenchyma. However, in the treatment group PTX 40 mg/kg, tumour cells were present at few places while other areas were found to be devoid of tumour cells and were clear. In addition, animals treated with PTX 60 mg/kg group showed presence of metastatic cells and formation of smaller tumour islands. These observations of our *in vitro* results together with the *in vivo* findings shows that PTX do qualify as an effective anti-metastatic agent. The known anti-cancer drugs suffer from high degrees of toxicity and thus there is an imperative rationale to develop combination regimens of PTX with other known anti-cancer drugs actively used against breast cancer. The basic principle for a combination therapy is to surmount individual drug limitations and to decrease the payload for each individual drug, thereby reducing the toxicity as well increasing their therapeutic efficacy [239-241]. Chemotherapy forms one of the major therapeutic interventions in the treatment of advanced breast cancer [82,84,85,90-92,242]. Anthracyclines such as doxorubicin (DOX) or adriamycin (ADR) comprise one of the treatment options in this scenario [242]. However, there are a large number of toxicity related issues are associated with the usage of doxorubicin [243,244]. In order to overcome these limitations, drug

delivery systems such as the entrapment of DOX in pegylated liposomes coated with methoxypolyethylene glycol (MPEG) are preferred [244,245]. These modifications not only increase their blood circulation time but also protect them from mononuclear phagocyte system apart from causing minimal toxicity to normal cells due to slower or sustained release [245]. Based on these properties, we have evaluated the combinatorial effects of PTX along with liposomal doxorubicin (Lipodox or LD) so as to increase its therapeutic efficacy in breast cancer cells. There are a few reports that have used combination of both PTX and DOX against cervical and leukemic cells [125,126]. However, no report regarding usage against breast cancer has been documented so far. In this context, the effects of combination therapy (PTX and LD) on various metastatic events *viz.* cellular proliferation, adhesion, migration, invasion and apoptosis had been demonstrated. LD was used in our present study since it is comparatively lesser toxic compared to DOX alone. The % viability of both PTX and LD in the ratio of 500:1 was determined using MTT assay at different doses both in combination as well as single agents respectively. It was found that PTX at doses of 3 mM, 4 mM and corresponding LD at 6 μ M and 8 μ M showed synergistic action where CI tends to be less than unity. This clearly indicates that the combination dose acts synergistically and is more potent than individual drugs. Based on these combination doses, anti-metastatic activity of the combination regimen was evaluated. The anti-proliferative activity of the combination regimen was further confirmed using colony formation assay which further confirmed that combination doses of C1 and C2 are more efficacious than individual dosage. We had shown that PTX inhibits the MAPK pathway that regulates the process of proliferation. Further, DOX also has shown to inhibit the same in breast cancer cells

[296]. In light of these evidences, we propose a similar mode of action for the combination doses in our experimental system as well. Flow cytometry was done to assess the cell cycle status of MDA-MB-231 cells upon PTX and LD treatment as well as their combinations (C1 and C2). It was found that treatment with PTX leads to a significant increase in G1 phase of the cell cycle. However, treatment with LD causes a G2-M cell cycle arrest significantly. PTX caused a G1 cell cycle arrest as demonstrated earlier by affecting the cyclinD1/cdk6 complex while in case of DOX a G2/M arrest had been reported [297]. We had found a similar observation in our experimental system as well. However, in the combination scenario a G1 phase cell cycle arrest was pronounced. The plausible reason is that since G1 phase precedes G2/M phase in the cell cycle, thus blockade in G1 phase by PTX shall not permit cells to bypass it in the combination scenario. Further, we had evaluated the effect of combination doses on cellular apoptosis. Both PTX and DOX are known to increase the apoptosis in cervical cancer [125]. Based on this, AnnexinV/FITC staining was performed to demonstrate the same in MDA-MB-231 cells. There was an increase in apoptosis in case of combination doses compared to individual treatments seen by an increase in number of apoptotic cells in both C1 and C2. To further corroborate our findings, ET/AO staining was performed. A similar effect was also observed in the combination regimen. These results clearly indicated that the combination of both PTX and LD caused an increase in apoptosis. However, molecular insight needs to be explored to unravel the plausible mechanism of action.

The metastatic cascade is a very complex event [6-8]. Accumulating mutations leads to cellular transformation and hyper-proliferation of the cells. These cancerous cells then loosen up their cell-cell as well as cell-ECM contacts thereby regulating the process of

cellular adhesion. Certain enzymes such as MMPs are being secreted that degrades the ECM and aids in paving the path for cancer cells to migrate and enter the bloodstream [32-35]. The tumour cells are then carried to distant sites via the bloodstream forming distant metastasis [8]. It should be noteworthy that both the processes of adhesion and proteolysis play an important role in the metastatic process by regulating the interaction of tumour cells with other cells and the underlying ECM, migration and survival cues [9]. In this regard, adhesion assay was done to evaluate the adhesive potential of MDA-MB-231 cells upon PTX, LD as well as their combinations to various ECM components viz. matrigel, collagen type IV, fibronectin, laminin and vitronectin. It was found that LD *per se* does not alter adhesion to any of the mentioned substrates. PTX at doses of 3 mM and 4 mM does affect adhesion. Further, the combination regimen showed a slight reduction in adhesion in comparison to use of PTX alone on matrigel, collagen type IV and laminin respectively. No change in adhesion was observed to vitronectin. These results clearly indicate that LD does not affect cellular adhesion to ECM components. However, in the combination regimen it is PTX that alters the same. We had earlier shown that PTX at sub-toxic doses affects cellular adhesion to ECM components and its allied receptors, integrins. We propose a similar mechanistic insight for the same in the combination scenario as well as in the combination with LD. The effect of combination was then evaluated on the activity of gelatinases such as MMP-2 and MMP-9 using gelatin zymography. Both these gelatinases degrade the collagen, a major constituent of basal lamina present in basement membrane. We observed MMP-9 activity in MDA-MB-231 cells to be very high. Further, MMP-9 in the condition media of MDA-MB-231 cells subjected to gelatin zymography was found to have a higher molecular weight than

corresponding MMP-9 from HT-1080. The plausible reason for such an observation is that MMP-9 might be associated with a small microglobulin that does not separate during the process of zymography and thus forms a high molecular complex [298]. We found that LD does not affect the activity of MMP-9 and thus it is rather PTX present in the combination regimen that brings about an alteration in the activity of MMP-9. Wound healing assay was done to assess the anti-migratory effect of combination regimens in MDA-MB-231 cells. It was observed that LD does not affect the process of motility, while PTX at both the doses (P1 and P2) impedes migration. In the combination regimen, a similar decrease in migration was observed. In short, we found out that LD *per se* does not affect the processes of adhesion, invasion and migration but it is rather the doses of PTX that brings about an alteration. It should be noted that anthracyclines such as DOX suffer from various toxicity related issues for the treatment of breast cancer [243,244]. However, it is still used in the clinics for its effectiveness [242,247,248]. Data from the combination studies clearly showed that PTX when used in conjunction with LD could target more metastatic pathways than LD alone. In a way, this combination shall serve to limit the doses of DOX as well achieve a wider target range along with PTX in our model system. Lastly we had evaluated the effect of combination of PTX and LD *in vivo*.

Here, we had used immuno-compromised nude mice (NIH-3) as the xenograft model system to demonstrate the *in vivo* efficacy of PTX, DOX and LD using MDA-MB-231 breast cancer cells. There was significant difference in combination groups i.e. Group 5 and 6 compared to the untreated control. The tumours from group 2 and 3 (DOX 4mg/kg as well as LD 4mg/kg) clearly demonstrates the effect of LD in the *in vivo* system leading to lower tumour volumes along with weights, because of the better half life and thereby

increased potency of LD. It should be clearly noted that although the tumour volumes represented for group 3 (LD 4 mg/kg) is much lesser than the combination groups i.e. group 5 PTX+LD (40 mg/kg and 1 mg/kg) and group 6, PTX+LD (40 mg/kg and 2 mg/kg), but the dose for LD given is two and four times the amount given to the latter groups. Thus, the combination surely plays a substantial role in delaying the tumour growth in nude mice at lower doses of both LD and PTX. Hence, in short the combination regime exhibited synergistic activity and inhibited cellular proliferation to a greater extent with regard to each drug used alone.

Summary and Conclusions

Cancer is a global wreck and the current therapeutic modalities fail to circumvent the associated deaths. Breast cancer is the most common form of cancer among women and second most leading cause of cancer related deaths worldwide. It is the outcome of multistep carcinogenesis and is associated with intense metabolic perturbations. The basic scheme for treatment includes surgery, radiotherapy and chemotherapy. Owing to high degrees of cytotoxicity and resistance there is an urgent need to identify new candidate entities to limit the current problems. One of the approaches in this regard is drug repositioning or finding new uses of the available drugs. It is assuredly becoming a concerning subject for Pharma companies and has indeed gained success in several incidences.

The most deadly aspect of cancer is its ability to spread, or metastasize. Therefore, search for an anti-metastatic compound is a crucial aspect of anti-cancer drug research. Metastasis is a stepwise process so drugs that can intervene in any of these events are clinically important. In this direction, our laboratory had discovered anti-metastatic property of a methyl-xanthine derivative, PTX using the B1F10 mouse melanoma model. In the current piece of work, we had investigated its potential against TNBC using MDA-MB-231 cells as our model system by *in vitro* and *in vivo* approaches. We had demonstrated the effect of PTX on integrin mediated adhesion and induced apoptosis upon loss of cellular adhesion in MDA-MB-231 cells. Further, we had evaluated its effect in combination with a potent anti-cancer agent, currently used in the treatment of breast cancer so as to improve the therapeutic efficacy of the same.

The summary of the results are as follows:

- PTX inhibits cellular proliferation in a dose and time dependent manner using MTT assay. IC₅₀ values observed at 24 hr, 48 hr and 72 hr were 9 mM, 3 mM, 2 mM respectively. This was further corroborated by a dose dependent decrease using colony formation assay.
- It hinders cell cycle progression at G0-G1 phase by affecting the levels of cyclinD1/cdk6 at sub-toxic doses. It also induces apoptosis as demonstrated by AnnexinV and ET/AO staining. This was further confirmed by a decrease in anti-apoptotic proteins such as Bcl-2 and Bcl-xL. It also affected the intrinsic pathway of apoptosis by modulating the expression and activities of both caspase 9 and caspase 3.
- PTX decreases adhesion significantly to ECM substrates (viz matrigel, collagen type1V, fibronectin and laminin) in a time and dose dependent manner. However, no significant change in adhesion was observed for vitronectin upon PTX treatment.
- It affected the activity of MMP-9 in a dose dependent manner using gelatin zymography and impedes cellular migration in wound scratch assay. PTX affected the cellular migration by disrupting the actin cytoskeleton and hampering the filopodia and lamellopodia formation. It also affected the RhoGTPases such as Rac and Rho in a dose-dependent manner.
- MDA-MB-231 demonstrated higher adhesive potential compared to MCF-7 to ECM components viz matrigel, collagen type1V, fibronectin, laminin and

vitronectin. It also expresses higher levels of integrins such as $\alpha 3$, $\alpha 5$, $\beta 1$, $\beta 3$, $\beta 5$, $\alpha V\beta 3$, $\alpha 5\beta 1$ and $\alpha V\beta 5$ compared to MCF-7.

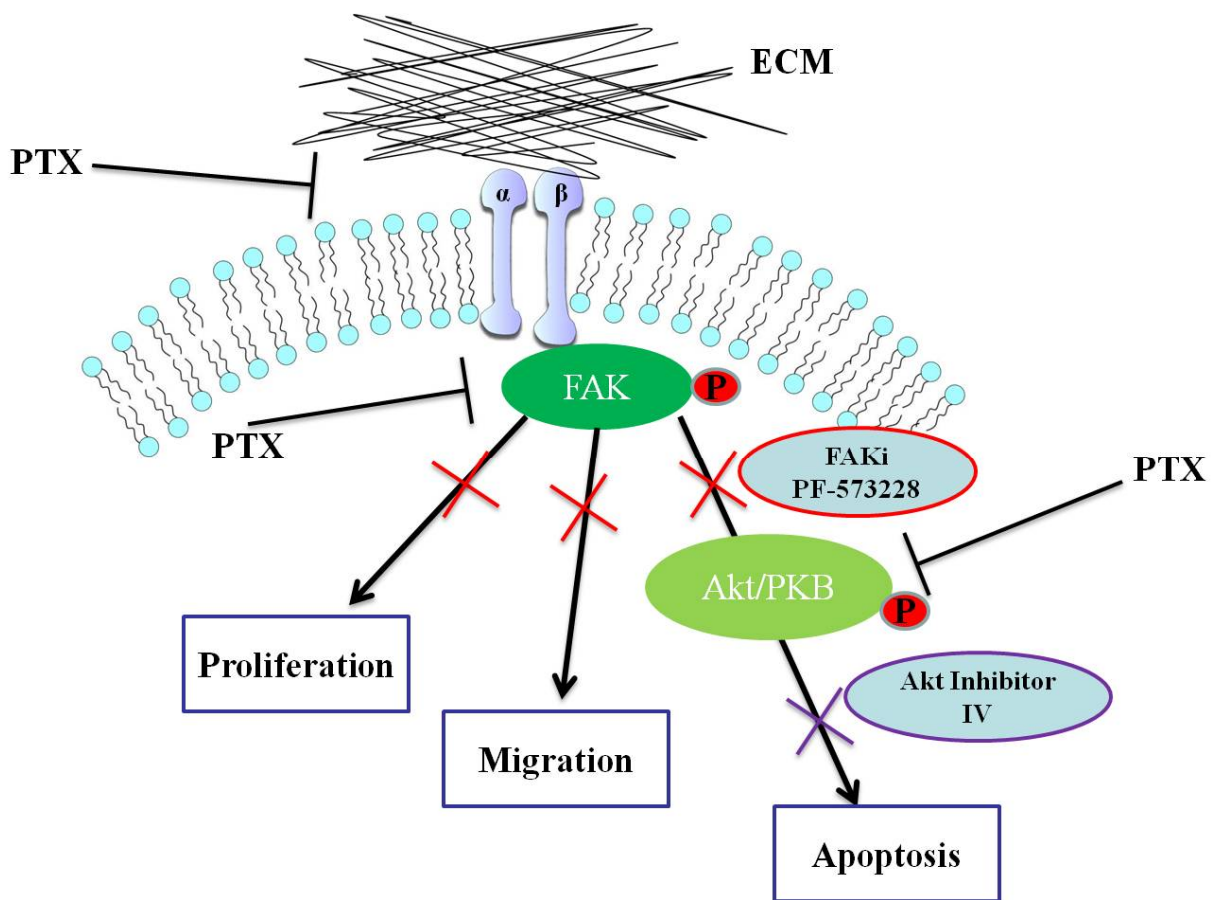
- PTX decreased the surface expression of integrins such as $\alpha 5$, $\beta 1$ and $\alpha 5\beta 1$ on MDA-MB-231 cells using flow cytometry. Further, it affects the surface localisation of $\alpha 5\beta 1$ using confocal microscopy. It lowered total protein levels of αV , $\alpha 3$, $\alpha 5$, $\beta 1$ and $\beta 3$ integrins respectively using western blotting. However, PTX treatment does not affect the transcriptional level of any of the integrins in MDA-MB-231 cells under investigation.
- PTX affected the FAK expression in a dose dependent manner that in turn regulates the MAPK and Akt signalling. It affected the Akt expression and its downstream mediators such as caspase 9, caspase 3 and PARP leading to cellular apoptosis. It affected the process of angiogenesis by inhibiting the expression of VEGF.
- PTX administration delays tumour growth in the xenograft model as well as inhibits the process of angiogenesis by inhibiting blood vessel formation using NOD-SCID mice. It also inhibits blood vessel formation using *in ovo* CAM assay. Further, PTX affects adhesion of MDA-MB-231 cells to lungs in the experimental metastasis model. Here, PTX treated groups showed lesser and smaller colonies compared to the untreated control.
- MTT assay for both lipodox and Adriamycin (ADR) showed that ADR is highly toxic at all time points viz. 24 hr, 48 hr, 72 hr. The combination was then developed using LD and PTX (1:500). Doses that CI less than 1 are synergistic. It was found that PTX at doses of 3 mM, 4 mM and corresponding LD at 6 μ M and

8 μ M showed synergistic action. Based on these combination doses, anti-metastatic activity of the combination regimen was evaluated. The doses were designated as PTX or P1 3 mM, PTX or P2 4 mM, LD or LD1 6 μ M, LD or LD2 8 μ M, combination C1 (P1 and LD1) and combination C2 (P2 and LD2) respectively. Further, colony formation showed a significant decrease in the combination treatments compared to single drugs alone.

- Flow Cytometry was further done to assess the cell cycle status. It was found that treatment with PTX leads to a significant increase in G1 phase of the cell cycle. Treatment with LD causes a G2-M cell cycle arrest. However, in the combination scenario a G1 phase cell cycle arrest was pronounced.
- ET/AO staining and AnnexinV/FITC staining was done to measure the apoptosis upon drug treatments. There was an increase in apoptosis in the combination compared to PTX and LD alone.
- Adhesion assay was carried out using various ECM components viz. matrigel, collagen type IV, fibronectin, laminin and vitronectin. It was found that LD *per se* does not alter adhesion to any of the mentioned substrates. Further, the combination regimen showed a similar reduction comparable to use of PTX alone. No change in adhesion was observed to vitronectin.
- The effect of PTX, LD and their combinations of gelatinases was studied by performing gelatin zymography. The combination regimens showed a similar decrease in MMP-9 activity as observed with PTX alone. A similar observation was accounted for cellular migration.

- Combination regimen of lipodox and PTX brings about a significant reduction in tumour volumes as compared to untreated control.

The key findings discoursed in the present research work provides a leading edge to investigate the effect of PTX in other model systems as well, so to ascertain its utilization in the proper management, design of newer combination regimens and treatment of metastasis in other cancers as well.



Probable mechanism of action of PTX in MDA-MB-231 cells.

Bibliography

1. R. Siegel, D. Naishadham, and A. Jemal. Cancer statistics, 2013. *CA: a cancer journal for clinicians*. 63:11-30 (2013).
2. J. Ferlay, H.R. Shin, F. Bray, D. Forman, C. Mathers, and D.M. Parkin. Estimates of worldwide burden of cancer in 2008: GLOBOCAN 2008. *Int J Cancer*. 127:2893-2917 (2010).
3. American Cancer Society. *Global Cancer Facts & Figures 2nd Edition*. Atlanta: American Cancer Society; 2011.
4. D. Hanahan and R.A. Weinberg. The hallmarks of cancer. *Cell*. 100:57-70 (2000).
5. D. Hanahan and R.A. Weinberg. Hallmarks of cancer: the next generation. *Cell*. 144:646-674 (2011).
6. G.P. Gupta and J. Massague. Cancer metastasis: building a framework. *Cell*. 127:679-695 (2006).
7. D.X. Nguyen, P.D. Bos, and J. Massague. Metastasis: from dissemination to organ-specific colonization. *Nature Reviews Cancer*. 9:274-284 (2009).
8. A. Irmisch and J. Huelsken. Metastasis: New insights into organ-specific extravasation and metastatic niches. *Exp Cell Res*. 319:1604-1610 (2013).
9. M. Bacac and I. Stamenkovic. Metastatic cancer cell. *Annu Rev Pathol*. 3:221-247 (2008).
10. S. Vanharanta and J. Massague. Origins of metastatic traits. *Cancer Cell*. 24:410-421 (2013).
11. T. Okegawa, R.C. Pong, Y. Li, and J.T. Hsieh. The role of cell adhesion molecule in cancer progression and its application in cancer therapy. *Acta Biochim Pol*. 51:445-457 (2004).
12. U. Cavallaro and E. Dejana. Adhesion molecule signalling: not always a sticky business. *Nat Rev Mol Cell Biol*. 12:189-197 (2011).
13. R.O. Hynes and A.D. Lander. Contact and adhesive specificities in the associations, migrations, and targeting of cells and axons. *Cell*. 68:303-322 (1992).
14. D.R. Coman. Decreased mutual adhesiveness, a property of cells from squamous cell carcinomas. *Cancer Research*. 4:625-629 (1944).
15. G. Bendas and L. Borsig. Cancer cell adhesion and metastasis: selectins, integrins, and the inhibitory potential of heparins. *Int J Cell Biol*. 2012:676731 (2012).
16. J. Behrens. The role of cell adhesion molecules in cancer invasion and metastasis. *Breast Cancer Res Treat*. 24:175-184 (1993).
17. B. Alberts, A. Johnson, J. Lewis, M. Raff, K. Roberts, and P. Walter. *Cell junctions, cell adhesion, and the extracellular matrix*. (2002).
18. R. Singhai, V.W. Patil, S.R. Jaiswal, S.D. Patil, M.B. Tayade, and A.V. Patil. E-Cadherin as a diagnostic biomarker in breast cancer. *N Am J Med Sci*. 3:227-233 (2011).
19. P.J. Kowalski, M.A. Rubin, and C.G. Klee. E-cadherin expression in primary carcinomas of the breast and its distant metastases. *Breast Cancer Res*. 5:R217-222 (2003).
20. S. Boudjadi, J.C. Carrier, and J.F. Beaulieu. Integrin alpha1 subunit is up-regulated in colorectal cancer. *Biomark Res*. 1:16 (2013).

21. G. Zhou, D. Chiu, D. Qin, L. Niu, J. Cai, L. He, D. Tan, and K. Xu. Expression of CD44v6 and integrin-beta1 for the prognosis evaluation of pancreatic cancer patients after cryosurgery. *Diagn Pathol.* 8:146 (2013).
22. M. Poettler, M. Unseld, K. Braemswig, A. Haitel, C.C. Zielinski, and G.W. Prager. CD98hc (SLC3A2) drives integrin-dependent renal cancer cell behavior. *Mol Cancer.* 12:169 (2013).
23. S. Subbaram and C.M. DiPersio. Integrin $\alpha 3\beta 1$ as a breast cancer target. *Expert opinion on therapeutic targets.* 15:1197-1210 (2011).
24. C. Boger, H. Kalthoff, S.L. Goodman, H.M. Behrens, and C. Rocken. Integrins and their ligands are expressed in non-small cell lung cancer but not correlated with parameters of disease progression. *Virchows Arch.* (2013).
25. T.D. Palmer, C.H. Martinez, C. Vasquez, K.E. Hebron, C. Jones-Paris, S.A. Arnold, S.M. Chan, V. Chalasani, J.A. Gomez-Lemus, A.K. Williams, J.L. Chin, G.A. Giannico, T. Ketova, J.D. Lewis, and A. Zijlstra. Integrin-Free Tetraspanin CD151 Can Inhibit Tumour Cell Motility upon Clustering and Is a Clinical Indicator of Prostate Cancer Progression. *Cancer Res.* (2013).
26. E. Pohec, M. Janik, D. Hoja-Lukowicz, P. Link-Lenczowski, M. Przybylo, and A. Litynska. Expression of integrins alpha3beta1 and alpha5beta1 and GlcNAc beta1,6 glycan branching influences metastatic melanoma cell migration on fibronectin. *Eur J Cell Biol.* (2013).
27. B. Al-Husein, A. Goc, and P.R. Somanath. Suppression of interactions between prostate tumour cell-surface integrin and endothelial ICAM-1 by simvastatin inhibits micrometastasis. *J Cell Physiol.* 228:2139-2148 (2013).
28. S. Nakamori, M. Kameyama, S. Imaoka, H. Furukawa, O. Ishikawa, Y. Sasaki, T. Kabuto, T. Iwanaga, Y. Matsushita, and T. Irimura. Increased expression of sialyl Lewisx antigen correlates with poor survival in patients with colorectal carcinoma: clinicopathological and immunohistochemical study. *Cancer Res.* 53:3632-3637 (1993).
29. K.J. Kim, A. Godarova, K. Seedle, M.H. Kim, T.A. Ince, S.I. Wells, J.J. Driscoll, and S. Godar. Rb Suppresses Collective Invasion, Circulation and Metastasis of Breast Cancer Cells in CD44-Dependent Manner. *PLoS One.* 8:e80590 (2013).
30. J.C. Adams. Molecular organisation of cell-matrix contacts: essential multiprotein assemblies in cell and tissue function. *Expert Rev Mol Med.* 4:1-24 (2002).
31. J.S. Desgrosellier and D.A. Cheresh. Integrins in cancer: biological implications and therapeutic opportunities. *Nat Rev Cancer.* 10:9-22 (2010).
32. M. Polette, B. Nawrocki-Raby, C. Gilles, C. Clavel, and P. Birembaut. Tumour invasion and matrix metalloproteinases. *Crit Rev Oncol Hematol.* 49:179-186 (2004).
33. I. Stamenkovic. Matrix metalloproteinases in tumour invasion and metastasis. *Semin Cancer Biol.* 10:415-433 (2000).
34. L.A. Shuman Moss, S. Jensen-Taubman, and W.G. Stetler-Stevenson. Matrix metalloproteinases: changing roles in tumour progression and metastasis. *Am J Pathol.* 181:1895-1899 (2012).
35. C.M. Overall and O. Kleinfeld. Tumour microenvironment - opinion: validating matrix metalloproteinases as drug targets and anti-targets for cancer therapy. *Nat Rev Cancer.* 6:227-239 (2006).

-
36. J.J. Bravo-Cordero, L. Hodgson, and J. Condeelis. Directed cell invasion and migration during metastasis. *Curr Opin Cell Biol.* 24:277-283 (2012).
 37. D.A. Lauffenburger and A.F. Horwitz. Cell migration: a physically integrated molecular process. *Cell.* 84:359-369 (1996).
 38. V.O. Paavilainen, E. Bertling, S. Falck, and P. Lappalainen. Regulation of cytoskeletal dynamics by actin-monomer-binding proteins. *Trends Cell Biol.* 14:386-394 (2004).
 39. L.M. Machesky. Lamellipodia and filopodia in metastasis and invasion. *FEBS Lett.* 582:2102-2111 (2008).
 40. C. Guilluy, R. Garcia-Mata, and K. Burridge. Rho protein crosstalk: another social network? *Trends Cell Biol.* 21:718-726 (2011).
 41. J. van Rijssel and J.D. van Buul. The many faces of the guanine-nucleotide exchange factor trio. *Cell Adh Migr.* 6:482-487 (2012).
 42. A. Murali and K. Rajalingam. Small Rho GTPases in the control of cell shape and mobility. *Cell Mol Life Sci.* (2013).
 43. R. Ananthakrishnan and A. Ehrlicher. The forces behind cell movement. *Int J Biol Sci.* 3:303-317 (2007).
 44. R.E. Mahaffy and T.D. Pollard. Kinetics of the formation and dissociation of actin filament branches mediated by Arp2/3 complex. *Biophys J.* 91:3519-3528 (2006).
 45. W.E. Allen, D. Zicha, A.J. Ridley, and G.E. Jones. A role for Cdc42 in macrophage chemotaxis. *J Cell Biol.* 141:1147-1157 (1998).
 46. C.D. Nobes and A. Hall. Rho GTPases control polarity, protrusion, and adhesion during cell movement. *J Cell Biol.* 144:1235-1244 (1999).
 47. P. Rickert, O.D. Weiner, F. Wang, H.R. Bourne, and G. Servant. Leukocytes navigate by compass: roles of PI3Kgamma and its lipid products. *Trends Cell Biol.* 10:466-473 (2000).
 48. E.E. Sander, S. van Delft, J.P. ten Klooster, T. Reid, R.A. van der Kammen, F. Michiels, and J.G. Collard. Matrix-dependent Tiam1/Rac signaling in epithelial cells promotes either cell-cell adhesion or cell migration and is regulated by phosphatidylinositol 3-kinase. *J Cell Biol.* 143:1385-1398 (1998).
 49. P.A. DiMilla, K. Barbee, and D.A. Lauffenburger. Mathematical model for the effects of adhesion and mechanics on cell migration speed. *Biophys J.* 60:15-37 (1991).
 50. T.J. Mitchison and L.P. Cramer. Actin-based cell motility and cell locomotion. *Cell.* 84:371-379 (1996).
 51. M. Amano, Y. Fukata, and K. Kaibuchi. Regulation and functions of Rho-associated kinase. *Exp Cell Res.* 261:44-51 (2000).
 52. K. Kaibuchi. Regulation of cytoskeleton and cell adhesion by Rho targets. *Prog Mol Subcell Biol.* 22:23-38 (1999).
 53. V. Niggli. Rho-kinase in human neutrophils: a role in signalling for myosin light chain phosphorylation and cell migration. *FEBS Lett.* 445:69-72 (1999).
 54. W.T. Chen. Mechanism of retraction of the trailing edge during fibroblast movement. *J Cell Biol.* 90:187-200 (1981).
 55. S.P. Palecek, A. Huttenlocher, A.F. Horwitz, and D.A. Lauffenburger. Physical and biochemical regulation of integrin release during rear detachment of migrating cells. *J Cell Sci.* 111 (Pt 7):929-940 (1998).
-

56. S.P. Palecek, C.E. Schmidt, D.A. Lauffenburger, and A.F. Horwitz. Integrin dynamics on the tail region of migrating fibroblasts. *J Cell Sci.* 109 (Pt 5):941-952 (1996).
57. Y. Miura, A. Kikuchi, T. Musha, S. Kuroda, H. Yaku, T. Sasaki, and Y. Takai. Regulation of morphology by rho p21 and its inhibitory GDP/GTP exchange protein (rho GDI) in Swiss 3T3 cells. *J Biol Chem.* 268:510-515 (1993).
58. A. Glading, P. Chang, D.A. Lauffenburger, and A. Wells. Epidermal growth factor receptor activation of calpain is required for fibroblast motility and occurs via an ERK/MAP kinase signaling pathway. *J Biol Chem.* 275:2390-2398 (2000).
59. J.P. Sleeman, I. Nazarenko, and W. Thiele. Do all roads lead to Rome? Routes to metastasis development. *Int J Cancer.* 128:2511-2526.
60. T. Dittmar, C. Heyder, E. Gloria-Maercker, W. Hatzmann, and K.S. Zanker. Adhesion molecules and chemokines: the navigation system for circulating tumour (stem) cells to metastasize in an organ-specific manner. *Clin Exp Metastasis.* 25:11-32 (2008).
61. A.F. Chambers, A.C. Groom, and I.C. MacDonald. Dissemination and growth of cancer cells in metastatic sites. *Nat Rev Cancer.* 2:563-572 (2002).
62. D.G. DeNardo, M. Johansson, and L.M. Coussens. Immune cells as mediators of solid tumour metastasis. *Cancer Metastasis Rev.* 27:11-18 (2008).
63. P. Friedl and K. Wolf. Tumour-cell invasion and migration: diversity and escape mechanisms. *Nat Rev Cancer.* 3:362-374 (2003).
64. G. Bergers and L.E. Benjamin. Tumourigenesis and the angiogenic switch. *Nat Rev Cancer.* 3:401-410 (2003).
65. M. Papetti and I.M. Herman. Mechanisms of normal and tumour-derived angiogenesis. *Am J Physiol Cell Physiol.* 282:C947-970 (2002).
66. A. Tandle, D.G. Blazer, 3rd, and S.K. Libutti. Antiangiogenic gene therapy of cancer: recent developments. *J Transl Med.* 2:22 (2004).
67. S.E. Singletary. Rating the risk factors for breast cancer. *Ann Surg.* 237:474-482 (2003).
68. T. Anothaisintawee, C. Wiratkapun, P. Lerdsitthichai, V. Kasamesup, S. Wongwaisayawan, J. Srinakaran, S. Hirunpat, P. Woodtichartpreecha, S. Boonlikit, Y. Teerawattananon, and A. Thakkinstian. Risk factors of breast cancer: a systematic review and meta-analysis. *Asia Pac J Public Health.* 25:368-387 (2013).
69. M. Iwasaki and S. Tsugane. Risk factors for breast cancer: epidemiological evidence from Japanese studies. *Cancer Sci.* 102:1607-1614 (2011).
70. J.R. Benson and I. Jatoi. The global breast cancer burden. *Future Oncol.* 8:697-702 (2012).
71. N. Bogdanova and T. Dork. Molecular genetics of breast and ovarian cancer: recent advances and clinical implications. *Balkan J Med Genet.* 15:75-80 (2012).
72. U.O. Njiaju and O.I. Olopade. Genetic determinants of breast cancer risk: a review of current literature and issues pertaining to clinical application. *Breast J.* 18:436-442 (2012).
73. K. Pavelic and K. Gall-Troselj. Recent advances in molecular genetics of breast cancer. *J Mol Med (Berl).* 79:566-573 (2001).

74. C.B. Matsen and L.A. Neumayer. Breast cancer: a review for the general surgeon. *JAMA Surg.* 148:971-979 (2013).
75. I. Alkatout, B. Order, W. Klapper, M.T. Weigel, W. Jonat, F.K. Schaefer, C. Mundhenke, and A. Wenners. Surgical impact of new treatments in breast cancer. *Minerva Ginecol.* 65:363-383 (2013).
76. S.I. Hayashi, H. Eguchi, K. Tanimoto, T. Yoshida, Y. Omoto, A. Inoue, N. Yoshida, and Y. Yamaguchi. The expression and function of estrogen receptor alpha and beta in human breast cancer and its clinical application. *Endocr Relat Cancer.* 10:193-202 (2003).
77. E.A. Ariazi, J.L. Ariazi, F. Cordera, and V.C. Jordan. Estrogen receptors as therapeutic targets in breast cancer. *Curr Top Med Chem.* 6:181-202 (2006).
78. G.M. Higa and R.G. Fell. Sex Hormone Receptor Repertoire in Breast Cancer. *Int J Breast Cancer.* 2013:284036 (2013).
79. J.R. Bellon, A. Katz, and A. Taghian. Radiation therapy for breast cancer. *Hematol Oncol Clin North Am.* 20:239-257, vii (2006).
80. P. Wachsberger, R. Burd, and A.P. Dicker. Tumour response to ionizing radiation combined with antiangiogenesis or vascular targeting agents: exploring mechanisms of interaction. *Clin Cancer Res.* 9:1957-1971 (2003).
81. D. Eriksson and T. Stigbrand. Radiation-induced cell death mechanisms. *Tumour Biol.* 31:363-372 (2010).
82. V. Malhotra and M.C. Perry. Classical chemotherapy: mechanisms, toxicities and the therapeutic window. *Cancer Biol Ther.* 2:S2-4 (2003).
83. V.A. Botchkarev. Molecular mechanisms of chemotherapy-induced hair loss. *J Invest Dermatol Symp Proc.* 8:72-75 (2003).
84. E. Espinosa, P. Zamora, J. Feliu, and M. Gonzalez Baron. Classification of anticancer drugs--a new system based on therapeutic targets. *Cancer Treat Rev.* 29:515-523 (2003).
85. F.J. Esteva, V. Valero, L. Pusztai, L. Boehnke-Michaud, A.U. Buzdar, and G.N. Hortobagyi. Chemotherapy of metastatic breast cancer: what to expect in 2001 and beyond. *Oncologist.* 6:133-146 (2001).
86. G.P. Margison, M.F. Santibanez Koref, and A.C. Povey. Mechanisms of carcinogenicity/chemotherapy by O6-methylguanine. *Mutagenesis.* 17:483-487 (2002).
87. G. Minotti, P. Menna, E. Salvatorelli, G. Cairo, and L. Gianni. Anthracyclines: molecular advances and pharmacologic developments in antitumour activity and cardiotoxicity. *Pharmacol Rev.* 56:185-229 (2004).
88. M. Binaschi, F. Zunino, and G. Capranico. Mechanism of action of DNA topoisomerase inhibitors. *Stem Cells.* 13:369-379 (1995).
89. K.E. Gascoigne and S.S. Taylor. How do anti-mitotic drugs kill cancer cells? *J Cell Sci.* 122:2579-2585 (2009).
90. A. Mohan and S. Ponnusankar. Newer Therapies for the Treatment of Metastatic Breast Cancer: a Clinical Update. *Indian J Pharm Sci.* 75:251-261 (2013).
91. P. den Hollander, M.I. Savage, and P.H. Brown. Targeted Therapy for Breast Cancer Prevention. *Front Oncol.* 3:250 (2013).

92. S.P. Gampenrieder, G. Rinnerthaler, and R. Greil. Neoadjuvant Chemotherapy and Targeted Therapy in Breast Cancer: Past, Present, and Future. *J Oncol.* 2013:732047 (2013).
93. W.D. Foulkes, I.E. Smith, and J.S. Reis-Filho. Triple-negative breast cancer. *N Engl J Med.* 363:1938-1948 (2010).
94. C.I. Herold and C.K. Anders. New targets for triple-negative breast cancer. *Oncology (Williston Park).* 27:846-854 (2013).
95. O. Engebraaten, H.K. Vollan, and A.L. Borresen-Dale. Triple-negative breast cancer and the need for new therapeutic targets. *Am J Pathol.* 183:1064-1074 (2013).
96. B.P. Schneider, E.P. Winer, W.D. Foulkes, J. Garber, C.M. Perou, A. Richardson, G.W. Sledge, and L.A. Carey. Triple-negative breast cancer: risk factors to potential targets. *Clin Cancer Res.* 14:8010-8018 (2008).
97. J.A. DiMasi, R.W. Hansen, and H.G. Grabowski. The price of innovation: new estimates of drug development costs. *J Health Econ.* 22:151-185 (2003).
98. A. Mullard. Could pharma open its drug freezers? *Nat Rev Drug Discov.* 10:399-400 (2011).
99. S.C. Gupta, B. Sung, S. Prasad, L.J. Webb, and B.B. Aggarwal. Cancer drug discovery by repurposing: teaching new tricks to old dogs. *Trends Pharmacol Sci.* 34:508-517 (2013).
100. L.J. Marnett. Aspirin and the potential role of prostaglandins in colon cancer. *Cancer Res.* 52:5575-5589 (1992).
101. S. Lee. Artemisinin, promising lead natural product for various drug developments. *Mini Rev Med Chem.* 7:411-422 (2007).
102. R. Gazak, D. Walterova, and V. Kren. Silybin and silymarin--new and emerging applications in medicine. *Curr Med Chem.* 14:315-338 (2007).
103. D. Ribatti and A. Vacca. Therapeutic renaissance of thalidomide in the treatment of haematological malignancies. *Leukemia.* 19:1525-1531 (2005).
104. P. Dua and R.P. Gude. Antiproliferative and antiproteolytic activity of pentoxifylline in cultures of B16F10 melanoma cells. *Cancer Chemother Pharmacol.* 58:195-202 (2006).
105. P. Dua, A. Ingle, and R.P. Gude. Suramin augments the antitumour and antimetastatic activity of pentoxifylline in B16F10 melanoma. *Int J Cancer.* 121:1600-1608 (2007).
106. A. Ratheesh, A. Ingle, and R.P. Gude. Pentoxifylline modulates cell surface integrin expression and integrin mediated adhesion of B16F10 cells to extracellular matrix components. *Cancer Biol Ther.* 6:1743-1752 (2007).
107. P. Dua and R.P. Gude. Pentoxifylline impedes migration in B16F10 melanoma by modulating Rho GTPase activity and actin organisation. *Eur J Cancer.* 44:1587-1595 (2008).
108. M.Z. Kamran and R.P. Gude. Preclinical evaluation of the antimetastatic efficacy of Pentoxifylline on A375 human melanoma cell line. *Biomed Pharmacother.* 66:617-626 (2012).
109. W.L. Ryan and M.L. Heidrick. Inhibition of cell growth in vitro by adenosine 3',5'-monophosphate. *Science.* 162:1484-1485 (1968).

-
110. C.L. Alexander, M. Edward, and R.M. MacKie. Pentoxifylline-induced modulation of melanoma cell growth, adhesion and lymphokine activated killer cell-mediated lysis. *Melanoma Res.* 9:31-39 (1999).
 111. H. Fujioka. Effects of dibutyryl cyclic AMP, theophylline or isobutylmethylxanthine on human renal cancer cell line (OUR-10) and normal human kidney cell. *Med J Osaka Univ.* 34:43-56 (1984).
 112. L.A. Rosenthal and K.J. Blank. Pentoxifylline- and caffeine-induced modulation of major histocompatibility complex class I expression on murine tumour cell lines. *Immunopharmacology.* 25:145-161 (1993).
 113. P.H. Wiernik, E. Paietta, O. Goloubeva, S.J. Lee, D. Makower, J.M. Bennett, J.L. Wade, C. Ghosh, L.S. Kaminer, J. Pizzolo, and M.S. Tallman. Phase II study of theophylline in chronic lymphocytic leukemia: a study of the Eastern Cooperative Oncology Group (E4998). *Leukemia.* 18:1605-1610 (2004).
 114. T. Hashida, S. Todo, and S. Imashuku. Role of adenosine 3':5'-cyclic monophosphate in antineoplastic effect of prostaglandins (PGE1, PGE2, PGD2 and PGA1) on human neuroblastoma cells. *Prostaglandins Leukot Essent Fatty Acids.* 33:61-68 (1988).
 115. A. Nakamura, T. Yamatani, T. Fujita, and T. Chiba. Mechanism of inhibitory action of prostaglandins on the growth of human gastric carcinoma cell line KATO III. *Gastroenterology.* 101:910-918 (1991).
 116. R.B. Clark and J.P. Perkins. Regulation of adenosine 3':5'-cyclic monophosphate concentration in cultured human astrocytoma cells by catecholamines and histamine. *Proc Natl Acad Sci U S A.* 68:2757-2760 (1971).
 117. S. Miwa, N. Sugimoto, N. Yamamoto, T. Shirai, H. Nishida, K. Hayashi, H. Kimura, A. Takeuchi, K. Igarashi, A. Yachie, and H. Tsuchiya. Caffeine induces apoptosis of osteosarcoma cells by inhibiting AKT/mTOR/S6K, NF-kappaB and MAPK pathways. *Anticancer Res.* 32:3643-3649 (2012).
 118. A. Lentini, C. Tabolacci, A. Nardi, P. Mattioli, B. Provenzano, and S. Beninati. Preclinical evaluation of the antineoplastic efficacy of 7-(2-hydroxyethyl)theophylline on melanoma cancer cells. *Melanoma Res.* 22:133-139.
 119. A. Lentini, C. Tabolacci, P. Mattioli, B. Provenzano, and S. Beninati. Antitumour activity of theophylline in combination with Paclitaxel: a preclinical study on melanoma experimental lung metastasis. *Cancer Biother Radiopharm.* 25:497-503.
 120. C.H. Langeveld, C.A. Jongenelen, J.J. Heimans, and J.C. Stoof. 8-Chloro-cyclic adenosine monophosphate, a novel cyclic AMP analog that inhibits human glioma cell growth in concentrations that do not induce differentiation. *Exp Neurol.* 117:196-203 (1992).
 121. M. Barancik, V. Bohacova, L. Gibalova, J. Sedlak, Z. Sulova, and A. Breier. Potentiation of anticancer drugs: effects of pentoxifylline on neoplastic cells. *Int J Mol Sci.* 13:369-382 (2012).
 122. A. Bravo-Cuellar, G. Hernandez-Flores, J.M. Lerma-Diaz, J.R. Dominguez-Rodriguez, L.F. Jave-Suarez, R. De Celis-Carrillo, A. Aguilar-Lemarroy, P. Gomez-Lomeli, and P.C. Ortiz-Lazareno. Pentoxifylline and the proteasome inhibitor MG132 induce apoptosis in human leukemia U937 cells through a

- decrease in the expression of Bcl-2 and Bcl-XL and phosphorylation of p65. *J Biomed Sci.* 20:13 (2013).
123. S. Gahlot, M.A. Khan, L. Rishi, and S. Majumdar. Pentoxifylline augments TRAIL/Apo2L mediated apoptosis in cutaneous T cell lymphoma (HuT-78 and MyLa) by modulating the expression of antiapoptotic proteins and death receptors. *Biochem Pharmacol.* 80:1650-1661 (2010).
124. G. Hernandez-Flores, P.C. Ortiz-Lazareno, J.M. Lerma-Diaz, J.R. Dominguez-Rodriguez, L.F. Jave-Suarez, C. Aguilar-Lemarroy Adel, R. de Celis-Carrillo, S. del Toro-Arreola, Y.C. Castellanos-Esparza, and A. Bravo-Cuellar. Pentoxifylline sensitizes human cervical tumour cells to cisplatin-induced apoptosis by suppressing NF-kappa B and decreased cell senescence. *BMC Cancer.* 11:483 (2011).
125. A. Bravo-Cuellar, P.C. Ortiz-Lazareno, J.M. Lerma-Diaz, J.R. Dominguez-Rodriguez, L.F. Jave-Suarez, A. Aguilar-Lemarroy, S. del Toro-Arreola, R. de Celis-Carrillo, J.E. Sahagun-Flores, J.E. de Alba-Garcia, and G. Hernandez-Flores. Sensitization of cervix cancer cells to Adriamycin by Pentoxifylline induces an increase in apoptosis and decrease senescence. *Mol Cancer.* 9:114 (2010).
126. J.M. Lerma-Diaz, G. Hernandez-Flores, J.R. Dominguez-Rodriguez, P.C. Ortiz-Lazareno, P. Gomez-Contreras, R. Cervantes-Munguia, D. Scott-Algara, A. Aguilar-Lemarroy, L.F. Jave-Suarez, and A. Bravo-Cuellar. In vivo and in vitro sensitization of leukemic cells to adriamycin-induced apoptosis by pentoxifylline. Involvement of caspase cascades and IkappaBalpha phosphorylation. *Immunol Lett.* 103:149-158 (2006).
127. A. Shoma, W. Eldars, N. Noman, M. Saad, E. Elzahaf, M. Abdalla, D.S. Eldin, D. Zayed, A. Shalaby, and H.A. Malek. Pentoxifylline and local honey for radiation-induced burn following breast conservative surgery. *Curr Clin Pharmacol.* 5:251-256 (2010).
128. B. Sinn, G. Tallen, G. Schroeder, B. Grassl, J. Schulze, V. Budach, and I. Tinhofer. Caffeine confers radiosensitization of PTEN-deficient malignant glioma cells by enhancing ionizing radiation-induced G1 arrest and negatively regulating Akt phosphorylation. *Mol Cancer Ther.* 9:480-488 (2010).
129. M. Magnusson, P. Hoglund, K. Johansson, C. Jonsson, F. Killander, P. Malmstrom, A. Weddig, and E. Kjellen. Pentoxifylline and vitamin E treatment for prevention of radiation-induced side-effects in women with breast cancer: a phase two, double-blind, placebo-controlled randomised clinical trial (Ptx-5). *Eur J Cancer.* 45:2488-2495 (2009).
130. H.K. Chopra, K.L. Chopra, K.K. Aggarwal, and S.K. Parashar. Pentoxifylline--a new drug for the treatment of intermittent claudication. *Indian Heart J.* 41:127-133 (1989).
131. M.T. De Sanctis, M.R. Cesarone, G. Belcaro, A.N. Nicolaidis, M. Griffin, L. Incandela, M. Bucci, G. Geroulakos, G. Ramaswami, S. Vasdekis, G. Agus, P. Bavera, and E. Ippolito. Treatment of intermittent claudication with pentoxifylline: a 12-month, randomized trial--walking distance and microcirculation. *Angiology.* 53 Suppl 1:S7-12 (2002).

132. D.M. Aviado and J.M. Porter. Pentoxifylline: a new drug for the treatment of intermittent claudication. Mechanism of action, pharmacokinetics, clinical efficacy and adverse effects. *Pharmacotherapy*. 4:297-307 (1984).
133. C.P. Samlaska and E.A. Winfield. Pentoxifylline. *J Am Acad Dermatol*. 30:603-621 (1994).
134. A. Ward and S.P. Clissold. Pentoxifylline. A review of its pharmacodynamic and pharmacokinetic properties, and its therapeutic efficacy. *Drugs*. 34:50-97 (1987).
135. H. Bessler, R. Gilgal, M. Djaldetti, and I. Zahavi. Effect of pentoxifylline on the phagocytic activity, cAMP levels, and superoxide anion production by monocytes and polymorphonuclear cells. *J Leukoc Biol*. 40:747-754 (1986).
136. M.C. Sha and C.M. Callahan. The efficacy of pentoxifylline in the treatment of vascular dementia: a systematic review. *Alzheimer Dis Assoc Disord*. 17:46-54 (2003).
137. N.I. Swislocki and J.M. Tierney. Effects of pentoxifylline on Ca²⁺-dependent transglutaminase in rat erythrocytes. *J Clin Pharmacol*. 29:775-780 (1989).
138. N.I. Swislocki and J.M. Tierney. Prevention by pentoxifylline of transient Ca²⁺ accumulation and transglutaminase activation in rat erythrocytes. *J Clin Pharmacol*. 31:531-536 (1991).
139. D.M. Cummings, S.K. Ballas, and M.J. Ellison. Lack of effect of pentoxifylline on red blood cell deformability. *J Clin Pharmacol*. 32:1050-1053 (1992).
140. H.J. Hinze, G. Bedessem, and A. Soder. [Structure of excretion products of 3,7-dimethyl-1-(5-oxo-hemyl)-xanthine (BL 191) in man]. *Arzneimittelforschung*. 22:1144-1151 (1972).
141. B. Beermann, R. Ings, J. Mansby, J. Chamberlain, and A. McDonald. Kinetics of intravenous and oral pentoxifylline in healthy subjects. *Clin Pharmacol Ther*. 37:25-28 (1985).
142. T.A. Bryce, J. Chamberlain, D. Hillbeck, and C.M. Macdonald. Metabolism and pharmacokinetics of ¹⁴C-pentoxifylline in healthy volunteers. *Arzneimittelforschung*. 39:512-517 (1989).
143. R.V. Smith, E.S. Waller, J.T. Doluisio, M.T. Bauza, S.K. Puri, I. Ho, and H.B. Lassman. Pharmacokinetics of orally administered pentoxifylline in humans. *J Pharm Sci*. 75:47-52 (1986).
144. H.J. Hinze, G. H. G. a. R. B. Bioavailability and pharmacokinetics of pentoxifylline and Trental 400 in man. *Pharmatherapeutica*. 1:160-171 (1976).
145. R. Fabia, D.L. Travis, M.F. Levy, B.S. Husberg, R.M. Goldstein, and G.B. Klintmalm. Effect of pentoxifylline on hepatic ischemia and reperfusion injury. *Surgery*. 121:520-525 (1997).
146. K. Kozaki, H. Egawa, L. Bermudes, N.J. Feduska, S. So, and C.O. Esquivel. Pentoxifylline inhibits production of superoxide anion and tumour necrosis factor by Kupffer cells in rat liver preservation. *Transplant Proc*. 25:3025-3026 (1993).
147. B.C. Tarlatzis, E.M. Kolibianakis, J. Bontis, M. Tousiou, S. Lagos, and S. Mantalenakis. Effect of pentoxifylline on human sperm motility and fertilizing capacity. *Arch Androl*. 34:33-42 (1995).
148. S.S. Chen and J.S. Liu. [Erythrocyte deformability in progressive muscular dystrophy and effect of pentoxifylline]. *Taiwan Yi Xue Hui Za Zhi*. 85:249-257 (1986).

149. D.K. Biswas, C.M. Ahlers, B.J. Dezube, and A.B. Pardee. Pentoxifylline and other protein kinase C inhibitors down-regulate HIV-LTR NF-kappa B induced gene expression. *Mol Med.* 1:31-43 (1994).
150. M. Diab-Assef, J.M. Reimund, J. Ezenfis, B. Duclos, M. Kedingler, and C. Foltzer-Jourdainne. The phosphodiesterase inhibitor, pentoxifylline, alters rat intestinal epithelial cell proliferation via changes in the expression of transforming growth factors. *Scand J Gastroenterol.* 37:206-214 (2002).
151. Y.L. Chiou, J.J. Shieh, and C.Y. Lin. Blocking of Akt/NF-kappaB signaling by pentoxifylline inhibit platelet-derived growth factor-stimulated proliferation in Brown Norway rat airway smooth muscle cells. *Pediatr Res.* 60:657-662 (2006).
152. S.L. Lin, R.H. Chen, Y.M. Chen, W.C. Chiang, T.J. Tsai, and B.S. Hsieh. Pentoxifylline inhibits platelet-derived growth factor-stimulated cyclin D1 expression in mesangial cells by blocking Akt membrane translocation. *Mol Pharmacol.* 64:811-822 (2003).
153. P.M. Fernandez, S.R. Patierno, and F.R. Rickles. Tissue factor and fibrin in tumour angiogenesis. *Semin Thromb Hemost.* 30:31-44 (2004).
154. H.H. Versteeg, C.A. Spek, M.P. Peppelenbosch, and D.J. Richel. Tissue factor and cancer metastasis: the role of intracellular and extracellular signaling pathways. *Mol Med.* 10:6-11 (2004).
155. F.R. Rickles, M. Shoji, and K. Abe. The role of the hemostatic system in tumour growth, metastasis, and angiogenesis: tissue factor is a bifunctional molecule capable of inducing both fibrin deposition and angiogenesis in cancer. *Int J Hematol.* 73:145-150 (2001).
156. A. Amirhosravi, T. Meyer, G. Warnes, M. Amaya, Z. Malik, J.P. Biggerstaff, F.A. Siddiqui, P. Sherman, and J.L. Francis. Pentoxifylline inhibits hypoxia-induced upregulation of tumour cell tissue factor and vascular endothelial growth factor. *Thromb Haemost.* 80:598-602 (1998).
157. M. Pinzani, F. Marra, A. Caligiuri, R. DeFranco, A. Gentilini, P. Failli, and P. Gentilini. Inhibition by pentoxifylline of extracellular signal-regulated kinase activation by platelet-derived growth factor in hepatic stellate cells. *Br J Pharmacol.* 119:1117-1124 (1996).
158. A. Danielsson, E. Karlsson, U. Delle, K. Helou, and C. Mercke. The biological effect of pentoxifylline on the survival of human head and neck cancer cells treated with continuous low and high dose-rate irradiation. *J Cancer Res Clin Oncol.* 131:459-467 (2005).
159. C. Nieder, F.B. Zimmermann, M. Adam, and M. Molls. The role of pentoxifylline as a modifier of radiation therapy. *Cancer Treat Rev.* 31:448-455 (2005).
160. K.L. Bennewith and R.E. Durand. Drug-induced alterations in tumour perfusion yield increases in tumour cell radiosensitivity. *Br J Cancer.* 85:1577-1584 (2001).
161. Y.X. Li, L.Q. Sun, K. Weber-Johnson, N. Paschoud, and P.A. Coucke. Potentiation of cytotoxicity and radiosensitization of (E)-2-deoxy-2'-(fluoromethylene) cytidine by pentoxifylline in vitro. *Int J Cancer.* 80:155-160 (1999).
162. D.T. Chua, C. Lo, J. Yuen, and Y.C. Foo. A pilot study of pentoxifylline in the treatment of radiation-induced trismus. *Am J Clin Oncol.* 24:366-369 (2001).

163. D.H. Wu, L. Liu, and L.H. Chen. [Radiosensitization by pentoxifylline in human hepatoma cell line HepG2 and its mechanism]. *Di Yi Jun Yi Da Xue Xue Bao.* 24:382-385 (2004).
164. D.H. Wu, L. Liu, and L.H. Chen. [Cytotoxicity of pentoxifylline and its effect on human hepatoma cell line Hep3b radiosensitivity]. *Nan Fang Yi Ke Da Xue Xue Bao.* 26:305-307 (2006).
165. B.A. Teicher, S.A. Holden, T.S. Herman, R. Epelbaum, A.B. Pardee, and B. Dezube. Efficacy of pentoxifylline as a modulator of alkylating agent activity in vitro and in vivo. *Anticancer Res.* 11:1555-1560 (1991).
166. K.S. Smith, B.A. Folz, E.G. Adams, and B.K. Bhuyan. Synergistic and additive combinations of several antitumour drugs and other agents with the potent alkylating agent adozelesin. *Cancer Chemother Pharmacol.* 35:471-482 (1995).
167. M. Futakuchi, K. Ogawa, S. Tamano, S. Takahashi, and T. Shirai. Suppression of metastasis by nuclear factor kappaB inhibitors in an in vivo lung metastasis model of chemically induced hepatocellular carcinoma. *Cancer Sci.* 95:18-24 (2004).
168. S. Gordon, M. Witul, H. Cohen, J. Sciandra, P. Williams, H. Gastpar, G.P. Murphy, and J.L. Ambrus. Studies on platelet aggregation inhibitors in vivo. VIII. Effect of pentoxifylline on spontaneous tumour metastasis. *J Med.* 10:435-443 (1979).
169. T. Grzela, M. Lazarczyk, J. Niderla, J. Golab, M.A. Lazarczyk, and P. Skopinski. Pentoxifylline promotes development of murine colon adenocarcinoma-derived metastatic tumours in liver. *Oncol Rep.* 10:1805-1809 (2003).
170. R.P. Gude, M.P. Chitnis, and S.G. Rao. Effect of pentoxifylline, a multidrug resistance reversal agent, on haemopoietic stem cell homing. *Cell Biol Int.* 18:79-84 (1994).
171. R.P. Gude, A.D. Ingle, and S.G. Rao. Inhibition of lung homing of B16F10 by pentoxifylline, a microfilament depolymerizing agent. *Cancer Lett.* 106:171-176 (1996).
172. R.P. Gude, M.M. Binda, A.L. Boquete, and R.D. Bonfil. Inhibition of endothelial cell proliferation and tumour-induced angiogenesis by pentoxifylline. *J Cancer Res Clin Oncol.* 127:625-630 (2001).
173. R.P. Gude, M.M. Binda, H.L. Presas, A.J. Klein-Szanto, and R.D. Bonfil. Studies on the mechanisms responsible for inhibition of experimental metastasis of B16-F10 murine melanoma by pentoxifylline. *J Biomed Sci.* 6:133-141 (1999).
174. N.L. Kovach, C.G. Lindgren, A. Fefer, J.A. Thompson, T. Yednock, and J.M. Harlan. Pentoxifylline inhibits integrin-mediated adherence of interleukin-2-activated human peripheral blood lymphocytes to human umbilical vein endothelial cells, matrix components, and cultured tumour cells. *Blood.* 84:2234-2242 (1994).
175. R. Gonzalez-Amaro, D. Portales-Perez, L. Baranda, J.M. Redondo, S. Martinez-Martinez, M. Yanez-Mo, R. Garcia-Vicuna, C. Cabanas, and F. Sanchez-Madrid. Pentoxifylline inhibits adhesion and activation of human T lymphocytes. *J Immunol.* 161:65-72 (1998).
176. M. Barczyk, S. Carracedo, and D. Gullberg. Integrins. *Cell Tissue Res.* 339:269-280 (2010).
177. Y. Takada, X. Ye, and S. Simon. The integrins. *Genome Biol.* 8:215 (2007).

178. A.L. Berrier and K.M. Yamada. Cell-matrix adhesion. *J Cell Physiol.* 213:565-573 (2007).
179. M. Vicente-Manzanares, C.K. Choi, and A.R. Horwitz. Integrins in cell migration--the actin connection. *J Cell Sci.* 122:199-206 (2009).
180. F. Aoudjit and K. Vuori. Integrin signaling in cancer cell survival and chemoresistance. *Chemother Res Pract.* 2012:283181 (2012).
181. R. Rathinam and S.K. Alahari. Important role of integrins in the cancer biology. *Cancer Metastasis Rev.* 29:223-237 (2010).
182. M.H. Ginsberg, A. Partridge, and S.J. Shattil. Integrin regulation. *Curr Opin Cell Biol.* 17:509-516 (2005).
183. C.J. Avraamides, B. Garmy-Susini, and J.A. Varner. Integrins in angiogenesis and lymphangiogenesis. *Nat Rev Cancer.* 8:604-617 (2008).
184. B.I. Ratnikov, A.W. Partridge, and M.H. Ginsberg. Integrin activation by talin. *J Thromb Haemost.* 3:1783-1790 (2005).
185. K.L. Wegener, A.W. Partridge, J. Han, A.R. Pickford, R.C. Liddington, M.H. Ginsberg, and I.D. Campbell. Structural basis of integrin activation by talin. *Cell.* 128:171-182 (2007).
186. R. Zaidel-Bar, S. Itzkovitz, A. Ma'ayan, R. Iyengar, and B. Geiger. Functional atlas of the integrin adhesome. *Nat Cell Biol.* 9:858-867 (2007).
187. K. Mitchell, K.B. Svenson, W.M. Longmate, K. Gkirtzimanaki, R. Sadej, X. Wang, J. Zhao, A.G. Eliopoulos, F. Berditchevski, and C.M. Dipersio. Suppression of integrin alpha3beta1 in breast cancer cells reduces cyclooxygenase-2 gene expression and inhibits tumourigenesis, invasion, and cross-talk to endothelial cells. *Cancer Res.* 70:6359-6367 (2010).
188. G.E. Morozevich, N.I. Kozlova, I.B. Cheglakov, N.A. Ushakova, M.E. Preobrazhenskaya, and A.E. Berman. Implication of alpha5beta1 integrin in invasion of drug-resistant MCF-7/ADR breast carcinoma cells: a role for MMP-2 collagenase. *Biochemistry (Mosc).* 73:791-796 (2008).
189. R.S. Sawhney, W. Liu, and M.G. Brattain. A novel role of ERK5 in integrin-mediated cell adhesion and motility in cancer cells via Fak signaling. *J Cell Physiol.* 219:152-161 (2009).
190. P.B. dos Santos, J.S. Zanetti, A. Ribeiro-Silva, and E.I. Beltrao. Beta 1 integrin predicts survival in breast cancer: a clinicopathological and immunohistochemical study. *Diagn Pathol.* 7:104 (2012).
191. N.E. Ramirez, Z. Zhang, A. Madamanchi, K.L. Boyd, L.D. O'Rear, A. Nashabi, Z. Li, W.D. Dupont, A. Zijlstra, and M.M. Zutter. The alpha(2)beta(1) integrin is a metastasis suppressor in mouse models and human cancer. *J Clin Invest.* 121:226-237 (2011).
192. M.D. Schaller, C.A. Borgman, B.S. Cobb, R.R. Vines, A.B. Reynolds, and J.T. Parsons. pp125FAK a structurally distinctive protein-tyrosine kinase associated with focal adhesions. *Proc Natl Acad Sci U S A.* 89:5192-5196 (1992).
193. M.J. van Nimwegen and B. van de Water. Focal adhesion kinase: a potential target in cancer therapy. *Biochem Pharmacol.* 73:597-609 (2007).
194. M. Luo and J.L. Guan. Focal adhesion kinase: a prominent determinant in breast cancer initiation, progression and metastasis. *Cancer Lett.* 289:127-139 (2010).

195. B. Geiger, J.P. Spatz, and A.D. Bershadsky. Environmental sensing through focal adhesions. *Nat Rev Mol Cell Biol.* 10:21-33 (2009).
196. C. Brakebusch and R. Fassler. The integrin-actin connection, an eternal love affair. *EMBO J.* 22:2324-2333 (2003).
197. S.K. Mitra and D.D. Schlaepfer. Integrin-regulated FAK-Src signaling in normal and cancer cells. *Curr Opin Cell Biol.* 18:516-523 (2006).
198. J. Zhao and J.L. Guan. Signal transduction by focal adhesion kinase in cancer. *Cancer Metastasis Rev.* 28:35-49 (2009).
199. M. Tong, K.W. Chan, J.Y. Bao, K.Y. Wong, J.N. Chen, P.S. Kwan, K.H. Tang, L. Fu, Y.R. Qin, S. Lok, X.Y. Guan, and S. Ma. Rab25 is a tumour suppressor gene with antiangiogenic and anti-invasive activities in esophageal squamous cell carcinoma. *Cancer Res.* 72:6024-6035 (2012).
200. A.P. Gilmore and L.H. Romer. Inhibition of focal adhesion kinase (FAK) signaling in focal adhesions decreases cell motility and proliferation. *Mol Biol Cell.* 7:1209-1224 (1996).
201. D.D. Schlaepfer and S.K. Mitra. Multiple connections link FAK to cell motility and invasion. *Curr Opin Genet Dev.* 14:92-101 (2004).
202. J.T. Parsons, K.H. Martin, J.K. Slack, J.M. Taylor, and S.A. Weed. Focal adhesion kinase: a regulator of focal adhesion dynamics and cell movement. *Oncogene.* 19:5606-5613 (2000).
203. J.H. Yoon, H.E. Kim, J.Y. Choi, H.J. Bae, and S.G. Lee. Caffeoylserotonin suppresses THP-1 monocyte adhesion and migration via inhibition of the integrin beta1/FAK/Akt signalling pathway. *Fitoterapia.* 83:1364-1370 (2012).
204. J. Zhou, F. Chen, J. Xiao, C. Li, Y. Liu, Y. Ding, P. Wan, X. Wang, J. Huang, and Z. Wang. Enhanced functional properties of corneal epithelial cells by coculture with embryonic stem cells via the integrin beta1-FAK-PI3K/Akt pathway. *Int J Biochem Cell Biol.* 43:1168-1177 (2011).
205. S. Saleem, J. Li, S.P. Yee, G.F. Fellows, C.G. Goodyer, and R. Wang. beta1 integrin/FAK/ERK signalling pathway is essential for human fetal islet cell differentiation and survival. *J Pathol.* 219:182-192 (2009).
206. A.R. Santos, R.G. Corredor, B.A. Obeso, E.F. Trakhtenberg, Y. Wang, J. Ponmattam, G. Dvorianchikova, D. Ivanov, V.I. Shestopalov, J.L. Goldberg, M.E. Fini, and M.L. Bajenaru. beta1 integrin-focal adhesion kinase (FAK) signaling modulates retinal ganglion cell (RGC) survival. *PLoS One.* 7:e48332 (2012).
207. P. Mehlen and A. Puisieux. Metastasis: a question of life or death. *Nat Rev Cancer.* 6:449-458 (2006).
208. G.W. McLean, N.O. Carragher, E. Avizienyte, J. Evans, V.G. Brunton, and M.C. Frame. The role of focal-adhesion kinase in cancer - a new therapeutic opportunity. *Nat Rev Cancer.* 5:505-515 (2005).
209. M.S. Aronsohn, H.M. Brown, G. Hauptman, and L.J. Kornberg. Expression of focal adhesion kinase and phosphorylated focal adhesion kinase in squamous cell carcinoma of the larynx. *Laryngoscope.* 113:1944-1948 (2003).
210. M. Heffler, V.M. Golubovskaya, K.M. Dunn, and W. Cance. Focal adhesion kinase autophosphorylation inhibition decreases colon cancer cell growth and enhances the efficacy of chemotherapy. *Cancer Biol Ther.* 14:761-772 (2013).

211. L.V. Owens, L. Xu, R.J. Craven, G.A. Dent, T.M. Weiner, L. Kornberg, E.T. Liu, and W.G. Cance. Overexpression of the focal adhesion kinase (p125FAK) in invasive human tumours. *Cancer Res.* 55:2752-2755 (1995).
212. V.M. Golubovskaya, M. Zheng, L. Zhang, J.L. Li, and W.G. Cance. The direct effect of focal adhesion kinase (FAK), dominant-negative FAK, FAK-CD and FAK siRNA on gene expression and human MCF-7 breast cancer cell tumorigenesis. *BMC Cancer.* 9:280 (2009).
213. T.R. Johnson, L. Khandrika, B. Kumar, S. Venezia, S. Koul, R. Chandhoke, P. Maroni, R. Donohue, R.B. Meacham, and H.K. Koul. Focal adhesion kinase controls aggressive phenotype of androgen-independent prostate cancer. *Mol Cancer Res.* 6:1639-1648 (2008).
214. A.R. Hess, L.M. Postovit, N.V. Margaryan, E.A. Seftor, G.B. Schneider, R.E. Seftor, B.J. Nickoloff, and M.J. Hendrix. Focal adhesion kinase promotes the aggressive melanoma phenotype. *Cancer Res.* 65:9851-9860 (2005).
215. K.M. Nicholson and N.G. Anderson. The protein kinase B/Akt signalling pathway in human malignancy. *Cell Signal.* 14:381-395 (2002).
216. J.A. Fresno Vara, E. Casado, J. de Castro, P. Cejas, C. Belda-Iniesta, and M. Gonzalez-Baron. PI3K/Akt signalling pathway and cancer. *Cancer Treat Rev.* 30:193-204 (2004).
217. B.T. Hennessy, D.L. Smith, P.T. Ram, Y. Lu, and G.B. Mills. Exploiting the PI3K/AKT pathway for cancer drug discovery. *Nat Rev Drug Discov.* 4:988-1004 (2005).
218. B.H. Jiang and L.Z. Liu. AKT signaling in regulating angiogenesis. *Curr Cancer Drug Targets.* 8:19-26 (2008).
219. G. Romano. The Role of the Dysfunctional Akt-Related Pathway in Cancer: Establishment and Maintenance of a Malignant Cell Phenotype, Resistance to Therapy, and Future Strategies for Drug Development. *Scientifica (Cairo).* 2013:317186 (2013).
220. Y. Liao and M.C. Hung. Physiological regulation of Akt activity and stability. *Am J Transl Res.* 2:19-42 (2010).
221. B.D. Manning and L.C. Cantley. AKT/PKB signaling: navigating downstream. *Cell.* 129:1261-1274 (2007).
222. S. Pugazhenti, A. Nesterova, C. Sable, K.A. Heidenreich, L.M. Boxer, L.E. Heasley, and J.E. Reusch. Akt/protein kinase B up-regulates Bcl-2 expression through cAMP-response element-binding protein. *J Biol Chem.* 275:10761-10766 (2000).
223. Y. Ogawara, S. Kishishita, T. Obata, Y. Isazawa, T. Suzuki, K. Tanaka, N. Masuyama, and Y. Gotoh. Akt enhances Mdm2-mediated ubiquitination and degradation of p53. *J Biol Chem.* 277:21843-21850 (2002).
224. T.M. Gottlieb, J.F. Leal, R. Seger, Y. Taya, and M. Oren. Cross-talk between Akt, p53 and Mdm2: possible implications for the regulation of apoptosis. *Oncogene.* 21:1299-1303 (2002).
225. L. Portt, G. Norman, C. Clapp, M. Greenwood, and M.T. Greenwood. Anti-apoptosis and cell survival: a review. *Biochim Biophys Acta.* 1813:238-259 (2011).

226. S. Elmore. Apoptosis: a review of programmed cell death. *Toxicol Pathol.* 35:495-516 (2007).
227. P. Meier and K.H. Vousden. Lucifer's labyrinth--ten years of path finding in cell death. *Mol Cell.* 28:746-754 (2007).
228. A. Degterev, M. Boyce, and J. Yuan. A decade of caspases. *Oncogene.* 22:8543-8567 (2003).
229. S. Fulda and K.M. Debatin. Extrinsic versus intrinsic apoptosis pathways in anticancer chemotherapy. *Oncogene.* 25:4798-4811 (2006).
230. S. Cory, D.C. Huang, and J.M. Adams. The Bcl-2 family: roles in cell survival and oncogenesis. *Oncogene.* 22:8590-8607 (2003).
231. P.N. Kelly and A. Strasser. The role of Bcl-2 and its pro-survival relatives in tumorigenesis and cancer therapy. *Cell Death Differ.* 18:1414-1424 (2011).
232. S. Willis, C.L. Day, M.G. Hinds, and D.C. Huang. The Bcl-2-regulated apoptotic pathway. *J Cell Sci.* 116:4053-4056 (2003).
233. S. Haupt, M. Berger, Z. Goldberg, and Y. Haupt. Apoptosis - the p53 network. *J Cell Sci.* 116:4077-4085 (2003).
234. J.D. Amaral, J.M. Xavier, C.J. Steer, and C.M. Rodrigues. The role of p53 in apoptosis. *Discov Med.* 9:145-152 (2010).
235. M.M. Gottesman. Mechanisms of cancer drug resistance. *Annu Rev Med.* 53:615-627 (2002).
236. U.A. Sartorius and P.H. Kramer. Upregulation of Bcl-2 is involved in the mediation of chemotherapy resistance in human small cell lung cancer cell lines. *Int J Cancer.* 97:584-592 (2002).
237. F. Aoudjit and K. Vuori. Integrin signaling inhibits paclitaxel-induced apoptosis in breast cancer cells. *Oncogene.* 20:4995-5004 (2001).
238. J.S. Damiano, L.A. Hazlehurst, and W.S. Dalton. Cell adhesion-mediated drug resistance (CAM-DR) protects the K562 chronic myelogenous leukemia cell line from apoptosis induced by BCR/ABL inhibition, cytotoxic drugs, and gamma-irradiation. *Leukemia.* 15:1232-1239 (2001).
239. G.R. Zimmermann, J. Lehar, and C.T. Keith. Multi-target therapeutics: when the whole is greater than the sum of the parts. *Drug Discov Today.* 12:34-42 (2007).
240. C. Reece, R. Kumar, D. Nienow, and A. Nehra. Extending the rationale of combination therapy to unresponsive erectile dysfunction. *Rev Urol.* 9:197-206 (2007).
241. T.A. Yap, A. Omlin, and J.S. de Bono. Development of therapeutic combinations targeting major cancer signaling pathways. *J Clin Oncol.* 31:1592-1605 (2013).
242. E. Andreopoulou and J.A. Sparano. Chemotherapy in Patients with Anthracycline- and Taxane-Pretreated Metastatic Breast Cancer: An Overview. *Curr Breast Cancer Rep.* 5:42-50 (2013).
243. Y.W. Zhang, J. Shi, Y.J. Li, and L. Wei. Cardiomyocyte death in doxorubicin-induced cardiotoxicity. *Arch Immunol Ther Exp (Warsz).* 57:435-445 (2009).
244. Y. Octavia, C.G. Tocchetti, K.L. Gabrielson, S. Janssens, H.J. Crijns, and A.L. Moens. Doxorubicin-induced cardiomyopathy: from molecular mechanisms to therapeutic strategies. *J Mol Cell Cardiol.* 52:1213-1225 (2012).

245. O. Tacar, P. Sriamornsak, and C.R. Dass. Doxorubicin: an update on anticancer molecular action, toxicity and novel drug delivery systems. *J Pharm Pharmacol.* 65:157-170 (2013).
246. C. Main, L. Bojke, S. Griffin, G. Norman, M. Barbieri, L. Mather, D. Stark, S. Palmer, and R. Riemsma. Topotecan, pegylated liposomal doxorubicin hydrochloride and paclitaxel for second-line or subsequent treatment of advanced ovarian cancer: a systematic review and economic evaluation. *Health Technol Assess.* 10:1-132 iii-iv (2006).
247. J.A. O'Shaughnessy. Pegylated liposomal doxorubicin in the treatment of breast cancer. *Clin Breast Cancer.* 4:318-328 (2003).
248. J. Lao, J. Madani, T. Puertolas, M. Alvarez, A. Hernandez, R. Pazo-Cid, A. Artal, and A. Anton Torres. Liposomal Doxorubicin in the treatment of breast cancer patients: a review. *J Drug Deliv.* 2013:456409 (2013).
249. A. Udhrain, K.M. Skubitz, and D.W. Northfelt. Pegylated liposomal doxorubicin in the treatment of AIDS-related Kaposi's sarcoma. *Int J Nanomedicine.* 2:345-352 (2007).
250. S.T. Duggan and G.M. Keating. Pegylated liposomal doxorubicin: a review of its use in metastatic breast cancer, ovarian cancer, multiple myeloma and AIDS-related Kaposi's sarcoma. *Drugs.* 71:2531-2558 (2011).
251. A.S. Manjappa, P.N. Goel, M.P. Vekataraju, K.S. Rajesh, K. Makwana, M. Ukawala, Y. Nikam, R.P. Gude, and R.S. Murthy. Is an alternative drug delivery system needed for docetaxel? The role of controlling epimerization in formulations and beyond. *Pharm Res.* 30:2675-2693 (2013).
252. T.C Chou, N. Martin. *CompuSyn Software for Drug Combinations and for General Dose-Effect Analysis, and User's Guide.* Paramus, NJ: ComboSyn 2007.
253. N.A. Franken, H.M. Rodermond, J. Stap, J. Haveman, and C. van Bree. Clonogenic assay of cells in vitro. *Nat Protoc.* 1:2315-2319 (2006).
254. D. Ribble, N.B. Goldstein, D.A. Norris, and Y.G. Shellman. A simple technique for quantifying apoptosis in 96-well plates. *BMC Biotechnol.* 5:12 (2005).
255. S. Wang, Q. Liu, Y. Zhang, K. Liu, P. Yu, J. Luan, H. Duan, Z. Lu, F. Wang, E. Wu, K. Yagasaki, and G. Zhang. Suppression of growth, migration and invasion of highly-metastatic human breast cancer cells by berbamine and its molecular mechanisms of action. *Mol Cancer.* 8:81 (2009).
256. H.S. Lee, E.Y. Seo, N.E. Kang, and W.K. Kim. [6]-Gingerol inhibits metastasis of MDA-MB-231 human breast cancer cells. *J Nutr Biochem.* 19:313-319 (2008).
257. T.H. Lin, T.W. Tan, T.H. Tsai, C.C. Chen, T.F. Hsieh, S.S. Lee, H.H. Liu, W.C. Chen, and C.H. Tang. D-pinitol Inhibits Prostate Cancer Metastasis through Inhibition of alphaVbeta3 Integrin by Modulating FAK, c-Src and NF-kappaB Pathways. *Int J Mol Sci.* 14:9790-9802 (2013).
258. S. Salot and R. Gude. MTA1-mediated transcriptional repression of SMAD7 in breast cancer cell lines. *Eur J Cancer.* 49:492-499 (2013).
259. R. Munoz, S. Man, Y. Shaked, C.R. Lee, J. Wong, G. Francia, and R.S. Kerbel. Highly efficacious nontoxic preclinical treatment for advanced metastatic breast cancer using combination oral UFT-cyclophosphamide metronomic chemotherapy. *Cancer Res.* 66:3386-3391 (2006).

260. B.A. Teicher. Tumour models for efficacy determination. *Mol Cancer Ther.* 5:2435-2443 (2006).
261. B. Weigelt, J.L. Peterse, and L.J. van 't Veer. Breast cancer metastasis: markers and models. *Nat Rev Cancer.* 5:591-602 (2005).
262. V. Guarneri and P. Conte. Metastatic breast cancer: therapeutic options according to molecular subtypes and prior adjuvant therapy. *Oncologist.* 14:645-656 (2009).
263. L. Bohm, W.P. Roos, and A.M. Serafin. Inhibition of DNA repair by Pentoxifylline and related methylxanthine derivatives. *Toxicology.* 193:153-160 (2003).
264. H.R. Dettelbach and D.M. Aviado. Clinical pharmacology of pentoxifylline with special reference to its hemorrheologic effect for the treatment of intermittent claudication. *J Clin Pharmacol.* 25:8-26 (1985).
265. D. Jacoby and E.R. Mohler, 3rd. Drug treatment of intermittent claudication. *Drugs.* 64:1657-1670 (2004).
266. H. Gastpar. The inhibition of cancer cell stickness by the methylxanthine derivative pentoxifylline (BL 191). *Thromb Res.* 5:277-289 (1974).
267. M. Zhang, Y.J. Xu, S.A. Mengi, A.S. Arneja, and N.S. Dhalla. Therapeutic potentials of pentoxifylline for treatment of cardiovascular diseases. *Exp Clin Cardiol.* 9:103-111 (2004).
268. C.L. D'Hellencourt, L. Diaw, P. Cornillet, and M. Guenounou. Differential regulation of TNF alpha, IL-1 beta, IL-6, IL-8, TNF beta, and IL-10 by pentoxifylline. *Int J Immunopharmacol.* 18:739-748 (1996).
269. M. Zhang, Y.J. Xu, H.K. Saini, B. Turan, P.P. Liu, and N.S. Dhalla. Pentoxifylline attenuates cardiac dysfunction and reduces TNF-alpha level in ischemic-reperfused heart. *Am J Physiol Heart Circ Physiol.* 289:H832-839 (2005).
270. D.R. Collingridge and S. Rockwell. Pentoxifylline improves the oxygenation and radiation response of BA1112 rat rhabdomyosarcomas and EMT6 mouse mammary carcinomas. *Int J Cancer.* 90:256-264 (2000).
271. P.J. Stork and J.M. Schmitt. Crosstalk between cAMP and MAP kinase signaling in the regulation of cell proliferation. *Trends Cell Biol.* 12:258-266 (2002).
272. A. Shmueli and M. Oren. Regulation of p53 by Mdm2: fate is in the numbers. *Mol Cell.* 13:4-5 (2004).
273. H.L. Glenn and B.S. Jacobson. Cyclooxygenase and cAMP-dependent protein kinase reorganize the actin cytoskeleton for motility in HeLa cells. *Cell Motil Cytoskeleton.* 55:265-277 (2003).
274. T.C. Chen, P. Wadsten, S. Su, N. Rawlinson, F.M. Hofman, C.K. Hill, and A.H. Schonthal. The type IV phosphodiesterase inhibitor rolipram induces expression of the cell cycle inhibitors p21(Cip1) and p27(Kip1), resulting in growth inhibition, increased differentiation, and subsequent apoptosis of malignant A-172 glioma cells. *Cancer Biol Ther.* 1:268-276 (2002).
275. H.C. Gallagher, C.L. Bacon, O.A. Odumeru, K.F. Gallagher, T. Fitzpatrick, and C.M. Regan. Valproate activates phosphodiesterase-mediated cAMP degradation: relevance to C6 glioma G1 phase progression. *Neurotoxicol Teratol.* 26:73-81 (2004).

276. D.O. Morgan. Cyclin-dependent kinases: engines, clocks, and microprocessors. *Annu Rev Cell Dev Biol.* 13:261-291 (1997).
277. G.A. Di Lullo, S.M. Sweeney, J. Korkko, L. Ala-Kokko, and J.D. San Antonio. Mapping the ligand-binding sites and disease-associated mutations on the most abundant protein in the human, type I collagen. *J Biol Chem.* 277:4223-4231 (2002).
278. A. Scorilas, A. Karameris, N. Arnogiannaki, A. Ardavanis, P. Bassilopoulos, T. Trangas, and M. Talieri. Overexpression of matrix-metalloproteinase-9 in human breast cancer: a potential favourable indicator in node-negative patients. *Br J Cancer.* 84:1488-1496 (2001).
279. Y.G. Shellman, M. Makela, and D.A. Norris. Induction of secreted matrix metalloproteinase-9 activity in human melanoma cells by extracellular matrix proteins and cytokines. *Melanoma Res.* 16:207-211 (2006).
280. Y. Okada, H. Tsuchiya, H. Shimizu, K. Tomita, I. Nakanishi, H. Sato, M. Seiki, K. Yamashita, and T. Hayakawa. Induction and stimulation of 92-kDa gelatinase/type IV collagenase production in osteosarcoma and fibrosarcoma cell lines by tumour necrosis factor alpha. *Biochem Biophys Res Commun.* 171:610-617 (1990).
281. C. Ries, H. Kolb, and P.E. Petrides. Regulation of 92-kD gelatinase release in HL-60 leukemia cells: tumour necrosis factor-alpha as an autocrine stimulus for basal- and phorbol ester-induced secretion. *Blood.* 83:3638-3646 (1994).
282. S.H. Kim, J. Turnbull, and S. Guimond. Extracellular matrix and cell signalling: the dynamic cooperation of integrin, proteoglycan and growth factor receptor. *J Endocrinol.* 209:139-151 (2011).
283. N.E. Reticker-Flynn, D.F. Malta, M.M. Winslow, J.M. Lamar, M.J. Xu, G.H. Underhill, R.O. Hynes, T.E. Jacks, and S.N. Bhatia. A combinatorial extracellular matrix platform identifies cell-extracellular matrix interactions that correlate with metastasis. *Nat Commun.* 3:1122 (2012).
284. F. Tang, R. Zhang, Y. He, M. Zou, L. Guo, and T. Xi. MicroRNA-125b induces metastasis by targeting STARD13 in MCF-7 and MDA-MB-231 breast cancer cells. *PLoS One.* 7:e35435 (2012).
285. S.L. Dalton, E. Scharf, R. Briesewitz, E.E. Marcantonio, and R.K. Assoian. Cell adhesion to extracellular matrix regulates the life cycle of integrins. *Mol Biol Cell.* 6:1781-1791 (1995).
286. M. Delcommenne and C.H. Streuli. Control of integrin expression by extracellular matrix. *J Biol Chem.* 270:26794-26801 (1995).
287. P. van der, H. Vloedgraven, S. Papapoulos, C. Lowick, W. Grzesik, J. Kerr, and P.G. Robey. Attachment characteristics and involvement of integrins in adhesion of breast cancer cell lines to extracellular bone matrix components. *Lab Invest.* 77:665-675 (1997).
288. J.E. Bartsch, E.D. Staren, and H.E. Appert. Adhesion and migration of extracellular matrix-stimulated breast cancer. *J Surg Res.* 110:287-294 (2003).
289. R. Korah, M. Boots, and R. Wieder. Integrin alpha5beta1 promotes survival of growth-arrested breast cancer cells: an in vitro paradigm for breast cancer dormancy in bone marrow. *Cancer Res.* 64:4514-4522 (2004).

290. S.L. Dalton, E.E. Marcantonio, and R.K. Assoian. Cell attachment controls fibronectin and alpha 5 beta 1 integrin levels in fibroblasts. Implications for anchorage-dependent and -independent growth. *J Biol Chem.* 267:8186-8191 (1992).
291. S.K. Mitra, D.A. Hanson, and D.D. Schlaepfer. Focal adhesion kinase: in command and control of cell motility. *Nat Rev Mol Cell Biol.* 6:56-68 (2005).
292. S.K. Mitra, D. Mikolon, J.E. Molina, D.A. Hsia, D.A. Hanson, A. Chi, S.T. Lim, J.A. Bernard-Trifilo, D. Ilic, D.G. Stupack, D.A. Cheresh, and D.D. Schlaepfer. Intrinsic FAK activity and Y925 phosphorylation facilitate an angiogenic switch in tumours. *Oncogene.* 25:5969-5984 (2006).
293. M.L. Jones, A.J. Shawe-Taylor, C.M. Williams, and A.W. Poole. Characterization of a novel focal adhesion kinase inhibitor in human platelets. *Biochem Biophys Res Commun.* 389:198-203 (2009).
294. T. Fernandes-Alnemri, G. Litwack, and E.S. Alnemri. CPP32, a novel human apoptotic protein with homology to *Caenorhabditis elegans* cell death protein Ced-3 and mammalian interleukin-1 beta-converting enzyme. *J Biol Chem.* 269:30761-30764 (1994).
295. S. Reagan-Shaw, M. Nihal, and N. Ahmad. Dose translation from animal to human studies revisited. *FASEB J.* 22:659-661 (2008).
296. A. Taherian and T. Mazoochi. Different Expression of Extracellular Signal-Regulated Kinases (ERK) 1/2 and Phospho-Erk Proteins in MBA-MB-231 and MCF-7 Cells after Chemotherapy with Doxorubicin or Docetaxel. *Iran J Basic Med Sci.* 15:669-677 (2012).
297. O. Bar-On, M. Shapira, and D.D. Hershko. Differential effects of doxorubicin treatment on cell cycle arrest and Skp2 expression in breast cancer cells. *Anticancer Drugs.* 18:1113-1121 (2007).
298. P.A. Snoek-van Beurden and J.W. Von den Hoff. Zymographic techniques for the analysis of matrix metalloproteinases and their inhibitors. *Biotechniques.* 38:73-83 (2005).

Publications

Publications

1. **P.N. Goel** and R.P Gude. Unravelling the antimetastatic potential of pentoxifylline, a methylxanthine derivative in human MDA-MB-231 breast cancer cells. *Molecular and cellular biochemistry*. 358:141-151 (2011).
2. **P.N. Goel** and R.P. Gude. Curbing the focal adhesion kinase and its associated signaling events by pentoxifylline in MDA-MB-231 human breast cancer cells. *Eur J Pharmacol*. 714:432-441 (2013).
3. **P.N. Goel** and R.P. Gude. Pentoxifylline Regulates the Cellular Adhesion and its Allied Receptors to Extracellular Matrix Components in Breast Cancer Cells. *Biomed Pharmacother* (2014) 68:93-99.
4. **P.N. Goel** and R.P. Gude. Delineating the Anti-Metastatic Potential of Pentoxifylline in Combination with Liposomal Doxorubicin against Breast Cancer Cells. *Biomed Pharmacother* (2014) 68:191-200.
5. **P.N. Goel**, S.P Singh, R.P Gude and M.K Chilakapati. Investigating the Effects of Pentoxifylline on Human Breast Cancer Cells Using Raman Spectroscopy *J Innov Opt Health Sci* (2014) 8(2): 1550004.

Unravelling the antimetastatic potential of pentoxifylline, a methylxanthine derivative in human MDA-MB-231 breast cancer cells

Peeyush N. Goel · R. P. Gude

Received: 21 February 2011 / Accepted: 21 June 2011 / Published online: 3 July 2011
© Springer Science+Business Media, LLC. 2011

Abstract Pentoxifylline (PTX), a methylxanthine derivative is a non-steroidal immunomodulating agent with unique hemorheologic properties. It is used in the treatment of intermittent claudication as it increases the amount of oxygen reaching tissues by increasing the flexibility of red blood cells. Recently, it has also shown to exhibit anti-metastatic and anti-angiogenic activities in B16F10 melanoma cells both in vitro as well as in vivo. As per the reports, the choice of drug in the treatment of breast cancer is paclitaxel, but the major limitation is its toxicity. However, the effects of PTX on metastatic processes in breast cancer are not currently known. Therefore, in this study, we have examined the effect of PTX in MDA-MB-231 human breast cancer cells. The MTT assay showed dose- and time-dependent decreases in cellular proliferation. The non-toxic concentration of PTX selected were 1, 2.5 and 5 mM for 24 h. PTX induced a G0-G1 cell-cycle arrest leading to apoptosis. Further, it affected adhesion to both the matrigel and collagen type-IV in a time- and dose-dependent manner. The PTX impeded the migration of MDA-MB-231 cells and also decreased the activities of both MMP-2 and MMP-9. Thus, PTX at non-toxic doses affected cellular proliferation, adhesion, migration and invasion. These results demonstrate its anti-metastatic effect on MDA-MB-231 cells, and further studies need to be carried out to understand the mechanism of action.

Keywords Pentoxifylline · MDA-MB-231 breast cancer cells · Proliferation · Adhesion · Migration · Matrix-metalloproteinases

Introduction

The most fruitful basis for the discovery of a new drug is to start with an old drug.

Sir James Black (Nobel Laureate, 1924–2010)

Cancer is an aggressive disease, an emperor of maladies, known to be existing as long as humanity has been existing and is currently the leading cause of deaths globally. Breast cancer is the second most diagnosed cancer worldwide with a total of 1.38 million cases [1]. The estimated new cases in United States for breast cancer alone is 0.2 million [2]. The multistep event of metastatic breast cancer involves the invasion of mammary carcinoma cells into the flanking tissues, paving their way to enter the systemic circulation, intravasating to target sites mainly the bones, lungs and central nervous system [3]. There has been a significant progress in the development of new diagnostic, prognostic and therapeutic strategies, but the survival rates for patients with metastatic disease has not changed markedly [4]. Conventional treatment modalities include surgery, followed by radiation and/or chemotherapy. One of the most common causes of the failure of a number of potential drugs is due to their high degree of cytotoxicity and the induction of resistance culminating to cause a limitation in therapy. Hence, investigations are often directed to understand the potential and therapeutic efficacy of drugs which are used in the treatment of other diseases and hence been shown to be non-cytotoxic, to act as anti-cancer or anti-metastatic agents.

P. N. Goel · R. P. Gude (✉)
Gude Lab, Advanced Centre for Treatment, Research & Education in Cancer (ACTREC), Tata Memorial Centre, Kharghar, Navi Mumbai 410210, India
e-mail: rgude@actrec.gov.in

Pentoxifylline (PTX), a methyl xanthine derivative (3,7 dimethyl-1-(5-oxohexyl xanthine) is used as a hemorheological agent in the treatment of peripheral vascular diseases [5]. This primarily occurs through the reduction in the whole blood viscosity and improved red blood cell flexibility [6]. The PTX can reduce cancer cell stickiness thereby increasing the circulating time of tumour cells in blood which can become a spotlight for the circulating immune cells [7]. It has shown to exert therapeutic benefits in cardiovascular diseases [8] and as an anti-inflammatory agent by decreasing the levels of TNF- α and other inflammatory cytokines [9, 10]. It improves tumour oxygenation by increasing tumour blood flow and sensitizes tumours to both the irradiation and alkylating agents [11, 12]. Further, being a phosphodiesterase inhibitor, it increases c-AMP levels. This could lead to the suppression of RAS and MAPK activities in variety of cells, such as NIH3T3 fibroblasts affecting proliferation [13]. Increased c-AMP is also associated with the attenuation of anti-apoptotic proteins, such as Bcl-2, MDM2 [14] and cytoskeletal reorganisation affecting motility in Hela and B16F10 cells [15, 16]. Our lab has earlier shown that the PTX affects cellular adhesion, in part by affecting the integrin surface expression in B16F10 cells [17]. We have also shown its activity against gelatinases [18] that degrades Collagen Type-IV, a primary determinant that makes the most of Extracellular Matrix, ECM [19] in B16F10 melanoma cells.

Our lab had earlier demonstrated the anti-metastatic activity of PTX on B16F10 melanoma cells [16–18]. Based on the literature, survey suggesting no reports of PTX on human breast cancer cells prompted us to demonstrate its anti-metastatic potential viz. cellular proliferation, adhesion, migration and invasion in human breast cancer cells using MDA-MB-231 cell line as a model for in vitro study.

Materials and methods

Cell lines

The MDA-MB-231 and HT-1080 cell lines were purchased from NCCS, Pune, India. The cell lines were maintained in Dulbecco's Modified Eagle Medium (DMEM, GIBCO) supplemented with 10% heat inactivated foetal bovine serum, FBS (GIBCO) and antibiotics (100 U/ml penicillin and 100 μ g/ml streptomycin). Cultures were maintained at 37°C in 5% CO₂ humidified atmosphere.

Materials

The PTX, MTT, propidium iodide(PI), ethidium bromide(EB), acridine orange(AO), mitomycin C and collagen Type IV were purchased from Sigma. RNase was

purchased from Merck and Matrigel from BD. All the other chemicals/reagents used were either of analytical grade or the highest purity commercially available.

Cellular proliferation using MTT cytotoxicity assay

The cell cytotoxicity assay was performed as mentioned earlier with a slight modification [18]. An initial inoculum of 4000 cells/well in exponential phase were seeded in 96-well plate (6-well replicates) and allowed to grow for the next 24 h. The PTX, prepared in complete media was added at varying doses (0.01–30 mM). Plates were then incubated at 37°C for 24, 48 and 72 h. The drug was removed, and then, the plates were washed twice with PBS. The MTT (1 mg/ml) was added to all the wells and incubated for 4 h. Plates were centrifuged, and the formazon crystals formed were dissolved in DMSO with intermittent shaking. The plate was read using the spectrophotometer at dual wavelengths of 540/690 nm as excitation and reference. IC₅₀, the concentration required to kill 50% of the cells by PTX was calculated. The graph was plotted in a logarithmic scale as percentage viability versus drug concentration.

Colony formation assay

The clonogenic assay was carried out as described earlier with slight modifications [20]. In brief, 300 cells were seeded in a 35 mm plate and allowed to stabilise. The PTX was later on added at different doses (1–20 mM). The drug was removed after an incubation period of 24 h, and the plates were gently washed twice with PBS. Complete media was added to each of the plates, and the cells were allowed to grow over a period of 8–10 days. Cells were fixed in chilled methanol and then stained with 0.5% crystal violet. Clones are considered to represent viable cells if they contain an excess of 50 cells, therefore, colonies with at least 50 cells were counted.

Cell cycle analysis using FACS

Sub-confluent plates were treated with varying non-toxic doses of PTX (1, 2.5 and 5 mM) for a period of 24 h. Cells were harvested, washed twice with PBS and later fixed with 70% chilled ethanol. The cells were then processed by treating them with RNase (0.5 mg/ml) and staining with PI(50 μ g/ml). Acquisition was done on FACS Calibur, and the results were analysed using Modfit software as previously described [18].

EB/AO staining for apoptosis

The basis of this assay is the discrimination of membrane integrity between the live and dead cells. EB/AO staining

was done as previously described [21]. 16,000 cells/well were seeded in triplicates in a 96-well format. Cells were treated with PTX at non-toxic doses for 24 h and then centrifuged. The cells were stained using EB/AO mix and observed under a Zeiss Axio inverted microscope. Images were captured at $\times 10$ magnification for three different fields of each particular well.

Cellular morphology in presence of PTX

The MDA-MB-231 cells were grown in 6-well plates and then treated with non-toxic doses of PTX for 24 h. Cells were fixed with 4% paraformaldehyde and observed under an inverted microscope. Haematoxylin-eosin (HE) staining was also performed to observe the cytopathic effects with a slight modification [18]. Sub-confluent cells grown on coverslips were treated with PTX as done earlier and fixed with 4% paraformaldehyde. The coverslips were washed with PBS and subjected to periodic staining with haematoxylin and eosin. Coverslips were mounted on glass slides with the aid of DPX mountant and observed under Zeiss upright microscope.

Adhesion assay

Adhesion to ECM substrates was carried out as per the protocol described earlier [18]. 96-well plates were treated with Matrigel (10 $\mu\text{g}/\text{ml}$) and Collagen type-IV (50 $\mu\text{g}/\text{ml}$) and kept at 4°C overnight for polymerisation. The plates were washed with PBS and then treated with 1% BSA for 2 h and kept in an incubator. Cells treated with non-toxic doses of PTX were harvested using Saline-EDTA. Subsequently, cells were suspended in 0.1% BSA containing plain DMEM and inoculated at a density of 3×10^4 cells/well. The effect of PTX on adhesion of MDA-MB-231 cells was evaluated at 15, 30, 45, 60 and 90 min. At each subsequent time point non-adherent cells were removed and wells were washed twice with PBS. The adherent cells were then determined using MTT.

Wound scratch assay

The wound healing assay was performed as per the earlier reports [22, 23]. Cells grown in 6-well plates were treated with 1 $\mu\text{g}/\text{ml}$ mitomycin C for 1 h. The cells were then lined off using a sterile tip, and the wells were washed to ensure that the wound area is devoid of cells. Non-toxic doses of PTX were added for 24 h and then fixed with 70% methanol. The wound width was measured using the Metamorph imaging software, and the results were plotted as percent wound closure with respect to control with varying doses of PTX.

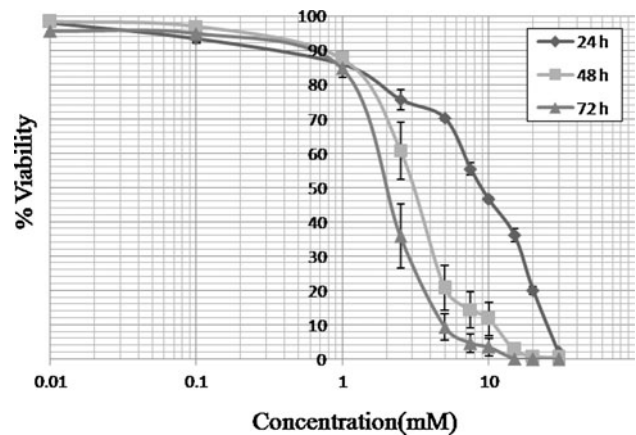


Fig. 1 PTX affects the proliferation potential of MDA-MB-231 cells. MTT assay was carried out to study the effect of 24, 48 and 72 h of PTX (0.01–30 mM) treatment on MDA-MB-231 cells. IC₅₀ was calculated from the dose effect plots considering untreated control as 100% viable. IC₅₀ for 24, 48 and 72 h was 9, 3 and 2 mM, respectively. Results are representative of three independent experiments

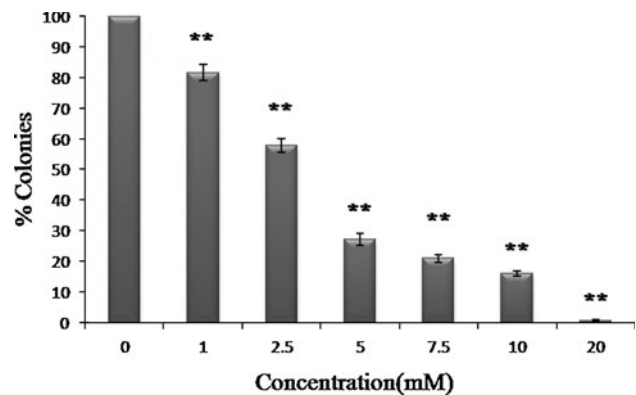


Fig. 2 PTX decreases the clonogenic potential. Cells were treated with PTX (1–20 mM) for 24 h and then allowed to grow further. Number of colonies at the end of 8 days of incubation were stained and counted. The plot represents the percentage colonies against increasing PTX concentration, considering the untreated control as 100% colonies. A significant dose-dependent decrease in colony formation is observed. Results are representative of three independent experiments \pm SE. $**P < 0.001$

Preparation of condition media and gelatin zymography

Sub-confluent plates were treated with non-toxic doses of PTX for 24 h. The cells were washed twice with PBS to remove serum traces. Plain DMEM was then added to each plate, and condition media was collected after 24 h. The media was concentrated using 30 kDa cut-off filters from millipore and normalised as per the individual cell counts. Samples (50 μl) were loaded onto 10% SDS-PAGE containing 0.1% gelatin as a substrate. The rest of the protocol was performed as per the method described earlier [24]. In addition, condition medium collected from HT-1080 was

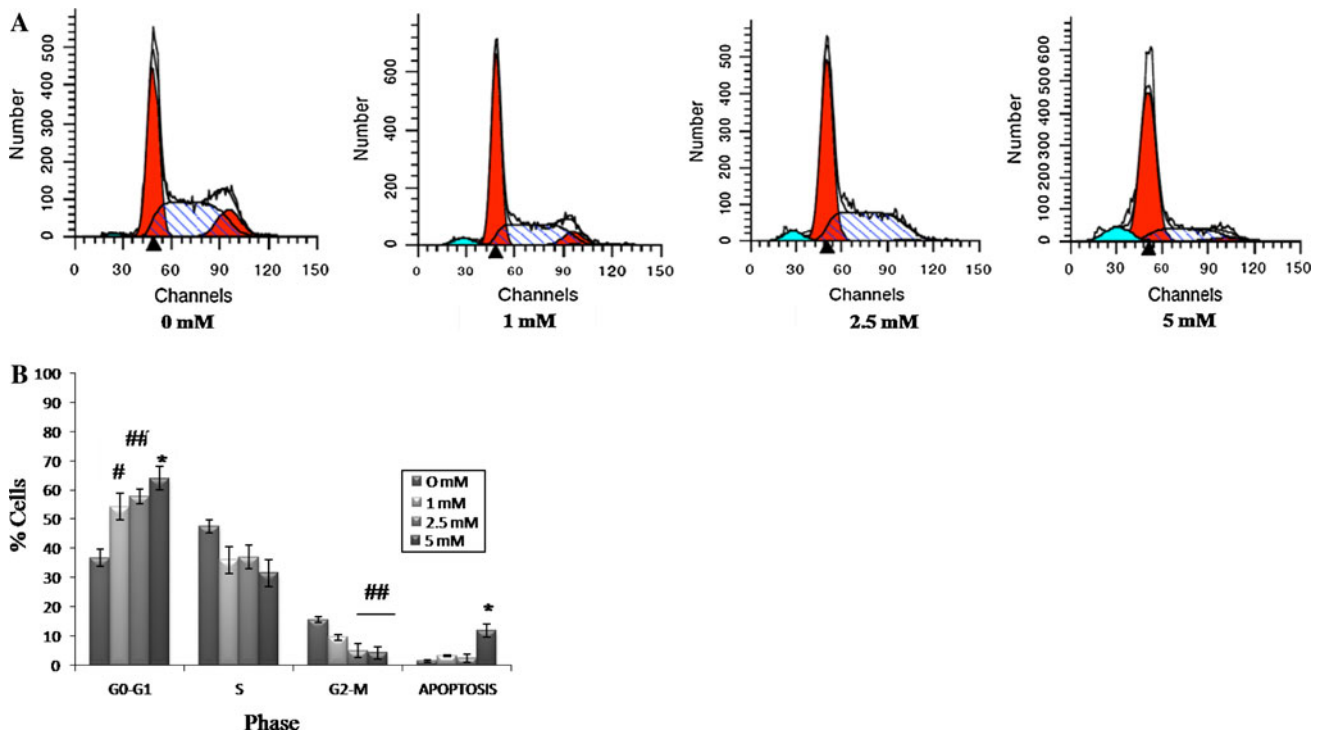
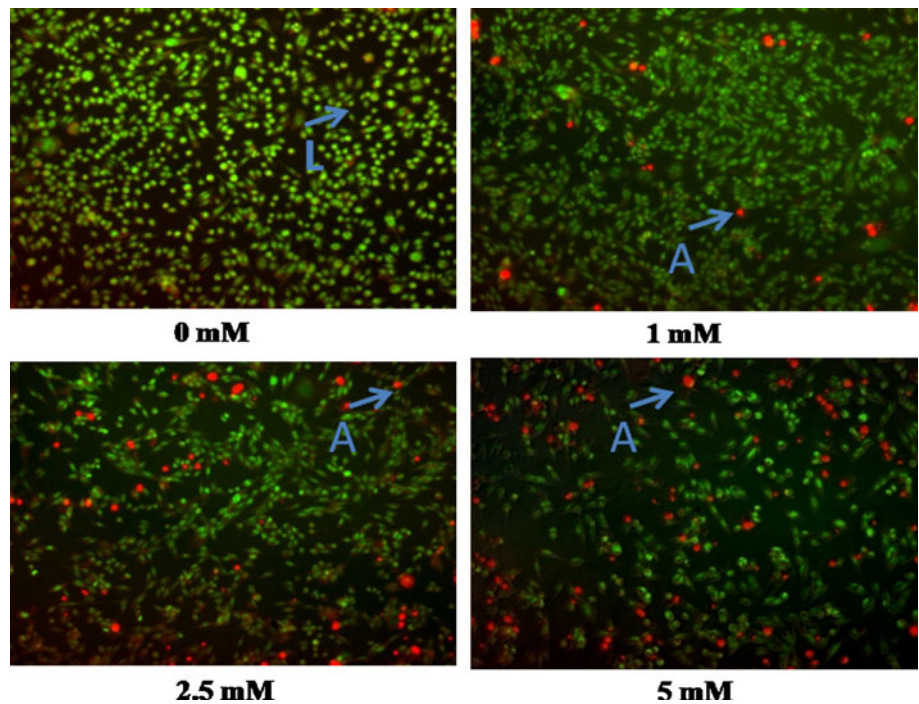


Fig. 3 PTX brings an alteration in the cell cycle. MDA-MB-231 cells treated with non-toxic concentrations of PTX for 24 h were stained with PI and acquired using FACS Calibur. **a** Ploidy level at non-toxic doses compared to control. **b** Graphical representation of PTX-treated cells in different phases of cellular cycle. PTX-treated

cells showed accumulation in G0-G1 phase, decrease in S and G2-M phases. A significant increase in apoptosis is evident. Results are representative of three independent experiments \pm SE. * $P < 0.005$, ^{##} $P < 0.03$, [#] $P < 0.05$

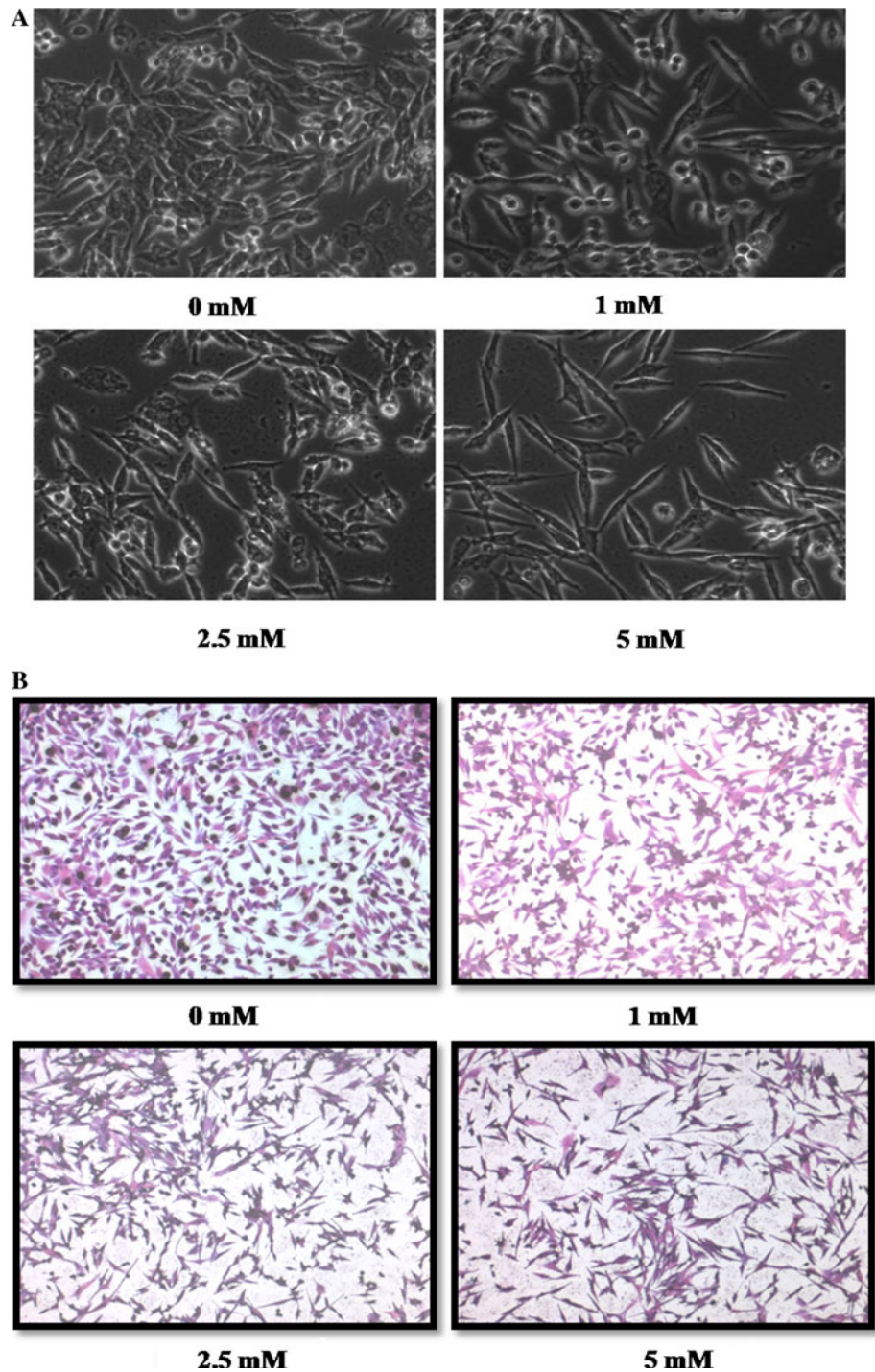
Fig. 4 EB/AO staining shows the apoptotic inducing activity of PTX. Cells treated with PTX in 96-well plates for 24 h were centrifuged and equal volumes of EB/AO were added. AO fluoresces green in live cells while EB fluoresces orange/red when intercalated with DNA in dead cells. PTX-treated cells showed an increase in apoptosis. Results are representative of three independent experiments



also processed and used as a positive control representing MMP-9, 92 kDa and MMP-2, 72 kDa. After electrophoresis, the gel was kept in developing buffer for at least

24 h. The gel was stained with 0.25% comassie brilliant blue R-250 and then destained. The gelatinase activity was visible as clear white zones in a dark background.

Fig. 5 Changes in cellular morphology upon PTX treatment. PTX was added to semi-confluent cells at non-toxic doses for 24 h. Cells were fixed and stained with H-E or left unstained. Cells exhibited a spindle appearance and decrease in cellular volume in PTX-treated groups. **a** Unstained cells, **b** H-E stained cells



ELISA of condition media

Enzyme linked immunosorbent assay (ELISA) was done as per the manufacturer's protocol. Both MMP-2 and MMP-9 activities in the condition media were, respectively, assessed using the kits from Calbiochem, MERCK (QIA63 and QIA56). The levels of both the gelatinases were determined. Percentage levels of decrease for respective

MMPs keeping the untreated as 100% were plotted against non-toxic doses of PTX.

Statistics

All experiments have been performed at least three times independently and are represented as Mean \pm SE. One

way ANOVA (Equal variances assumed) was used for statistical significance and $P < 0.05$ is considered significant.

Results

PTX affects cellular proliferation in dose-dependent manner

The MTT assay was performed to determine the IC_{50} of PTX in a time- and dose-dependent manner (24, 48 and 72 h). As seen in Fig. 1, IC_{50} showed a significant decrease as exposure time of PTX was increased. The observed IC_{50} of PTX on MDA-MB-231 was 9, 3 and 2 mM after 24, 48 and 72 h, respectively. Further, a dose-dependent decrease in cell viability is seen at all the time intervals. Based on this observation, the subsequent experiments were carried out at non-toxic doses such as 1, 2.5 and 5 mM of PTX for a 24 h exposure.

Cancer cells have self-sufficiency to growth signals [25] and can form clones. The PTX (1–20 mM) shows a dose-dependent decrease in colony formation (Fig. 2) leading to 81.7, 57.14, 16.11 and 0.75% at 1, 2.5, 10 and 20 mM, respectively, compared with untreated cells ($P < 0.001$). Thus, only a fraction of seeded cells are able to self-reproduce themselves with increasing the concentration of PTX.

PTX brings an alteration in cell cycle profile and induces apoptosis

The FACS was performed to evaluate the ploidy state of MDA-MB-231 cells treated with PTX. As is evident from Fig. 3a, the PTX induces a G0-G1 block. There was a significant increase from 36.81 ± 2.87 to 57.85 ± 2.5 , 62.74 ± 4.68 at 2.5 and 5 mM, respectively, compared with the control ($P < 0.03$). Further, a dose-dependent increase in apoptosis was also observed (Fig. 3b). The EB/AO staining was further done to study the apoptotic activity of PTX at non-toxic doses on MDA-MB-231 cells. An increase in apoptotic cells is observed at 1, 2.5 and 5 mM which are depicted as red-coloured cells compared with live green-coloured cells (Fig. 4).

PTX affects cellular morphology and adhesion

The PTX-treated cells showed a spindle-shaped characteristic, lesser spreading and hypertrophy compared to untreated cells (Fig. 5a and b). Further, to check the anti-adhesive potential of PTX, adhesion assay using ECM substrates was done. A significant reduction is seen in

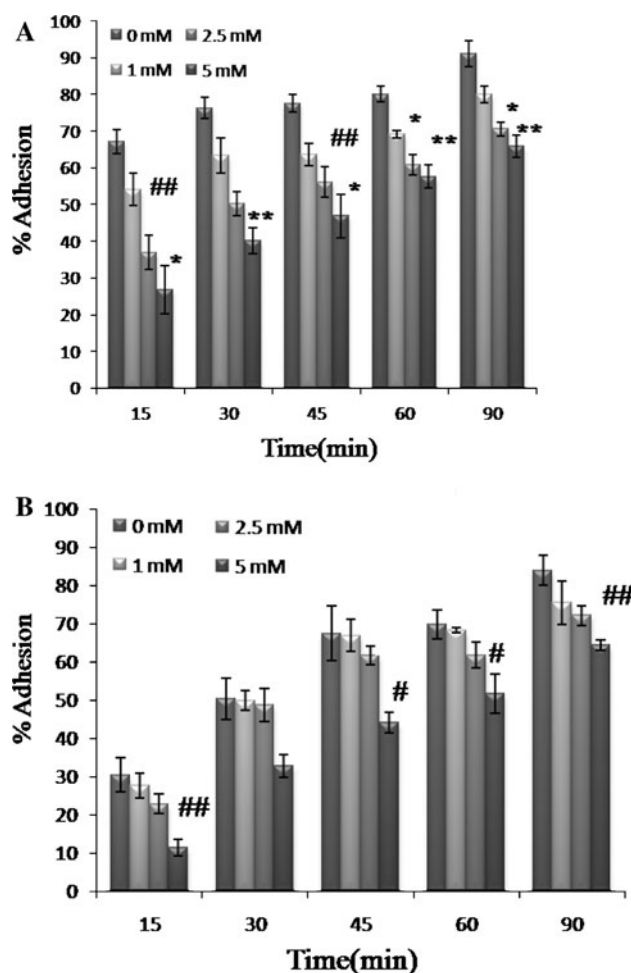


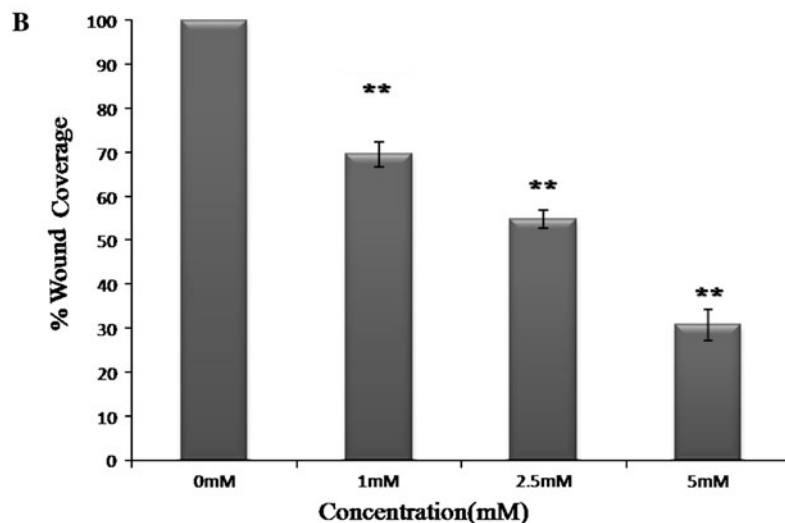
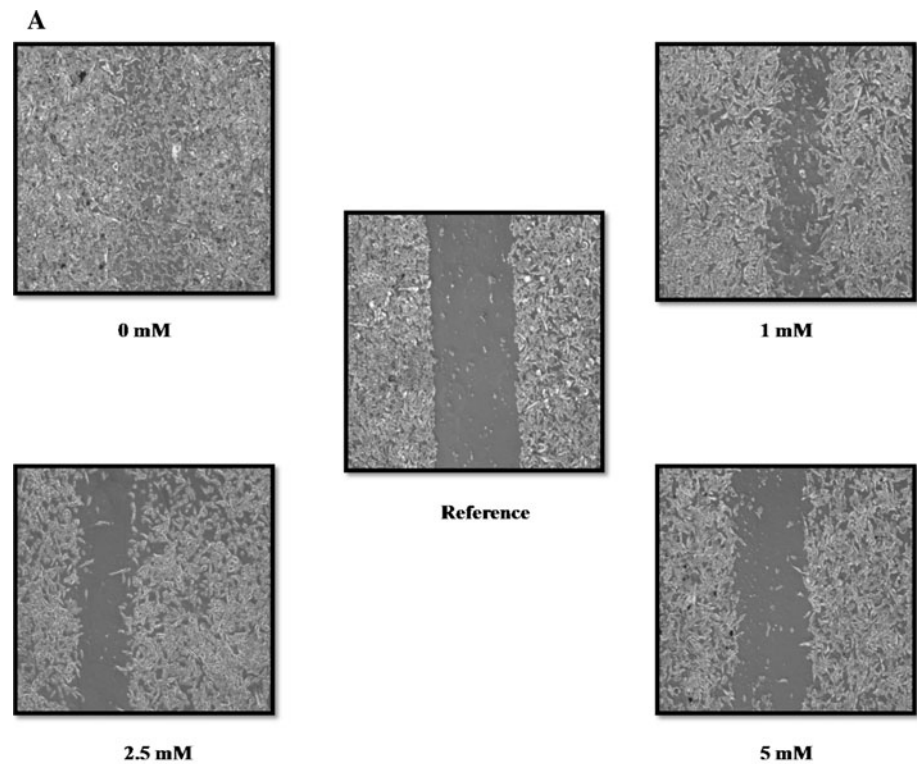
Fig. 6 PTX decreases the adhesion to ECM substrates. Cells were treated with non-toxic doses of PTX for 24 h, harvested and allowed to adhere to plates for 15, 30, 45, 60 and 90 min. Time- and dose-dependent kinetics of adhesion to **a** Matrigel and **b** Collagen type-IV. PTX-treated cells showed a decrease in adherence at all time points. Values are representative of three independent experiments \pm SE. # $P < 0.05$, ## $P < 0.03$, * $P < 0.005$, ** $P < 0.001$

PTX-treated cell adherence to both matrigel and collagen type-IV at different time points. Cells treated with PTX at 2.5, 5 mM showed an adherence of 70.51 ± 1.97 and 65.84 ± 3 compared to 91.08 ± 3.62 for untreated cells at 90 min ($P < 0.005$) with matrigel (Fig. 6a). In contrast, adherence to the collagen type-IV at 5 mM was 64.4 ± 1.30 compared to 83.94 ± 3.84 for untreated ($P < 0.03$) at 90 min (Fig. 6b). Thus, PTX affected adhesion to both matrigel and collagen type-IV at non-toxic doses.

PTX impedes cellular motility

The PTX at non-toxic doses showed a significant reduction in motility of MDA-MB-231 cells (Fig. 7a). At 1, 2.5 and 5 mM, the wound coverage is 69.54 ± 2.93 , 54.87 ± 2.02

Fig. 7 Cellular motility impeded by PTX. Cells grown in 6-well plates were scratched using a sterile tip. Wound coverage was then monitored in the presence of PTX for 24 h at non-toxic doses. Initial and final wound widths were measured for control and treated groups. A representative picture of $\times 10$ magnification is shown as reference taken at initial zero time point. **a** Wound coverage in untreated control and PTX-treated groups. **b** Quantitative representation of wound coverage. A significant reduction in the migration at all the non-toxic doses can be seen. Values are representative of three independent experiments \pm SE. $**P < 0.001$ compared with untreated control



and 30.84 ± 3.53 , respectively, (Fig. 7b) compared to control ($P < 0.001$).

PTX affects the activity of gelatinases

The activities of both the gelatinases MMP-2 and MMP-9 were checked by subjecting the condition media to gelatin zymography. A dose-dependent decrease in MMP-9 was observed (Fig. 8a). At 2.5 mM and 5 mM, there were reductions to 21.59 and 32.37% compared with control ($P < 0.005$). MMP-2 levels showed a marginal decrease

(Fig. 8b) at non-toxic doses. It was also seen that MDA-MB-231 cells expressed higher levels of MMP-9 compared to MMP-2. We have further investigated this using ELISA. It was observed that PTX reduced MMP-9 expression in a dose-dependent manner (Fig. 9a). At 1, 2.5 and 5 mM, there was a significant reduction to 74.76 ± 3.77 , 71.25 ± 6.07 and 66.32 ± 5.82 , respectively, compared with control ($P < 0.03$). The MMP-2 levels (Fig. 9b) further showed minor decrease to 92.31 ± 1.44 , 95.83 ± 0.86 , 93.20 ± 0.82 at 1, 2.5 and 5 mM, respectively, compared with control ($P < 0.05$). Further, it was observed that

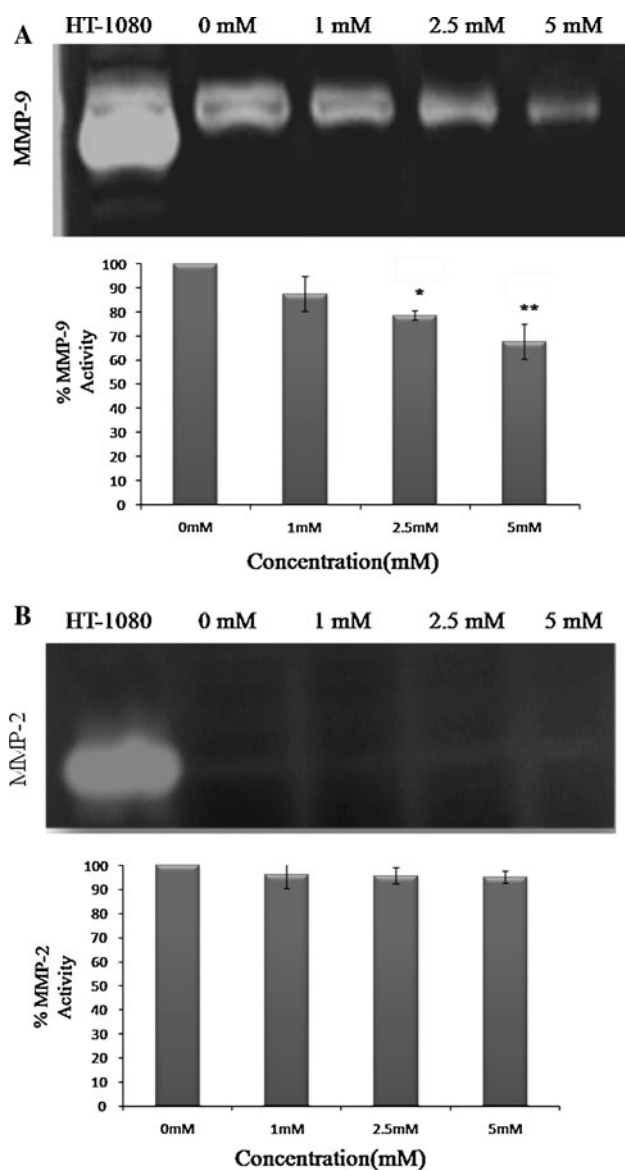


Fig. 8 Gelatin zymography of PTX-treated condition media. Condition media was collected from untreated and PTX-treated cells after 24 h. MMP-2 and MMP-9 activity were observed using gelatin zymography. Gelatinase activity is visible as clear *white zones* in dark background. **a** MMP-9 activity **b** MMP-2 activity. Quantification was done using densitometry considering untreated as 100%. Values are representative of three independent experiments \pm SE. * $P < 0.005$, ** $P < 0.001$ compared with untreated control

MDA-MB-231 cells exhibited higher levels of MMP-9 compared with MMP-2 (~6.6 fold).

Discussion

The present investigation addresses the effect of PTX on human breast cancer cells. A methylxanthine is a

methylated form of xanthine, a purine base. It includes caffeine, Theobromine, Theophylline, PTX, etc. These inhibit the activity of phosphodiesterase and have been shown to exert anti-cancerous effects [26]. The PTX is the drug of choice based on its hydrophilic nature due to its maximal solubility in aqueous among other derivatives, such as caffeine [12]. This indeed is a pharmacological advantage in therapeutic scenario.

Breast cancer is the second most diagnosed cancer worldwide [1, 2]. It starts off as a local disease but eventually metastasise to lymph nodes and distant organs, such as lung, liver and bones [3, 27]. The primary cause for cancer-related deaths is the dissemination of tumour cells into the bloodstream making a destination to different target sites. This process starts when a transformed cell accumulates mutations in the genes regulating the key essential pathways, leading to uncontrolled proliferation and its outgrowth [25]. The detachment from the primary mass makes it a liable candidate to participate in the next round of confrontation with other physical barriers. Cells having the capability to show increased adhesion, invasion and migration participate in further metastatic sequel [28]. Thus, targeting the initial metastatic events such as adhesion, migration and invasion which are the key cardinal signatures surely holds a promise to target the multistep metastatic occurrence.

The pharmacokinetics as well as the safety profiles for the existing drugs are well understood. Thus, any later discovered role can be harnessed to the field of clinical trials. This can eventually help drug developers to bypass the assessment costs [29]. In view of this, we have evaluated the anti-metastatic potential of PTX in human breast cancer cells. Previous studies from our lab have shown that PTX exerts anti-metastatic activity in B16F10 murine melanoma cells [16–18]. In the present work, we have extended our approach to MDA-MB-231 human breast cancer cells.

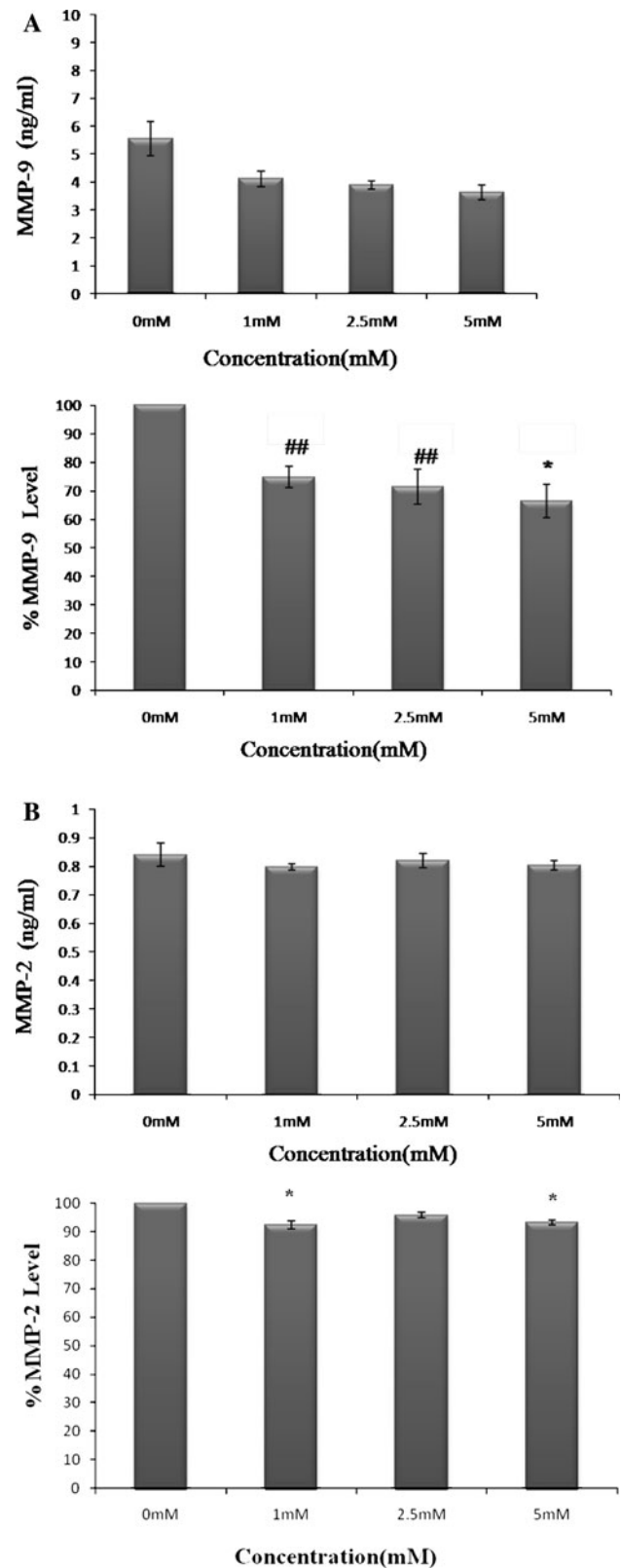
The initial evaluation of PTX on MDA-MB231 cells was done using a MTT cytotoxic assay for 24, 48 and 72 h. A dose- and time-dependent decreases in cellular proliferation were observed that confirms the anti-proliferative potential of PTX. There was a decrease in IC_{50} at all the time points. Further, it was found out that at 24 h treatment with PTX about 86.05, 75.62 and 70.25% cells were viable at 1, 2.5 and 5 mM, respectively. So, we decided to check the efficacy of doses ≤ 5 mM to carry out our further experiments. The clonogenic assay further corroborated its anti-proliferative potential. It has been earlier reported that increased c-AMP levels lead to the suppression of RAS and MAPK activity affecting proliferation [13]. Thus, it is quite possible that PTX might modulate the activity of MAPK affecting proliferation.

Severe morphological and motility characteristic changes were observed in MDA-MB-231 cells at the non-toxic

Fig. 9 PTX affects the levels of gelatinases. ELISA of condition medium was done to check the levels of gelatinases. PTX affects the levels of MMP-9(a) in a dose-dependent manner while affecting the MMP-2(b) slightly. The untreated cells are represented having 100% respective MMP levels. MDA-MB-231 cells expressed higher levels of MMP-9 compared to MMP-2. Values are representative of three independent experiments \pm SE. $^{##}P < 0.03$, $^{*}P < 0.005$

doses. This might be due to the cytoskeletal alterations associated with phosphodiesterase inhibitors, which lead to increased c-AMP levels [15, 16]. We have earlier shown that PTX affects migration by modulating Rho GTPase activity and actin organisation in B16F10 cells due to phosphodiesterase inhibition [16]. Further, PTX induced a cell cycle arrest at G1 phase of cell cycle followed by apoptotic death. This observation is consistent with other anticancer agents that are phosphodiesterase inhibitors [30, 31]. The PTX has been earlier shown to down regulate cyclin D1 levels in mesangial cells that abrogate cdk4 activity [32]. Both cyclinD1/cdk4 complexes are required to traverse the G1 phase. Thus, in light of this observation, we propose a similar mechanism of action in MDA-MB-231 cells as well. The EB/AO staining was performed to distinguish live from apoptotic cells. The AO fluoresces green in live cells and EB fluoresces orange/red when intercalated with DNA in dead cells [33]. The AO being an inclusion dye penetrates cells making the nucleus look green while ET an exclusion dye penetrates only those cells which have lost their integrity [34]. The PTX-treated MDA-MB231 cells showed an increase in apoptosis at a concentration of 5 mM. Thus, apart from inducing a cell cycle block it also leads to apoptosis. A significant reduction in the adhesion potential of MDA-MB-231 cells to both matrigel and collagen type-IV, a major ECM component [19] was observed. This might be due to the alteration in the surface molecules such as integrins that regulate the adhesion capability at cell substratum interface.

One major family of proteinases associated with the process of tumorigenesis is the MMPs [35]. Both MMP-2 and MMP-9 are the major gelatinases playing a key role in the degradation of collagen type-IV and gelatin [36, 37]. We observed that PTX inhibited MMP-9 activity significantly, but marginally affecting MMP-2 activity using gelatin zymography. Further, MDA-MB-231 cells expressed higher levels of MMP-9 in comparison to MMP-2. It had been reported earlier that MMP-9 expression is a positive prognostic marker in node-negative breast cancer [38]. The TNF- α is a potent transcriptional activator of MMP-9 [39, 40]. The PTX has been shown to inhibit TNF- α -induced MMP-9 secretion in HL60 leukaemia cells [41]. Based on these evidences, we propose a similar mechanism of action in this scenario as well. Further, MMPs have been shown to regulate the process of apoptosis, and the elevated MMP-9 levels correlate with decreased apoptosis [35].



Therefore, the decrease in MMP-9 activity by PTX could also be attributed to increased apoptotic activity in breast cancer cells.

In conclusion, we have for the first time described that PTX inhibits the key metastatic events of MDA-MB-231 human breast cancer cells. It affects proliferation, adhesion, migration as well as invasion even at non-toxic doses. Thus, it surely qualifies as a suitable candidate for the usage as a therapeutic agent in the treatment of metastatic breast cancer.

Acknowledgments The authors acknowledge the support of grant from the ACTREC, Tata Memorial Centre. Mr. Peeyush N. Goel is supported by CSIR-Junior Research Fellowship. The authors would also like to thank Shimul Salot for providing technical assistance.

Conflict of Interest None.

References

1. Ferlay J, Shin HR, Bray F, Forman D, Mathers C, Parkin DM (2010) Estimates of worldwide burden of cancer in 2008: GLOBOCAN 2008. *Int J Cancer* 127:2893–2917
2. Jemal A, Siegel R, Xu J, Ward E (2010) Cancer statistics, 2010. *CA Cancer J Clin* 60:277–300
3. Nguyen DX, Bos PD, Massague J (2009) Metastasis: from dissemination to organ-specific colonization. *Nat Rev Cancer* 9:274–284
4. Guarneri V, Conte P (2009) Metastatic breast cancer: therapeutic options according to molecular subtypes and prior adjuvant therapy. *Oncologist* 14:645–656
5. Dettelbach HR, Aviado DM (1985) Clinical pharmacology of pentoxifylline with special reference to its hemorrheologic effect for the treatment of intermittent claudication. *J Clin Pharmacol* 25:8–26
6. Jacoby D, Mohler ER 3rd (2004) Drug treatment of intermittent claudication. *Drugs* 64:1657–1670
7. Gastpar H (1974) The inhibition of cancer cell stickiness by the methylxanthine derivative pentoxifylline (BL 191). *Thromb Res* 5:277–289
8. Zhang M, Xu YJ, Mengi SA, Arneja AS, Dhalla NS (2004) Therapeutic potentials of pentoxifylline for treatment of cardiovascular diseases. *Exp Clin Cardiol* 9:103–111
9. D'Hellencourt CL, Diaw L, Cornillet P, Guenounou M (1996) Differential regulation of TNF alpha, IL-1 beta, IL-6, IL-8, TNF beta, and IL-10 by pentoxifylline. *Int J Immunopharmacol* 18:739–748
10. Zhang M, Xu YJ, Saini HK, Turan B, Liu PP, Dhalla NS (2005) Pentoxifylline attenuates cardiac dysfunction and reduces TNF-alpha level in ischemic-reperfused heart. *Am J Physiol Heart Circ Physiol* 289:H832–H839
11. Collingridge DR, Rockwell S (2000) Pentoxifylline improves the oxygenation and radiation response of BA1112 rat rhabdomyosarcomas and EMT6 mouse mammary carcinomas. *Int J Cancer* 90:256–264
12. Bohm L, Roos WP, Serafin AM (2003) Inhibition of DNA repair by pentoxifylline and related methylxanthine derivatives. *Toxicology* 193:153–160
13. Stork PJ, Schmitt JM (2002) Crosstalk between cAMP and MAP kinase signaling in the regulation of cell proliferation. *Trends Cell Biol* 12:258–266
14. Shmueli A, Oren M (2004) Regulation of p53 by Mdm2: fate is in the numbers. *Mol Cell* 13:4–5
15. Glenn HL, Jacobson BS (2003) Cyclooxygenase and cAMP-dependent protein kinase reorganize the actin cytoskeleton for motility in HeLa cells. *Cell Motil Cytoskeleton* 55:265–277
16. Dua P, Gude RP (2008) Pentoxifylline impedes migration in B16F10 melanoma by modulating Rho GTPase activity and actin organisation. *Eur J Cancer* 44:1587–1595
17. Ratheesh A, Ingle A, Gude RP (2007) Pentoxifylline modulates cell surface integrin expression and integrin mediated adhesion of B16F10 cells to extracellular matrix components. *Cancer Biol Ther* 6:1743–1752
18. Dua P, Gude RP (2006) Antiproliferative and antiproteolytic activity of pentoxifylline in cultures of B16F10 melanoma cells. *Cancer Chemother Pharmacol* 58:195–202
19. Di Lullo GA, Sweeney SM, Korkko J, Ala-Kokko L, San Antonio JD (2002) Mapping the ligand-binding sites and disease-associated mutations on the most abundant protein in the human, type I collagen. *J Biol Chem* 277:4223–4231
20. Franken NA, Rodermond HM, Stap J, Haveman J, van Bree C (2006) Clonogenic assay of cells in vitro. *Nat Protoc* 1:2315–2319
21. Ribble D, Goldstein NB, Norris DA, Shellman YG (2005) A simple technique for quantifying apoptosis in 96-well plates. *BMC Biotechnol* 5:12
22. Pichot CS, Hartig SM, Xia L, Arvanitis C, Monisvais D, Lee FY, Frost JA, Corey SJ (2009) Dasatinib synergizes with doxorubicin to block growth, migration, and invasion of breast cancer cells. *Br J Cancer* 101:38–47
23. Lee HS, Seo EY, Kang NE, Kim WK (2008) [6]-Gingerol inhibits metastasis of MDA-MB-231 human breast cancer cells. *J Nutr Biochem* 19:313–319
24. Wang S, Liu Q, Zhang Y, Liu K, Yu P, Liu K, Luan J, Duan H, Lu Z, Wang F, Wu E, Yagasaki K, Zhang G (2009) Suppression of growth, migration and invasion of highly-metastatic human breast cancer cells by berbamine and its molecular mechanisms of action. *Mol Cancer* 8:81
25. Hanahan D, Weinberg RA (2000) The hallmarks of cancer. *Cell* 100:57–70
26. Hirsh L, Dantes A, Suh BS, Yoshida Y, Hosokawa K, Tajima K, Kotsuji F, Merimsky O, Amsterdam A (2004) Phosphodiesterase inhibitors as anti-cancer drugs. *Biochem Pharmacol* 68:981–988
27. Weigelt B, Peterse JL, van't Veer LJ (2005) Breast cancer metastasis: markers and models. *Nat Rev Cancer* 5:591–602
28. Gupta GP, Massague J (2006) Cancer metastasis: building a framework. *Cell* 127:679–695
29. DiMasi JA, Hansen RW, Grabowski HG (2003) The price of innovation: new estimates of drug development costs. *J Health Econ* 22:151–185
30. Chen TC, Wadsten P, Su S, Rawlinson N, Hofman FM, Hill CK, Schonthal AH (2002) The type IV phosphodiesterase inhibitor rolipram induces expression of the cell cycle inhibitors p21(Cip1) and p27(Kip1), resulting in growth inhibition, increased differentiation, and subsequent apoptosis of malignant A-172 glioma cells. *Cancer Biol Ther* 1:268–276
31. Gallagher HC, Bacon CL, Odumeru OA, Gallagher KF, Fitzpatrick T, Regan CM (2004) Valproate activates phosphodiesterase-mediated cAMP degradation: relevance to C6 glioma G1 phase progression. *Neurotoxicol Teratol* 26:73–81
32. Lin SL, Chen RH, Chen YM, Chiang WC, Tsai TJ, Hsieh BS (2003) Pentoxifylline inhibits platelet-derived growth factor-stimulated cyclin D1 expression in mesangial cells by blocking Akt membrane translocation. *Mol Pharmacol* 64:811–822
33. Polo ML, Arnoni MV, Riggio M, Wargon V, Lanari C, Novaro V (2010) Responsiveness to PI3K and MEK inhibitors in breast cancer. Use of a 3D culture system to study pathways related to hormone independence in mice. *PLoS One* 5:e10786
34. Renvoize C, Biola A, Pallardy M, Breard J (1998) Apoptosis: identification of dying cells. *Cell Biol Toxicol* 14:111–120
35. Egeblad M, Werb Z (2002) New functions for the matrix metalloproteinases in cancer progression. *Nat Rev Cancer* 2:161–174

36. Kessenbrock K, Plaks V, Werb Z (2010) Matrix metalloproteinases: regulators of the tumor microenvironment. *Cell* 141:52–67
37. Farina HG, Pomies M, Alonso DF, Gomez DE (2006) Antitumor and antiangiogenic activity of soy isoflavone genistein in mouse models of melanoma and breast cancer. *Oncol Rep* 16:885–891
38. Scorilas A, Karameris A, Arniogiannaki N, Ardavanis A, Bassilopoulos P, Trangas T, Talieri M (2001) Overexpression of matrix-metalloproteinase-9 in human breast cancer: a potential favourable indicator in node-negative patients. *Br J Cancer* 84: 1488–1496
39. Shellman YG, Makela M, Norris DA (2006) Induction of secreted matrix metalloproteinase-9 activity in human melanoma cells by extracellular matrix proteins and cytokines. *Melanoma Res* 16:207–211
40. Okada Y, Tsuchiya H, Shimizu H, Tomita K, Nakanishi I, Sato H, Seiki M, Yamashita K, Hayakawa T (1990) Induction and stimulation of 92-kDa gelatinase/type IV collagenase production in osteosarcoma and fibrosarcoma cell lines by tumor necrosis factor alpha. *Biochem Biophys Res Commun* 171:610–617
41. Ries C, Kolb H, Petrides PE (1994) Regulation of 92 kD gelatinase release in HL-60 leukemia cells: tumor necrosis factor-alpha as an autocrine stimulus for basal- and phorbol ester-induced secretion. *Blood* 83:3638–3646



Molecular and Cellular pharmacology

Curbing the focal adhesion kinase and its associated signaling events by pentoxifylline in MDA-MB-231 human breast cancer cells



Peeyush N. Goel, Rajiv P. Gude*

Gude Lab, Advanced Centre for Treatment, Research & Education in Cancer (ACTREC), Tata Memorial Centre, Kharghar, Navi Mumbai 410210, India

ARTICLE INFO

Article history:

Received 22 January 2013

Received in revised form

2 July 2013

Accepted 4 July 2013

Available online 16 July 2013

Keywords:

Pentoxifylline

MDA-MB-231 Breast cancer cells

Focal Adhesion Kinase

RhoGTPases

Proliferation

Apoptosis

ABSTRACT

Pentoxifylline (PTX) is a methylxanthine derivative currently being used in the treatment of peripheral vascular diseases. Recently, we had evaluated its action in human MDA-MB-231 breast cancer cells. PTX exhibited anti-metastatic activity by affecting key processes such as proliferation, adhesion, migration, invasion and apoptosis. In light of the preliminary findings, the present work accounts for the possible mechanistic insights of the pathways affected by PTX. Aberrant Focal Adhesion Kinase (FAK) signaling forms a key determinant in breast cancer and in view of this fact we had investigated downstream processes regulated by FAK. PTX at sub-toxic doses lowers the level of activated FAK, Extracellular Regulated Kinase or Mitogen Activated Protein Kinase (ERK/MAPK), Protein Kinase B (PKB/Akt) affecting cellular proliferation and survival. It blocks G1/S phase of cell cycle by inhibiting the expression of Cyclin D1/Cdk6. Further, it modulates the activities of RhoGTPases and alters actin organization resulting in decreased motility. PTX also delays tumor growth and inhibited blood vessel formation *in vivo*. In purview of these findings, PTX surely qualifies as a suitable prospect in the intervention of breast cancer.

© 2013 Elsevier B.V. All rights reserved.

1. Introduction

“All things are poison, and nothing is without poison; only the dose permits something not to be poisonous.” (Paracelsus, 1493–1541).

Cancer is a global wreck and the current therapeutic modalities fail to circumvent the associated deaths. Breast cancer is the most commonest form of cancer among women and second most leading cause of cancer related deaths worldwide (Ferlay et al., 2010). It is the outcome of multistep carcinogenesis and is associated with intense metabolic perturbations (Oakman et al., 2011). The basic scheme for treatment includes surgery, radiotherapy and chemotherapy. Owing to high degrees of cytotoxicity and resistance there is an urgent need to identify new candidate entities to limit the current problems. One of the approaches in this regard is drug repositioning or finding new uses of the available drugs. It is assuredly becoming a concerning subject for pharma companies and has indeed gained success in several incidences (Mullard, 2011). Pentoxifylline ([1-(5-oxohexyl)-3,7-dimethyl-xanthine], oxpentifylline, PTX) is a theobromine derivative used in treatment of peripheral vascular diseases (De Sanctis et al., 2002). Several reports show that it has therapeutic effects in

various cellular diseases and processes such as liver degeneration, oxidative stress, inflammatory diseases, renal failure and cancer (Fabia et al., 1997; D'Hellencourt et al., 1996; Zhang et al., 2004). It is a phosphodiesterase inhibitor that increases c-AMP levels hindering the processes such as proliferation, migration and apoptosis (Hirsh et al., 2004). It has shown to exert anti-metastatic effects in both mouse B16F10 melanoma and human MDA-MB-231 breast cancer cells (Dua and Gude, 2006; Goel and Gude, 2011). Thus, it surely qualifies as an attractive drug for therapy with a few side effects and being relatively non-toxic at therapeutic doses (Harris et al., 2010).

Cells are the basic entities of life composed of biomolecules such as nucleic acids, carbohydrates, proteins, lipids and water. The enigma of life is dictated by the regulatory efforts of these biomolecules. Hence, any disruption in this organization confers a pathological state. Focal Adhesion Kinase (FAK) is one of the attractive targets for anti-cancer therapy since it integrates diverse signaling pathways viz. cellular proliferation, migration, angiogenesis and apoptosis (Parsons et al., 2000; Luo and Guan, 2010). Once activated by a key phosphorylation at tyrosine³⁹⁷ residue ensures successive signaling events such as activation of PI3K/Akt signaling, a central pathway regulating apoptosis (Zhao and Guan, 2009). Levels of both FAK and PI3K/Akt are upregulated in breast cancers (Luo and Guan, 2010; Hennessy et al., 2005). It also regulates the functioning of RhoGTPases and MAPK signaling that aids the process of cellular migration and proliferation (Mitra et al., 2005; Mitra et al., 2006).

* Corresponding author. Tel.: +91 022 27405084; fax: +91 022 27405083.

E-mail addresses: peeyushgoel29@gmail.com (P.N. Goel), rgude@actrec.gov.in, rpgude@yahoo.com (R.P. Gude).

In our previous work we have investigated the effects of PTX at sub-toxic doses on various metastatic events in MDA-MB-231 cells (Goel and Gude, 2011). The present work addresses the key mechanistic and molecular insights for the same. Further, *in vivo* evaluation had been performed to corroborate the *in vitro* observations. In light of these findings, PTX emerges as a suitable therapeutic modality for the management of breast cancer.

2. Material and methods

2.1. Reagents and antibodies

Pentoxifylline, Beta-tubulin, Phalloidin/FITC, Fibronectin, FAK Inhibitor or FAKi (PF-573228), Triton X-100, Bovine Serum Albumin (BSA), 1,4-diazabicyclo[2.2.2]octane (DABCO), Paraformaldehyde, Cytochalasin B were purchased from Sigma (India). pFAK (Tyr397), ERK1/2, pERK1/2, Akt, pAkt (Thr308), Cyclin D1, Cdk4, Cdk6, Cleaved Caspase 3, Cleaved Caspase 9, Cleaved PARP, Bcl-2, Bcl-xL and Mcl-1 antibodies were purchased from Cell Signaling Technology (MA, USA) while antibodies against VEGF, p53, FAK were purchased from Santa Cruz (CA, USA). Caspase detection and Annexin V/FITC kits were purchased from Invitrogen (India). G-LISA activation assay and DNA binding assay kits were purchased from Cytoskeleton (Denver, USA) and Active Motif (CA, USA). All the other chemicals/reagents used were either of analytical grade or highest purity that were commercially available.

2.2. Cell culture

MDA-MB-231 human breast cancer cells were purchased from NCCS (Pune, India) and maintained in 10% Dulbecco's Modified Eagle Medium (DMEM, Gibco), supplemented with 10% heat inactivated fetal bovine serum, (FBS, Gibco). Cell Cultures were maintained at 37 °C in 5% CO₂ humidified atmosphere as described earlier (Goel and Gude, 2011).

2.3. Western blotting

Western blotting was carried out as described earlier with slight modifications (Salot and Gude, 2012). Cells were lysed in modified radioimmunoprecipitation assay (RIPA) buffer containing 50 mM Tris, 150 mM NaCl, 1% NP-40, 0.5% sodium deoxycholate, 0.1% SDS, 5 mM EDTA, 1 mM Na orthovanadate, 1 mM PMSF and protease inhibitor cocktail. The FAK stimulation study was performed by pre-coating the plates with fibronectin (20 µg/ml). Cells were seeded and harvested at different time points *viz.* 30 min, 60 min and 120 min respectively. The FAK inhibitor study was performed by treating the cells with 10 µM, 20 µM of PF-573228 for 1 h. Cells were later harvested and proceeded for electrophoresis. 50 µg protein was loaded on 8% SDS-PAGE gel and then electroblotted to PVDF membranes. The membranes were processed by blocking in 5% BSA and subsequently incubated with primary and secondary antibodies along with intermittent washings using Tris-Buffered Saline-Tween 20 (TBST). Beta-tubulin was used as a loading control. Signal detection was done using the Pierce Femto Chemiluminescence system.

2.4. Wound healing assay

Wound healing assay was performed as described earlier (Goel and Gude, 2011). Cells were pre-treated with DMSO (vehicle control), 10 µM and 20 µM of PF-573228 for 1 h. A scratch was made using a sterile tip and then media was added to the plates. Plates were fixed in 70% methanol after 24 h and the images were captured using upright microscope (Carl Zeiss, Germany).

2.5. G-LISA assays for Rho GTPases

The assay was performed as per the manufacturer's instructions. Both Rac and Rho activation assay kits were used for determination of active levels of GTPases in cellular lysates. Briefly, 50 µg of cell lysates (Untreated, PTX treated 1 mM, 2.5 mM and 5 mM) were added to the active Rac or Rho coated plates. Plates were then incubated with intermittent shaking. Primary and secondary antibodies were added sequentially for 1 h each. Color development was seen by addition of HRP detection reagent and then the reaction was stopped by addition of stop reagent. Plates were then read at 490 nm using a spectrophotometer. The results were plotted as % activity considering untreated control as 100%.

2.6. Actin staining

Cells (untreated and PTX treated) were grown on coverslips and then fixed using 4% paraformaldehyde. Coverslips were washed and then permeabilised using 0.1% Triton X100. Cells were then overlaid with 20 µl of Phalloidin mixture and then subsequently with equal volume of 4% BSA. Coverslips were then washed with PBS and mounted on a clean glass slide using 4% DABCO and then sealed with the help of nail paint. A positive control was also set up by the treatment of MDA-MB-231 cells with cytochalasin B (10 µg/ml and 20 µg/ml) for 30 min. The coverslips were then processed in a similar way as done with PTX treated samples. Images were then acquired at 63 × using the LSM 510 META laser scanning microscope from Carl Zeiss, Germany. Images were later analyzed using the software LSM 510 as done earlier (Dua and Gude, 2008).

2.7. AnnexinV/FITC staining

Apoptosis detection was done as per the instructions provided by the company. Briefly, 1 × 10⁶ cells (untreated and PTX treated) were suspended in 100 µl Annexin binding buffer and treated with 5 µl Annexin FITC solution along with 1 µl PI (100 µg/ml). The samples were incubated for 15 min and then 400 µl of Annexin binding buffer was added. Acquisition was done using FACS calibur and analysis was performed using Cell Quest software.

2.8. Caspase 3 and caspase 9 activation assays

Cell lysates were prepared for untreated control and PTX treated samples *viz.* 1 mM, 2.5 mM and 5 mM using caspase lysis buffer, supplied as a part of kit component. 200 µg of protein solution was added with subsequent addition of substrates Leucine–Glutamate–Histidine–Aspartate (LEHD), Aspartate–Glutamate–Valine–Aspartate (DEVD) for caspase-9 and caspase-3 respectively in a 96-well plate format. Plate was incubated for at least 2 h at 37 °C and later read at 405 nm in a spectrophotometer. Results were plotted as % fold increase considering untreated control to be unity.

2.9. DNA binding assay for NF-(kappa)B

TransAM™ assay kit was purchased from Active motif for DNA binding activity of the transcription factor NF-(kappa)B. Wells coated with the desired sequence for binding were incubated with 20 µg of nuclear extracts (untreated and PTX treated). Incubation was thereafter done with both primary and secondary antibodies respectively for 1 h each. The developing solution was then added to the wells for a colorimetric reaction. The reaction was stopped using a stop solution and the plate was read at 450 nm in a spectrophotometer. DNA binding activity was plotted as % NF-(kappa)B activity considering activity for untreated sample as 100%.

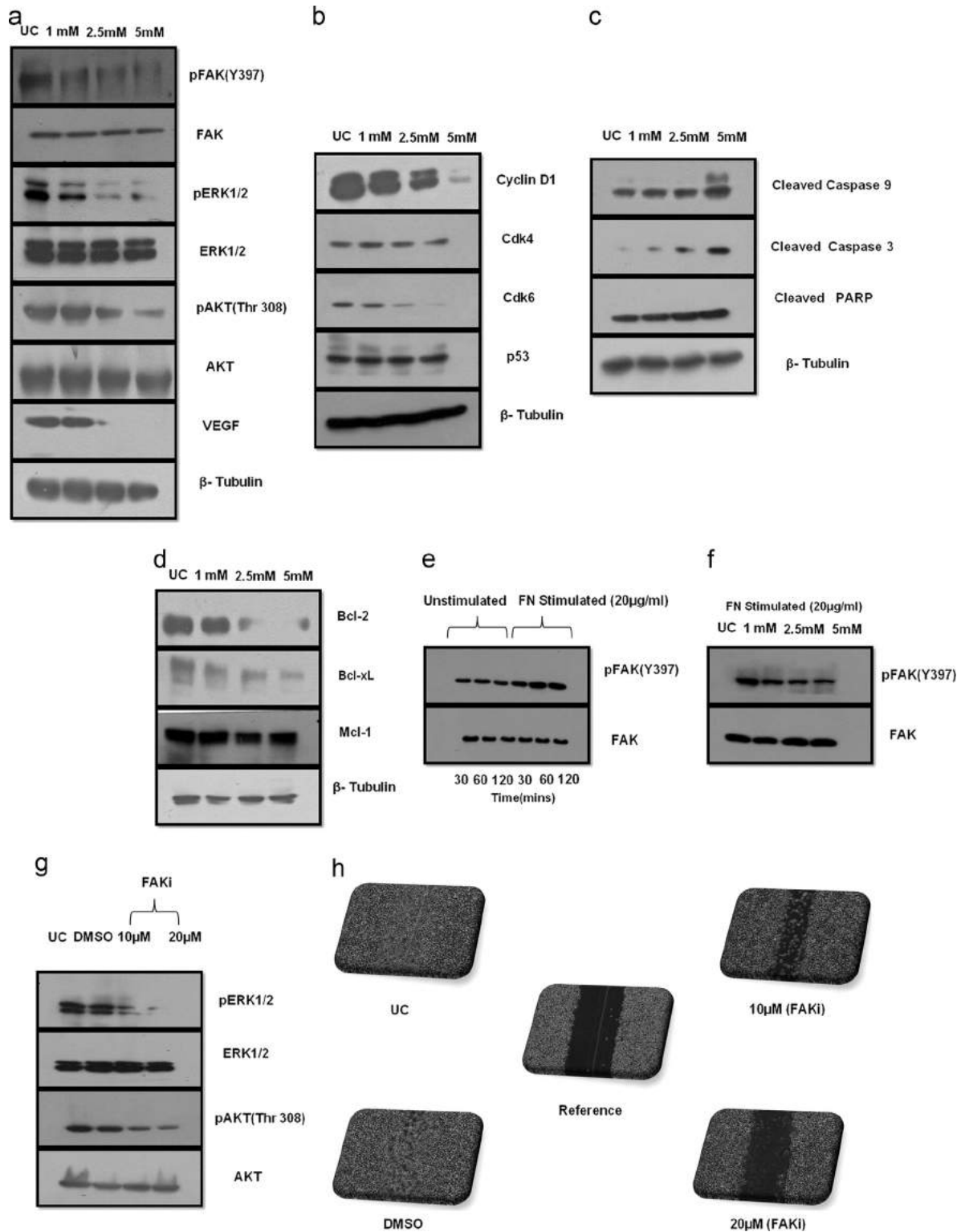


Fig. 1. Dose dependent effects of PTX on FAK pathway and other associated molecules: MDA-MB-231 cells were treated with sub-toxic doses of PTX (1 mM, 2.5 mM and 5 mM) along with untreated control for 24 h. Western blotting was done to study the effects of PTX on protein expression (a). Dose dependent decrease in activated levels of FAK, ERK1/2 and Akt is seen along with decreased levels of VEGF (b). PTX affects G1/S cell cycle mediators CyclinD1/Cdk6 while levels of Cdk4 and p53 remain unchanged (c) and (d). Increase in levels of active caspases 9 and 3 along with the downstream effector PARP that results in apoptosis, while levels of anti-apoptotic proteins (Bcl-2, Bcl-xL) were decreased. No change in levels of Mcl-1 observed. There was an increase in pFAK levels upon stimulation with Fibronectin (20 μ g/ml) compared to unstimulated cells at different time points viz. 30 min, 60 min and 120 min respectively (e). PTX treatment of fibronectin stimulated cells at sub-toxic doses lowered the levels of active FAK (f). Further, the treatment of cells using PF-573228 (FAK inhibitor or FAKi) at 10 μ M and 20 μ M resulted in lowering of the active levels of both ERK1/2 and pAkt (g). It also impedes migration of MDA-MB-31 cells in wound healing assay, suggestive of the fact that FAK indeed has a tumorigenic role in the process of metastasis (h). DMSO was used as a vehicle control.

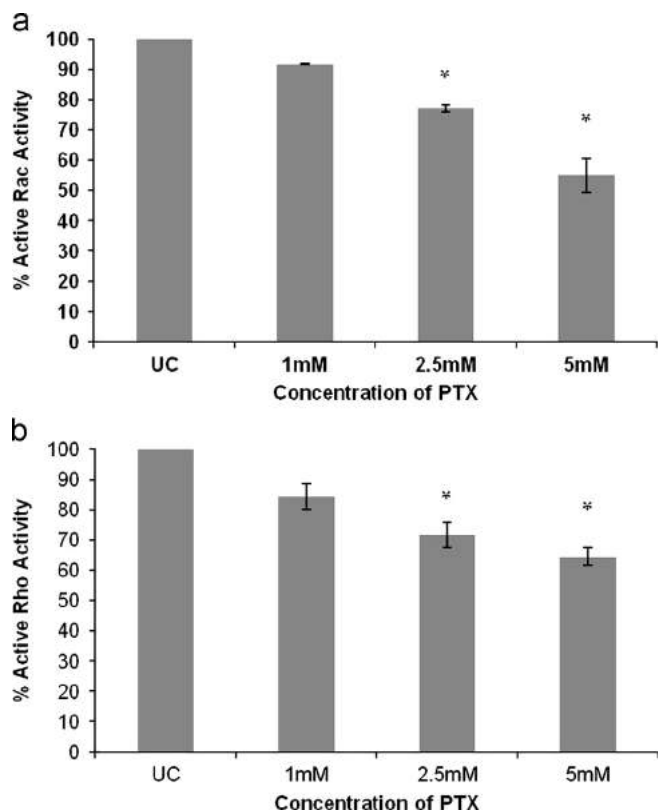


Fig. 2. Decrease in activity of active Rho GTPases upon PTX treatment: G-LISA assays were performed to score the activities of PTX on active Rac and RhoA. A significant reduction is observed at sub-toxic doses of 2.5 mM and 5 mM in levels of (a) active Rac and (b) RhoA respectively. Values are representative of three independent experiments mean \pm S.E.M * $P < 0.05$.

2.10. In vivo xenograft model

2×10^6 MDA-MB-231 cells were inoculated into the right flank of 6–8 week old female NOD-SCID mice respectively as described earlier (Munoz et al., 2006). The animals were obtained from Animal Facility at ACTREC after the Institutional Animal Ethical Committee clearance. When the tumors had grown to an average size of 50 mm³ mice were randomized and divided into 3 groups ($n=5$). (a) PBS only (b) PTX 40 mg/kg and (c) PTX 60 mg/kg. PTX was administered intraperitoneally (i.p) for a period of 9 days consecutively. Tumor volume and animal weight were measured on alternate days. Tumor volume was measured using Vernier calipers and calculated using the formula $1/2ab^2$ where a is the longer diameter and b is the shorter one (Munoz et al., 2006).

2.11. In vivo intradermal model for angiogenesis

1×10^6 MDA-MB-231 cells were injected intradermally into the ventral side of 6–8 week old female NOD-SCID mice respectively as per the protocol followed earlier (Dua et al., 2007). When palpable tumors were observed mice were randomized into 3 groups ($n=5$) as described previously. (a) PBS only (b) PTX 40 mg/kg and (c) PTX 60 mg/kg. Administration of PTX was done intraperitoneally for 9 days. Tumor volumes and animal weight were measured as done earlier. Mice were sacrificed on day 15th after the treatment schedule was completed. The intradermal skin bearing tumors was excised for counting blood vessel density around the localized tumor.

2.12. Statistical analysis

All the experiments were performed at least thrice independently. Results are represented as Mean \pm S.E.M respectively. One way ANOVA (Equal variances assumed) was used for statistical significance and results where $P < 0.05$ were considered statistically significant.

3. Results

3.1. PTX affects the expression of active FAK and its downstream effectors

Several studies have demonstrated that FAK regulates the processes of cell proliferation, angiogenesis, migration and apoptosis. To evaluate whether PTX inhibits the phosphorylation of FAK/ERK/Akt, protein levels of VEGF and the other apoptotic proteins, MDA-MB-231 cells were treated at with sub-toxic doses of PTX. Fig. 1A shows that PTX significantly inhibited the activation of FAK, ERK1/2 and Akt shown by the decrease in the phosphorylation status. Further, PTX inhibited the protein levels of VEGF, Cyclin D1, Cdk6, Bcl-2 and Bcl-xL in a dose dependent manner (Fig. 1a, b, and d). On the other hand there was a dose dependent increase in levels of cleaved caspase-9, 3 and Poly-ADP Ribose Polymerase (PARP) (Fig. 1d). However, no change in protein levels were observed for p53, Cdk4 and Mcl-1 respectively (Fig. 1b and d). An increase in pFAK levels was observed upon stimulation with fibronectin (20 μ g/ml) compared to unstimulated cells at different time points viz. 30 min, 60 min and 120 min respectively (Fig. 1e). PTX treatment at sub-toxic doses affects the levels of activated FAK in fibronectin treated cells confirming that cells are sensitive to PTX treatment (Fig. 1f). Further, the treatment of cells using PF-573228 (FAK inhibitor) resulted in lowering of the active levels of both ERK1/2 and pAkt (Fig. 1g). It also impedes migration of MDA-MB-31 cells which is suggestive of the fact that FAK indeed has a tumorigenic role in the process of metastasis (Fig. 1h).

3.2. Inhibition of the activities of RhoGTPases by PTX

The effect of PTX on the family of RhoGTPases such as Rac and Rho which are largely associated with cytoskeletal alterations and migration was seen in MDA-MB-231 cells. G-LISA assays have an advantage over other traditional methods such as pull-down assays since it requires lesser starting material, time and the results are quantitative. The Rac or Rho G-LISA[®] kit contains a Rac/Rho-GTP-binding protein linked to the wells of a 96 well plate. Active, GTP-bound Rac/Rho in cell lysates binds to the well while inactive GDP-bound Rac/Rho is removed during successive washing steps. Cell lysates treated with sub-toxic doses of PTX (1 mM, 2.5 mM and 5 mM) shows a concentration dependent decrease in activities of both the GTPases respectively. The decrease is significant at 2.5 mM and 5 mM which is 77.145 ± 1.2 , 54.9 ± 5.54 and 71.58 ± 4.31 , 64.43 ± 2.83 for levels of Rac and Rho respectively, compared to untreated control (Fig. 2a and b).

3.3. Effect of PTX on actin cytoskeleton arrangement

The effect of sub-toxic doses of PTX on actin organization was seen in MDA-MB-231 cells. Cells treated with various sub-toxic doses of PTX were fixed and stained with phalloidin-FITC, that specifically stains filamentous actin in the cell. Confocal images captured at 600 \times magnification showed disappearance of extensions protruding at cellular surface, i.e filopodia as well as lamellopodia in a concentration dependent manner upon PTX

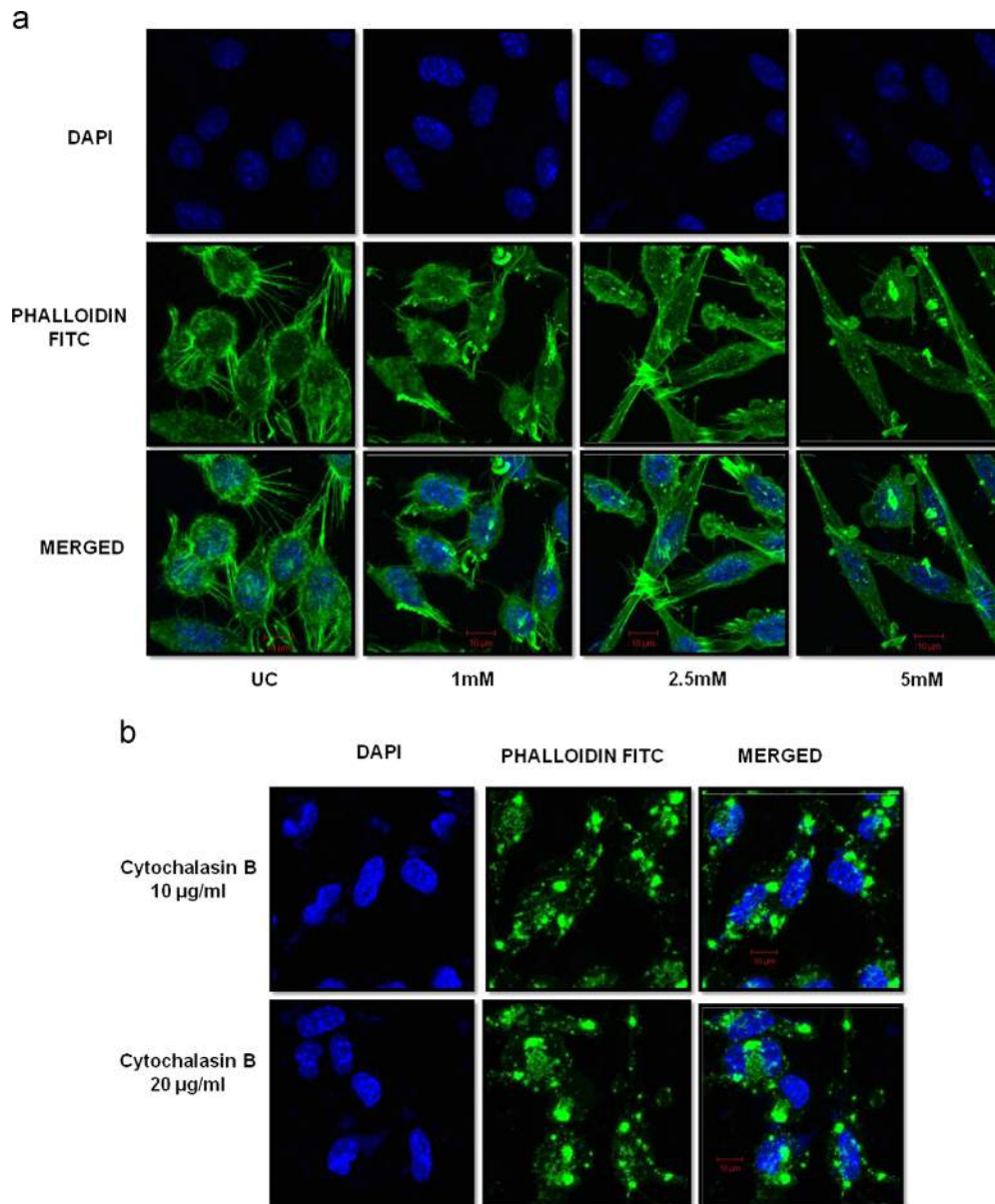


Fig. 3. Effect of PTX on actin staining in MDA-MB-231 cells: Sub-confluent cells were treated with PTX and then subjected to Phalloidin/FITC staining (a). A dose dependent decrease in actin structures such as filopodia (seen as protrusions arising from cell surface) and lamellopodia is seen (b). Cells treated with Cytochalasin B at concentrations of 10 $\mu\text{g/ml}$ and 20 $\mu\text{g/ml}$ were used as positive control. Loss of actin structures is distinctly visible. (Scale-10 μm).

treatment (Fig. 3a). Positive control showed actin depolymerization by disruption of actin fibers (Fig. 3b).

3.4. PTX showed an increase in apoptosis in MDA-MB-231 cells

AnnexinV/FITC staining was performed to assess the apoptotic status of MDA-MB-231 cells on treatment with sub-toxic doses of PTX. AnnexinV has an affinity for Phosphatidylserine (PS) found on the inner leaflet of non-apoptotic cells. However, PS translocates to the outer membrane of apoptotic cells. There is an increase in the early apoptotic cells (shown in the lower right quadrant) as well as late apoptotic cells (upper right quadrant) in a dose dependent manner compared to the untreated control (Fig. 4).

3.5. PTX enhances the activities of cleaved caspases 9 and 3

Caspases exist in an inactive zymogenic form that needs to be processed to be active. This functional form can then recognize target sequences in its substrates initiating the apoptotic process.

PTX showed a significant dose-dependent increase in activities of both caspase-9, caspase-3 at 2.5 mM and 5 mM respectively compared to uninduced control. The synthetic peptides labeled with para-nitroalanine used were LEHD for caspase-9 and DEVD for caspase-3. The active form of these caspases is directly proportional to their substrate specific cleavage ability. Caspase-9 activity showed an increase of $34 \pm 1.26\%$, $43 \pm 5.5\%$ while in case of caspase-3 the increase was $34 \pm 5.2\%$, $65 \pm 2.2\%$ at 2.5 mM and 5 mM compared to the untreated control (Fig. 5a and b).

3.6. DNA binding activity of NF-(kappa)B is not affected upon PTX treatment

MDA-MB-231 cells were assessed for DNA binding ability of transcription factor NF-(kappa)B using TransAM[®] Flexi Kit. Nuclear extracts prepared at sub-toxic doses of PTX were subjected to DNA ELISA in a 96-well format. No changes in NF-(kappa)B activity was observed with increasing concentration of PTX. However, there was a slight non-significant decrease in % NF-(kappa)B binding

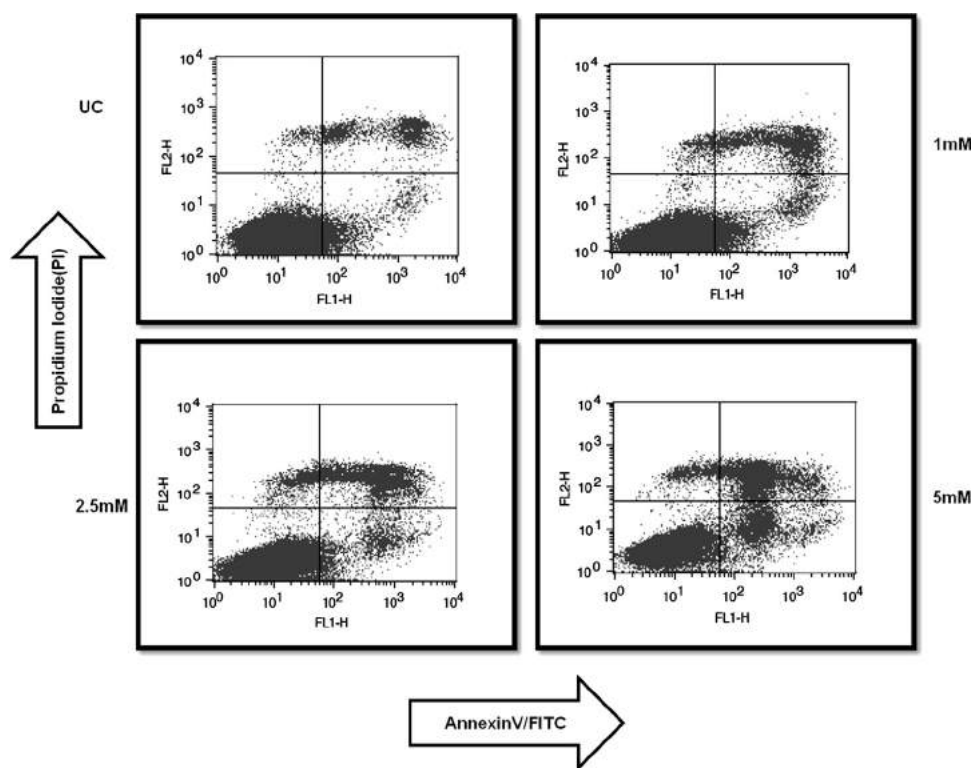


Fig. 4. AnnexinV/FITC Staining shows the Apoptotic inducing activity of PTX: Cells treated with sub-toxic doses of PTX were stained with AnnexinV, a molecule with high affinity towards Phosphotidyl Serine (PS) found on outer surface of apoptotic cells. Increase in number of apoptotic cells is visible with increasing doses of PTX (lower and upper right quadrants) respectively. X-axis represents AnnexinV/FITC while Y-axis denotes Propidium Iodide (PI).

activity at 5 mM, i.e. $94.54 \pm 0.54\%$ compared to untreated control being 100% (Fig. 6).

3.7. Tumor growth delay in SCID mice after PTX treatment

MDA-MB-231 cells were implanted subcutaneously into the right flank to allow tumors to grow. Tumor latency period observed was 5 days. PTX was administered intraperitoneally only from the day 9, when the average tumor volume was more than 50 mm^3 (Teicher, 2006) till day 17, i.e. for a period of 9 days. PTX, showed a significant tumor growth delay from day 13th to day 21st when animals were sacrificed. Tumor volume on 17th and 21st days were $554.20 \pm 78.05 \text{ mm}^3$, $1397 \pm 108.2 \text{ mm}^3$ for untreated control while $280.92 \pm 37.13 \text{ mm}^3$, $912.91 \pm 106.16 \text{ mm}^3$ for PTX (40 mg/kg) and $239 \pm 22 \text{ mm}^3$, $895 \pm 98.50 \text{ mm}^3$ for PTX (60 mg/kg) groups respectively (Fig. 7a). Animal weights were measured alternately after PTX administration to observe the dose associated toxicity in animals. There was no decrease in body weights on PTX treatment (Fig. 7b).

3.8. Decrease in blood vessel formation upon PTX treatment

MDA-MB-231 cells implanted intradermally showed palpable tumors on day 3rd. PTX was administered from 4th day onward when an average tumor volume was greater than $1\text{--}2 \text{ mm}^3$ since lesser volumes restrain the tumors to derive nutrition (Naumov et al., 2006). Hence, angiogenesis occurs only after achieving volumes greater than 2 mm^3 . PTX was administered for a period of 9 days as done earlier. Tumor volumes and animal weight were measured every alternate day. There as a delay in tumor growth as seen by reduced tumor burden compared to control group. Tumor volume was $145.6 \pm 24.32 \text{ mm}^3$ for untreated while it was $75.44 \pm 10.95 \text{ mm}^3$, $73.64 \pm 15 \text{ mm}^3$ for PTX treated viz. 40 mg/kg and

60 mg/kg groups respectively (Fig. 8a). No significant weight loss was observed (Fig. 8b). Mice were sacrificed on day 15th and the skin was carefully removed using forceps to visualize the growth of blood vessels around the tumor. A significant reduction in blood vessels was being observed (Fig. 8c). Average number of blood vessels visible were 6.8 ± 0.8 , 3.8 ± 0.8 , 2.8 ± 0.58 for untreated and PTX treated (40 mg/kg and 60 mg/kg) groups respectively (Fig. 8d).

4. Discussion

Breast cancer, being a global issue and the second most leading cause of cancer related deaths among women, needs an effective management and treatment. The largest proportions of deaths are due to disseminated tumors that form distant metastasis rather than the localized ones. Chemotherapy as well as radiotherapy forms an elaborate and systematic plan of treatment for patients with metastasis since surgery encompasses the scope of operating confined tumors in majority of the cases. In a given cell, multiple pathways team up to regulate cellular functioning. Over/under expression of diverse biomolecules may lead to a diseased state such as cancer. One of the key determinants is FAK, a non-receptor tyrosine kinase that regulates myriad of cell signaling pathways. This orchestration network embraces key metastatic attributes such as proliferation, migration, invasion, apoptosis as well as angiogenesis (Parsons et al., 2000; Luo and Guan, 2010). The increased levels of FAK form a positive correlation with the invasive behavior from a benign state (McLean et al., 2005). It phosphorylates a large number of substrates which in turn regulate downstream signaling events.

The present work is an extension to our previous results documenting that PTX at sub-toxic doses exert anti-metastatic

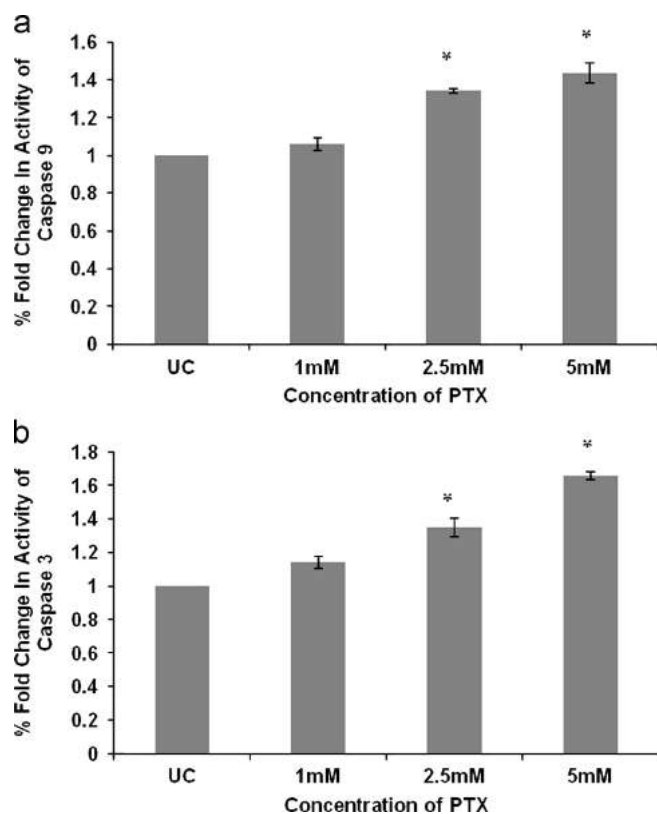


Fig. 5. Increase in activity of Cleaved Caspase-9 and Caspase-3 upon PTX treatment: Cells treated with sub-toxic doses of PTX were harvested and cell lysates were prepared. A 96-well format was used to determine the activity of caspases. Caspase activity was determined using substrates: LEHD, DEVD specific for caspase 9 and caspase 3. A significant fold change is observed at 2.5 mM and 5 mM in activities of (a) caspase-9 and (b) caspase-3 respectively. Values are representative of three independent experiments mean \pm S.E.M. * $P < 0.05$.

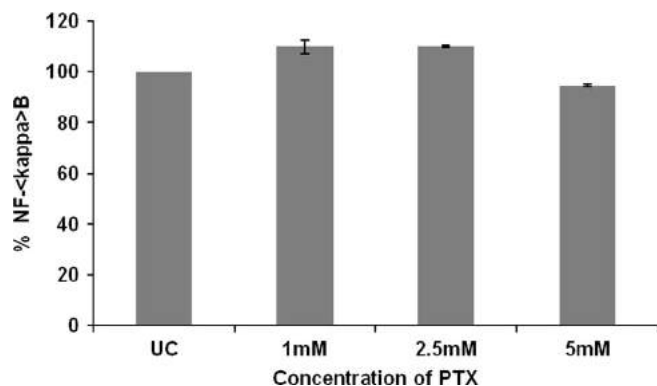


Fig. 6. PTX does not alter the DNA binding ability of NF-(kappa)B: PTX treated cells were harvested and then nuclear extracts were prepared to evaluate the DNA binding ability of NF-(kappa)B using TransAM[®] Flexi Kit. No significant change is observed upon PTX treatment.

effects in human MDA-MB-231 cells. We have earlier shown that PTX affected cellular proliferation, induced a G1/S cell cycle arrest, impeded cellular migration, adherence to ECM components and decreased the activity of MMP-9 affecting invasion (Goel and Gude, 2011). In the current investigation, the mechanistic insights have been explored so as to unscramble the molecular determinants associated with anti-metastatic mechanisms of PTX. It is being routinely used in clinical settings for treatment of intermittent claudication and other vascular diseases (Dettelbach and Aviado, 1985). Thus, it is indeed a drug of choice due to its

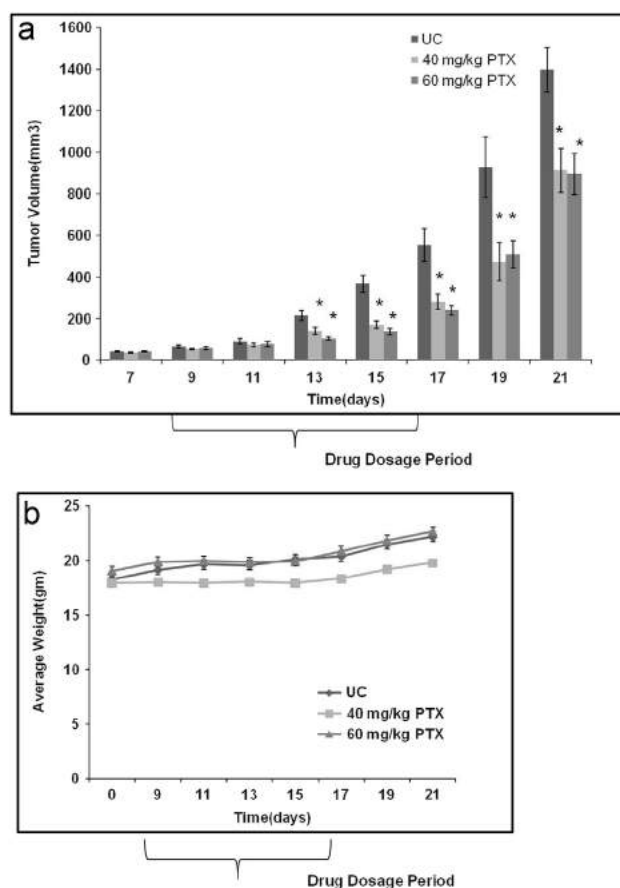


Fig. 7. PTX shows a tumor growth delay in Xenograft model: MDA-MB-231 cells were implanted into the right flanks of 6–8 week old female NOD-SCID mice. PTX treatment (40 mg/kg and 60 mg/kg) was given intraperitoneally when tumors attained a minimum tumor volume of 50 mm³, i.e. from day 9th to day 17th (a). Tumor growth delay is observed upon PTX treatment (b). No significant weight loss was observed during the course of PTX treatment. Values are representative of mean \pm S.E.M. * $P < 0.05$.

pharmacological values such as less toxicity and high water solubility that scores it to be a suitable candidate for bio therapeutics.

The present study shows a down regulation of activated FAK levels. We also found out that increased levels of activated FAK upon Fibronectin stimulation were sensitive to PTX treatment. FAK regulates the processes of cellular proliferation via the MAPK as well as Akt pathways (Mitra and Schlaepfer, 2006; Jones et al., 2009). In our present study we found out a dose dependent effect of FAKi on activated form of MAPK and Akt levels. It also impedes the cellular migration using wound scratch assay. These results further confirm that FAK is a key regulator of tumorigenesis and thus targeting FAK holds a key promise for therapeutic intervention. Earlier studies have shown that PTX inhibited ERK or MAPK pathway in human ovarian cancer cells (Hernandez-Flores et al., 2011). Further, it has also shown to inhibit Akt activation and its translocation in smooth muscle cells and mesangial cells respectively (Chiou et al., 2006; Lin et al., 2003). FAK inhibition is associated with decrease in Akt levels where it is a critical downstream intercessor of FAK survival signaling that protects the cells from apoptosis. A dose dependent decrease was observed in the levels of both activated forms of ERK1/2 and Akt. Further, ERK2 has been shown to regulate levels of VEGF, a potent activator of angiogenesis (Mitra et al., 2006). PTX had been earlier shown to inhibit VEGF release in human MCF-7 and A549 cancer cells (Amirkhosravi et al., 1998). We observed a similar decrease in

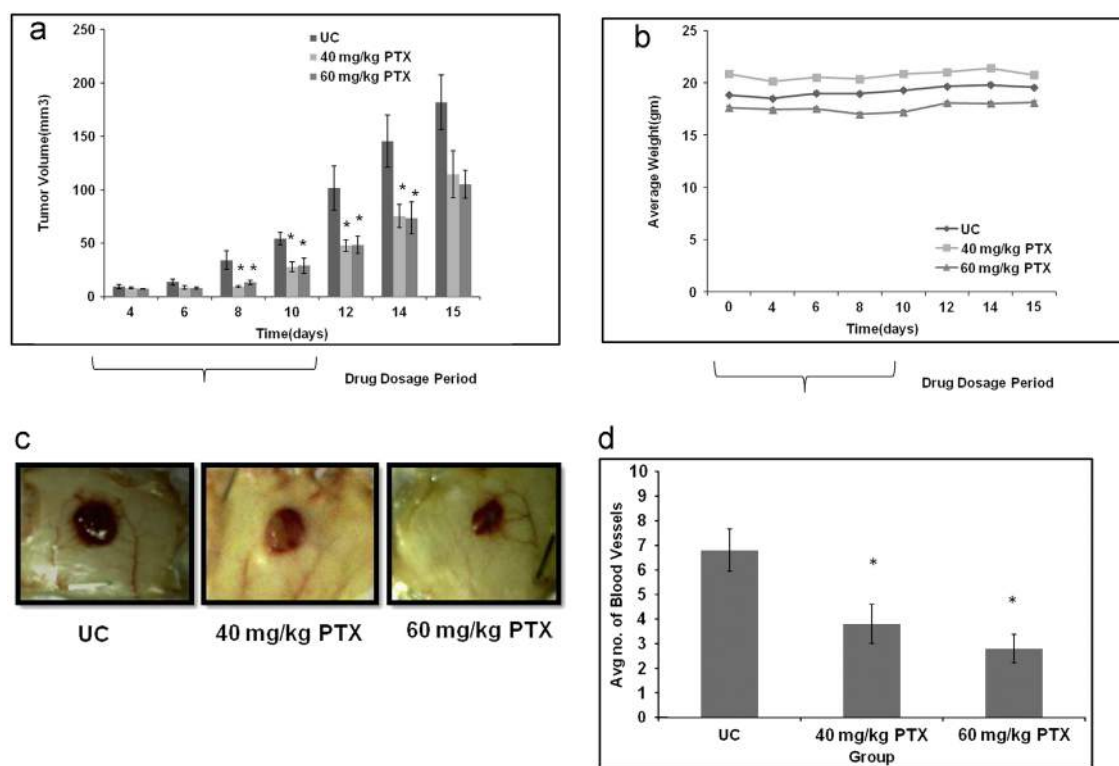


Fig. 8. PTX affects blood vessel formation in intradermal model of angiogenesis: MDA-MB-231 cells were implanted intradermally into 6–8 week old female NOD-SCID mice respectively. After palpable tumors were visible, PTX was given intraperitoneally at doses of 40 mg/kg and 60 mg/kg, i.e. from day 4th to day 12th (a). Tumor burden decreased during the course of PTX treatment (b). Changes in body weight were insignificant upon PTX treatment (c) and (d). Skin bearing the tumors was later excised and photographed. Blood vessels around tumors were then counted and plotted. Values are representative of mean \pm S.E.M. * $P < 0.05$.

cellular levels of VEGF, suggestive of its anti-angiogenic action as well. This result was further affirmed by our *in vivo* findings where PTX at 40 mg/kg and 60 mg/kg inhibited blood vessel and tumor formation.

PTX induced a G1/S cell cycle blockage in our earlier observations. Both cyclin D1 as well as Cdk4/6 are required to crisscross this cell cycle phase. PTX has been associated to lower cyclin D1 levels in mesangial cells that may abolish Cdk4 activity (Lin et al., 2003). However, PTX inhibited both CyclinD1/Cdk6 in our model system without affecting Cdk4 levels. Apart from cell cycle blockage we had observed increase in apoptosis as well. This result was further confirmed using AnnexinV/FITC staining that showed higher number of apoptotic cells (both early and late) compared to the controls. Akt regulates the activity of caspase-9 by phosphorylating it, preventing its activation and upregulates the Bcl-2 expression via c-AMP Response Element Binding Protein (Manning and Cantley, 2007; Pugazhenthii et al., 2000). We found a dose dependent increase in levels as well as activities of cleaved caspase-9 and its downstream effector caspase, i.e. cleaved caspase-3 levels. A dose dependent increase in protein levels of cleaved PARP was also observed. Caspase-3 is an executioner caspase since it is responsible for the proteolytic cleavage of many key proteins such as the PARP (Fernandes-Alnemri et al., 1994). Further, decrease in both Bcl-2 and Bcl-xL levels was ascertained. However, decrease in Bcl-xL was less pronounced than Bcl-2 levels while no changes in Mcl-1 levels were observed. These observations clearly indicated that PTX might be able to modulate the FAK/Akt axis to induce apoptosis in MDA-MB-231 cells. Both NF-(κ)B and p53 are reported to be the potential activator and repressor of FAK promoter respectively suggesting that abnormal expression in either could play a role in regulating FAK expression in breast cancer (Golubovskaya et al., 2004). However, to our surprise DNA binding study for NF-(κ)B activity showed a slight change at 5 mM that was rather insignificant

indicative of the fact that PTX does not affect the activity of NF-(κ)B in our model system. These findings are in accordance to the earlier findings that suggest PTX does not alter NF-(κ)B levels (Rishi et al., 2009; Shamsara et al., 2012). Further, no change in p53 expression was observed. Thus, it can be hypothesized that PTX might affect FAK independently of NF-(κ)B activation and there might be a different mechanism that may govern for this action of PTX in lowering the levels of activated FAK.

PTX has shown to hamper the migration of MD-MB-231 cells and affect the cellular morphology in a dose-dependent manner (Goel and Gude, 2011). A distinct family of small GTPases such as RhoGTPases functions by alternating between an active, GTP bound and an inactive, GDP bound states (van Rijssel and van Buul, 2012). These members are involved in diverse processes such as migration, cytoskeletal reorganization and metastasis (Guilluy et al., 2011). PTX has shown to inhibit migration in B16F10 melanoma by the modulation of RhoGTPase activity (Dua and Gude, 2008). We observed a significant decrease in the active levels of both Rac, Rho GTPases at 2.5 mM and 5 mM that clearly confirms our earlier findings. Further, cell morphology upon PTX treatment using Haematoxylin-Eosin (HE) staining (see Supplement Fig. 1) showed that cells appear to be more elongated upon PTX treatment. We postulated that this effect might be due to certain cytoskeletal disruption responsible for maintaining the cellular integrity. PTX has shown to act as an actin depolymerizing agent in B16F10 cells (Dua and Gude, 2008). Based on this fact we had performed actin staining using Phalloidin labeled with fluorochrome FITC. The cells showed similar morphological changes as observed with HE staining. Further, there was a loss of filopodia and lamellopodia upon PTX treatment which further validate our earlier findings. These results clearly document that PTX affected cellular motility and cytoskeletal organization via inhibition of RhoGTPases.

Preclinical evaluation of any chemotherapeutic agent forms an integral aspect in therapeutic scenario. *In vivo* studies were done to test the efficacy of PTX using NOD-SCID mice. The doses were calculated based on body surface area (Reagan-Shaw et al., 2008). There was a significant tumor growth delay upon PTX treatment indicative of a stronger evidence for clinical potential. However, no significant difference in tumor volume was observed between the two groups of PTX 40 mg/kg and 60 mg/kg *per se*. Intradermal model for evaluating anti-angiogenic activity showed a promising role for PTX as well. Dose dependent decrease in blood vessel as well as tumor development was observed. Further, there was no significant weight loss noticeable during the course of the treatment.

Drug repositioning is an active area in research that offers several advantages such as known pharmacokinetics of existing drugs, safety profiles and lower assessment costs (DiMasi et al., 2003). In view of these facts PTX do promise to be one of the liable candidates for the treatment of breast cancer along with other anti-cancer agents being currently used in the treatment of this deadly disease.

In conclusion, our results indicate that PTX effectively modulates the FAK/ERK/Akt and RhoGTPase signaling pathways that may be responsible for the inhibitory effect of PTX in MDA-MB-231 breast cancer cells. These observations of our *in vitro* results together with the *in vivo* findings show that PTX does qualify as an effective anti-metastatic agent. The key findings discoursed in the present research work provide a leading edge to investigate its effect in other model systems as well, so to ascertain its utilization in the proper management and treatment of metastasis of other cancers as well.

Conflict of interest statement

None declared.

Acknowledgments

We acknowledge grant support from ACTREC, Tata Memorial Center. Mr. Peeyush N. Goel is supported by CSIR-Senior Research Fellowship. The authors would also like to thank Manohar Parker for providing technical assistance, Animal House, confocal and flow cytometry facilities. The authors would also like to give special thanks to Darshana Jain and Ankit Kumar Jain for their valuable suggestions.

Appendix A. Supporting information

Supplementary data associated with this article can be found in the online version at <http://dx.doi.org/10.1016/j.ejphar.2013.07.004>.

References

- Amirkhosravi, A., Meyer, T., Warnes, G., Amaya, M., Malik, Z., Biggerstaff, J.P., Siddiqui, F.A., Sherman, P., Francis, J.L., 1998. Pentoxifylline inhibits hypoxia-induced upregulation of tumor cell tissue factor and vascular endothelial growth factor. *Thromb. Haemost.* 80, 598–602.
- Chiou, Y.L., Shieh, J.J., Lin, C.Y., 2006. Blocking of Akt/NF-kappaB signaling by pentoxifylline inhibits platelet-derived growth factor-stimulated proliferation in brown Norway rat airway smooth muscle cells. *Pediatr. Res.* 60, 657–662.
- D'Hellencourt, C.L., Diaw, L., Cornillet, P., Guenounou, M., 1996. Differential regulation of TNF alpha, IL-1 beta, IL-6, IL-8, TNF beta, and IL-10 by pentoxifylline. *Int. J. Immunopharmacol.* 18, 739–748.
- De Sanctis, M.T., Cesarone, M.R., Belcaro, G., Nicolaidis, A.N., Griffin, M., Incandela, L., Bucci, M., Geroulakos, G., Ramaswami, G., Vasdekis, S., Agus, G., Bavera, P., Ippolito, E., 2002. Treatment of intermittent claudication with pentoxifylline: a 12-month, randomized trial—walking distance and microcirculation. *Angiology* 53 (Suppl. 1), S7–S12.
- Detelbach, H.R., Aviado, D.M., 1985. Clinical pharmacology of pentoxifylline with special reference to its hemorrheologic effect for the treatment of intermittent claudication. *J. Clin. Pharmacol.* 25, 8–26.
- DiMasi, J.A., Hansen, R.W., Grabowski, H.G., 2003. The price of innovation: new estimates of drug development costs. *J. Health Econ.* 22, 151–185.
- Dua, P., Gude, R.P., 2006. Antiproliferative and antiproteolytic activity of pentoxifylline in cultures of B16F10 melanoma cells. *Cancer Chemother. Pharmacol.* 58, 195–202.
- Dua, P., Gude, R.P., 2008. Pentoxifylline impedes migration in B16F10 melanoma by modulating Rho GTPase activity and actin organization. *Eur. J. Cancer* 44, 1587–1595.
- Dua, P., Ingle, A., Gude, R.P., 2007. Suramin augments the antitumor and antimetastatic activity of pentoxifylline in B16F10 melanoma. *Int. J. Cancer* 121, 1600–1608.
- Fabia, R., Travis, D.L., Levy, M.F., Husberg, B.S., Goldstein, R.M., Klintmalm, G.B., 1997. Effect of pentoxifylline on hepatic ischemia and reperfusion injury. *Surgery* 121, 520–525.
- Ferlay, J., Shin, H.R., Bray, F., Forman, D., Mathers, C., Parkin, D.M., 2010. Estimates of worldwide burden of cancer in 2008: GLOBOCAN 2008. *Int. J. Cancer* 127, 2893–2917.
- Fernandes-Alnemri, T., Litwack, G., Alnemri, E.S., 1994. CPP32, a novel human apoptotic protein with homology to *Caenorhabditis elegans* cell death protein Ced-3 and mammalian interleukin-1 beta-converting enzyme. *J. Biol. Chem.* 269, 30761–30764.
- Goel, P.N., Gude, R.P., 2011. Unravelling the antimetastatic potential of pentoxifylline, a methylxanthine derivative in human MDA-MB-231 breast cancer cells. *Mol. Cell Biochem.* 358, 141–151.
- Golubovskaya, V., Kaur, A., Cance, W., 2004. Cloning and characterization of the promoter region of human focal adhesion kinase gene: character of nuclear kappa B and p53 binding sites. *Biochim. Biophys. Acta* 1678, 111–125.
- Guilluy, C., Garcia-Mata, R., Burrige, K., 2011. Rho protein crosstalk: another social network? *Trends Cell Biol.* 21, 718–726.
- Harris, E., Schulzke, S.M., Patole, S.K., 2010. Pentoxifylline in preterm neonates: a systematic review. *Paediatr. Drugs* 12, 301–311.
- Hennessy, B.T., Smith, D.L., Ram, P.T., Lu, Y., Mills, G.B., 2005. Exploiting the PI3K/AKT pathway for cancer drug discovery. *Nat. Rev. Drug Discov.* 4, 988–1004.
- Hernandez-Flores, G., Ortiz-Lazareno, P.C., Lerma-Diaz, J.M., Dominguez-Rodriguez, J.R., Jave-Suarez, L.F., Aguilar-Lemarroy Adel, C., de Celis-Carrillo, R., del Toro-Arreola, S., Castellanos-Esparza, Y.C., Bravo-Cuellar, A., 2011. Pentoxifylline sensitizes human cervical tumor cells to cisplatin-induced apoptosis by suppressing NF-kappa B and decreased cell senescence. *BMC Cancer* 11, 483.
- Hirsh, L., Dantes, A., Suh, B.S., Yoshida, Y., Hosokawa, K., Tajima, K., Kotsuji, F., Merimsky, O., Amsterdam, A., 2004. Phosphodiesterase inhibitors as anti-cancer drugs. *Biochem. Pharmacol.* 68, 981–988.
- Jones, M.L., Shawe-Taylor, A.J., Williams, C.M., Poole, A.W., 2009. Characterization of a novel focal adhesion kinase inhibitor in human platelets. *Biochem. Biophys. Res. Commun.* 389, 198–203.
- Lin, S.L., Chen, R.H., Chen, Y.M., Chiang, W.C., Tsai, T.J., Hsieh, B.S., 2003. Pentoxifylline inhibits platelet-derived growth factor-stimulated cyclin D1 expression in mesangial cells by blocking Akt membrane translocation. *Mol. Pharmacol.* 64, 811–822.
- Luo, M., Guan, J.L., 2010. Focal adhesion kinase: a prominent determinant in breast cancer initiation, progression and metastasis. *Cancer Lett.* 289, 127–139.
- Manning, B.D., Cantley, L.C., 2007. AKT/PKB signaling: navigating downstream. *Cell* 129, 1261–1274.
- McLean, G.W., Carragher, N.O., Avizienyte, E., Evans, J., Brunton, V.G., Frame, M.C., 2005. The role of focal-adhesion kinase in cancer—a new therapeutic opportunity. *Nat. Rev. Cancer* 5, 505–515.
- Mitra, S.K., Hanson, D.A., Schlaepfer, D.D., 2005. Focal adhesion kinase: in command and control of cell motility. *Nat. Rev. Mol. Cell Biol.* 6, 56–68.
- Mitra, S.K., Mikolon, D., Molina, J.E., Hsia, D.A., Hanson, D.A., Chi, A., Lim, S.T., Bernard-Trifilo, J.A., Ilic, D., Stupack, D.G., Cheresch, D.A., Schlaepfer, D.D., 2006. Intrinsic FAK activity and Y925 phosphorylation facilitate an angiogenic switch in tumors. *Oncogene* 25, 5969–5984.
- Mitra, S.K., Schlaepfer, D.D., 2006. Integrin-regulated FAK-Src signaling in normal and cancer cells. *Curr. Opin. Cell Biol.* 18, 516–523.
- Mullard, A., 2011. Could pharma open its drug freezers? *Nat. Rev. Drug Discov.* 10, 399–400.
- Munoz, R., Man, S., Shaked, Y., Lee, C.R., Wong, J., Francia, G., Kerbel, R.S., 2006. Highly efficacious nontoxic preclinical treatment for advanced metastatic breast cancer using combination oral UFT-cyclophosphamide metronomic chemotherapy. *Cancer Res.* 66, 3386–3391.
- Naumov, G.N., Bender, E., Zurakowski, D., Kang, S.Y., Sampson, D., Flynn, E., Watnick, R.S., Straume, O., Akslen, L.A., Folkman, J., Almog, N., 2006. A model of human tumor dormancy: an angiogenic switch from the nonangiogenic phenotype. *J. Natl. Cancer Inst.* 98, 316–325.
- Oakman, C., Tenori, L., Biganzoli, L., Santarpia, L., Cappadona, S., Luchinat, C., Di Leo, A., 2011. Uncovering the metabolomic fingerprint of breast cancer. *Int. J. Biochem. Cell Biol.* 43, 1010–1020.
- Parsons, J.T., Martin, K.H., Slack, J.K., Taylor, J.M., Weed, S.A., 2000. Focal adhesion kinase: a regulator of focal adhesion dynamics and cell movement. *Oncogene* 19, 5606–5613.
- Pugazhenthis, S., Nesterova, A., Sable, C., Heidenreich, K.A., Boxer, L.M., Heasley, L.E., Reusch, J.E., 2000. Akt/protein kinase B up-regulates Bcl-2 expression through cAMP response element-binding protein. *J. Biol. Chem.* 275, 10761–10766.

- Reagan-Shaw, S., Nihal, M., Ahmad, N., 2008. Dose translation from animal to human studies revisited. *FASEB J.* 22, 659–661.
- Rishi, L., Gahlot, S., Kathania, M., Majumdar, S., 2009. Pentoxifylline induces apoptosis *in vitro* in cutaneous T cell lymphoma (HuT-78) and enhances FasL mediated killing by upregulating Fas expression. *Biochem. Pharmacol.* 77, 30–45.
- Salot, S., Gude, R., 2012. MTA1-mediated transcriptional repression of SMAD7 in breast cancer cell lines. *Eur. J. Cancer.*
- Shamsara, J., Behravan, J., Falsoleiman, H., Mohammadpour, A.H., Ramezani, M., 2012. The effects of pentoxifylline administration on NF κ B P50 transcription factor expression. *ARYA Atheroscler.* 7, 133–137.
- Teicher, B.A., 2006. Tumor models for efficacy determination. *Mol. Cancer Ther.* 5, 2435–2443.
- van Rijssel, J., van Buul, J.D., 2012. The many faces of the guanine-nucleotide exchange factor trio. *Cell Adh. Migr.* 6.
- Zhang, M., Xu, Y.J., Mengi, S.A., Arneja, A.S., Dhalla, N.S., 2004. Therapeutic potentials of pentoxifylline for treatment of cardiovascular diseases. *Exp. Clin. Cardiol.* 9, 103–111.
- Zhao, J., Guan, J.L., 2009. Signal transduction by focal adhesion kinase in cancer. *Cancer Metastasis Rev.* 28, 35–49.



Available online at
ScienceDirect
 www.sciencedirect.com

Elsevier Masson France
EM|consulte
 www.em-consulte.com



Original article

Pentoxifylline regulates the cellular adhesion and its allied receptors to extracellular matrix components in breast cancer cells



Peeyush N. Goel, Rajiv P. Gude*

Gude Lab, Advanced Centre for Treatment, Research & Education in Cancer (ACTREC), Tata Memorial Centre, Kharghar, Navi Mumbai, Maharashtra 410210, India

ARTICLE INFO

Article history:

Received 24 August 2013

Accepted 24 September 2013

Keywords:

Pentoxifylline
 Extracellular Matrix (ECM)
 Integrins
 MDA-MB-231 cells
 Experimental metastasis

ABSTRACT

Pentoxifylline (PTX) is a methylxanthine derivative that improves blood flow by decreasing its viscosity. Being an inhibitor of platelet aggregation, it can thus reduce the adhesiveness of cancer cells prolonging their circulation time. This delay in forming secondary tumours makes them more prone to immunological surveillance. Recently, we have evaluated its anti-metastatic efficacy against breast cancer, using MDA-MB-231 model system. In view of this, we had ascertained the effect of PTX on adhesion of MDA-MB-231 cells to extracellular matrix components (ECM) and its allied receptors such as the integrins. PTX affected adhesion of breast cancer cells to matrigel, collagen type IV, fibronectin and laminin in a dose dependent manner. Further, PTX showed a differential effect on integrin expression profile. The experimental metastasis model using NOD-SCID mice showed lesser tumour island formation when treated with PTX compared to the control. These findings further substantiate the anti-adhesive potential of PTX in breast cancer and warrant further insights into the functional regulation.

© 2013 Elsevier Masson SAS. All rights reserved.

1. Introduction

“The nontoxic curative compound remains undiscovered but not undreamt”.

James F. Holland

Cancer is a major health concern in the global scenario, accounting for the second most leading cause of deaths among all ages and sexes [1]. The majority of cancer related deaths are due to the dissemination of tumour cells from the primary to distant target sites, a process referred to as metastasis. It is indeed a very complex phenomenon and thus targeting metastasis holds a great promise for anticancer therapy. During the process of metastasis, tumour cells need to invade their surroundings and surpass these barriers. The ability to alter cellular migration and adhesion to the extracellular matrix (ECM) components helps the tumour cells to bypass these obstructions, paving a passage into circulation for distant localisation. Cellular adhesion is an important biological phenomenon required for the functioning of living organisms. The cells transmit signals from their environment via different surface

receptors that act as the relaying switches. One of the crucial members among this family are the integrins that mediate both cell–cell as well as cell to ECM interactions. A typical integrin is a heterodimer made up of α and β subunits linked non-covalently. A total of 18 α and 8 β subunits have been identified till date that forms a total of 24 $\alpha\beta$ distinct combinations [2]. The normal functioning of an organism requires the regulated coordination between the cells as well as their extracellular milieu. These interactions play a very important role in diverse aspects of cellular behaviour such as cellular adhesion, proliferation, apoptosis and angiogenesis.

Binding of ECM molecules/ligands to the integrins leads to clustering and subsequently promotes the localised aggregation of signalling moieties culminating in downstream intracellular signalling. Conversely, cytoplasmic signals modulates the integrin functioning and thus regulate cellular dynamics. Hence, integrins orchestrate both outside–inside and inside–outside signalling events. Extracellular ligation of integrins triggers a large variety of signal transduction events such as proliferation, invasion, migration, survival or apoptosis angiogenesis, immunity and homeostasis [3–6].

Numerous studies have documented marked differences in surface expression and distribution of integrins in malignant breast tumours compared with pre-neoplastic tumours of the same type. Integrins such as αv , $\alpha 3$, $\alpha 5$, $\beta 1$, and $\alpha v\beta 3$ are being involved in the process of cancer progression [7]. A large number of reports are suggestive of the correlation between integrin expression and breast cancer metastasis. Integrin $\alpha 3\beta 1$ is

* Corresponding author. Tel.: +91 022 274 05084; fax: +91 022 274 05083.

E-mail addresses: peeyushgoel29@gmail.com (P.N. Goel), rajivgude@yahoo.in, rgude@actrec.gov.in (R.P. Gude).

associated with the process of tumourigenesis and invasion [8] while $\alpha v\beta 3$, $\alpha v\beta 5$, $\alpha 5\beta 1$ are associated with breast cancer progression [3]. Expression of $\alpha 5\beta 1$ is highly up regulated in drug resistant breast carcinoma cells and associated with the ability to regulate invasion via MMP-2 [9]. Moreover, $\alpha v\beta 3$ is associated with Mitogen Activated Protein Kinase (MAPK) signalling affecting proliferation [10] while $\beta 1$ is an indicator for survival in breast cancer [11]. However, $\alpha 2\beta 1$ has been shown to play a key role of metastasis suppressor in a spontaneous model of breast carcinoma [12].

Pentoxifylline (1-[5-oxohexyl]-3,7-dimethyl-xanthine), oxpentifylline, PTX) is a methylxanthine derivative that elevates c-AMP by inhibiting the phosphodiesterase activity. It is being used clinically for the treatment of intermittent claudication and peripheral vascular diseases [13]. PTX has been shown to inhibit the integrin-mediated adherence of IL-2 activated human peripheral blood lymphocytes to human endothelial cells, matrix components and tumour cells [14]. It also inhibited the integrin-mediated adhesion and activation of human T lymphocytes [15]. Further, we have earlier shown in our laboratory that PTX modulates integrin expression in B16F10 mouse melanoma cells [16]. Based on these observations, we propose to investigate the effect of PTX on the adhesion of human breast MDA-MB-231 cells to ECM components as well as its allied receptors, integrins. Further, we have also demonstrated the effect of PTX *in vivo* using experimental metastasis model. These studies surely scores PTX to be a promising agent for targeting metastasis in breast cancer.

2. Material and methods

2.1. Reagents and antibodies

Pentoxifylline, matrigel, collagen type IV, fibronectin, laminin, vitronectin, MTT, beta-tubulin, bovine serum albumin (BSA) and paraformaldehyde were purchased from Sigma-Aldrich (India). Antibodies against integrins such as αv , $\alpha 2$, $\alpha 3$, $\alpha 5$, $\beta 1$, $\beta 3$ and $\beta 5$ were purchased from Santa Cruz (CA, USA). Fluorescein isothiocyanate (FITC) labeled secondary antibodies were acquired from Invitrogen (India). All the other chemicals/reagents used were either of analytical grade or highest purity that were commercially available.

2.2. Cell culture

MDA-MB-231 and MCF-7 human breast cancer cell lines were purchased from NCCS (Pune, India). The cells were maintained in 10% Dulbecco's Modified Eagle Medium (DMEM, GIBCO) supplemented with 10% heat inactivated foetal bovine serum (FBS, GIBCO). Primocin was added at a concentration of 100 $\mu\text{g}/\text{mL}$. The cells were maintained at 37 °C in 5% CO₂ humidified atmosphere as described earlier [17].

2.3. Adhesion assay

Adhesion of breast cancer cells to different to ECM components was proceeded as per the protocol described earlier [17,18]. Briefly, 96 well plates were pre-coated with matrigel (10 $\mu\text{g}/\text{mL}$), collagen type IV (10 $\mu\text{g}/\text{mL}$), fibronectin (2.5 $\mu\text{g}/\text{mL}$), laminin (5 $\mu\text{g}/\text{mL}$) and vitronectin (2.5 $\mu\text{g}/\text{mL}$). The plates were then kept at 4 °C for polymerisation overnight. Subsequently, the plates were washed with PBS and then treated with 1% BSA. MDA-MB-231 cells treated with sub-toxic doses of PTX (0 mM, 1 mM, 2.5 mM and 5 mM) were then harvested using saline EDTA. Cells were then seeded at a density of 3×10^4 per well suspended in 0.1% BSA containing plain DMEM. A percentage relative adhesion was then calculated for PTX treated cells at different time points viz. 15, 30, 45, 60 and 90 min.

Differences in adhesion to ECM components was also compared between MDA-MB-231 and MCF-7 cells using the above mentioned substrates at different time points viz. 15, 30, 45, 60 and 90 min respectively.

2.4. Flow cytometry

Surface expression of integrins viz. αv , $\alpha 2$, $\alpha 3$, $\alpha 5$, $\beta 1$, $\beta 3$ and $\beta 5$ was compared between MDA-MB-231 as well as MCF-7 cell lines. The effect of PTX at sub-toxic doses was then evaluated on MDA-MB-231 cells. Briefly, cells were harvested using saline EDTA and then fixed using 4% paraformaldehyde. Approximately 1×10^6 cells were treated with 1 μg of the respective integrin (αv , $\alpha 2$, $\alpha 3$, $\alpha 5$, $\beta 1$, $\beta 3$ and $\beta 5$) antibody. Cells were mixed thoroughly and kept at 4 °C for an hour. Subsequently, cells were washed using fluorescence activated cell sorting (FACS) buffer twice and then incubated with FITC labelled secondary antibody for 1 h at 4 °C. Cells were washed twice using FACS buffer and then finally suspended in it. Acquisition was done on FACS Calibur and the results were analysed using Cell Quest software as done earlier [19].

2.5. Western blotting

Western blotting was carried out as per the procedure followed earlier [20]. Cells treated with sub-toxic doses of PTX were harvested using saline EDTA and then lysed using modified Radio-Immuno Precipitation Assay (RIPA) buffer. Fifty micrograms protein were then loaded on an 8% SDS-PAGE gel and then run at constant current of 25 mA. After, the electrophoresis the protein was electro-blotted onto PVDF membranes overnight at a constant voltage of 20 V. Membranes were later blocked using 5% BSA for 1 h. Subsequently, the membranes were incubated with primary (αv , $\alpha 2$, $\alpha 3$, $\alpha 5$, $\beta 1$, $\beta 3$ and $\beta 5$) and secondary (HRP labelled) antibodies for 1 h each. Washings were done using Tris-Buffered Saline-Tween 20 (TBST) after an each successive step. β -tubulin was used as a loading control. The membranes were finally processed for signal detection using Pierce Femto Chemiluminescence system.

2.6. In vivo experimental metastasis

The animal experiments were performed after the approval from the ethical clearance committee at ACTREC. Briefly, 1×10^6 cells were injected intravenously (IV) into the tail vein of 6–8 weeks old female NOD-SCID mouse. Three groups ($n = 5$) were being formed:

- PBS only;
- PTX 40 mg/kg;
- PTX 60 mg/kg.

PTX was injected intraperitoneally (i.p) from day 1 to day 9 continuously. Animals were sacrificed when found to be moribund. The lungs were being excised and then fixed in buffered formalin solution. The tissues were then sectioned and stained using Haemotoxylin-Eosin as done earlier [18]. Images were then captured using an upright microscope from Zeiss (Germany) at 10 × magnification.

2.7. Chick Chorioallontic Membrane (CAM) assay

Fertilized eggs from White Leghorn hen were placed in an incubator at 37 °C under approximately 70% humid conditions. The eggs were then kept at 37 °C for 5 days prior to PTX treatment. PTX (400 μg) was added through a small window made using a sterile scalpel. The eggs were then resealed using parafilm and incubated

further at 37 °C. The experiment was terminated on the subsequent day and photographs were taken after cut opening of the eggs.

2.8. Statistical analysis

All the experiments were performed at least thrice independently. Results are represented as mean \pm SEM respectively. One way ANOVA (equal variances assumed) was used for statistical significance and results where $P < 0.05$ were considered statistically significant.

3. Results and discussion

3.1. MDA-MB-231 display higher adhesion potential than MCF-7 using ECM substrates

Cells inside the body are firmly glued to supporting matrix i.e. the ECM. This ECM not only provides structural support but also provides a means of regulating cellular behaviour [21]. It has been well documented that metastatic cancer cells showed a differential adhesive behaviour to tumour microenvironment [22]. Based on this observation, we have carried out the experiments to understand the differences in adhesion between the two breast cancer cell lines viz. MDA-MB-231 and MCF-7. The latter is a non-metastatic cell line compared to MDA-MB-231 that is highly

invasive and exhibits a high metastatic potential [23]. MDA-MB-231 cells displayed a significant and high adhesive potential to the ECM components at different time points 15, 30, 45, 60 and 90 min respectively as shown in Fig. 1A–E. Percentage relative adhesion for MCF-7 was 25.97 ± 6.30 , 11.2 ± 4.71 , 29.12 ± 3.84 , 23.15 ± 1.40 , 55.21 ± 5.95 as compared to 80.08 ± 2.1 , 69.82 ± 3.86 , 90.91 ± 0.58 , 45.63 ± 2.99 , 71.4 ± 2.48 for MDA-MB-231 against matrigel, collagen type IV, fibronectin, laminin and vitronectin respectively at 60 min ($P < 0.05$). This observation supports the fact that metastatic cells do show a differential affinity towards their microenvironment.

3.2. PTX affects adhesion to ECM substrates in MDA-MB-231 cells

Based on the ability of higher adhesion of MDA-MB-231 cells prompted us to evaluate the effects of PTX at sub-toxic doses on the ECM substrates as well. We have earlier shown that PTX affects adhesion to both matrigel and collagen type IV in a dose dependent manner [17]. Further, it has been well reported that ECM governs the life cycle and expression of integrins [24,25]. In the present study, we had demonstrated its anti-adhesive potential to ECM substrates such as fibronectin, laminin and vitronectin respectively. A dose-dependent decrease in percentage relative adhesion was being observed against both fibronectin and laminin represented in Fig. 2A and B. However, sub-toxic doses of PTX had no significant effect on adhesion to vitronectin as can be seen in Fig. 2C. Percentage relative adhesion was found out to be

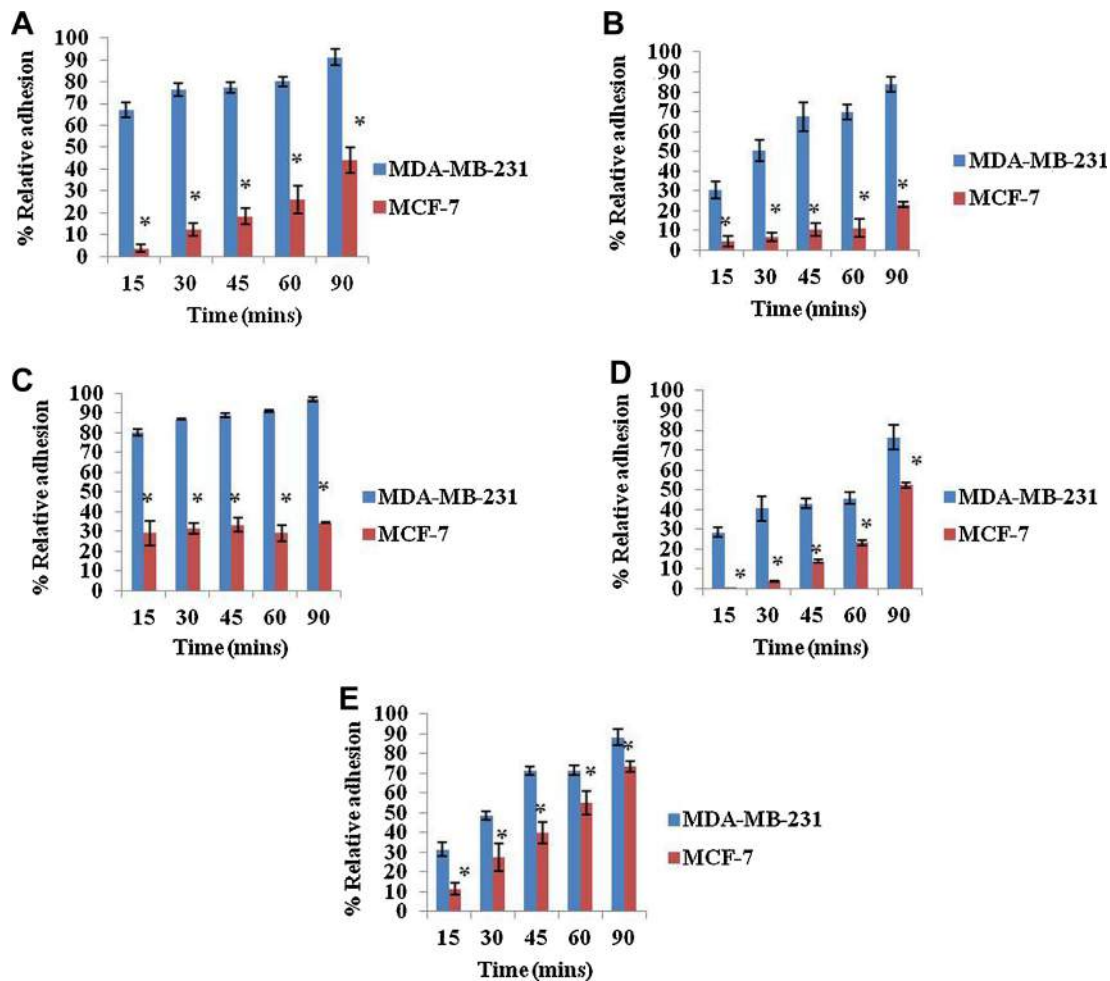


Fig. 1. MDA-MB-231 cells exhibit higher adhesive potential to ECM components than MCF-7 cells. Adhesive potential was compared between MDA-MB-231 and MCF-7 cells towards ECM components at different time points (15, 30, 45, 60 and 90 min). MDA-MB-231 cells showed higher adhesion to (A) matrigel, (B) collagen type IV, (C) fibronectin, (D) laminin, (E) vitronectin compared to lower metastatic MCF-7 cells. Values are representative of three independent experiments (mean \pm SEM). * $P < 0.05$.

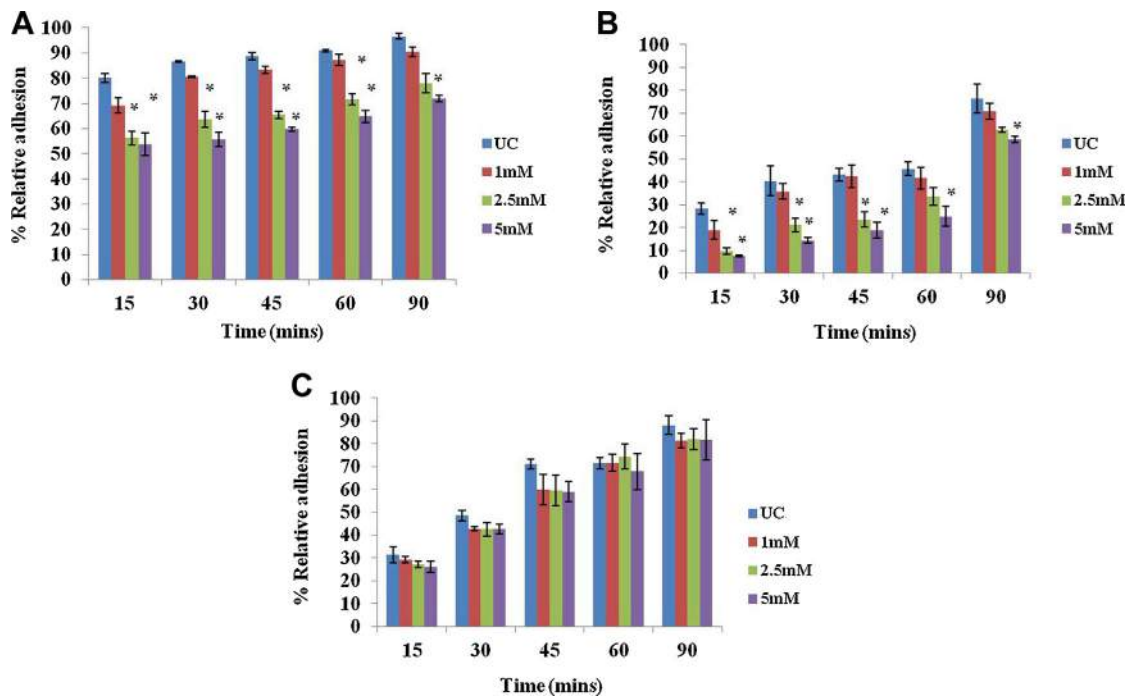


Fig. 2. PTX affects adhesion of MDA-MB-231 to fibronectin and laminin in a dose dependent manner. Adhesion assays were performed to evaluate the effect of sub-toxic doses of PTX (0 mM, 1 mM, 2.5 mM and 5 mM) on MDA-MB-231 cells using ECM substrates at different time points viz. 15, 30, 45, 60, 90 min. PTX affected the adhesion to both (A) fibronectin and (B) laminin in a dose dependent manner, while no change was observed in case of (C) vitronectin. Values are representative of three independent experiments (mean \pm SEM). * $P < 0.05$.

80.16 \pm 1.74, 69.11 \pm 3.03, 56.13 \pm 2.77, 53.78 \pm 4.57 for fibronectin and 28.43 \pm 2.47, 18.90 \pm 4.11, 9.81 \pm 1.40, 7.44 \pm 0.31 against laminin at PTX doses of 0 mM, 1 mM, 2.5 mM, 5 mM respectively ($P < 0.05$). These results clearly envisage the need to appraise the effect of PTX on integrin receptors that might play a crucial role in regulating the adhesion potential of MDA-MB-231 cells.

3.3. MDA-MB-231 exhibits differences in surface expression of integrins compared to MCF-7

Both breast cell lines were being tested for differences in surface expression of integrins using flow cytometry. MDA-MB-231 cells exhibited significantly higher levels of integrins such as α v, α 3, α 5, β 1, β 3 and β 5 (Fig. 3A, C–G) compared to MCF-7.

However, there was no marked difference observed in the surface expression of integrin α 2 between the two cell lines as shown in Fig. 3B. These observations are consistent with the earlier report [26]. Hence, these results clearly demonstrate that deviations in surface expression of integrins between the two cell lines might be one of the possible reasons for differential adhesive behaviour.

3.4. PTX demonstrates a differential effect on integrins expression in MDA-MB-231 cells

As per our previous observations regarding differences in integrin expression between two breast cancer cell lines, we have further compared both the surface and total expression status of integrins upon PTX treatment at sub-toxic doses in MDA-MB-231

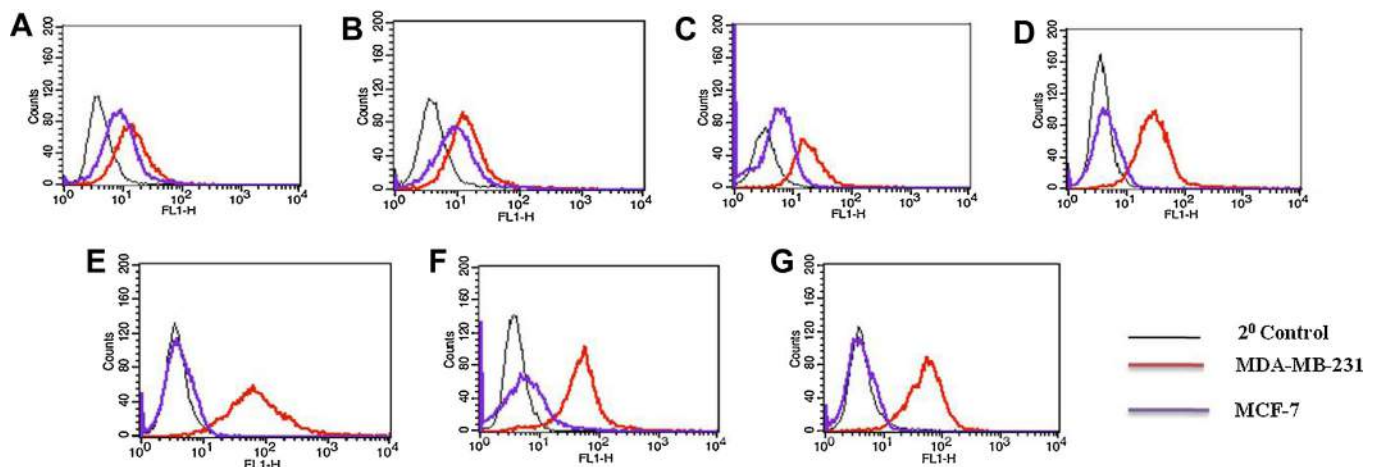


Fig. 3. MDA-MB-231 displayed higher surface expression of integrins compared to MCF-7 cells. Flow cytometry was performed to compare the surface expression of integrins (A) α v, (B) α 2, (C) α 3, (D) α 5, (E) β 1, (F) β 3 and (G) β 5 between MDA-MB-231 and MCF-7 cells respectively. MDA-MB-231 cells expressed higher levels of all the integrins under investigation except α 2.

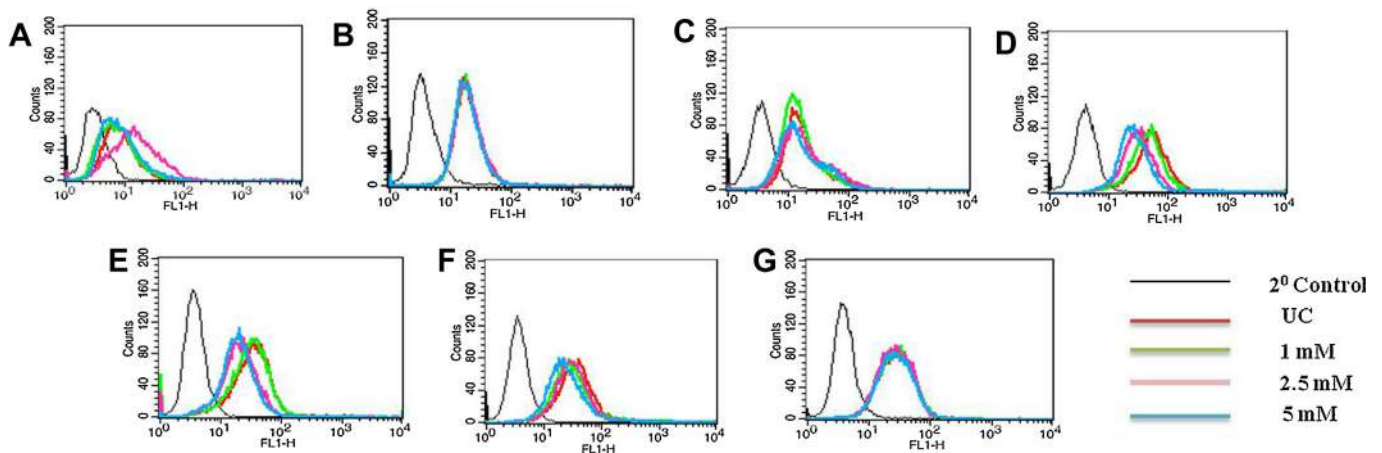


Fig. 4. PTX affects surface expression of integrins $\alpha 5$ and $\beta 1$ using flow cytometry in MDA-MB-231 cells. MDA-MB-231 cells were treated with sub-toxic doses of PTX (0 mM, 1 mM, 2.5 mM and 5 mM) to evaluate its effect on surface expression of integrins (A) αv , (B) $\alpha 2$, (C) $\alpha 3$, (D) $\alpha 5$, (E) $\beta 1$, (F) $\beta 3$ and (G) $\beta 5$. PTX affects surface expression of integrins $\alpha 5$ and $\beta 1$ markedly while no effect was observed for αv , $\alpha 2$, $\alpha 3$, $\beta 3$ and $\beta 5$ subunits respectively.

cells. A differential effect was being observed upon PTX treatment. PTX affected the surface expression of integrins $\alpha 5$ and $\beta 1$ significantly (Fig. 4D and E). The relative mean fluorescence intensity (MFI) was found out to be 90.55 ± 6.81 , 70.49 ± 7.27 , 57.34 ± 1.22 for integrin $\alpha 5$ while 81 ± 11.80 , 64.65 ± 4.74 , 61.23 ± 3.84 for integrin $\beta 1$ at PTX doses of 1 mM, 2.5 mM and 5 mM, considering the MFI for untreated control to be 100% ($P < 0.05$) (Supplementary Fig. S1). A decrease in surface expression was also observed for integrin $\beta 3$ at 5 mM but it was rather insignificant (Fig. 4F). It has been well documented that MDA-MB-231 cells show the highest adhesion potential to fibronectin [27], and this was also confirmed by adhesion assay. Further, PTX decreased the adhesion towards fibronectin in a dose dependent manner. Integrin $\alpha 5\beta 1$ is well-characterised receptor for fibronectin and shown to be highly elevated in breast tumours and is associated with resistance to apoptosis by chemotherapeutic drugs [9,28,29]. A decrease in surface expression of both $\alpha 5$ and $\beta 1$ subunits can be plausible explanation for PTX mediated anti-adhesive effects on fibronectin. This observation is in consistency with the earlier report that loss of fibronectin leads to decrease in expression of $\alpha 5\beta 1$ integrin [30]. The changes in total protein levels were also confirmed by western blotting that further showed a dose-dependent reduction in total levels of both the integrins (Fig. 5). However, for integrins αv , $\alpha 2$, $\alpha 3$, $\beta 3$ and $\beta 5$ there was no change in surface expression observed (Fig. 4A–C, F, G). Although there was a decrease in total protein levels being observed for integrins αv , $\alpha 3$ and $\beta 3$ (Fig. 5), no change in protein levels was seen for integrins $\alpha 2$ and $\beta 5$ (Fig. 5). Integrin $\alpha 2\beta 1$ is known to play a role in metastasis suppression [12] and thus no effect of PTX on surface and total protein levels of $\alpha 2\beta 1$ could thus be well justified. This differential outcome of PTX upon integrin expression might be due to its effect on degradation–synthesis axis for surface receptor modulation or rather integrin transport [16]. Further, in our recent report we have found that PTX modulates the FAK signalling pathway affecting cellular proliferation, migration, survival and angiogenesis [20]. These findings do implicate the anti-metastatic activity of PTX by regulation of cell-ECM adhesion via integrins.

3.5. PTX affects adhesion using *in vivo* experimental metastasis model and angiogenesis in Chick Chorioallontic Membrane assay

Previous reports from our lab have established that PTX pre-treated melanoma cells showed lesser tumour island formation in C57/BL6 mice [16]. In our model system MDA-MB-231 cells were injected intravenously and PTX administration was started at the same day for a period of 9 days. Mice were being sacrificed after a

period of 30 days and the lungs were excised. Numerous tumour islands were being present in the untreated group. These islands were both large and small being present throughout the lung parenchyma (Fig. 6A). However, in the treatment group PTX 40 mg/kg, tumour cells were present at few places while other areas were found to be devoid of tumour cells and were clear. In addition, animals treated with PTX 60 mg/kg group showed presence of metastatic cells and formation of smaller tumour islands (Fig. 6B and C). The quantitative assessment results showed an average of

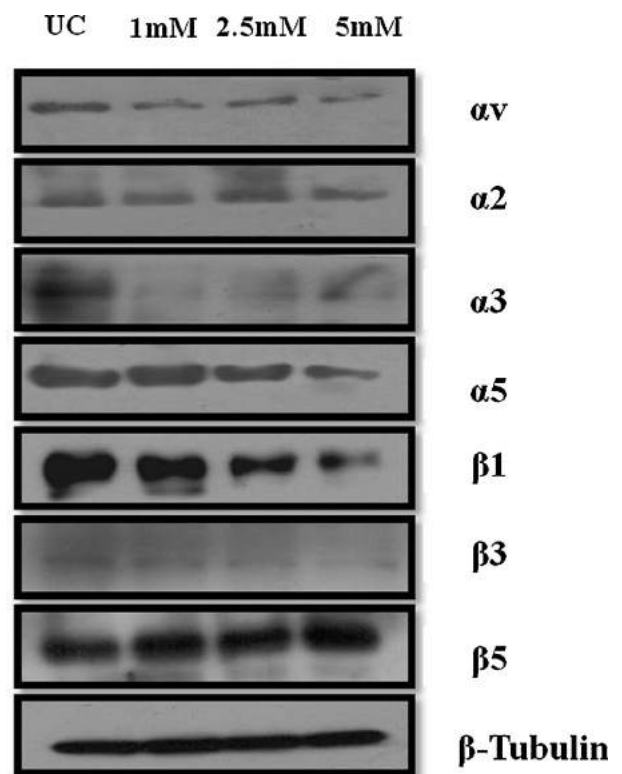


Fig. 5. Changes in total protein levels of integrins upon PTX treatment in MDA-MB-231 cells. Western blotting was done to assess PTX associated changes in total protein levels of integrins αv , $\alpha 2$, $\alpha 3$, $\alpha 5$, $\beta 1$, $\beta 3$ and $\beta 5$. PTX at sub-toxic doses 1 mM, 2.5 mM, 5 mM. affected the levels of αv , $\alpha 3$, $\alpha 5$, $\beta 1$ and $\beta 3$. However, no change was observed for $\alpha 2$ and $\beta 5$ subunits. Beta-tubulin was used as a loading control.

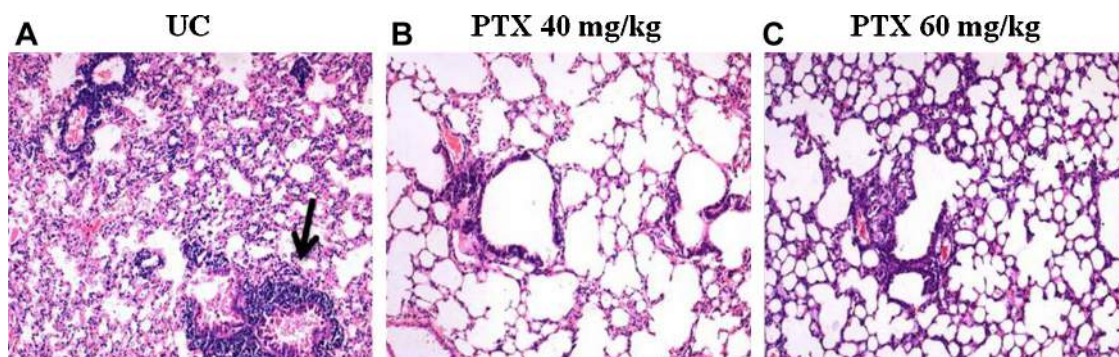


Fig. 6. PTX treatment displayed lessened metastatic potential using *in vivo* experimental metastasis model. MDA-MB-231 cells were injected intravenously into the tail vein of 6–8 week old female NOD-SCID mice. Mice were divided into three groups: (A) control treated with PBS, (B) PTX 40 mg/kg and (C) PTX 60 mg/kg and treated for a period of 9 consecutive days via intraperitoneal route. Mice were sacrificed after a month, lungs were excised and later Haematoxylin-Eosin stained. Control groups showed presence of many large and small tumour colonies compared to PTX treated groups.

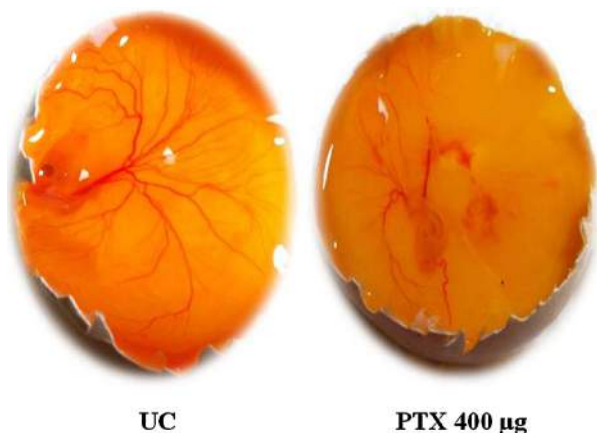


Fig. 7. PTX affects blood vessel formation using *in ovo* CAM assay. Fertilized eggs were procured and kept in an incubator maintained at 37 °C under humidifying conditions. The eggs were kept for a period of 5 days before PTX treatment and then incubated further. Photographs were taken after the eggs were cut open. PTX treatment caused reduction in blood vessel density around the growing embryo, suggestive of its anti-angiogenic activity.

7 ± 0.69 , 2.3 ± 0.3 , 3 ± 0.34 tumour islands/field for untreated, 40 mg/kg and 60 mg/kg PTX groups respectively ($P < 0.05$) (Supplementary Fig. S2). This observation clearly demonstrates anti-adhesive properties of PTX using *in vivo* model system. Further, we have evaluated the effect of PTX on angiogenesis using *in ovo* model CAM assay. Integrins are known to be involved in the process of angiogenesis as well [6,31]. We had earlier shown that PTX inhibits blood vessel formation in NOD-SCID mice [20]. CAM assay was performed as an additional validation to corroborate our earlier findings and we did observe a decrease in blood vessel formation around the growing embryo (Fig. 7). The present study thus clearly highlights the potential of PTX as an anti-adhesive and anti-angiogenic agent in the present model system.

Disclosure of interest

The authors declare that they have no conflicts of interest concerning this article.

Acknowledgements

We acknowledge grant support from ACTREC, Tata Memorial Centre. Mr. Peeyush N. Goel is supported by CSIR-Senior Research Fellowship. The authors would also like to thank Manohar Parker for providing technical assistance during animal experimentation.

The authors are also grateful for the support by Animal house, Confocal and flow cytometry facilities. The authors also thank Miss Nirosha Konduru for helping during the course of experiments.

Appendix A. Supplementary data

Supplementary data associated with this article can be found in the online version, at <http://dx.doi.org/10.1016/j.biopha.2013.09.002>.

References

- [1] Siegel R, Naishadham D, Jemal A. Cancer statistics, 2013. *CA Cancer J Clin* 2013;63:11–30.
- [2] Bendas G, Borsig L. Cancer cell adhesion and metastasis: selectins, integrins, and the inhibitory potential of heparins. *Int J Cell Biol* 2012;676731.
- [3] Desgrosellier JS, Cheresh DA. Integrins in cancer: biological implications and therapeutic opportunities. *Nat Rev Cancer* 2010;10:9–22.
- [4] Vicente-Manzanares M, Choi CK, Horwitz AR. Integrins in cell migration – the actin connection. *J Cell Sci* 2009;122:199–206.
- [5] Aoudjit F, Vuori K. Integrin signaling in cancer cell survival and chemoresistance. *Chemother Res Pract* 2012;283181.
- [6] Avraamides CJ, Garmy-Susini B, Varner JA. Integrins in angiogenesis and lymphangiogenesis. *Nat Rev Cancer* 2008;8:604–17.
- [7] Rathinam R, Alahari SK. Important role of integrins in the cancer biology. *Cancer Metastasis Rev* 2010;29:223–37.
- [8] Mitchell K, Svenson KB, Longmate WM, Gkirtzimanaki K, Sadej R, Wang X, et al. Suppression of integrin alpha3beta1 in breast cancer cells reduces cyclooxygenase-2 gene expression and inhibits tumorigenesis, invasion, and cross-talk to endothelial cells. *Cancer Res* 2010;70:6359–67.
- [9] Morozovitch GE, Kozlova NI, Cheglakov IB, Ushakova NA, Preobrazhenskaya ME, Berman AE. Implication of alpha5beta1 integrin in invasion of drug-resistant MCF-7/ADR breast carcinoma cells: a role for MMP-2 collagenase. *Biochemistry (Mosc)* 2008;73:791–6.
- [10] Sawhney RS, Liu W, Brattain MG. A novel role of ERK5 in integrin-mediated cell adhesion and motility in cancer cells via Fak signaling. *J Cell Physiol* 2009;219:152–61.
- [11] dos Santos PB, Zanetti JS, Ribeiro-Silva A, Beltrao EI. Beta 1 integrin predicts survival in breast cancer: a clinicopathological and immunohistochemical study. *Diagn Pathol* 2012;7:104.
- [12] Ramirez NE, Zhang Z, Madamanchi A, Boyd KL, O'Rear LD, Nashabi A, et al. The alpha(2)beta(1) integrin is a metastasis suppressor in mouse models and human cancer. *J Clin Invest* 2011;121:226–37.
- [13] Zhang M, Xu YJ, Mengi SA, Arneja AS, Dhalla NS. Therapeutic potentials of pentoxifylline for treatment of cardiovascular diseases. *Exp Clin Cardiol* 2004;9:103–11.
- [14] Kovach NL, Lindgren CG, Fefer A, Thompson JA, Yednock T, Harlan JM. Pentoxifylline inhibits integrin-mediated adherence of interleukin-2-activated human peripheral blood lymphocytes to human umbilical vein endothelial cells, matrix components, and cultured tumor cells. *Blood* 1994;84:2234–42.
- [15] Bruynzeel I, van der Raaij LM, Stoof TJ, Willemze R. Pentoxifylline inhibits T-cell adherence to keratinocytes. *J Invest Dermatol* 1995;104:1004–7.
- [16] Ratheesh A, Ingle A, Gude RP. Pentoxifylline modulates cell surface integrin expression and integrin mediated adhesion of B16F10 cells to extracellular matrix components. *Cancer Biol Ther* 2007;6:1743–52.
- [17] Goel PN, Gude RP. Unravelling the antimetastatic potential of pentoxifylline, a methylxanthine derivative in human MDA-MB-231 breast cancer cells. *Mol Cell Biochem* 2011;358:141–51.

- [18] Dua P, Ingle A, Gude RP. Suramin augments the antitumor and antimetastatic activity of pentoxifylline in B16F10 melanoma. *Int J Cancer* 2007;121:1600–8.
- [19] Lin TH, Tan TW, Tsai TH, Chen CC, Hsieh TF, Lee SS, et al. D-pinitol inhibits prostate cancer metastasis through inhibition of alphaVbeta3 integrin by modulating FAK, c-Src and NF-kappaB pathways. *Int J Mol Sci* 2013;14:9790–802.
- [20] Goel PN, Gude RP. Curbing the focal adhesion kinase and its associated signalling events by pentoxifylline in MDA-MB-231 human breast cancer cells. *Eur J Pharmacol* 2013;714:432–41.
- [21] Kim SH, Turnbull J, Guimond S. Extracellular matrix and cell signalling: the dynamic cooperation of integrin, proteoglycan and growth factor receptor. *J Endocrinol* 2011;209:139–51.
- [22] Reticker-Flynn NE, Malta DF, Winslow MM, Lamar JM, Xu MJ, Underhill GH, et al. A combinatorial extracellular matrix platform identifies cell-extracellular matrix interactions that correlate with metastasis. *Nat Commun* 2012;3:1122.
- [23] Tang F, Zhang R, He Y, Zou M, Guo L, Xi T. MicroRNA-125b induces metastasis by targeting STARD13 in MCF-7 and MDA-MB-231 breast cancer cells. *PLoS One* 2012;7:e35435.
- [24] Dalton SL, Scharf E, Briesewitz R, Marcantonio EE, Assoian RK. Cell adhesion to extracellular matrix regulates the life cycle of integrins. *Mol Biol Cell* 1995;6:1781–91.
- [25] Delcommenne M, Streuli CH. Control of integrin expression by extracellular matrix. *J Biol Chem* 1995;270:26794–801.
- [26] van der P, Vloedgraven H, Papapoulos S, Lowick C, Grzesik W, Kerr J, et al. Attachment characteristics and involvement of integrins in adhesion of breast cancer cell lines to extracellular bone matrix components. *Lab Invest* 1997;77:665–75.
- [27] Bartsch JE, Staren ED, Appert HE. Adhesion and migration of extracellular matrix-stimulated breast cancer. *J Surg Res* 2003;110:287–94.
- [28] Korah R, Boots M, Wieder R. Integrin alpha5beta1 promotes survival of growth-arrested breast cancer cells: an in vitro paradigm for breast cancer dormancy in bone marrow. *Cancer Res* 2004;64:4514–22.
- [29] Aoudjit F, Vuori K. Integrin signaling inhibits paclitaxel-induced apoptosis in breast cancer cells. *Oncogene* 2001;20:4995–5004.
- [30] Dalton SL, Marcantonio EE, Assoian RK. Cell attachment controls fibronectin and alpha 5 beta 1 integrin levels in fibroblasts. Implications for anchorage-dependent and -independent growth. *J Biol Chem* 1992;267:8186–91.
- [31] Kim S, Bell K, Mousa SA, Varner JA. Regulation of angiogenesis in vivo by ligation of integrin alpha5beta1 with the central cell-binding domain of fibronectin. *Am J Pathol* 2000;156:1345–62.



Available online at
ScienceDirect
 www.sciencedirect.com

Elsevier Masson France
EM|consulte
 www.em-consulte.com



Original article

Delineating the anti-metastatic potential of pentoxifylline in combination with liposomal doxorubicin against breast cancer cells



Peeyush N. Goel, Rajiv P. Gude*

Gude Lab, Advanced Centre for Treatment, Research & Education in Cancer (ACTREC), Tata Memorial Centre, Kharghar, Navi Mumbai 410210, Maharashtra, India

ARTICLE INFO

Article history:

Received 5 October 2013

Accepted 11 November 2013

Keywords:

Pentoxifylline

Lipodox

Combination therapy

Breast cancer

Xenograft model

ABSTRACT

Breast cancer remains the second most prevalent cancer worldwide. Several anticancer drugs are being currently used in the treatment of breast cancer. However, owing to high cytotoxicity, induced resistance and cost ineffectiveness, there is an urgent need to develop newer therapeutic regimens that limit the current problems. One of the approaches in this regard is the formulation of combination therapies whereby multiple drugs are being delivered at relatively lesser dose that surely confines the aforesaid problems. In this purview, we had evaluated the effects of pentoxifylline, a methylxanthine derivative and liposomal doxorubicin (Lipodox), an anthracycline in combination to evaluate their anti-metastatic activities both *in vitro* and *in vivo* against breast cancer cells. The combination regime exhibited synergistic activity and inhibited cellular proliferation to a greater extent with regard to each drug used alone.

© 2013 Elsevier Masson SAS. All rights reserved.

1. Introduction

“The next step – the complete cure – is almost sure to follow”.
 Kenneth Endicott

Cancer in the present scenario tends to be one of the most leading causes of worldwide deaths [1]. It is rather a syndrome characterised by uncontrolled proliferation and the spread of abnormal cells. As per the latest global statistics, an estimated 12.7 million cancer cases around the world were reported by World Health Organisation (WHO). This number is anticipated to rise towards 21 million by the year 2030 [2,3]. Several mutations are necessitated by a cell to transform and eventually proliferate, forming a primary tumor, which when being localised or confined at a particular site can easily be treated by surgically removing the same. However, most cancer related deaths are not caused by this primary mass but due to disseminated tumor cells from these primary tumors at distant sites via the bloodstream. This process is referred to as metastasis and is the prime cause of cancer related deaths [4].

Breast cancer is the second most common cancer with nearly 1.38 million cases [2]. Triple negative breast cancer (TNBC) is a

heterogeneous entity that makes it a daunting task for diagnosis and treatment. This sub-group lack the expression of estrogen receptor, progesterone receptor and HER-2. Further, such tumors are difficult to manage since hormonal therapies as well as HER-2 targeted therapies are incompetent. Thus, no other systemic therapies exists other than chemotherapy [5]. At present, a large number of anticancer drugs for targeting metastatic breast cancer are currently available in the market, such as the anthracyclines, taxanes, anti-metabolites and platinum analogues [6]. A high expenditure and time are the requisites for the initial evaluation of any drug to reach the clinics. Thus, it becomes favourable to evaluate several known drugs used in other clinical settings for targeting cancer, a process referred to as drug repositioning. It also helps in bypassing the assessment costs since the pharmacokinetics and safety profiles for the available drugs are substantially inferred [7]. This indeed has provided success to the pharmaceutical companies in the preceding times [8].

Pentoxifylline (3,7, dimethyl-1-(5-oxohexyl xanthine) or PTX) is a methylxanthine derivative that inhibits the phosphodiesterase activity leading to increased c-AMP levels [9]. It is currently used for the treatment of peripheral vascular diseases [10]. Further, it has been shown to increase the effectiveness of both radiotherapy and chemotherapy [11,12]. Our lab had earlier demonstrated that PTX exerts anti-metastatic effects in both melanoma and breast cancers, respectively [13–16]. Thus, there is an imperative rationale to develop combination regimens of PTX with other known anticancer drugs actively used against breast cancer. The basic principle for a combination therapy is to surmount individual

* Corresponding author. Tel.: +91 22 274 050 84; fax: +91 22 274 050 83.

E-mail addresses: peeyushgoel29@gmail.com (P.N. Goel), rgude@actrec.gov.in, rajivgude@yahoo.in (R.P. Gude).

drug limitations and to decrease the payload for each individual drug, thereby, reducing the toxicity as well increasing their therapeutic efficacy [17]. Chemotherapy represents one of the major therapeutic interventions in the treatment of advanced breast cancer. Among the various classes of known anticancer agents, anthracyclines {such as doxorubicin (DOX) or adriamycin (ADR)} comprise one of the primary options in this scenario. Their ability to inhibit topoisomerases as well as intercalate between DNA base pairs, terminates the process of DNA replication and culminates into the death of rapidly dividing cells. These also result in the generation of free radicals, causing lipid peroxidation leading to cellular death [18]. However, there are a large number of toxicity related issues, such as cardiotoxicity, suppression of bone marrow, nausea, vomiting and baldness associated with the usage of doxorubicin. In order to overcome these limitations, drug delivery systems, such as the entrapment of DOX in pegylated liposomes coated with methoxypolyethylene glycol (MPEG) are preferred. These modifications not only increase their blood circulation time but also protect them from mononuclear phagocyte system apart from causing minimal toxicity to normal cells due to slower or sustained release [19].

Based on these properties, we have evaluated the combinatorial effects of PTX along with liposomal doxorubicin (Lipodox or LD) so as to increase its therapeutic efficacy in breast cancer cells. There are a few reports that have used combination of both PTX and DOX against cervical and leukemic cells [20,21]. However, no report regarding usage against breast cancer has been documented so far. In this context, the effects of combination therapy (PTX and LD) on various metastatic events *viz.* cellular proliferation, adhesion, migration, invasion and apoptosis have been demonstrated along with *in vivo* evaluation using MDA-MB-231 breast cancer cells as the model system in the present study.

2. Materials and methods

2.1. Cell Lines and animals

Human (TNBC) MDA-MB-231 (TNBC) and fibrosarcoma HT-1080 (TNBC) cell lines were purchased from NCCS, Pune, India. The cells were maintained in Dulbecco's Modified Eagle Medium (DMEM, GIBCO) supplemented with 10% heat inactivated foetal bovine serum, FBS (GIBCO). Cultures were kept up at 37 °C in 5% CO₂ humidified atmosphere [14].

Six to eight old week female nude mice (NIH-3) were procured from the animal house facility at ACTREC, Tata Memorial Centre after clearance from Institutional ethical approval committee (IEAC). The animals were maintained under sterilised conditions.

2.2. Materials

Pentoxifylline, MTT or (3-(4,5-dimethylthiazol-2-yl)-2,5-diphenyltetrazoliumbromide), bovine serum albumin (BSA), propidium iodide (PI), gelatin, ethidium bromide (EB), acridine orange (AO), mitomycin C, fibronectin, laminin, vitronectin and collagen type IV were purchased from Sigma. RNase was purchased from Merck, 30 kDa cut-off filters were obtained from Millipore and Matrigel from BD Biosciences. Plain and liposomal doxorubicin (Lipodox) were purchased from Sigma and Sun pharmaceutical Ltd, respectively. AnnexinV/FITC staining kit was purchased from Invitrogen (India). All other chemicals or reagents used were either of analytical grade or highest purity that were commercially available.

2.3. MTT cytotoxicity assay

MTT assay for determining cellular viability was performed as done earlier [22]. Briefly, 4000, 2000 and 1500 cells per well were

seeded into 96-well plates for 24 h, 48 h and 72 h, respectively. The cells were incubated at 37 °C in a 5% CO₂ incubator for 24 h. Complete media containing DOX and LD were added in logarithmic doses (0.001 μM–1000 μM) respectively. The drug was removed at subsequent time points (24–72 h) and the plates were washed with PBS twice. MTT solution was then added to each of the wells and the plates were incubated for 4 h at 37 °C. Plates were then centrifuged at 1500 rpm for 20 min. The supernatant was discarded and DMSO was added to dissolve the formazan crystals along with intermittent shaking. The plates were then read using a spectrophotometer at dual wavelengths of 540/690 nm. The inhibitory concentration at which 50% of cell viability is observed (IC₅₀) values were then calculated using a logarithmic graph by plotting % viability vs drug concentration. The cell viability for combination study was also determined by MTT assay. Here, PTX:LD was taken in the ratio of 500:1 and synergistic doses were evaluated using compusyn software [23]. The doses evaluated for combination regimens were then designated and abbreviated as P1 (3 mM) or P2 (4 mM) for PTX, LD1 (6 μM) or LD2 (8 μM) for LD and C1 (P1 and LD1) or C2 (P2 and LD2) for combination doses, respectively.

2.4. Colony formation assay

Briefly, 600 cells were being seeded in a 35 mm plate and allowed to stabilise overnight. The following day combination regimens were added for another 24 h and incubated at 37 °C. Cells were washed with PBS and complete medium was added. The cells were then allowed to multiply over a period of 8–10 days as done previously. Cells were finally washed with PBS and fixed in chilled methanol. Staining was then performed using 0.5% crystal violet. Colonies with at least 50 cells were counted and the results were plotted as percentage colonies vs drug treatment.

2.5. Cell cycle distribution using flow cytometry

Sub-confluent cultures were treated with combination doses (P1 or P2, LD1 or LD2 and C1 or C2) for a period of 24 h and then harvested. Cells were later washed using PBS and fixed using 70% chilled ethanol. Cells were centrifuged, suspended in PBS followed by treatment using RNase (0.5 mg/mL) and PI (50 μg/mL). The cells were acquired using FACS Calibur and the results analysed using Modfit software [14].

2.6. AnnexinV/FITC staining

Apoptotic cells were determined using AnnexinV/FITC staining protocol as done previously [15]. Briefly, 1 × 10⁶ cells for each of the following groups *viz.* P1 or P2, LD1 or LD2 and C1 or C2 were suspended in 100 μL 1 × Annexin binding buffer. The cells were then treated using 5 μL AnnexinV/FITC along with 1 μL of PI (100 μg/mL) solutions. The samples were mixed thoroughly and incubated at room temperature for 15 min. Thereafter, the final volume was made till 500 μL using Annexin binding buffer and the samples were kept on ice. Acquisition was done using FACS Calibur and the results were analysed using Cell Quest Pro software.

2.7. EB/AO staining

EB/AO staining for differentiating the live and dead cells was performed as mentioned earlier [24]. Briefly, 16000 cells/well were seeded in triplicates using a 96-well plate. Cells were then treated with different combination regimens as described, for a period of 24 h. The plates were centrifuged and 1:1 ratio of EB/AO mix was added to the wells. The plates were later observed under a Zeiss

Axio inverted microscope (Germany) and images were captured at 10× magnification.

2.8. Adhesion assay

Adhesion to extracellular matrix components (ECM) was carried out as described earlier [16]. Then, 96-well plates were coated using Matrigel (10 µg/mL), collagen type IV (10 µg/mL), fibronectin (2.5 µg/mL), laminin (5 µg/mL) and vitronectin (2.5 µg/mL). The plates were kept for polymerisation at 4 °C overnight, washed with PBS and then blocking was done using 1% BSA. Cells treated with varying combination regimens were harvested using saline–EDTA and seeded at a density of 3×10^4 cells/well for 30 min. The percent relative adhesion against each substrate was then calculated considering the adhesion of control/untreated cells to be 100%.

2.9. Gelatin zymography

Sub-confluent plates were treated with different combination regimen as described earlier for 24 h [14]. Cells were then washed with PBS and plain DMEM was added. The condition media was thereafter collected after 24 h as done previously. The condition media was later concentrated using 30 kDa cut-off filters and normalised as per the individual cell counts. Samples were then loaded onto 10% SDS–PAGE containing 0.1% gelatin as a substrate. The condition medium obtained from HT-1080 was used as a positive control. The gel was later kept in developing buffer after electrophoresis for 24 h. Staining was done using 0.25% Commassie Brilliant Blue R-250 and then de-staining in

a mixture of water: methanol: acetic acid (5:4:1). The gelatinase activity was detected as visible white zones in a dark background.

2.10. Wound scratch assay

Changes in cellular motility were determined using wound healing assay as done earlier [14]. Cells were grown in 6-well plates and then treated with 1 µg/mL mitomycin C for an hour. Cells in the centre of the plate were scratched using a sterile tip and washed with PBS. Combination regimen doses of PTX and LD (P1 or P2, LD1 or LD2 and C1 or C2) were added for another 24 h. The plates were then washed using PBS and fixed using chilled methanol. Wound widths were then measured using Metamorph imaging software. The results were plotted as % wound closure with respect to control vs drug regimen, considering untreated to be 100%.

2.11. In vivo xenograft model

Briefly, 2×10^6 MDA-MB-231 cells were injected into the right flank of 6–8 week old female Nude (NIH-3) mice. Mice were then divided into 6 groups ($n = 5$) namely:

- untreated or UC (PBS only);
- DOX (4 mg/kg);
- LD (4 mg/kg);
- PTX 60 mg/kg;
- PTX + LD (40 mg/kg and 1 mg/kg);
- PTX + LD (40 mg/kg and 2 mg/kg).

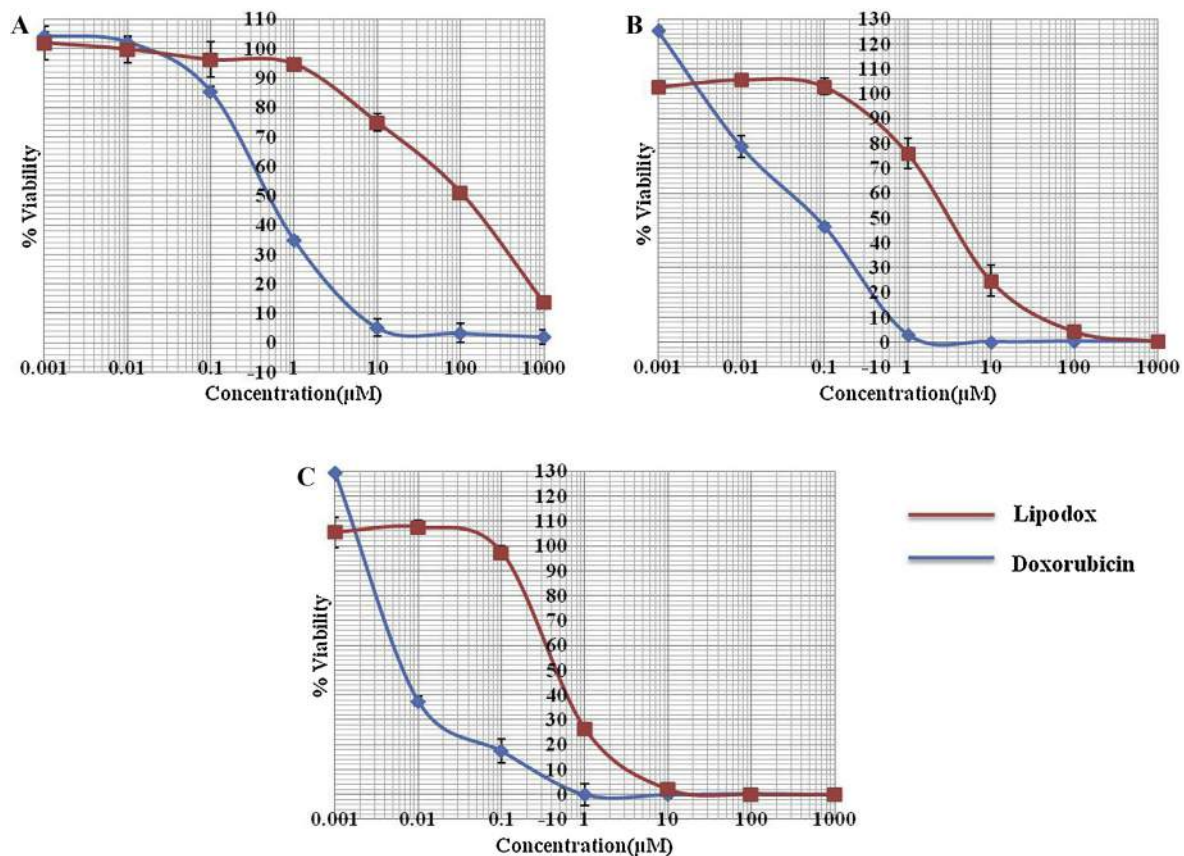


Fig. 1. Comparison of cytotoxicity for Doxorubicin (DOX) and liposomal doxorubicin (Lipodox or LD). MTT assay was performed to determine the percent viability in MDA-MB-231 cells at (A) 24 h (B) 48 h (C) 72 h in MDA-MB-231 cells using DOX and LD. Results are representative of three independent experiments mean \pm SEM.

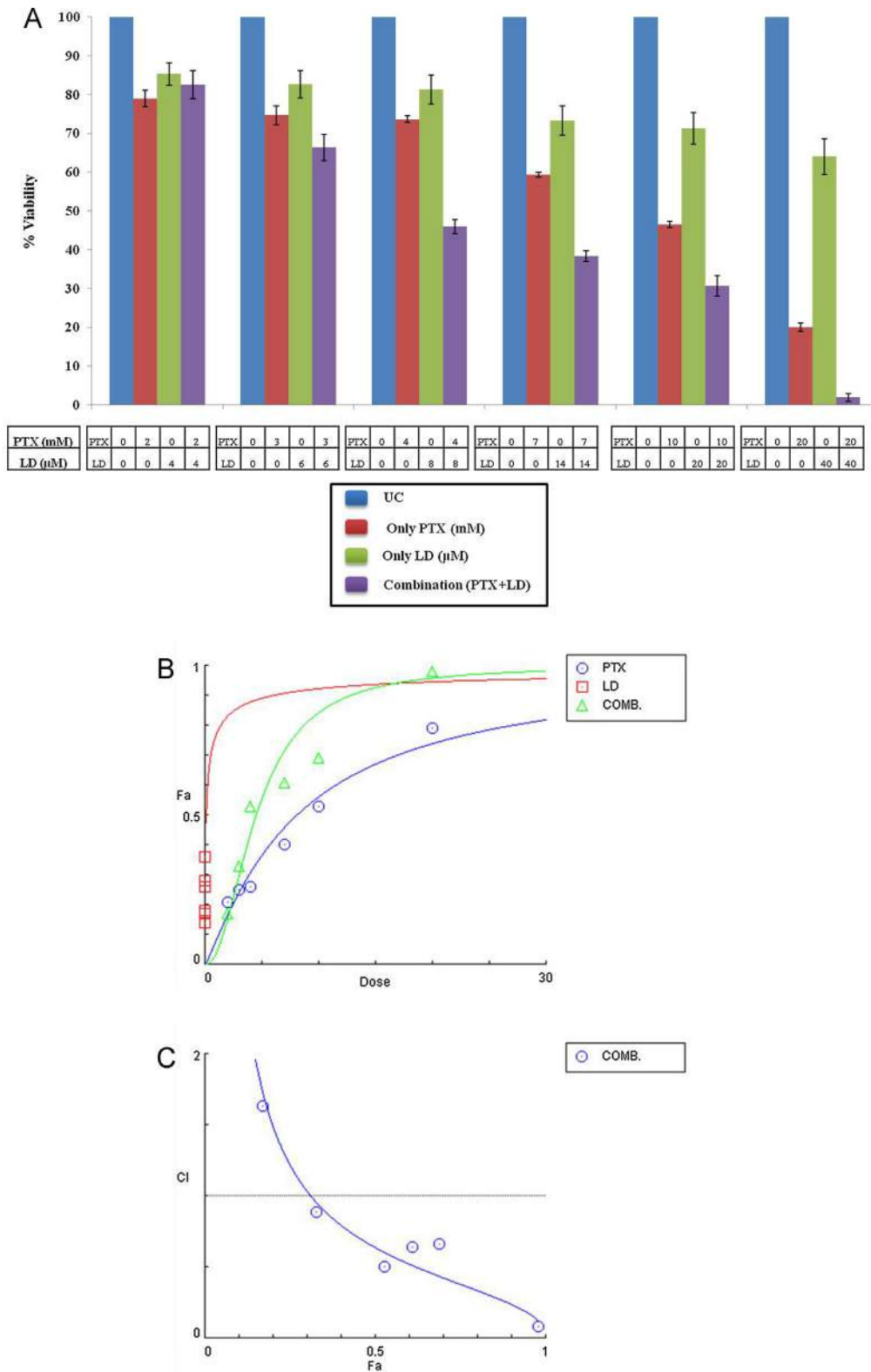


Fig. 2. Effect of combination doses of PTX and LD. Combination regimen was evaluated for PTX and LD for 24 h study in the ratio of 500:1. A. Representation of % viability for individual doses of PTX, LD as well as their combination doses. B. Dose-effect curve of PTX, LD and combination. C. Combination Index (CI) plot for different combinations. CI values less than 1 are representative of synergism.

PTX was administered intraperitoneally (ip) for a period of 9 days consecutively while DOX/LD were injected intravenously (iv) once a week for 2 weeks, respectively. The tumor volumes and animal weights were measured alternately. The tumor volume was calculated using the formula $1/2ab^2$ where “a” is the longer diameter and “b” is the shorter one [15,25].

2.12. Statistics

The experiments were performed at least thrice independently and the values represented are indicative of mean \pm SEM. One way ANOVA (equal variances assumed) was used for statistical significance where $P < 0.05$ was considered to be statistically significant.

3. Results and discussion

3.1. Lipodox exhibited lesser cytotoxicity than plain doxorubicin in MDA-MB-231 cells

Anthracyclines, such as DOX is being used extensively in the treatment of advanced breast cancer [6,26–28]. However, toxicity related issues, such as the cardiotoxicity forms a major obstacle in the treatment scenario. MTT assay was done to evaluate the toxicity of DOX and LD at different time points, viz. 24 h, 48 h and 72 h respectively (Fig. 1A–C). It was found that DOX is highly toxic to MDA-MB-231 cells when compared to LD at these time points. IC₅₀ was found to be 0.5 μM, 0.09 μM, 0.006 μM for DOX compared to 100 μM, 3.5 μM, 0.4 μM in case of LD at 24 h, 48 h and 72 h. Hence, LD was chosen for combination therapy in our model system due to sustained release of the drug and least toxicity.

3.2. Synergism in the cytotoxicity profile for the combination regimen of pentoxifylline and lipodox

PTX is a hydrophilic drug and thus readily soluble, providing a therapeutic advantage [29]. Further, it has shown to exert anti-metastatic effects in breast cancer cells [14–16]. This prompted us to evaluate its effect in combination with other known anticancer agent, such as anthracyclines (e.g. Doxorubicin). LD was used in our present study since it is comparatively lesser toxic compared to DOX alone. The % viability of both PTX and LD in the ratio of 500:1 was determined using MTT assay at different doses both in combination as well as single agents respectively (Fig. 2A). Combination index (CI) was determined by the use of Compusyn software (Table 1). A value of CI > 1 means antagonism, CI = 1 represents additive and CI < 1 indicates synergism [23]. It was found that PTX at doses of 3 mM, 4 mM and corresponding LD at 6 μM and 8 μM showed synergistic action where CI tends to be less than unity (Table 1). The dose-effect curve and CI plot are represented in Fig. 2B and C, respectively. Further, it can be seen that there is a reduction in IC₅₀ values for both the drugs in concern (Table 2). The IC₅₀ computed by software comes to be approximately 8.1 mM, 110 μM for PTX and LD. However, in the combination scenario it is found to be close to 4.5 mM, 9 μM for PTX and LD with CI < 1. This clearly indicates that the combination dose acts synergistically and is more potent than individual drugs. Based on these combination doses, anti-metastatic activity of the combination regimen was evaluated. The doses were designated as P1 (3 mM), P2 (4 mM) for PTX, LD1 (6 μM), LD2 (8 μM) for LD and C1 (P1 and LD1), C2 (P2 and LD2) for combination. It can be further seen that the viability at these combination doses (C1 and C2) is much lower than that of individual effects (Fig. 2A). The anti-proliferative activity of the combination regimen was further confirmed using colony formation assay. The % colony formation was 54.12 ± 4.14% (P1), 44.22 ± 1.90% (P2), 16.75 ± 0.70% (LD1), 4.88 ± 1.17% (LD2), 6.22 ± 1.24% (C1) and 1.59 ± 0.23% (C2) (*P* < 0.05). The results are shown in Fig. 3. In our earlier work, we had shown PTX to inhibit the

Table 1

Combination index (CI) values for actual experimental points.

Total dose (PTX and LD)	Effect (Fa)	Combination index (CI)
2.004	0.17	1.63463
3.006	0.33	0.88569
4.008	0.53	0.50458
7.014	0.61	0.64374
10.02	0.69	0.65971
20.04	0.98	0.08417

Table 2

Data for Fa=0.5 i.e. Effect at 50% inhibition.

Drug/combination	Combination index (CI)	PTX dose (mM)	LD dose (mM)
PTX		8.07922	
LD			0.10972
Combination	0.63782	4.49159	0.00898

mitogen activated protein kinase (MAPK) pathway that regulates the process of proliferation [15]. Further, DOX also has shown to inhibit the same in breast cancer cells [30]. In light of these evidences, we propose a similar mode of action for the combination doses in our experimental system as well.

3.3. Changes in cell cycle progression and increased apoptosis upon treatment with the combination regimen

Flow cytometry was done to assess the cell cycle status of MDA-MB-231 cells upon PTX and LD treatment as well as their combinations (C1 and C2) represented in Fig. 4A. PI is an intercalating dye that has an affinity towards nucleic acids and thus upon binding to DNA its fluorescence changes. It was found that treatment with PTX leads to a significant increase in G1 phase of the cell cycle (64.58 ± 2.58% for P1, 60.90 ± 2.57% for P2 while for UC it was 38.4 ± 3.22%) (*P* < 0.05). However, treatment with LD causes a G2–M cell cycle arrest significantly (49.93 ± 2.14% for LD1, 68.35 ± 3.44% for LD2 and 14.9 ± 1.11% for UC) (*P* < 0.05) as shown in Fig. 4B. PTX caused a G1 cell cycle arrest as demonstrated earlier by affecting the cyclinD1/cdk6 complex [14,15] while in case of DOX a G2–M arrest had been reported [31]. We had found a similar observation in our experimental system as well. However, in the combination scenario, a G1 phase cell cycle arrest was pronounced (Table 3). The plausible reason is that since G1 phase precedes G2–M phase in the cell cycle, thus blockade in G1 phase by PTX shall not permit cells to bypass it in the combination scenario.

We had earlier observed that combination doses showed a synergistic effect in affecting cellular proliferation. Further, we wanted to check whether these doses cause an increase in apoptosis or not. Both PTX and DOX are known to increase the apoptosis in cervical cancer [20]. Based on this, AnnexinV/FITC staining was performed to demonstrate the same in MDA-MB-231 cells. The basis for this assay is that phosphatidylserine (PS) present in the inner leaflet of the membrane translocates to the outer region in apoptotic cells. This PS has a high affinity for AnnexinV binding. There was an increase in apoptosis in case of

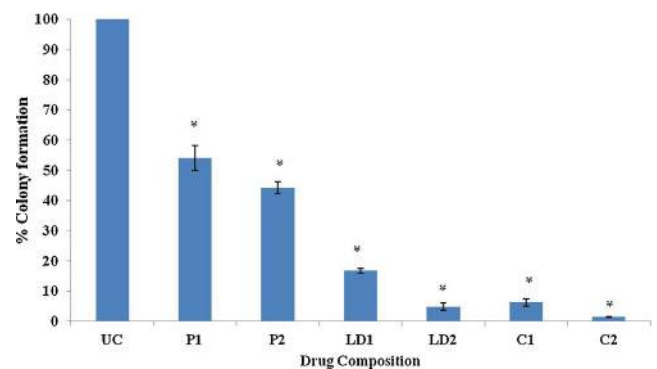


Fig. 3. Clonogenic assay for the combination. Colony formation assay was done to evaluate the anti-proliferative effect of PTX, LD and their combinations. A significant decrease in colony formation was observed in case of C1 and C2. Results are representative of three independent experiments Mean ± SEM. (*P* < 0.05).

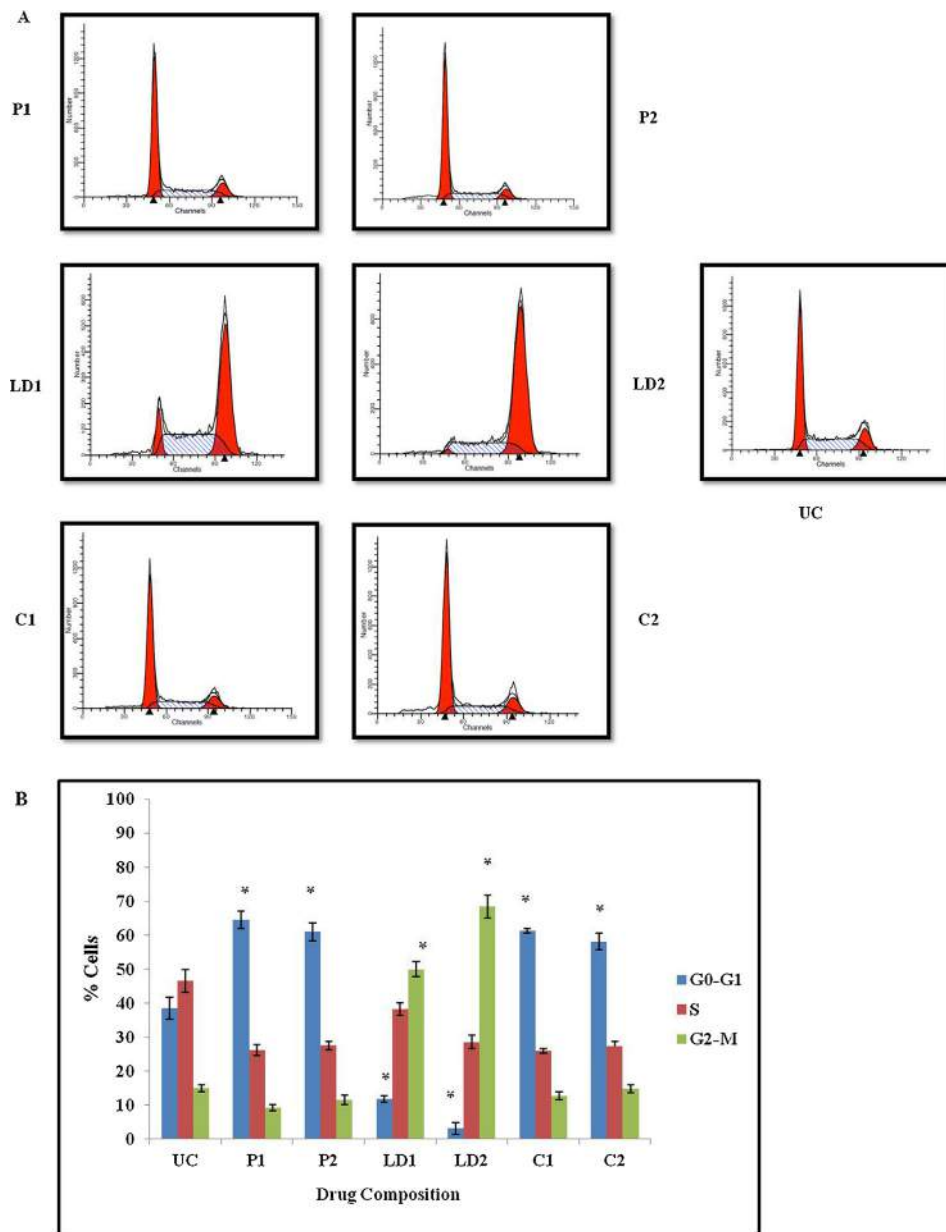


Fig. 4. Cell cycle distribution. Flow cytometry was done to determine the cell cycle status in MDA-MB-231 cells treated with PTX, LD or combinations. A. Ploidy status of the cells. B. Graphical representation of the cells present in different phases of cellular cycle. Results are indicative of three independent experiments Mean \pm SEM. ($P < 0.05$).

combination doses compared to individual treatments as it can be seen by increase in number of apoptotic cells in both the upper right and lower right quadrants of both C1 and C2 plots (Fig. 5). To further corroborate our findings, ET/AO staining was performed. AO is an inclusion dye that penetrates both live and dead cells showing a green fluorescence while ET is an exclusion dye that penetrates only the dead cells showing a red fluorescence [24].

Table 3

Tabulation for cell cycle analysis using flow cytometry.

	G0-G1	S	G2-M
UC	38.4 \pm 3.22	46.5775 \pm 3.40	14.9025 \pm 1.11
P1	64.5875 \pm 2.57	26.2125 \pm 1.64	9.2 \pm 0.98
P2	60.905 \pm 2.57	27.4925 \pm 1.31	11.605 \pm 1.36
LD1	11.8625 \pm 0.92	38.21 \pm 1.93	49.93 \pm 2.14
LD2	3.07 \pm 1.69	28.58 \pm 1.92	68.35 \pm 3.44
C1	61.2775 \pm 0.75	25.95 \pm 0.78	12.7725 \pm 1.13
C2	58.0275 \pm 2.45	27.275 \pm 1.43	14.695 \pm 1.17

ET has a dominating effect over AO staining. A similar effect was also observed in the combination regimen (Fig. 6). These results clearly indicate that the combination of both PTX and LD causes an increase in apoptosis. However, molecular insight needs to be explored to unravel the plausible mechanism of action.

3.4. Alterations in cellular adhesion, invasion and migration for the combination treatment

The metastatic cascade is a very complex event [32]. Accumulating mutations lead to cellular transformation and hyper-proliferation of the cells. These cancerous cells then loosen up their cell-cell as well as cell-ECM contacts thereby regulating the process of cellular adhesion. Certain enzymes, such as matrix metalloproteinases (MMPs) are being secreted that degrades the ECM and aids in paving the path for cancer cells to migrate and enter the bloodstream. The tumor cells are then carried to distant sites via the bloodstream forming distant metastasis. It should be

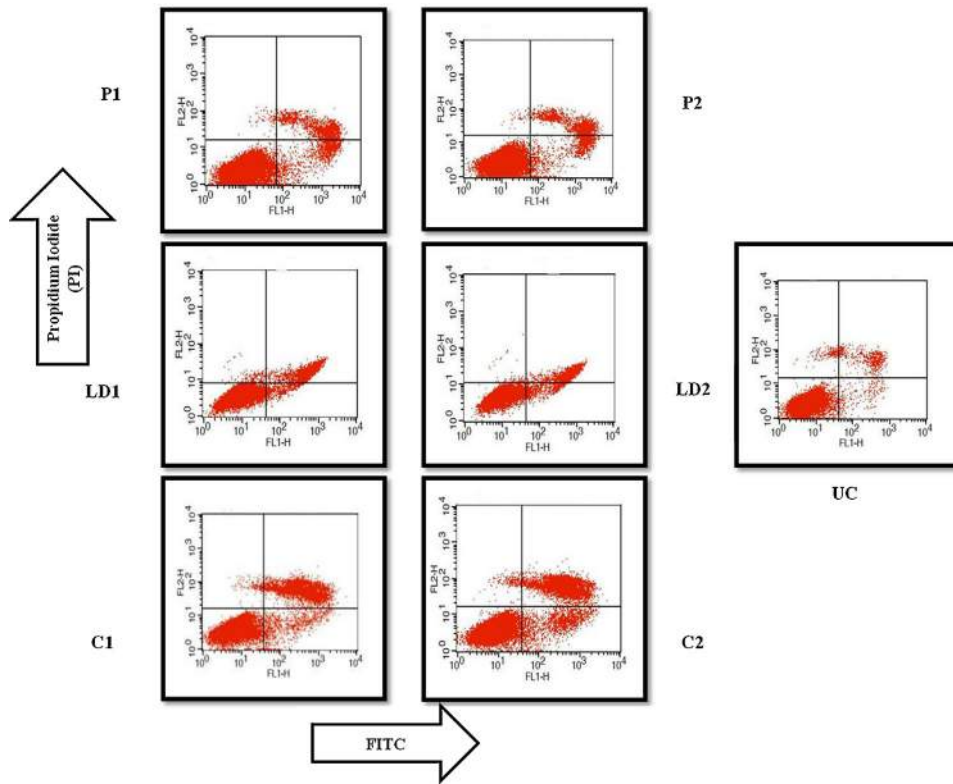


Fig. 5. AnnexinV/FITC staining for apoptotic determination. Sub-confluent cells treated with combination doses showed an enhancement in apoptosis compared to treatment with single drugs alone. AnnexinV binds to the phosphatidylserine present on the outer membrane of apoptotic cells. X and Y axis represents FITC and PI fluorescence respectively.

noteworthy that both the processes of adhesion and proteolysis play an important role in the metastatic process by regulating the interaction of tumor cells with other cells and the underlying ECM, migration and survival cues [33].

In this regard, adhesion assay was done to evaluate the adhesive potential of MDA-MB-231 cells upon PTX, LD as well as their combinations to various ECM components viz. matrigel, collagen type IV, fibronectin, laminin and vitronectin (Fig. 7). It was found

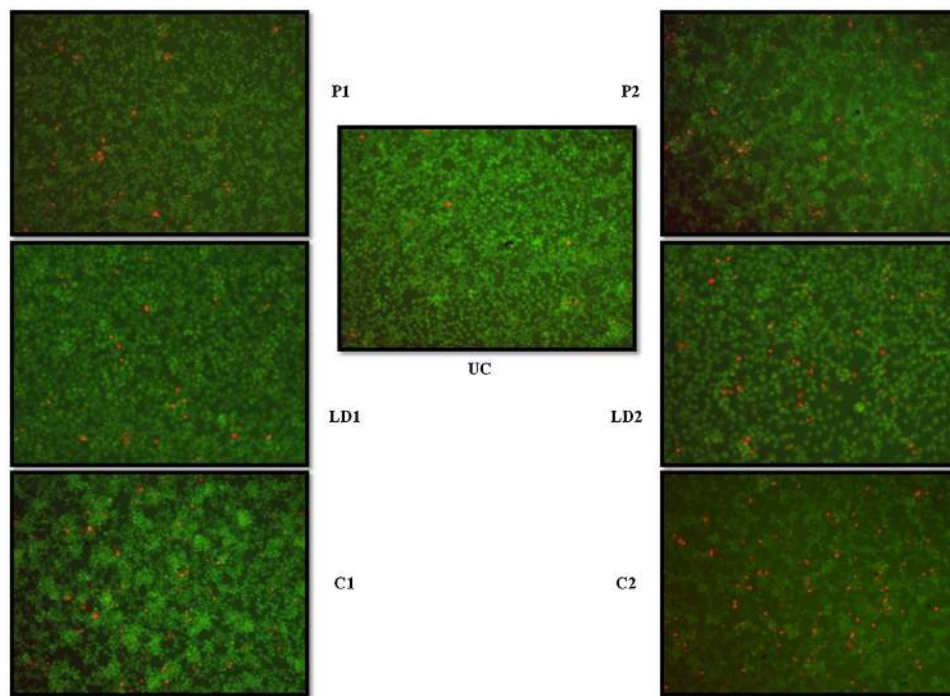


Fig. 6. EB/AO staining for differentiating live and dead cells. The differences between live and dead cells for MDA-MB-231 cells treated with different combinations were determined using EB/AO staining. AO stains the live cells that appear green while apoptotic cells appear reddish coloured. Images were captured using Axio Inverted microscope (Germany).

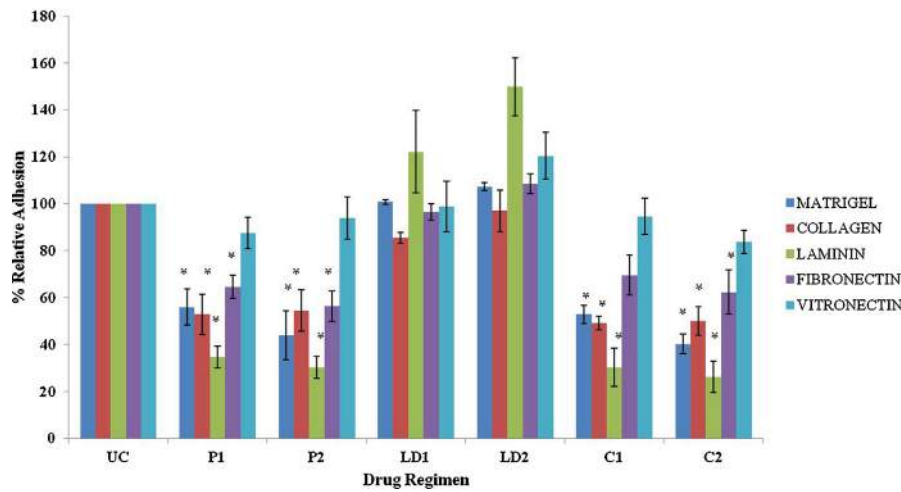


Fig. 7. Adhesion assay to ECM components. Adhesion was evaluated in drug treated cells for 30 min using different ECM substrates viz. Matrigel, collagen type IV, fibronectin, laminin and vitronectin. The % relative adherence was then calculated. Results are representative of three independent experiments mean \pm SEM. ($P < 0.05$).

that LD *per se* does not alter adhesion to any of the mentioned substrates. PTX at doses of 3 mM and 4 mM does affect adhesion. The adhesion for (P1 and P2) was found out to be $55.96 \pm 7.78\%$; $43.87 \pm 10.48\%$ for matrigel, $52.8 \pm 8.52\%$; $54.44 \pm 8.81\%$ for collagen type IV, $64.55 \pm 5\%$; $56.34 \pm 6.53\%$ for fibronectin and $34.53 \pm 4.68\%$; $30.3 \pm 4.6\%$ for laminin ($P < 0.05$). Further, the combination regimen showed a slight reduction in adhesion in comparison to use of PTX alone on matrigel, collagen type IV and laminin, respectively. The combination doses (C1 and C2) showed $52.7 \pm 3.94\%$, $40.19 \pm 4.21\%$ adhesion to matrigel, $49.092.91\%$; $49.97 \pm 6.17\%$ to collagen, $69.55 \pm 8.59\%$; $62.28 \pm 9.4\%$ to fibronectin and $30.3 \pm 8.04\%$; $26.2 \pm 6.78\%$ for laminin considering the adhesion of untreated control to be 100%. No change in adhesion was observed to vitronectin. These results clearly indicate that LD does not affect cellular adhesion to ECM components. However, in the combination regimen, it is PTX that alters the same. We had earlier shown that PTX at sub-toxic doses affects cellular adhesion to ECM components and its allied receptors, integrins [16].

We propose a similar mechanistic insight for the same in the combination scenario as well in the combination with LD.

The effect of combination was then evaluated on the activity of gelatinases, such as MMP-2 and MMP-9 using gelatin zymography. Both these gelatinases degrade the collagen, a major constituent of basal lamina present in basement membrane [34]. We observed MMP-9 activity in MDA-MB-231 cells to be very high. This observation is consistent to earlier findings where MMP-9 had been shown to serve as a prognostic marker for node-negative

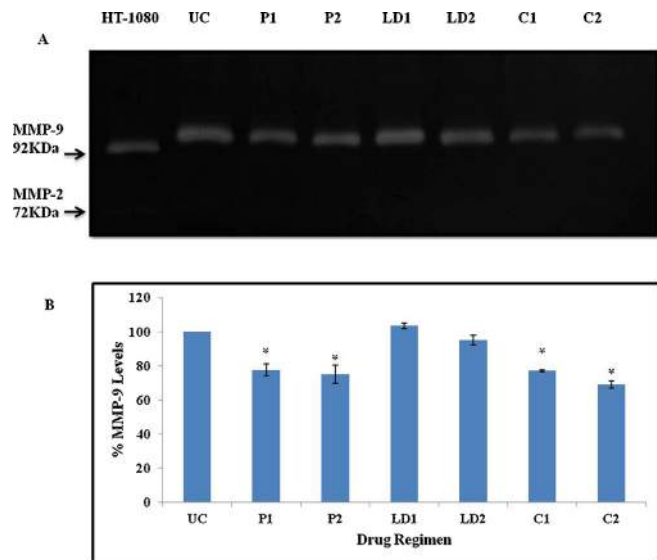


Fig. 8. Gelatin zymography using condition media. The effect of PTX, LD and combinations was done to evaluate changes in the activity of gelatinases. HT-1080 was used as positive control. A. Representative zymograms. B. Graphical representation for changes in activity of MMP-9 considering activity in control to be 100%. Results are representative of three independent experiments mean \pm SEM. ($P < 0.05$).

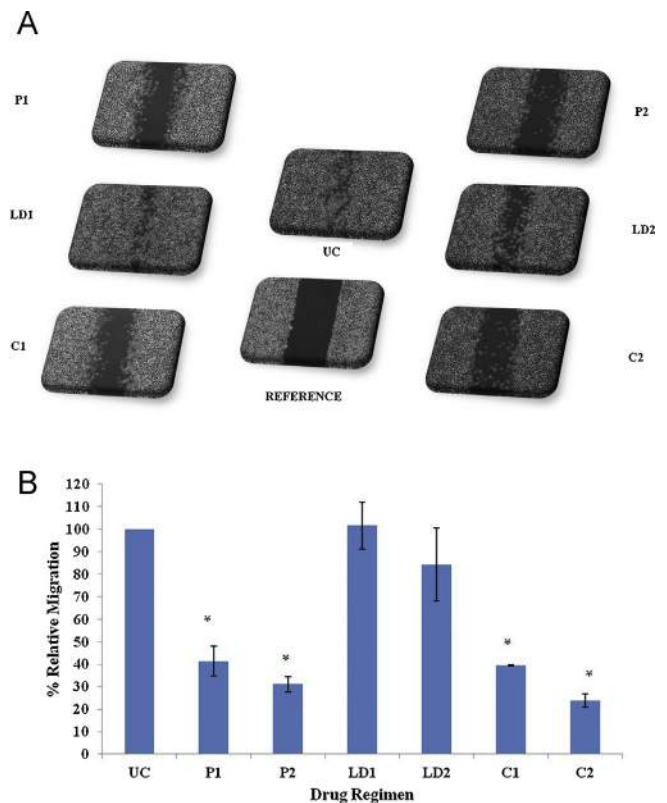


Fig. 9. Changes in cellular motility. Wound healing assay was performed to ascertain the anti-motility effects in MDA-MB-231 cells using different combination regimens. A. Wound images captured after 24 h of drug exposure. Reference represents wound at zero hour. B. % wound coverage considering wound closure in control to be 100%. The results are indicative of three independent experiments Mean \pm SEM. ($P < 0.05$).

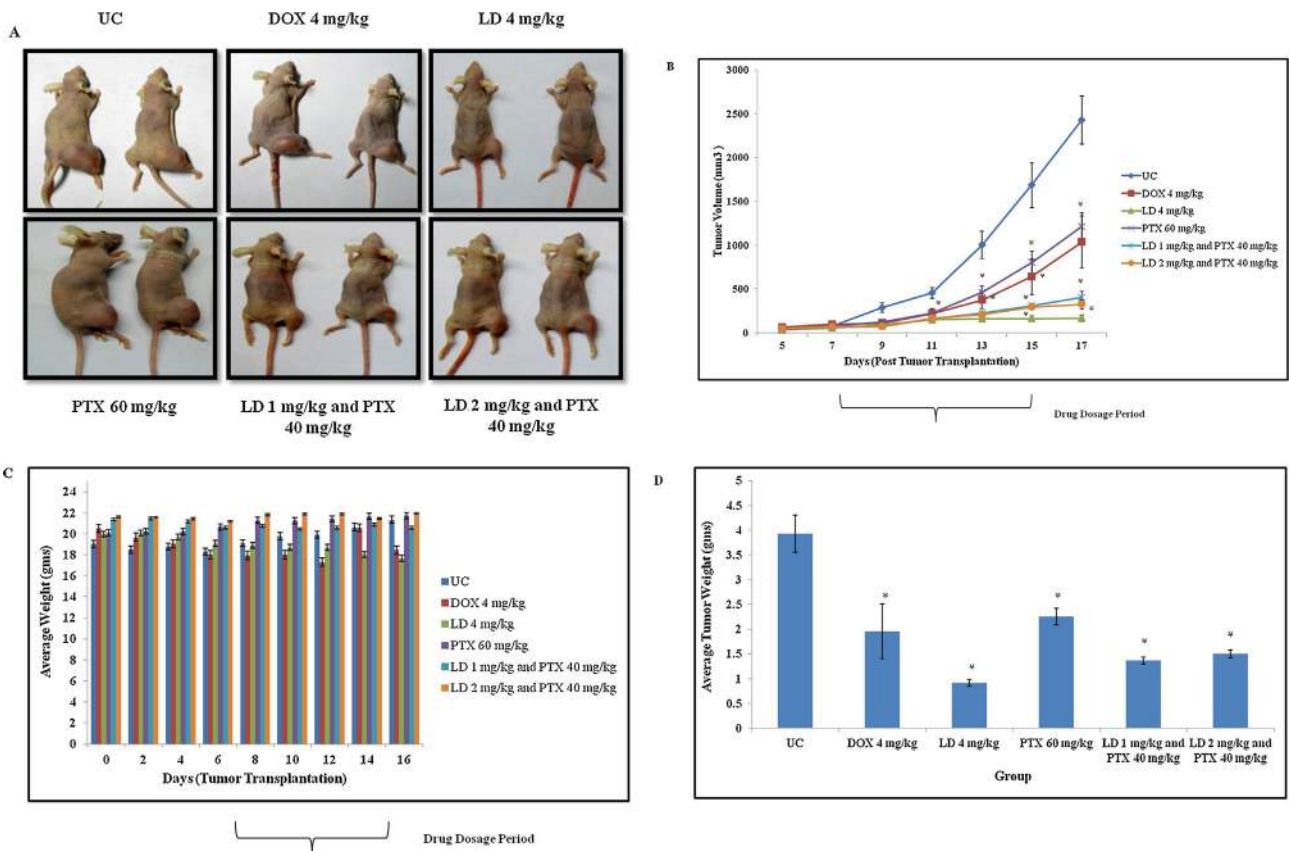


Fig. 10. *In vivo* xenograft model. MDA-MB-231 cells injected sub-cutaneously into nude mice were subjected to treatment using DOX, LD, PTX and their combinations. Mice were sacrificed on day 17th and tumors were excised. A. Images of animals showing tumor grown on the right flank (B) Tumor volumes (C) animal weights at alternate days and (D) average weights of excised tumors.

breast cancer [35]. The % MMP-9 activity was $77.60 \pm 3.46\%$, $75.12 \pm 5.21\%$, $103.51 \pm 1.75\%$, $95.1 \pm 2.98\%$, $77.08 \pm 0.57\%$, $68.94 \pm 2.08\%$ for P1, P2, LD1, LD2, C1 and C2, respectively considering the control to be 100% (Fig. 8A and B). The condition media from HT-1080 was used as a positive control that shows the activity of both gelatinases i.e. MMP-9 (92 kDa) and MMP-2 (72 kDa). Further, MMP-9 in the condition media of MDA-MB-231 cells subjected to gelatin zymography, was found to have a higher molecular weight than corresponding MMP-9 from HT-1080. The plausible reason for such an observation is that MMP-9 might be associated with a small microglobulin that does not separate during the process of zymography and thus, forming a high molecular complex [36].

Wound healing assay was done to assess the anti-migratory effect of combination regimens in MDA-MB-231 cells. It was observed that LD does not affect the process of motility, though at dose of $8 \mu\text{M}$, there was a decrease in migration (approximately 16%). PTX at both the doses (P1 and P2) impedes migration. In the combination regimen, a similar decrease in migration was observed. The % migration was $41.35 \pm 6.63\%$, $31.12 \pm 3.45\%$, $101.58 \pm 10.49\%$, $84.22\% \pm 16.20$, $39.51 \pm 0.24\%$, $23.78 \pm 2.90\%$ for P1, P2, LD1, LD2, C1 and C2, respectively considering the control to be 100% ($^*P < 0.05$). The changes in cellular motility are represented in Fig. 9A and B.

In short, we found out that LD *per se* does not affect the processes of adhesion, invasion and migration but it is rather the doses of PTX that brings about an alteration. It should be noted that anthracyclines, such as DOX suffer from various toxicity related issues for the treatment of breast cancer. However, it is still used in the clinics for its effectiveness. Data from the combination studies clearly showed that PTX when used in conjunction with LD could

target more metastatic pathways than LD alone. In a way, this combination shall serve to limit the doses of DOX as well achieve a wider target range along with PTX in our model system.

3.5. Combination delays tumor growth using *in vivo* xenograft model

In vivo studies form an integral part of chemotherapy. Thus, pre-clinical studies are required to establish the anti-metastatic activities of drugs under investigation. Here, we had used immuno-compromised nude mice (NIH-3) as the xenograft model system to demonstrate the *in vivo* efficacy of PTX, DOX and LD using MDA-MB-231 breast cancer cells. Tumor latency period was found out to be around 4 days. Mice were separated into 6 groups ($n = 5$) as already mentioned. When tumors had reached an approximately 50 mm^3 [37] i.e. by day 7th drug dosage was initiated. The treatment regimen given was as follows:

- group 1 [Untreated or UC (PBS only)];
- group 2 [DOX (4 mg/kg)];
- group 3 [LD (4 mg/kg)];
- group 4 [PTX 60 mg/kg];
- group 5 [PTX + LD (40 mg/kg and 1 mg/kg)];
- group 6 [PTX + LD (40 mg/kg and 2 mg/kg)].

PTX was administered intraperitoneally (ip) in groups 4, 5 and 6 for a period of 9 days consecutively (day 7th till 15th) while DOX/LD was being injected intravenously (groups 2, 3, 5 and 6), once a week for 2 weeks respectively (day 7th and 14th). Mice were sacrificed on day 17th. Representative images are shown in Fig. 10A. The tumor volumes were found out to be $2429.24 \pm 275.85 \text{ mm}^3$, $1035.53 \pm 298.97 \text{ mm}^3$, $167.9 \pm$

38.06 mm³, 1211.263 ± 161.96 mm³, 403.8 ± 69.06 mm³ and 327.1 ± 53.79 mm³ for untreated, DOX (4 mg/kg), LD (4 mg/kg), PTX (60 mg/kg), PTX + LD (40 mg/kg and 1 mg/kg) and PTX + LD (40 mg/kg and 2 mg/kg) groups, respectively (Fig. 10B) (^{*}*P* < 0.05). Further, there were no significant changes in average animal weights in any of the groups under investigation (Fig. 10C). The tumors were also excised and weighed. There was significant difference in combination groups i.e. group 5 and 6 compared to the untreated control (Fig. 10D). The tumors from group 2 and 3 (DOX 4 mg/kg as well as LD 4 mg/kg) clearly demonstrates the effect of LD in the *in vivo* system leading to lower tumor volumes along with weights, because of the better half-life and thereby increased potency of LD (Fig. 10B and D). It should be clearly noted that although the tumor volumes represented for group 3 (LD 4 mg/kg) is much lesser than the combination groups i.e. group 5 PTX + LD (40 mg/kg and 1 mg/kg) and group 6, PTX + LD (40 mg/kg and 2 mg/kg), but the dose for LD given is two and four times the amount given to the latter groups. Thus, the combination surely plays a substantial role in delaying the tumor growth in nude mice at lower doses of both LD and PTX.

Disclosure of interest

The authors declare that they have no conflicts of interest concerning this article.

Acknowledgements

We acknowledge grant support from ACTREC, Tata Memorial Centre. Mr. Peeyush N. Goel is being supported by fellowship from CSIR. The authors also thank Manohar Parker and Nirosha Konduru for providing technical assistance. The authors would like to convey special thanks to the animal house for maintenance of nude mice, flow cytometry and microscopy facilities for their invaluable support.

References

- [1] Siegel R, Naishadham D, Jemal A. Cancer statistics, 2013. *CA: Cancer J Clin* 2013;63:11–30.
- [2] Ferlay J, Shin HR, Bray F, Forman D, Mathers C, Parkin DM. Estimates of worldwide burden of cancer in 2008: GLOBOCAN 2008. *Int J Cancer* 2010;127:2893–917.
- [3] Bray F, Jemal A, Grey N, Ferlay J, Forman D. Global cancer transitions according to the Human Development Index (2008–2030): a population-based study. *Lancet Oncol* 2012;13:790–801.
- [4] Irmisch A, Huelsken J. Metastasis: New insights into organ-specific extravasation and metastatic niches. *Exp Cell Res* 2013;319:1604–10.
- [5] Carey L, Winer E, Viale G, Cameron D, Gianni L. Triple negative breast cancer: disease entity or title of convenience? *Nat Rev Clin Oncol* 2010;7:683–92.
- [6] Andreopoulou E, Sparano J. Chemotherapy in patients with anthracycline and taxane-pretreated metastatic breast cancer: an overview. *Curr Breast Cancer Rep* 2013;5:42–50.
- [7] DiMasi JA, Hansen RW, Grabowski HG. The price of innovation: new estimates of drug development costs. *J Health Econ* 2003;22:151–85.
- [8] Mullard A. Could pharma open its drug freezers? *Nat Rev Drug Discov* 2011;10:399–400.
- [9] Hirsh L, Dantes A, Suh BS, Yoshida Y, Hosokawa K, Tajima K, et al. Phosphodiesterase inhibitors as anti-cancer drugs. *Biochem Pharmacol* 2004;68:981–8.
- [10] Zhang M, Xu YJ, Mengi SA, Arneja AS, Dhalla NS. Therapeutic potentials of pentoxifylline for treatment of cardiovascular diseases. *Exp Clin Cardiol* 2004;9:103–11.
- [11] Misirlioglu C, Demirkasimoglu T, Kucukplakci B, Sanri E, Altundag K. Pentoxifylline and alpha-tocopherol in prevention of radiation-induced lung toxicity in patients with lung cancer. *Med Oncol* 2007;24:308–11.
- [12] Bravo-Cuellar A, Hernandez-Flores G, Lerma-Diaz JM, Dominguez-Rodriguez JR, Jave-Suarez LF, De Celis-Carrillo R, et al. Pentoxifylline and the proteasome inhibitor MG132 induce apoptosis in human leukemia U937 cells through a decrease in the expression of Bcl-2 and Bcl-XL and phosphorylation of p65. *J Bio Sci* 2013;20:13.
- [13] Dua P, Gude RP. Anti-proliferative and antiproteolytic activity of pentoxifylline in cultures of B16F10 melanoma cells. *Cancer Chemother Pharmacol* 2006;58:195–202.
- [14] Goel PN, Gude RP. Unravelling the anti-metastatic potential of pentoxifylline, a methylxanthine derivative in human MDA-MB-231 breast cancer cells. *Mol Cell Biochem* 2011;358:141–51.
- [15] Goel PN, Gude RP. Curbing the focal adhesion kinase and its associated signaling events by pentoxifylline in MDA-MB-231 human breast cancer cells. *Eur J Pharmacol* 2013;714:432–41.
- [16] Goel PN, Gude RP. Pentoxifylline regulates the cellular adhesion and its allied receptors to extracellular matrix components in breast cancer cells. *Biomed Pharmacother* 2013. 10.1016/j.biopha.2013.09.002.
- [17] Zimmermann GR, Lehar J, Keith CT. Multi-target therapeutics: when the whole is greater than the sum of the parts. *Drug Discov Today* 2007;12:34–42.
- [18] Octavia Y, Tocchetti CG, Gabrielson KL, Janssens S, Crijns HJ, Moens AL. Doxorubicin-induced cardiomyopathy: from molecular mechanisms to therapeutic strategies. *J Mol Cell Cardiol* 2012;52:1213–25.
- [19] Tacar O, Sriamornsak P, Dass CR. Doxorubicin: an update on anticancer molecular action, toxicity and novel drug delivery systems. *J Pharm Pharmacol* 2012;65:157–70.
- [20] Bravo-Cuellar A, Ortiz-Lazareno PC, Lerma-Diaz JM, Dominguez-Rodriguez JR, Jave-Suarez LF, Aguilar-Lemarroy A, et al. Sensitization of cervix cancer cells to adriamycin by pentoxifylline induces an increase in apoptosis and decrease senescence. *Mol Cancer* 2010;9:114.
- [21] Lerma-Diaz JM, Hernandez-Flores G, Dominguez-Rodriguez JR, Ortiz-Lazareno PC, Gomez-Contreras P, Cervantes-Munguia R, et al. In vivo and in vitro sensitization of leukemic cells to adriamycin-induced apoptosis by pentoxifylline. Involvement of caspase cascades and IκBα phosphorylation. *Immunol Lett* 2006;103:149–58.
- [22] Manjappa AS, Goel PN, Vekataraju MP, Rajesh KS, Makwana K, Ukawala M, et al. Is an alternative drug delivery system needed for docetaxel? The role of controlling epimerization in formulations and beyond. *Pharm Res* 2013;30:2675–93.
- [23] Chou T, Martin N. CompuSyn Software for drug combinations and for general dose-effect analysis and user's guide. Paramus, NJ: ComboSyn; 2007.
- [24] Ribble D, Goldstein NB, Norris DA, Shellman YG. A simple technique for quantifying apoptosis in 96-well plates. *BMC Biotechnol* 2005;5:12.
- [25] Munoz R, Man S, Shaked Y, Lee CR, Wong J, Francia G, et al. Highly efficacious nontoxic pre-clinical treatment for advanced metastatic breast cancer using combination oral UFT-cyclophosphamide metronomic chemotherapy. *Cancer Res* 2006;66:3386–91.
- [26] Nicolini A, Carpi A. Advanced breast cancer: an update and controversies on diagnosis and therapy. *Biomed Pharmacother* 2003;57:439–46.
- [27] Nicolini A, Giardino R, Carpi A, Ferrari P, Anselmi L, Colosimo S, et al. Metastatic breast cancer: an updating. *Biomed Pharmacother* 2006;60:548–56.
- [28] Gennari A, D'Amico M. Anthracyclines in the management of metastatic breast cancer: state of the art. *Eur J Cancer Suppl* 2011;9:11–5.
- [29] Otsuka M, Matsuda Y. Programmable drug release of highly water-soluble pentoxifylline from dry-coated wax matrix tablets. *J Pharm Sci* 1995;84:443–7.
- [30] Taherian A, Mazoochi T. Different expression of extracellular signal-regulated kinases (ERK) 1/2 and phospho-Erk proteins in MBA-MB-231 and MCF-7 cells after chemotherapy with doxorubicin or docetaxel. *Iran J of Basic Med Sci* 2012;15:669–77.
- [31] Bar-On O, Shapira M, Hershko DD. Differential effects of doxorubicin treatment on cell cycle arrest and Skp2 expression in breast cancer cells. *Anticancer Drugs* 2007;18:1113–21.
- [32] Nguyen DX, Bos PD, Massague J. Metastasis: from dissemination to organ-specific colonization. *Nat Rev Cancer* 2009;9:274–84.
- [33] Bacac M, Stamenkovic I. Metastatic cancer cell. *Annu Rev Pathol* 2008;3:221–47.
- [34] Sanes JR, Engvall E, Butkowski R, Hunter DD. Molecular heterogeneity of basal laminae: isoforms of laminin and collagen IV at the neuromuscular junction and elsewhere. *J Cell Biol* 1990;111:1685–99.
- [35] Scorilas A, Karameris A, Arnoyianni N, Ardavanis A, Bassilopoulos P, Trangas T, et al. Overexpression of matrix metalloproteinase-9 in human breast cancer: a potential favourable indicator in node-negative patients. *Br J Cancer* 2001;84:1488–96.
- [36] Snoek-van Beurden PA, Von den Hoff JW. Zymographic techniques for the analysis of matrix metalloproteinases and their inhibitors. *Biotechniques* 2005;38:73–83.
- [37] Teicher BA. Tumor models for efficacy determination. *Mol Cancer Ther* 2006;5:2435–43.

Investigating the effects of Pentoxifylline on human breast cancer cells using Raman spectroscopy

Peeyush N. Goel*, S. P. Singh[†], C. Murali Krishna^{†,‡}
and R. P. Gude*

*Gude Lab, ACTREC, Tata Memorial Center
Kharghar, Navi Mumbai 410210 India

[†]Chilakapati Lab, ACTREC, Tata Memorial Center
Kharghar, Navi Mumbai 410210 India

[‡]mchilakapati@actrec.gov.in

Received 21 February 2014

Accepted 24 March 2014

Published 25 April 2014

Breast cancer is one of the leading causes of cancer-related deaths in a global scenario. In the present study, biochemical changes exerted upon Pentoxifylline (PTX) treatment had been appraised in human breast cancer cells using Raman spectroscopy. There are no clinically approved methods to monitor such therapeutic responses available. The spectral profiling is suggestive of changes in DNA, protein and lipid contents showing a linear relationship with drug dosage. Further, multivariate analysis using principal-component based linear-discriminant-analysis (PC-LDA) was employed for classifying the control and the PTX treated groups. These findings support the feasibility of Raman spectroscopy as an alternate/adjunct label-free, objective method for monitoring drug-induced modifications against breast cancer cells.

Keywords: Pentoxifylline; MDA-MB-231 breast cancer cells; Raman spectroscopy; spectra; multivariate analysis.

1. Introduction

Cancer is the leading cause of worldwide deaths. It is a micro-evolutionary process based on its ability to render genetic alterations, compete and confer unlimited replication potential to the cells.¹ One of the main reasons for cancer-related deaths is the dissemination of tumor cells to different target sites, a process referred to as metastasis. Breast cancer accounts for the second most leading cause of

cancer-related deaths.² The treatment regimen encompasses surgery, radiotherapy followed by chemotherapy. Metastatic breast cancer poses a big challenge for treatment owing to limited therapeutic interventions.

Therapeutic switching or finding newer uses of currently available drugs is one of the most challenging and exciting areas of research in the pharmaceutical industry.³ Pentoxifylline (PTX),

This is an Open Access article published by World Scientific Publishing Company. It is distributed under the terms of the Creative Commons Attribution 3.0 (CC-BY) License. Further distribution of this work is permitted, provided the original work is properly cited.

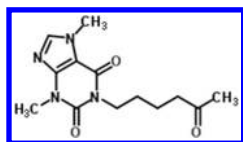


Fig. 1. Structure of Pentoxifylline, a tri-substituted xanthine derivative designated chemically as 1-(5-oxohexyl)-3,7-dimethylxanthine.

1-(5-oxohexyl)-3,7-dimethyl-xanthine (structure shown in Fig. 1) belongs to a class of hemorrheologic agents. It is being used in the treatment of peripheral vascular diseases.⁴ Being a phosphodiesterase inhibitor, it elevates the levels of c-AMP thereby affecting various aspects of cellular behavior associated with metastasis. However, various c-AMP elevators such as forskolin, IBMX, dibutyl cAMP are excluded from chemotherapeutic regimens due to their toxicity.⁵ Recently, PTX has been shown to exert anti-metastatic activity in MDA-MB-231 human breast cancer cells.⁶ At sub-toxic doses (1, 2.5 and 5 mM), PTX affects cellular proliferation, cellular invasion and migration. It induced a cell cycle block at G1 phase followed by apoptosis. However, alterations in the biochemical design/structure in breast cancer cells upon PTX treatment needs to be sought out. The biochemical framework comprises of proteins, carbohydrates, lipids and nucleic acid. It is the combinatorial endeavours of these biomolecules that form and regulate the functioning of living organization. Thus, investigation of the changes in the intracellular milieu of breast cancer cells upon PTX treatment will explore its targeted action.

PTX has shown to affect protein catabolism and suppress protein levels promoting hepatoprotective effects.^{7,8} It causes a decrease in oxidized lipid products and alters membrane fluidity.^{9–11} Further, it also regulates homologous recombination repair and carbohydrate metabolism.^{12,13} Various modalities such as use of complex cellular techniques, immunohistological analysis for determining drug associated changes are relatively less sensitive and preclude the complete scenario of the associated effects.¹⁴ Hence, newer techniques that surpass these drawbacks and limitations need to be explored.

Raman spectroscopy, an analytical technique based on vibrational spectroscopy is sensitive to biochemical variations and provides molecular fingerprints. It has been applied to a variety of applications ranging from medicine to forensic sciences.^{15–18} A typical Raman spectrum is the result of

inelastic scattering leading to a shift in the frequency of the incident excitation light. The wavelength shift is specific and thus can provide information about chemical and structural state of a biomolecule. The greatest benefit of this technique is its label-free nature and noninvasive perception.¹⁹ It has the advantage of having minimum interference from water bands which makes it more appropriate for biomedical applications²⁰ and provides an easy, chemical-free and nondestructive method for studying cells *in vitro*, cell drug interactions as well as for distinguishing neoplastic from normal tissues.^{21–32}

Each tumor is composed of several distinct cell populations and thus the potential and efficacy of chemotherapy is largely governed by the presence of most chemosensitive or rather least resistant cell populations. Identification of a resistant/sensitive phenotype in cancer cells from the patients can enhance the efficacy of therapy. Various studies on identification of multi-drug resistant phenotypes in ovarian and leukemic cells had demonstrated the prospective of Raman spectroscopy as an objective and label-free cell sensor.^{22,33,34} Along the similar lines, we have extended our approach to assess the biochemical alterations in breast cancer cells upon PTX treatment at sub-toxic doses.

2. Materials and Methods

2.1. Cell line and culture conditions

MDA-MB-231, human breast cancer cell line was procured from National Centre for Cell Sciences (NCCS), Pune, India. Cells were maintained in Dulbecco's modified, Eagle medium (DMEM, GIBCO) supplemented with 10% heat inactivated fetal bovine serum (FBS) (GIBCO) and antibiotics (100 U/mL penicillin and 100 μ g/mL streptomycin). Cell cultures were maintained at 37°C in 5% CO₂ humidified atmosphere.

2.2. Cell viability assay

Briefly, 5000 cells/well were seeded into a 96-well plate format. After 24 h, PTX (1–30 mM) was added in complete medium and incubated for another 24 h. 10 μ L KineticBlue™ solution was then added into medium and incubated at 37°C overnight. Optical density was recorded at 570–600 nm for the plate and the blank intensity was deducted from the test samples. The results were plotted in a

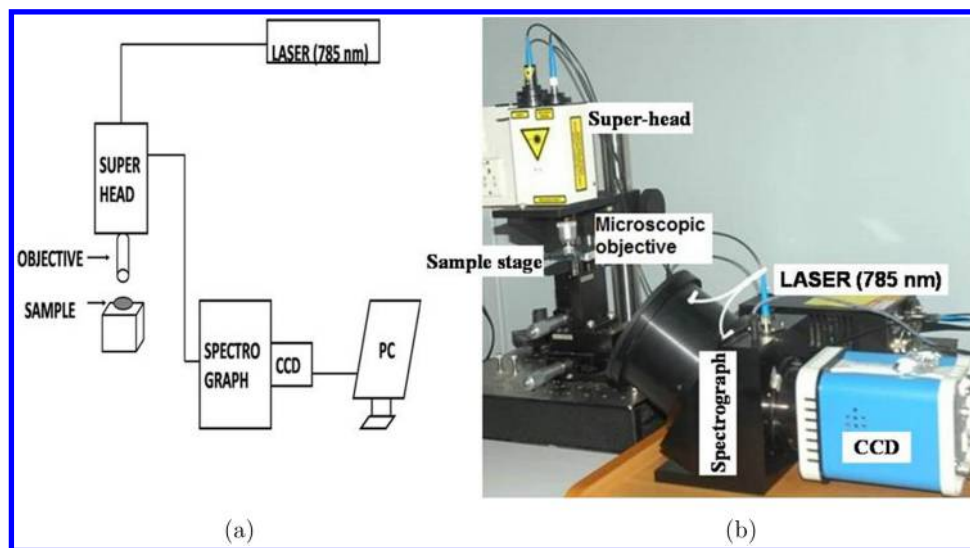


Fig. 2. Raman microprobe employed for acquiring spectrum from cell pellets. (a) Schematic Representation, (b) Photographic representation.

logarithmic scale where the x -axis represents % viability and the y -axis represents concentration of PTX (mM).

2.3. Preparation of cells for Raman spectroscopy

Cells were seeded in 100 mm plates (BD Biosciences) containing complete medium (DMEM with serum). When the cells reached a confluency of about 70–80%, plain medium (DMEM without serum) was added for synchronizing cells. Nutritional elimination (by removing serum) is a commonly used method for cell synchronization and causes the cells to accumulate in G1 phase of the cell cycle. Following this, different doses of PTX (0, 1 2.5 and 5 mM) were added to each of the plates and incubated for 24 h. Cells were washed twice with phosphate buffered saline (PBS) and then removed using saline-EDTA. Cells were later harvested by centrifugation at 1500 rpm for 5 min and cell pellets were collected. Plates were taken in duplicates for control as well as for PTX treated groups and the experiments were repeated thrice.

2.4. Spectral acquisition

Raman spectra from cell pellets, placed on a calcium fluoride (CaF_2) window, were acquired using fiber-optic Raman microprobe system (Horiba-Jobin-Yvon, France). Briefly, the system consisted of a

laser of 785 nm wavelength (PI-ECL-785-300-FC, Process Instruments) as an excitation source, HE 785 spectrograph (Horiba-Jobin-Yvon, France) coupled with CCD (1024x256-BIDD-SYN, Synapse) as dispersion and detection elements, respectively. Optical filtering of unwanted noise, including Rayleigh signals was executed through “SuperHead”, the auxiliary component of the system. Optical fibers were employed to connect the excitation and detection systems. Raman microprobe was assembled by coupling a 50X microscopic objective (Nikon, NA 0.8) to the “SuperHead”. The spectrograph was equipped with a fixed grating of 950 gr/mm and spectral resolution as per the manufacturer’s specification was $\sim 4 \text{ cm}^{-1}$. Photographic representation of the instrument is shown in Fig. 2. A total of 204 spectra were acquired with the following parameters: laser power-40 mW, integration time-10s and averaged over six accumulations.

2.5. Spectral pre-processing and multivariate analysis

Spectral pre-processing of Raman spectra from the control and PTX treated cells was performed using Labspec 5.0 software (Horiba-Jobin-Yvon) as per the standard protocol described earlier.^{35,36} In the first step, the wavelength dependency of the detector and the polarization dependence of the optical elements were measured using a calibration standard (standard reference material number -2241;

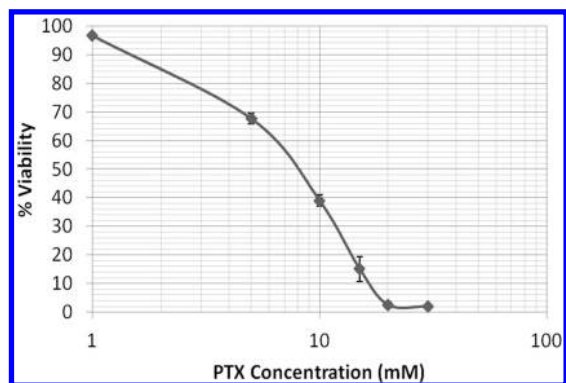


Fig. 3. Cell viability assay. Cells were seeded in 96-well format and different doses of PTX (1–30 mM) were added for 24 h. After, overnight incubation on adding Kinetic blue, absorbance was recorded at 570–600 nm. Results were plotted in log scale where x -axis represent % Viability and y -axis corresponds to PTX concentration (mM).

NIST, Gaithersburg, MD, USA). The measured Raman spectra were divided by spectrum associated with the instrument response. Spectral contribution of optical elements i.e., the background signals were obtained by acquiring spectra of CaF_2 window without the sample under similar conditions. The response corrected background spectrum was then subtracted. In order to remove the influence of slow-moving fluorescence background, first derivative spectrum was computed using Savitzky–Golay filter mechanism (window size-3). Correction for spectral differences due to relative intensity changes was performed by vector normalization. First derivative and vector normalized spectra were interpolated in $800\text{--}1800\text{ cm}^{-1}$ region^{16,22,26,28,31–33} and used as input for multivariate analysis by principal component-linear discriminant analysis (PC-LDA). PC-LDA models were then validated by leave-one-out cross-validation (LOOCV). Algorithms for these analyses were implemented in MATLAB-(Mathworks Inc., USA) based software using in-house codes.³⁷

The average spectra were computed from the background subtracted spectra prior to derivatization. This was performed by averaging the y -axis variations, keeping the x -axis constant for each class and the baseline corrections by fitting a 5th-order polynomial function. These baseline corrected spectra were used for spectral comparisons across all groups. Difference spectra was generated by subtracting the average spectra of cells treated with different sub-toxic concentrations of PTX viz. 1, 2.5 and 5 mM, from the control cells.

3. Results and Discussion

3.1. PTX affects cellular viability and proliferation

The foremost step to elucidate the cytotoxic effects of PTX was to perform a cell viability assay. As shown in Fig. 3, a dose-dependent decrease in cell viability was observed with approximate 100% cell death at 20 mM. Inhibitory concentration₅₀ (IC_{50}) i.e., the concentration required to kill half the population of cells was observed to be approximately 8 mM. A famous axiom in toxicology by Paracelsus states, “The dose makes the poison”. As per the doctrine, it is the dose that determines the outcome of a biological process. In our study, we have therefore evaluated the effects of PTX at sub-toxic doses i.e., doses exhibiting a maximal of 30% toxicity or till IC_{30} . Higher doses have been excluded from the same in purview of this rationale. Based on these observations, doses within sub-toxic range were selected i.e., 1, 2.5 and 5 mM for Raman studies. In an independent study, these sub-toxic doses of PTX have shown to minimally affect the normal or nontumorigenic HaCaT cells. The survival fraction of the normal cells at these sub-toxic doses was found to be around 90%.³⁸ In view of reported facts, the sub-toxic doses used in our study were found to be more detrimental against the breast cancer cells compared to normal cells.

PTX affects cellular proliferation which is evident by the viability curve. In our earlier work we had shown that PTX caused a G1 cell cycle block inducing apoptosis in breast cancer cells.⁶ This observation is in accordance to the earlier reports that describe an increase in c-AMP, upon phosphodiesterase inhibition thus inducing a G1 block. c-AMP is 3'-5'-cyclic adenosine monophosphate that functions as a secondary messenger. It is known to alter gene expression by its effect on c-AMP response element-binding protein (CREB).

Being a transcription factor, CREB thus regulates gene expression by binding to a DNA sequence (5'-TGACGTCA-3') referred to as the c-AMP response elements (CRE).³⁹ In light of this, we propose a similar mode of action for PTX.

3.2. Analysis of Raman spectral profiles

Several studies have conclusively demonstrated that wavelength of 660 nm or above do not induce photodamage.^{40–43} In accordance to these observations

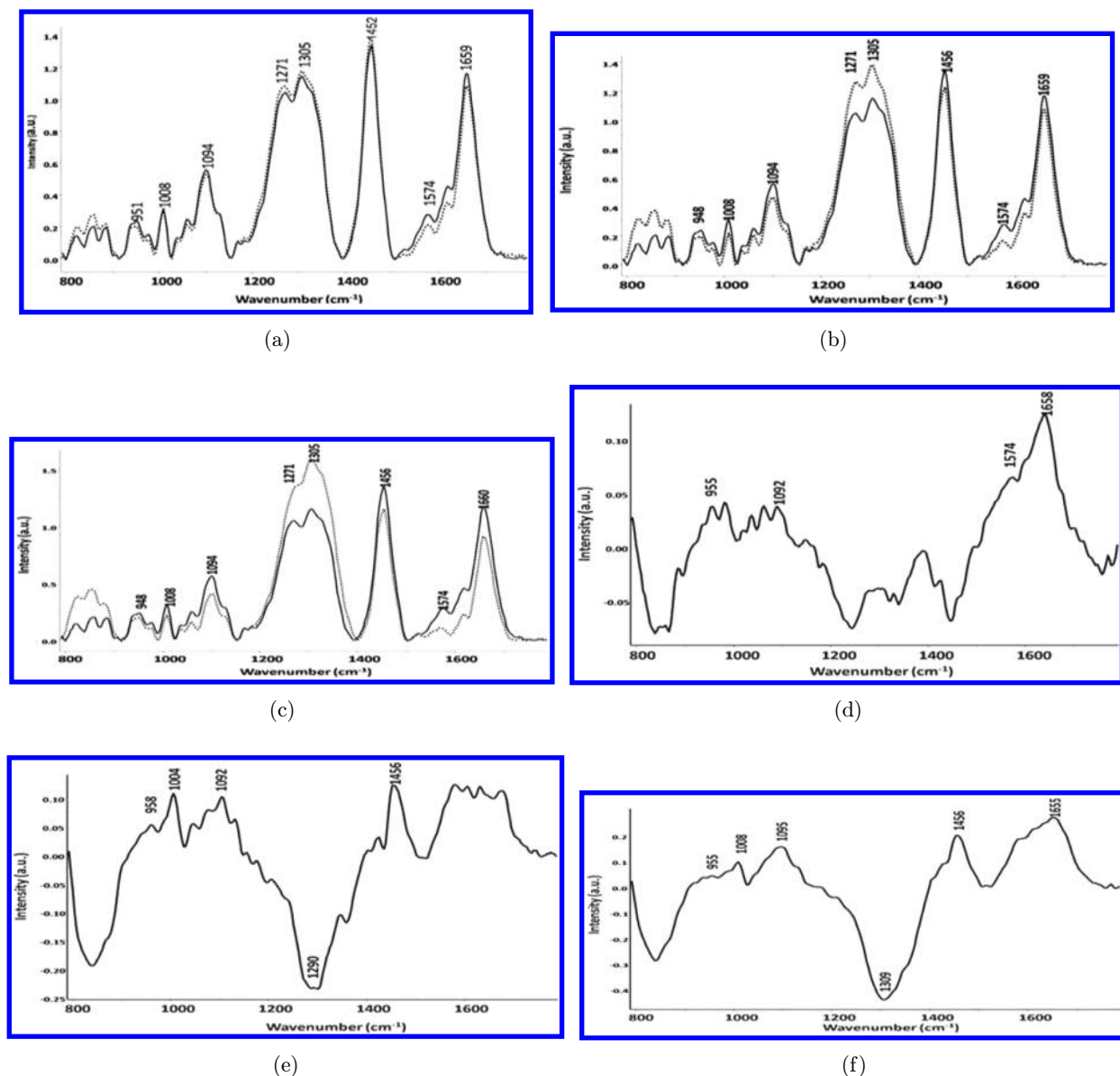


Fig. 4. Mean spectra of MDA-MB-231 cells: control (solid line), PTX treated (broken line) (a)-1 mM, (b)-2.5 mM, (c)-5 mM. Comparison of difference spectra across control and treatment groups (d): Control – 1 mM PTX treatment, (e): Control– 2.5 mM PTX treatment and (f): Control — 5 mM PTX treatment.

in the present study, breast cancer cells treated with PTX that were exposed to 785 nm excitation do not show any photodamage. Therefore, the observed differences in the spectra could be attributed to differential drug treatment regimens.

The mean baseline corrected Raman spectra in the range of 800–1800 cm^{-1} for the control (solid line) and PTX treated (broken line) MDA-MB-231 cells for 24 h are shown in Figs. 4(a)–4(c). Differences in Raman bands associated with DNA backbone, DNA ring bases, lipids and protein vibrations were observed. The band at 1094 cm^{-1} is considered

as an internal standard for DNA content and has been assigned to the symmetric stretching vibration mode of PO_2^{2-} backbone in DNA. As can be seen from Figs. 4(a)–4(c), intensity of the peak at 1094 cm^{-1} is less in PTX-treated groups in comparison to the controls, suggesting changes in the DNA content due to drug intervention. This observation is also supported by a similar variation observed in the guanine band at 1576 cm^{-1} . Cells treated with 5 mM PTX showed low DNA content as compared to control and the other treatment groups. A linear increase with drug dosage was

observed for the bands around 1280 cm^{-1} (= CH bending of lipids) and 1305 cm^{-1} (CH_3/CH_2 bending of phospholipids) suggesting changes in lipid profile upon PTX exposure.^{44–47} This is in concordance with already mentioned reports on PTX affecting membrane fluidity by altering lipids.^{9–11} Minor changes in free amino acids indicated by the bands around 950 cm^{-1} (proline), phenylalanine (1008 cm^{-1}), 1620 cm^{-1} (tryptophan), suggesting changes in overall protein content after drug treatment were also observed. This is further supported by the decrease in the intensity of amide I band around 1660 cm^{-1} . Alterations in these bands serve as a probe for the conformational variability, which could arise due to drug treatment. The intensity of the band at 1660 cm^{-1} decreases linearly with drug dosage in the treatment groups with respect to control, suggesting a decrease in the protein content upon drug treatment.

In the next step, to highlight the spectral differences between the control and treatment groups distinctly, difference spectra were computed. The subtraction of mean spectra is one of the conventional ways of identifying spectral differences over a selected spectral range. It can provide the information regarding moieties being altered. The mean spectra of cells treated with 1, 2.5 and 5 mM PTX were subtracted from that of the control group. The positive bands characterize the control group while the negative bands represent PTX-treated groups. A reduction in the protein and DNA content marked by positive amide I (1660 cm^{-1}) and DNA (1094 cm^{-1}) bands was observed, Fig. 4(d). These differences were more pronounced in cells treated with higher doses of PTX i.e., 2.5 and 5 mM. Changes in lipid profile due to drug treatment, evident by the negative bands around 1280 and 1305 cm^{-1} , were also observed. As shown in Figs. 4(e) and 4(f), the intensity of positive DNA band ($1094, 1574\text{ cm}^{-1}$) was highest for the cells treated with 5 mM drug, indicating that the cells treated with 5 mM PTX have the lowest DNA content. This observation was consistent with the other two doses as well. These changes can be attributed to the fact that increase in *c*-AMP, upon PTX treatment, leads to differential regulation of CRE sequences of DNA. This sequence consists of guanine nucleotides and thus can be designated as a point for this distinctive execution. PTX has been earlier shown to inhibit DNA content of neuroblastoma cells.¹¹ Further it decreases cells in S phase (duplication phase) which is also indicative of

decrease in DNA content. Positive bands at phenylalanine, CH_2 (1450 cm^{-1}), and amide I suggest that cells treated with PTX exhibited decrease in overall protein content in comparison to the control group. Overall, major changes in DNA, protein and lipids were observed upon drug treatment. These changes do appear to have a linear relationship with drug concentration i.e., cells treated with highest dose of 5 mM exhibits maximal changes followed by 1 and 2.5 mM dosage, respectively.

3.3. Multivariate analysis

The next step of classification between control and treated cells was explored using the PC-LDA method. PCA is a routinely used method for data compression and visualization. It describes data variance by identifying a new set of orthogonal features known as principal components (PCs) or factors. For visual discrimination, we project each of the spectra in the newly formed co-ordinate space of selected PCs. While PCA aims to identify features that represent variance among complete data, LDA provides data classification based on an optimized criteria leading to better class separation. In LDA, the classification criterion is identified using the scatter measure of within class and between class variance. LDA can be used in companion with PCA to increase the efficiency of the classification. For this, PCA scores obtained using a set of significant PCs with maximum variance amongst data, are used as input data for LDA-based classification. It has an advantage of eliminating or minimizing noise from the data and concentrates on variables important for classification. In our analysis, significant PCs ($p < 0.05$) were selected as input for LDA. In order to avoid over-fitting of the data, as a thumb rule, total number of factors selected for analysis were less than half the number of the spectra in the smallest group.^{48–50} First derivative and vector normalized spectra were fed in to MATLAB-based algorithm and PC-LDA using 15 factors with $\sim 73\%$ classification efficiency was performed. Profiles of PCs also known as factor loadings can provide vital clues on biochemical variations among different classes. Loading plots of factor 1 and 2 that lead to delineation among control and treated groups are presented in Fig. 5. Corroborating spectral variability suggested by difference spectra loading plots also suggest differences in protein and lipid content of control and

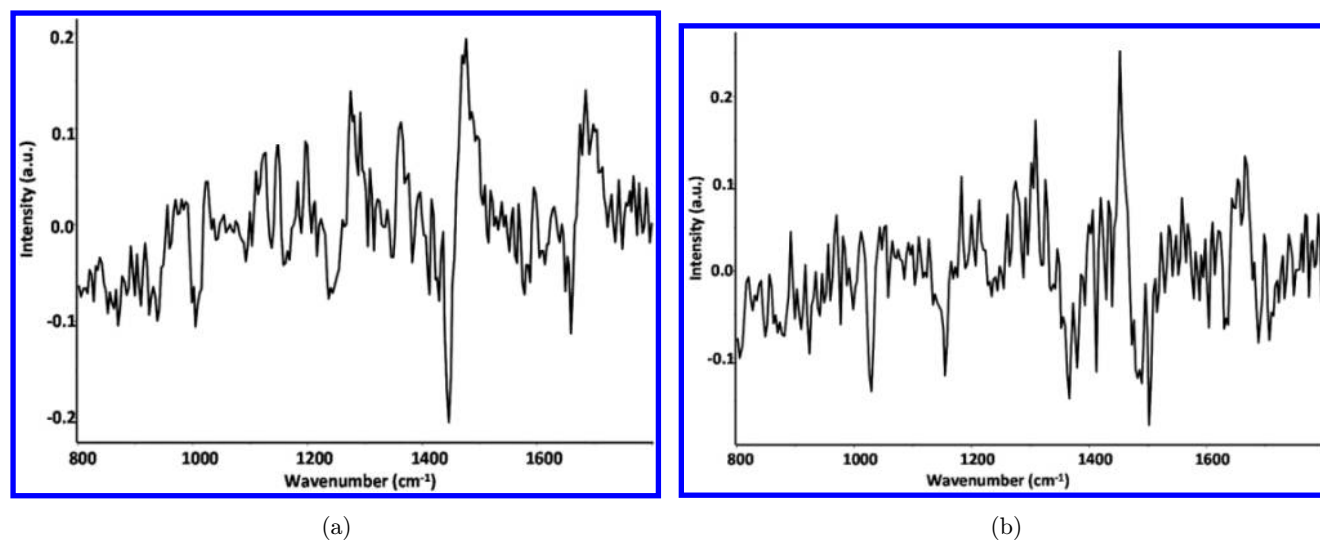


Fig. 5. Loading plots of factors used for classification (a) Factor 1 (b) Factor 2.

treated group. The first PC (PC1) has two major bands that correspond to CH_3/CH_2 bending modes of phospholipids and CH_2 stretching modes, respectively. In the second component (PC2) the main peak features correspond to $=\text{CH}$ bending of lipids and amide I, in addition to smaller bands similar to PC1.

The scatter plot generated using score of factor 1 and factor 2 is shown in Fig. 6. It can be seen that the spectra of cells treated with 1 mM drug (\blacklozenge) showed an overlap with control cells (\triangle) while

separate clusters belonging to the spectra from other two groups i.e., 2.5 (\blacksquare) and 5 mM (\bullet) were obtained. This observation can be best explained as per the fact that, as 1 mM corresponds to the lowest sub-toxic dose, it might have a minimal effect on the biochemical environment of cells in comparison to cells treated with other two higher sub-toxic doses. The same results are presented in Table 1. As can be seen, 39/53 spectra of control cells were correctly classified. A total of 14 spectra were misclassified, of these 10 were with cells treated with 1 mM drug

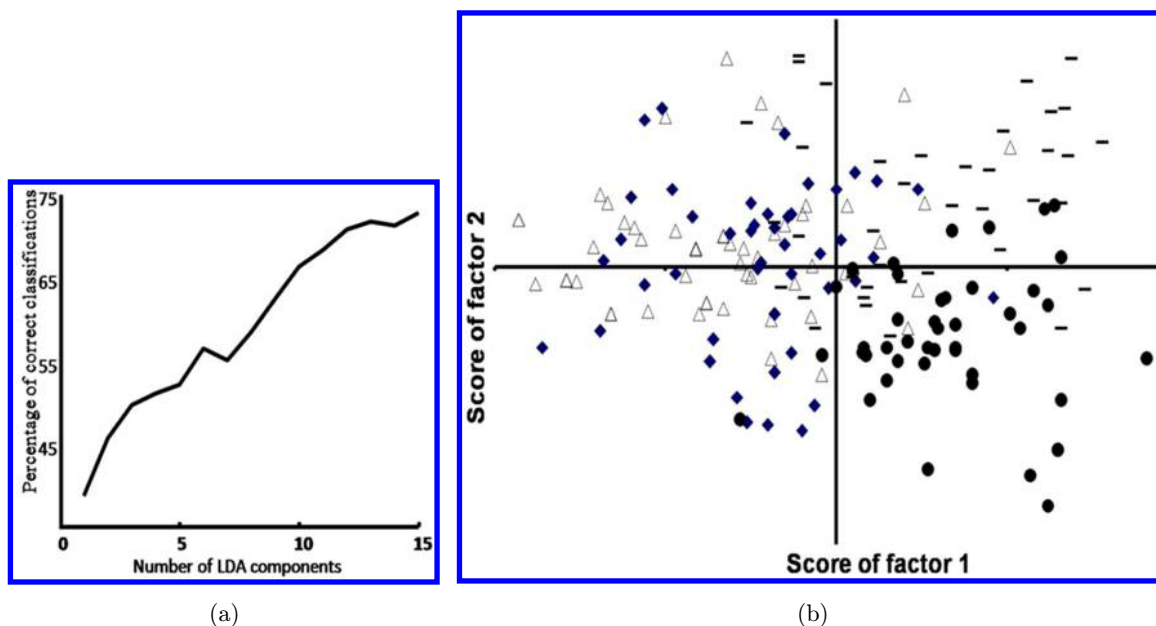


Fig. 6. PC-LDA of control cells (\triangle) and the cells treated with 1 (\blacklozenge), 2.5 (\blacksquare), and 5 mM drug doses (\bullet). (a) Scree plot (b) Scatter plot.

Table 1. Summary of classification after PC-LDA and LOOCV between control and PTX-treated MDA-MB-231 cells (diagonal elements are true positive predictions and ex-diagonal elements are false positive predictions).

	Untreated	1 mM	2.5 mM	5 mM
Untreated	39/53	10	1	3
1 mM	7	37/53	6	3
2.5 mM	2	5	33/47	7
5 mM	3	1	8	39/51
Leave-one-out-cross validation				
Untreated	29/53	17	3	4
1 mM	10	32/53	7	4
2.5 mM	7	8	23/47	9
5 mM	5	1	14	31/51

dose and remaining 4 with other two doses i.e., 2.5 and 5 mM. A similar trend was observed for cells treated with 1 mM drug dose, here 37/53 spectra were correctly classified (70%) and maximum misclassifications were observed with control cells. This can be explained on the basis of previously described fact that cells treated with 1 mM dose might not have acquired enough changes in their biochemical milieu with respect to control or untreated cells. Further, a dose of 1 mM exerts mere 10% cytotoxicity and therefore misclassification with control cell population is expected. In case of cells treated with 2.5 mM or the median drug dose, 33/47 spectra were correctly classified (70%). Here of the 14 misclassifications, 7 were with cells treated with 5 mM drug dose. Only two spectra were misclassified with control group. Similarly, in case of cells treated with 5 mM drug dose, 39/51 spectra were correctly classified (76%). Of the 12 misclassifications, 8 were with cells treated with 2.5 mM drug dose and only 1 spectrum was misclassified with the control cells, suggesting that cells had undergone biochemical changes reflected by the decreased misclassification with the control group. In addition, we had employed LOOCV, a commonly used method for the validation of results of supervised analysis, in the absence of an independent test dataset. As can be seen from Table 1, 29 of the 53 spectra from control groups were correctly classified; of the 24 misclassification, 17 blend with cells treated with minimal drug dose i.e., 1 mM. Similarly, of the total 53 spectra acquired from cells treated with 1 mM drug, 32 were correctly classified and among 21 misclassifications, 10 were with the control group which was consistent with our earlier

observations. Further, of the total 47 spectra of cells treated with 2.5 mM, 23 were correctly classified. A closer view of Table 1 reveals that the misclassifications were distributed across all the groups with minimal numbers contributed by the untreated group. About 31 out of 51 spectra from cells treated with 5 mM drug dose were correctly assorted. Most importantly, only 5 and 1 spectra were misclassified with control and cells treated with 1 mM dose, respectively. Overall findings indicate that control and treated cells can be categorized but with a varying efficiency. The differential sensitivity of cells in a pellet toward PTX treatment could be a plausible explanation for such misclassifications. It should be noteworthy that most of the misclassifications are among groups harboring overlapping features. Further, the doses used in our studies i.e., 1, 2.5 and 5 mM are relatively sub-toxic and far below the cytotoxic dose of the drug. The maximal toxicity undertaken in the present study at 5 mM dose is around 30%. Thus, overlaps and misclassifications are expected within the different doses under investigation. At higher toxic doses, such misclassifications may be minimal but such high doses shall be deleterious for cells. These high doses are generally avoided from therapeutic point of view and thus had been excluded in the present study as well.

Additionally, it is important to note that Raman spectra in the present study were acquired using cell pellets rather than single cells. As per the manufacturer specifications, the laser spot size of the setup is $\sim 5-10 \mu\text{m}$ and the probing volume is ~ 500 cubic microns suggesting that in a pellet, the probing beam can encounter a stack of heterogeneous population of cells (drug sensitive or resistant) raising a possibility that the probed area could be at many different cellular components as well as many cells.

4. Conclusions

Earlier studies on cell pellets had demonstrated the potential of Raman spectroscopy in classifying single cell type among a mixed cancer cell population, HPV detection, discrimination of wild and multi-drug resistant cell types.^{22,33,34,51,52} In the present study, we had explored the usage of cell pellets to identify the cellular changes impinged upon PTX treatment. Mean and difference spectra suggest

major changes in DNA, lipid and protein profile of cells due to drug treatment, which is consistent with existing literature. These changes appear to have a linear relationship with drug dosage. Variations in DNA content can be primarily due to increase in c-AMP level that regulates the action of CREB protein, a transcription factor that affects the CRE of DNA. Multivariate analysis PC-LDA demonstrated the feasibility of categorizing control and treated groups. Overlaps among spectra of cells treated with different drug doses can be ascribed to differential activity of the drug on cells, selection of relatively sub-toxic doses and presence of heterogeneous (sensitive/resistant) cell populations. The findings of the study supports the applicability of Raman spectroscopic method as a valuable real time, label-free cell sensor in assessing PTX induced differential changes in breast cancer cells.

Conflict of Interest

None Declared

Acknowledgments

We acknowledge grant support from ACTREC, Tata Memorial Centre. Mr. Peeyush N. Goel is supported by CSIR-Senior Research fellowship and Mr. S. P. Singh is supported by ACTREC Senior Research fellowship. The Raman spectrometer employed in the study was procured from DBT project BT/PRI11282/MED/32/83/2008, entitled "Development of *in vivo* laser Raman spectroscopy methods for diagnosis of oral precancerous and cancerous conditions, Department of Biotechnology, Government of India".

References

1. G. Tarafa, D. Tuck, D. Ladner, M. Topazian, R. Brand, C. Deters, V. Moreno, G. Capella, H. Lynch, P. Lizardi, J. Costa, "Mutational load distribution analysis yields metrics reflecting genetic instability during pancreatic carcinogenesis," *Proc. Natl. Acad. Sci. USA* **105**, 4306–4311 (2008).
2. J. Ferlay, H. R. Shin, F. Bray, D. Forman, C. Mathers, D. M. Parkin, "Estimates of worldwide burden of cancer in 2008: GLOBOCAN 2008," *Int. J. Cancer* **127**, 2893–2917 (2010).
3. A. Mullard, "Could pharma open its drug freezers?," *Nat. Rev. Drug. Discov.* **10**(6), 399–400 (2011).
4. M. Zhang, Y. J. Xu, S. A. Mengi, A. S. Arneja, N. S. Dhalla, "Therapeutic potentials of pentoxifylline for treatment of cardiovascular diseases," *Exp. Clin. Cardiol.* **9**(2), 103–111 (2004).
5. L. Hirsh, A. Dantes, B. S. Suh, Y. Yoshida, K. Hosokawa, K. Tajima, F. Kotsuji, O. Merimsky, A. Amsterdam, "Phosphodiesterase inhibitors as anti-cancer drugs," *Biochem. Pharmacol.* **68**(6), 981–988 (2004).
6. P. N. Goel, R. P. Gude, "Unravelling the antimetastatic potential of pentoxifylline, a methylxanthine derivative in human MDA-MB-231 breast cancer cells," *Mol. Cell. Biochem.* **358**(1–2), 141–151 (2011).
7. G. Biolo, B. Ciocchi, A. Bosutti, R. Situlin, G. Toigo, G. Guarnieri, "Pentoxifylline acutely reduces protein catabolism in chronically uremic patients," *Am. J. Kidney Dis.* **40**(6), 1162–1172 (2002).
8. M. K. Chae, S. G. Park, S.-O. Song, E. S. Kang, B. S. Cha, H. C. Lee, B.-W. Lee, "Pentoxifylline attenuates Methionine- and Choline-deficient-diet-induced steatohepatitis by suppressing TNF- α expression and endoplasmic reticulum stress," *Exp. Diabetes Res.* **2012**, 1–8 (2012).
9. C. O. Zein, R. Lopez, X. Fu, J. P. Kirwan, L. M. Yerian, A. J. McCullough, S. L. Hazen, A. E. Feldstein, "Pentoxifylline decreases oxidized lipid products in nonalcoholic steatohepatitis: New evidence on the potential therapeutic mechanism," *Hepatology* **56**(4), 1291–1299 (2012).
10. Y. Sato, T. Miura, Y. Suzuki, "Interaction of pentoxifylline with human erythrocytes. III. Comparison of fluidity change of erythrocyte membrane caused by S-adenosyl-L-methionine with that by pentoxifylline," *Chem. Pharm. Bull. (Tokyo)* **39**(2), 468–473 (1991).
11. A. Amirkhosravi, G. Warnes, J. Biggerstaff, Z. Malik, K. May, J. L. Francis, "The effect of pentoxifylline on spontaneous and experimental metastasis of the mouse Neuro2a neuroblastoma," *Clin. Exp. Metastasis* **15**(4), 453–461 (1997).
12. L. Bohm, "Inhibition of homologous recombination repair with Pentoxifylline targets G2 cells generated by radiotherapy and induces major enhancements of the toxicity of cisplatin and melphalan given after irradiation," *Radiat. Oncol.* **1**(1), 12 (2006).
13. S. S. B. R. Ambrus Jr, "Effect of pentoxifylline on carbohydrate metabolism in type ii diabetics," *Arch. Intern. Med.* **150**(4), 921–921 (1990).
14. D. Lin, J. Lin, Y. Wu, S. Feng, Y. Li, Y. Yu, G. Xi, H. Zeng, R. Chen, "Investigation on the interactions of lymphoma cells with paclitaxel by Raman spectroscopy," *Spectroscopy* **25**(1), 23–32 (2011).
15. E. V. Efremov, F. Ariese, C. Gooijer, "Achievements in resonance Raman spectroscopy review of a

- technique with a distinct analytical chemistry potential," *Anal. Chim. Acta.* **606**(2), 119–134 (2008).
16. A. Nijssen, S. Koljenovic, T. C. Bakker Schut, P. J. Caspers, G. J. Puppels, "Towards oncological application of Raman spectroscopy," *J. Biophotonics* **2**(1–2), 29–36 (2009).
 17. E. B. Hanlon, R. Manoharan, T. W. Koo, K. E. Shafer, J. T. Motz, M. Fitzmaurice, J. R. Kramer, I. Itzkan, R. R. Dasari, M. S. Feld, "Prospects for in vivo Raman spectroscopy," *Phys. Med. Biol.* **45**(2), R1–59 (2000).
 18. A. Mahadevan-Jansen, R. R. Richards-Kortum, "Raman spectroscopy for the detection of cancers and precancers," *J. Biomed. Opt.* **1**(1), 31–70 (1996).
 19. J. R. Baena, B. Lendl, "Raman spectroscopy in chemical bioanalysis," *Curr. Opin. Chem. Biol.* **8**(5), 534–539 (2004).
 20. D. Naumann, "FT-Infrared and FT-Raman spectroscopy in biomedical research," *App. Spectrosc. Rev.* **236**(2–3), 239–298 (2001)
 21. K. W. Short, S. Carpenter, J. P. Freyer, J. R. Mourant, "Raman spectroscopy detects biochemical changes due to proliferation in mammalian cell cultures," *Biophys. J.* **88**(6), 4274–4288 (2005).
 22. C. M. Krishna, G. Kegelaer, I. Adt, S. Rubin, V. B. Kartha, M. Manfait, G. D. Sockalingum, "Combined Fourier transform infrared and Raman spectroscopic approach for identification of multidrug resistance phenotype in cancer cell lines," *Biopolymers* **82**(5), 462–470 (2006).
 23. R. J. Swain, G. Jell, M. M. Stevens, "Non-invasive analysis of cell cycle dynamics in single living cells with Raman micro-spectroscopy," *J. Cell. Biochem.* **104**(4), 1427–1438 (2008).
 24. M. V. Chowdary, K. K. Kumar, J. Kurien, S. Mathew and C. M. Krishna, "Discrimination of normal, benign, and malignant breast tissues by Raman spectroscopy," *Biopolymers* **83**(5), 556–569 (2006).
 25. R. Malini, K. Venkatakrishna, J. Kurien, K. M. Pai, L. Rao, V. B. Kartha, C. M. Krishna, "Discrimination of normal, inflammatory, premalignant, and malignant oral tissue: A Raman spectroscopy study," *Biopolymers* **81**(3), 179–193 (2006).
 26. J. Guo, W. Cai, B. Du, M. Qian, Z. Sun, "Raman spectroscopic investigation on the interaction of malignant hepatocytes with doxorubicin," *Biophys. Chem.* **140**(1–3), 57–61 (2009).
 27. W. Xie, Y. Ye, A. Shen, L. Zhou, Z. Lou, X. Wang, J. Hu, "Evaluation of DNA-targeted anti-cancer drugs by Raman spectroscopy," *Vib. Spectrosc.* **47**(2), 119–123 (2008).
 28. S. Akyuz, A. E. Ozel, K. Balci, T. Akyuz, A. Coker, E. D. Arisan, N. Palavan-Unsal, A. Ozalpan, "Raman micro-spectroscopic analysis of cultured HCT116 colon cancer cells in the presence of roscovitine," *Spectrochim. Acta A Mol. Biomol. Spectrosc.* **78**(5), 1540–1547 (2011).
 29. K. Brautigam, T. Bocklitz, M. Schmitt, P. Rosch, J. Popp, "Raman spectroscopic imaging for the real-time detection of chemical changes associated with docetaxel exposure," *Chemphyschem* **14**(3), 550–553 (2013).
 30. R. N. Aravalli, J. Choi, S. Mori, D. Mehra, J. Dong, J. C. Bischof, E. N. Cressman, "Spectroscopic and calorimetric evaluation of chemically induced protein denaturation in HuH-7 liver cancer cells and impact on cell survival," *Technol. Cancer Res. Treat.* **11**(5), 467–473 (2012).
 31. K. Hartmann, M. Becker-Putsche, T. Bocklitz, K. Pachmann, A. Niendorf, P. Rosch, J. Popp, "A study of Docetaxel-induced effects in MCF-7 cells by means of Raman microspectroscopy," *Anal. Bioanal. Chem.* **403**(3), 745–753 (2012).
 32. K. le Roux, L. C. Prinsloo, A. A. Hussein, N. Lall, "A micro-Raman spectroscopic investigation of leukemic U-937 cells treated with *Crotalaria agatiflora* Schweinf and the isolated compound madurensine," *Spectrochim. Acta A Mol. Biomol. Spectrosc.* **95**, 547–554 (2012).
 33. C. Murali Krishna, G. Kegelaer, I. Adt, S. Rubin, V. B. Kartha, M. Manfait, G. D. Sockalingum, "Characterisation of uterine sarcoma cell lines exhibiting MDR phenotype by vibrational spectroscopy," *Biochim. Biophys. Acta* **1726**(2), 160–167 (2005).
 34. C. M. Krishna, G. D. Sockalingum, G. Kegelaer, S. Rubin, V. B. Kartha, M. Manfait, "Micro-Raman spectroscopy of mixed cancer cell populations," *Vib. Spectrosc.* **38**(1), 95–100 (2005).
 35. A. Nijssen, K. Maquelin, L. F. Santos, P. J. Caspers, T. C. Bakker Schut, J. C. den Hollander, M. H. Neumann, G. J. Puppels, "Discriminating basal cell carcinoma from perilesional skin using high wavenumber Raman spectroscopy," *J. Biomed. Opt.* **12**(3), 034004 (2007).
 36. S. P. Singh, A. Sahu, A. Deshmukh, P. Chaturvedi, C. M. Krishna, "In vivo Raman spectroscopy of oral buccal mucosa: A study on malignancy associated changes (MAC)/cancer field effects (CFE)," *Analyst* **138**(14), 4175–4182 (2013).
 37. A. D. Ghanate, S. Kothiwale, S. P. Singh, D. Bertrand, C. M. Krishna, "Comparative evaluation of spectroscopic models using different multivariate statistical tools in a multicancer scenario," *J. Biomed. Opt.* **16**(2), 025003 (2011).
 38. A. Bravo-Cuellar, P. C. Ortiz-Lazareno, J. M. Lerma-Diaz, J. R. Dominguez-Rodriguez, L. F. Jave-Suarez, A. Aguilar-Lemarro, S. del Toro-Arreola, R. de Celis-Carrillo, J. E. Sahagun-Flores, J. E. de Alba-Garcia,

- G. Hernandez-Flores, "Sensitization of cervix cancer cells to Adriamycin by Pentoxifylline induces an increase in apoptosis and decrease senescence," *Mol. Cancer* **9**, 114–127 (2010).
39. A. J. Shaywitz, M. E. Greenberg, "CREB: A stimulus-induced transcription factor activated by a diverse array of extracellular signals," *Annu. Rev. Biochem.* **68** 821–861 (1999).
 40. G. J. Puppels, F. F. M. de Mul, C. Otto, J. Greve, M. Robert-Nicoud, D. J. Arndt-Jovin, T. M. Jovin, "Studying single living cells and chromosomes by confocal Raman microspectroscopy," *Nature* **347** (6290), 301–303 (1990).
 41. G. J. Puppels, H. S. Garritsen, G. M. Segers-Nolten, F. F. de Mul, J. Greve, "Raman microspectroscopic approach to the study of human granulocytes," *Biophys. J.* **60**(5), 1046–1056 (1991).
 42. G. J. Puppels, J. H. F. Olminkhof, G. M. J. Segers-Nolten, C. Otto, F. F. M. de Mul, J. Greve, "Laser irradiation and Raman spectroscopy of single living cells and chromosomes: Sample degradation occurs with 514.5 nm but not with 660 nm laser light," *Exp. Cell Res.* **195**(2), 361–367 (1991).
 43. F. Bonnier, S. M. Ali, P. Knief, H. Lambkin, K. Flynn, V. McDonagh, C. Healy, T. C. Lee, F. M. Lyng, H. J. Byrne, "Analysis of human skin tissue by Raman microspectroscopy: Dealing with the background," *Vib. Spectrosc.* **61**(0), 124–132 (2012).
 44. S. R. Hawi, W. B. Campbell, A. Kajdacsy-Balla, R. Murphy, F. Adar, K. Nithipatikom, "Characterization of normal and malignant human hepatocytes by Raman microspectroscopy," *Cancer Lett.* **110**(1–2), 35–40 (1996).
 45. W. T. Cheng, M. T. Liu, H. N. Liu, S. Y. Lin, "Micro-Raman spectroscopy used to identify and grade human skin pilomatrixoma," *Microsc. Res. Tech.* **68**(2), 75–79 (2005).
 46. Z. Movasaghi, S. Rehman, I. U. Rehman, "Raman spectroscopy of biological tissues," *App. Spectrosc. Rev.* **42**(5), 493–541 (2007).
 47. I. Notingher, C. Green, C. Dyer, E. Perkins, N. Hopkins, C. Lindsay, L. L. Hench, "Discrimination between ricin and sulphur mustard toxicity in vitro using Raman spectroscopy," *J. R. Soc. Interface* **1**(1), 79–90 (2004).
 48. T. C. Bakker Schut, R. Wolthuis, P. J. Caspers, G. J. Puppels, "Real-time tissue characterization on the basis of in vivo Raman spectra," *J. Raman Spectrosc.* **33**(7), 580–585 (2002).
 49. P. Crow, B. Barrass, C. Kendall, M. Hart-Prieto, M. Wright, R. Persad, N. Stone, "The use of Raman spectroscopy to differentiate between different prostatic adenocarcinoma cell lines," *Br. J. Cancer* **92**(12), 2166–2170 (2005).
 50. T. J. Harvey, E. Gazi, A. Henderson, R. D. Snook, N. W. Clarke, M. Brown, P. Gardner, "Factors influencing the discrimination and classification of prostate cancer cell lines by FTIR microspectroscopy," *Analyst* **134**(6), 1083–1091 (2009).
 51. E. Vargis, Y. W. Tang, D. Khabele, A. Mahadevan-Jansen, "Near-infrared Raman microspectroscopy detects high-risk human papillomaviruses," *Transl. Oncol.* **5**(3), 172–179 (2012).
 52. K. M. Ostrowska, A. Malkin, A. Meade, J. O'Leary, C. Martin, C. Spillane, H. J. Byrne, F. M. Lyng, "Investigation of the influence of high-risk human papillomavirus on the biochemical composition of cervical cancer cells using vibrational spectroscopy," *Analyst* **135**(12), 3087–3093 (2010).